TECHNISCHE UNIVERSITÄT MÜNCHEN

Fakultät für Maschinenwesen

Lehrstuhl für Hubschraubertechnologie

A Hierarchical Probabilistic Approach to Rotorcraft Preliminary Design

Dominik Wirth

Vollständiger Abdruck der von der Fakultät für Maschinenwesen der Technischen Universität München zur Erlangung des akademischen Grades eines Doktor-Ingenieurs (Dr.-Ing.) genehmigten Dissertation.

Vorsitzender: Prof. Dr. mont. habil. Dr. rer. nat. h. c. Ewald Werner

Prüfende der Dissertation: 1. Prof. Dr.-Ing. Manfred Hajek

2. Prof. Dr.-Ing. Mirko Hornung

Die Dissertation wurde am 12.03.2018 bei der Technischen Universität München eingereicht und durch die Fakultät für Maschinenwesen am 17.09.2018 angenommen.

To Family & Friends.

Abstract

Contemporary preliminary design methodologies for rotorcraft are built around empirical methods, and hence are limited in their capabilities and validity to the domain of the underlying set of data. While these methods excel in the evolutionary strategy characterizing the rotorcraft developments of the past decades, the ability to explore alternative configurations and technologies is lacking. However, rising expectations for future rotorcraft call for the infusion of new technologies and the exploration of novel configurations, pushing the established methodologies beyond their limits. A paradigm change towards model-based approaches for the preliminary design of rotorcraft is needed. This work addresses this need through the development of a novel methodology for rotorcraft preliminary design.

As model-based methodologies do not exhibit the intrinsic robustness of contemporary empirically-driven methods, the incorporation of dedicated elements addressing the model-related uncertainty in the design problem is essential. Hence, the methodology developed here integrates probabilistic elements into the design logic, aiming at prioritizing and quantifying the model-related uncertainty. Based on the stochastic properties of the particular design problem, a robust design is derived in which the relevant uncertainty is controlled. Crucially, design margins for robustness are identified per design parameter, improving the visibility of uncertainty propagation in the design space compared to historical approaches.

Furthermore, the methodology adopts a Systems-Engineering-inspired mindset, characterized by a requirement-driven approach and the progressive decomposition of the design problem. This hierarchical approach is reflected both in the design and modeling strategies. In a model-based design environment, it is considered as crucial to develop the system model and the design synchronously. To this end, a three-tiered modeling strategy of varying fidelity is developed, tailored to the particular needs of each distinct design phase. A methodical and traceable strategy ensuring consistency when transitioning across model-fidelity levels is developed. The above outlined attributes are merged into a coherent methodology for preliminary design.

The methodology is tested with a demonstration case. A generic preliminary design problem in a fictive Urban Air Mobility scenario is investigated. Three different rotorcraft configurations are included in the example case, namely a conventional helicopter, a tiltrotor, and a novel, fully-electric configuration capable of vertical flight. The cases successfully demonstrate the viability of the developed methodology for quantifying and controlling the model-related uncertainty prevalent in model-based preliminary design. The design margins required for turning the deterministic reference designs into robust designs decrease continuously while progressing through the preliminary design tiers. Interestingly, it is found that the design margins required for robustness at the end of the preliminary design phase are moderate. Hence, it is concluded that the developed methodology provides an effective framework for the broad adoption of model-based methodologies in the field.

Kurzfassung

Gegenwärtige Methoden für den Drehflüglervorentwurf basieren auf empirischen Verfahren. Deren Anwendungsbereich ist hinsichtlich der prädiktiven Fähigkeiten und der Validität auf die Domäne des ihrer Genese zu Grunde liegenden Datensatzes beschränkt. Während diese Methoden einen hohen Nutzwert in einer evolutionären Entwicklungsstrategie aufweisen, welche die Drehflüglerentwicklungen der vergangenen Jahrzehnte auszeichnete, so sind diese jedoch ungeeignet für die Untersuchung alternativer Konfigurationen und Technologien. Steigende Anforderungen an zukünftige Drehflügler bedingen allerdings die Exploration neuer Technologien und die Evaluierung neuartiger Konzepte und stellen bestehende Verfahren daher vor unüberbrückbare Aufgaben. Ein Paradigmenwechsel hin zu modellbasierten Verfahren wird daher als zwingend erachtet. Die vorliegende Arbeit adressiert diesen Bedarf durch die Entwicklung einer neuartigen Methodik für den Drehflüglervorentwurf.

Da modellbasierte Methoden nicht die intrinsischen Robustheitseigenschaften gegenwärtiger empirischer Methoden aufweisen, ist die Einbettung dedizierter Elemente für die Handhabung der modellbezogenen Unsicherheit in der Auslegungsaufgabe essentiell. Die hier entwickelte Methodik integriert daher probabilistische Elemente in die Entwicklungslogik, welche auf die relative Gewichtung und Quantifizierung der modellbezogenen Unsicherheit zielen. Aus der Analyse der stochastischen Eigenschaften einer spezifischen Auslegungsaufgabe wird ein robuster Entwurf ermittelt, in welchem die relevante Unsicherheit kontrolliert wird. Die Identifizierung der Entwurfsmargen pro Auslegungsparameter ist dabei elementar, da somit die Sichtbarkeit der Fortpflanzung der Unsicherheit in den Auslegungsraum gegenüber bestehenden Verfahren deutlich erhöht wird.

Die entwickelte Auslegungsmethodik übernimmt mit der anforderungsgetriebenen Vorgehensweise sowie der progressiven Dekomposition der Auslegungsaufgabe elementare Bestandteile des Systems Engineering. Dieser hierarchische Ansatz wird sowohl in der Entwicklungs- als auch in der Modellierungsstrategie offenbar. In einer modellbasierten Auslegungsmethodik ist es von entscheidender Bedeutung, die Entwicklung des Systemmodells und des Entwurfs synchron voranzutreiben. Vor diesem Hintergrund wird eine dreistufige Modellierungsstrategie verschiedener Modellierungsgüte entwickelt und auf den jeweiligen Bedarf der diskreten Vorentwurfsphasen angepasst. Ein methodisches und nachverfolgbares Verfahren zur Sicherstellung eines konsistenten Übergangs zwischen den Modellierungsebenen wird entwickelt. Die voranstehend aufgeführten Attribute werden in einer kohärenten Methodik für den Drehflüglervorentwurf zusammengeführt.

Die Methodik wird in einem Anwendungsfall getestet. Eine generische Vorentwurfsaufgabe auf Basis eines fiktiven Szenarios für die Einbindung von Luftfahrzeugen in urbane Mobilitätskonzepte (“Urban Air Mobility”) wird untersucht. Mit einem konventionellem Hubschrauber, einem Kipprotorflugzeug, sowie einem neuartigen, vollelektrisch angetriebenem Drehflüglerkonzept werden drei verschiedene Konfigurationen in die Studie einbezogen. Diese Anwendungsbeispiele belegen eindrücklich die Eignung der entwickelten Methodik zur Quantifizierung und Beherrschung der

modellbezogenen Unsicherheit in Vorentwurfsaufgaben. Die notwendigen Entwurfsmargen zur Transformation des deterministischen in einen robusten Entwurf sinken kontinuierlich während des Durchlaufens der verschiedenen Vorentwurfsphasen. Die am Ende des Vorentwurfs verbleibenden Robustheitsmargen sind dabei äußerst moderat. Die entwickelte Methodik wird daher als effektives Rahmenwerk für eine breite Anwendung modellbasierter Verfahren im Bereich des Drehflüglervorentwurfs bewertet.

Contents

List of Figures

List of Tables

Notation

List of symbols

A	Rotor disc area
$battType$	Type of battery
c	Rotor blade chord
$\overline{c}_d$	Rotor blade mean drag coefficient
c_T/σ	Rotor blade loading
DGM	Design Gross Mass
e	Specific energy density
EM	Empty Mass
η_{mot}	Electric motor efficiency
η_{pe}	Power electronics efficiency
η_{prop}	Propeller efficiency
η_{tot}	Total propulsive efficiency
f_{RC}	Rotorcraft equivalent flat plate drag area
f_{Int}	Battery integration factor
g	Gravitational acceleration constant on earth
k_{DL}	Rotorcraft vertical download factor
k_{FF}	Fuel flow installation losses factor
L/D	Rotorcraft Lift-to-Drag ratio; $L/D = \frac{WV}{P_{req}}$
M	Mass
n_{blades}	Number of rotor blades
n_c	Number of instances per uncertainty factor in the probabilistic analysis
n_f	Number of factors subjected to uncertainty in the probabilistic analysis
$\mathcal{F}$	Set of events in the probability space $\mathcal{P}$
P_{req}	Required Power
PA	Physical Architecture
PL	Power Loading
R	Rotor radius
RA	Requirements Architecture
$rcType$	Type of rotorcraft
S	Parameter space spanned by $\vec{p}$
sfc	Specific fuel consumption
T	Rotor thrust
TA	Technical Architecture
tr	Rotor blade taper ratio
U	Battery voltage

V	Rotorcraft velocity with respect to the air
v	Induced velocity of the rotor, perpendicular to the rotor disk
V_{hold}	Rotorcraft holding speed
V_{max}	Rotorcraft maximum speed
V_{tip}	Rotor tip speed
V_z	Rotorcraft vertical speed, positive for climb
W	Weight, $W = Mg$
Z_p	Density altitude
$\vec{d}$	Design parameters, where $\vec{d} \in PA \subset \vec{p}$
$\vec{p}$	Vector of the complete set of model parameters
$\vec{r}$	Vector of requirements
$\vec{s}$	Vector of flight state parameters
$\vec{t}$	Technical model parameters, where $\vec{t} \in TA \subset \vec{p}$
$\vec{y}$	Vector of system state parameters

Greek symbols

χ_{EM}	Uncertainty control variable on empty mass
δ	Prefix for an accompanying model parameter vector, indicating the vector contains entries describing variability
Δ_{DGM}	Design Gross Mass difference between robust and reference designs, $\Delta_{DGM} = DGM_{rob} - DGM_{ref}$
Δ_{EM}	Empty Mass fraction difference between robust and reference designs, $\Delta_{EM} = (EM/DGM)_{rob} - (EM/DGM)_{ref}$
Δ_{Tn}	Robust Design Margin at design tier n
κ	induced power factor indicating the ratio between real induced power to ideal power
μ	Advance ratio
Ω	Set of possible outcomes of a particular probability space $\mathcal{P}$
Ω_{rotor}	Rotor rotational speed
ρ	Air density
σ	Rotor solidity
Θ	Rotor blade twist

Subscripts

batt	Battery
cell	Battery cell

computed	Parameter value computed from sub-model at lower level
dep	Dependent parameter
DoF	Degree of Freedom
feas	feasible
hover	Hovering flight domain
indep	Independent parameter
n	Level of system hierarchy *n*
$n \pm j$	Index of system-hierarchy level *j* levels above/below level *n*
prop	Proposed parameter
prosp	Prospect parameter
ref	Index of the (deterministic) reference design
req	requirement
rob	Index of the robust design
rotor	Rotor parameter
s	Specified parameter
sel	Selected subset of parameters
size	Parameter sizing dependent parameter
sys	system
T2+	Index of Tier-2 scenario boosted by Concurrent Engineering
Tn	Index of tier *n*
uncert	Uncertainty parameter

Acronyms

AMRDEC	United States Army Aviation and Missile Research, Development and Engineering Center
BET	Blade-Element-Theory
CAT	Commercial Air Transport
CDF	Cumulative Distribution Function
CE	Concurrent Engineering
CFD	Computational Fluid Dynamics
CG	Center of Gravity
ConOps	Concept of Operations
DGM	Design Gross Mass
DL	Disk Loading
DLR	German Aerospace Center
EASA	European Aviation Safety Agency
EM	Empty Mass
eVTOL	Electric Vertical Takeoff and Landing (Aircraft)
FA	Functional Architecture
FAA	Federal Aviation Administration
FEA	Finite Element Analysis
H/C	Helicopter
HOGE	Hover out of Ground Effect
ICAO	International Civil Aviation Organization
IDL	Iterative Design Loop
IFR	Instrument Flight Rules
INCOSE	International Council on Systems Engineering
IPPD	Integrated Product and Process Development
ISA	ICAO International Standard Atmosphere
ISO	International Organization for Standardization
IV&V	Integration, Verification and Validation
LCC	Life-Cycle Costs
LHS	Latin Hypercube Sampling
MBSE	Model-Based Systems Engineering
MCP	Maximum Continuous Power

MDP	Model Development Process
MoE	Measure of Effectiveness
MoP	Measure of Performance
MR	Main Rotor
NASA	National Aeronautics and Space Administration
NDARC	NASA Design and Analysis of Rotorcraft
ONERA	The French Aerospace Lab
PA	Physical Architecture
PDF	Probability Density Function
PDT	Probability Distribution Type
PL	Power Loading
QE	Quality Engineering
qMC	quasi-Monte-Carlo (Method)
R/C	Rotorcraft
RA	Requirements Architecture
RADP	Robust Architectural Design Process
RAM	Reliability, Availability, and Maintainability
RSM	Response Surface Methodology
SE	Systems Engineering
SLS	Sea Level Standard Conditions
STOL	Short Takeoff and Landing
T/R	Tiltrotor (Aircraft)
T0	Tier 0
T1	Tier 1
T2	Tier 2
$T2_+$	Tier-2 scenario boosted by Concurrent Engineering
TA	Technical Architecture
TOP	Takeoff Power
UAM	Urban Air Mobility
UL	Useful Load
UMDO	Uncertainty-Based Multidisciplinary Design Optimization
VTOL	Vertical Takeoff and Landing

1. Introduction

1.1. Motivation

The immense level of cost and risk associated with the development of a new rotorcraft in conjunction with a global acceptance of the limitations of contemporary vertical flight platforms regarding their performance and noise has long led the rotorcraft community opting to refresh legacy platforms in favor of new developments, as Sinsay and Nunez observe [1]. This evolutionary approach has been adequate as long as these systems were able to meet the stakeholders demands. In recent years, however, a continuous rise in operational and societal expectations towards rotorcraft is evident. Rotorcraft are asked to operate at greater speeds and ranges, more cost-efficiently, while enhancing safety, availability and alleviating the environmental footprint in terms of noise and emissions [1–4].

Besides these technical challenges, the rotorcraft community is experiencing an unprecedented level of commercial pressure in a now global and increasingly sensitive environment. The major share of the committed Life-Cycle Costs (LCC) and development risks of complex systems is imposed by project decisions taken early in the development cycle, i.e. during the conceptual and preliminary design stages. However, these initial phases in design saw comparatively little attention in terms of process and methodology evolution in recent aeronautical research. This is particularly the case for the rotorcraft sector, which has a history of trailing the advances made in its fixed-wing counterpart. Implementing modern Systems Engineering (SE) processes, which are designed to master the complexity and interdisciplinary nature of complex systems, has introduced vast improvements in cost and schedule adherence in other engineering fields [5]. In the rotorcraft field, the low number and evolutionary character of recent development projects has delayed the adoption of such holistic approaches to product design in preliminary design methodologies.

The above-mentioned increasing expectations for future rotorcraft are pushing the evolution of existing legacy platforms and technologies beyond their limits [2, 6]. This poses a major challenge for the rotorcraft community, whose capability to develop new concepts has atrophied in the past decades [7]. Contemporary preliminary design methodologies are typically based on empirical approaches, which are derived from but also limited to the particular basis of knowledge and experience of the designing entity. Consequently, these methods excel in developing concepts reflecting their product legacy but globally are not set up to explore alternative technologies or new concepts [2, 8–11]. The apparent need for the infusion of new technologies and the exploration of new concepts increases the complexity of rotorcraft development even further, while the validity of contemporary design methodologies deteriorates. For instance, revolutionary technologies such as electric and distributed propulsion are emerging, substantially expanding the design space beyond established paradigms. To enable the exploration of this expanded domain, a transition to model-based design methodologies is concluded to be imperative [11, 12]. It is desirable for

these novel methods to integrate with modern product development processes like SE, mandating a methodology which is compatible with the hierarchical approach to design adopted in SE. However, model-based approaches do not offer the intrinsic robustness of empirical methods, and hence require dedicated means to handle uncertainty [9].

1.2. Research Objectives and Scope of this Work

The main objective of this work is the development of a novel, model-based methodology for the preliminary design of rotorcraft. In view of the preceding discussion in chapter 1.1, the following objectives for the development of the methodology are set:

- Modern preliminary design methodologies need to be able to design and analyze generic rotorcraft configurations, and to assess novel technologies and concepts, implying the need for a model-based design environment.
- A SE mindset is adopted, characterized by its requirement-driven approach and a progressive decomposition of the design problem. This hierarchical approach to design calls for equally hierarchical modeling strategies for model-based preliminary design methodologies. The use of models of varying fidelity adapted to the needs of the different preliminary design stages is targeted. The development of a corresponding modeling strategy is thus a major objective of this work.
- The validity of design decisions taken at prior stages of the design process based on the prediction of system characteristics derived from differing model fidelity is an area of concern in hierarchical model-based design, yet a distinct feature of hierarchical design approaches. A prerequisite for establishing validity is a consistent and traceable evolution of the representation of the design candidates throughout the hierarchical design process. To this end, the development of a suitable methodology for transitioning between discrete levels of varying model fidelity is pursued.
- Dedicated means of uncertainty handling are required to grant model-based approaches validity. The incorporation of elements which enable the quantification and control of uncertainty related to the model-based nature of the approach is hence another key objective of this work.

1.3. Document Structure

An overview of rotorcraft preliminary design is provided in chapter 2.1, with a focus on contemporary methodologies and modeling practices. The field of model-based design is reviewed in chapter 2.2. Subsequently, chapter 2.3 introduces possible sources of uncertainty in a model-based design environment. A classification of uncertainty in this context follows. Existing approaches to handling uncertainty are reviewed. Thereafter, the main challenges related to hierarchical model-based design are discussed in chapter 2.4, before the required characteristics of modern preliminary design methodologies and modeling techniques derived from the information presented in the

preceding chapters are summarized in chapter 2.5.

The methodology developed here is outlined in chapter 3. The overall preliminary design process developed in the frame of this work is introduced in chapter 3.1. Modifications and improvements to the standard SE design process are incorporated to enable the hierarchical and probabilistic approach to preliminary design. Chapter 3.2 presents the modeling strategy developed and tailored to the needs of this novel preliminary design methodology. The modifications and improvements to the standard SE design process are then delineated in detail in chapter 3.3.

A test of the developed methodology is conducted in chapter 4 through the application to a fictive rotorcraft preliminary design problem. Three different rotorcraft types are investigated, including a Helicopter, a Tiltrotor (Aircraft) and an Electric Vertical Takeoff and Landing (Aircraft).

Based on the findings of the test cases, the developed design methodology is discussed within chapter 5. The evolution of the obtained designs over the distinct preliminary design phases is analyzed in chapter 5.1, followed by a comparison of the deterministically sized reference design on the one hand, and the derived robust design on the other hand in chapter 5.2. A synthesis of the simplifications and assumptions and their potential impact on the obtained results is outlined in chapter 5.3, leading into a discussion of the applicability of the proposed methodology to practical preliminary design problems in chapter 5.4. A differentiation against contemporary approaches is provided.

Finally, conclusions and recommendations for future investigations and improvements are given in chapter 6.

2. Modeling Aspects in Preliminary Design

2.1. An Overview of Rotorcraft Preliminary Design

2.1.1. Conventional versus Integrated Product Development

Ehrlenspiel and Meerkamm generally differentiate between *conventional* and *integrated* product development in organizations [13]. Conventional product development processes are characterized as sequential in nature. The individual activities are performed in a rather isolated manner. Whereas efforts to establish integrated views, i.e. views aiming at providing a holistic view of the product in the context of its foreseen market, do exist, these activities are typically performed in subsequent loops and are insufficiently pronounced, as Ehrlenspiel and Meerkamm observe.

Integrated Product Development, on the other hand, applies holistic and multidisciplinary methodologies, processes and organizations, while making minimal and sustainable use of resources, targeting the development of cost-effective and high-quality products with the entire product life-cycle in mind [14, 15]. Integrated Product Development procedurally and technically integrates all involved entities into a collaborative environment through all phases of product design [14, 16].

A steady trend towards an increasing degree of specialization within organizations is observed by Ehrlenspiel and Meerkamm, who see in this trend the logical reaction to the significant advances made in all fields of science in the past decades, which demand highly specialized individuals to be mastered. In this regard, the rapid development of the computer sciences has been a catalyst for the field of aeronautical engineering. Inevitably, this development triggered a change in working culture towards a distributed and highly specialized division of work [13]. Correspondingly, the technical and organizational complexity in modern product development has increased significantly. Cost and schedule overruns are commonly listed among the primary shortcomings attributed to applying conventional product development processes in today's environment [13].
The superiority of Integrated Product Development processes in modern environments is now universally agreed [13–15]. In aerospace, Systems Engineering provides the most-widely-used framework for integrated product development [9].[1] Whereas the application rate of SE principles inside aerospace is highest in the space sector, and strong efforts are observable in the fixed-wing world, the adoption rate within the rotorcraft community is, not uncharacteristically, trailing those fields. Whereas the need for a paradigm change towards integrated design processes is agreed, the adoption rate in practice is slow, and conventional product development remains predominant today in many organizations.

Only little research is available on modern product development processes specific to rotorcraft. One prominent contribution was made by Schrage in the form of the Integrated Product and Process Development (IPPD) methodology [12]. The *Georgia Tech Generic IPPD Methodology*

[1] Also illustrated by the availability of reference handbooks published by SAE International [17], National Aeronautics and Space Administration (NASA) [18] or the Federal Aviation Administration (FAA) [19].

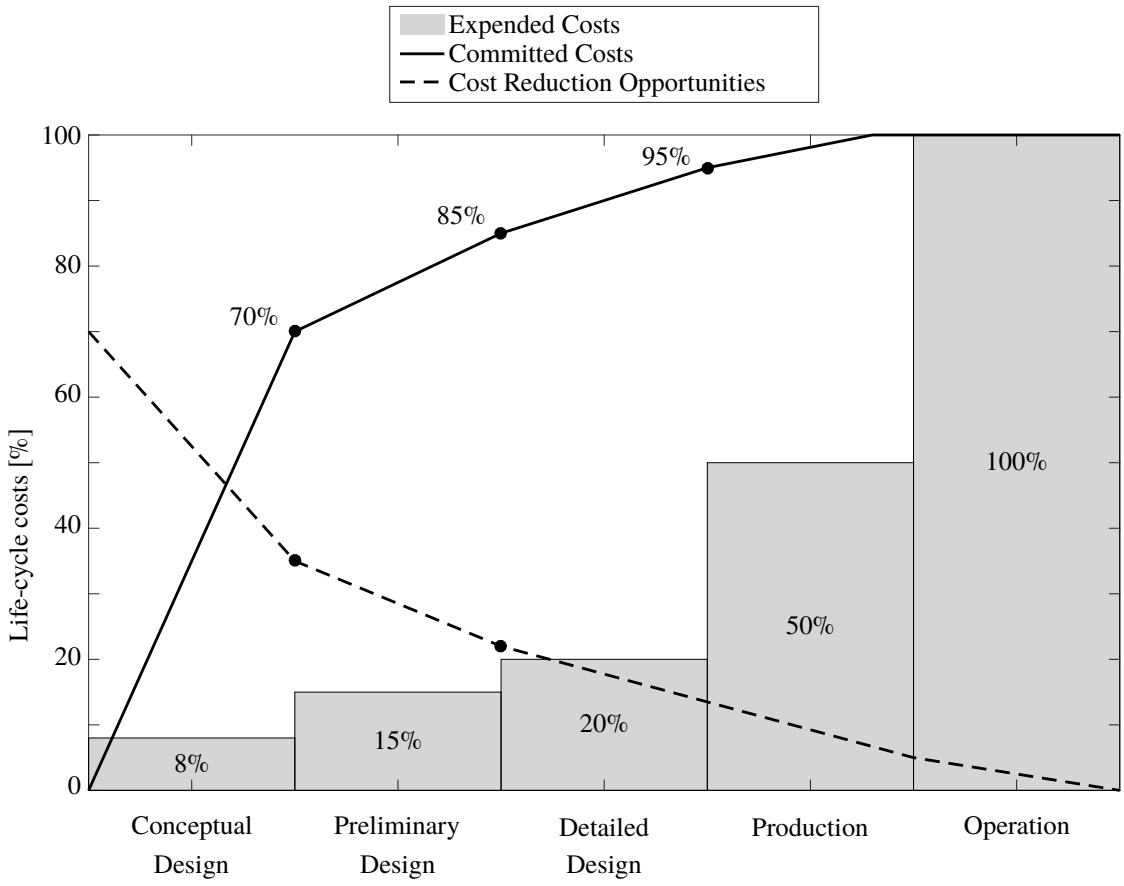

Figure 1 Overview of typical cost relations over a system life-cycle, data from [5, 9]

incorporates a systematic approach to product design similar to SE, but enriched with elements collectively labeled "Quality Engineering (QE) principles and routines", which aim at cost optimization. Schrage advocates for the addition of these QE elements based on the hypothesis that SE processes cause development costs to be locked in already at the conceptual design stage, thus leading to the conclusion that SE is indeed required in IPPD, but is not sufficient. Figure 1 shows a typical cost characteristic of a complex system over its life-cycle, indicating that the major share of the LCC is in fact already committed to at early stages of the development. Consequently, subsequent work in this context at Georgia Tech aimed at preserving design freedom until a later stage in the development process, for instance by Mavris and DeLaurentis [20]. In an attempt to facilitate Concurrent Engineering (CE), Ashok et al. apply relational-design techniques to a SE approach to rotorcraft drive system optimization [21]. The primary objective is to decouple the design disciplines. Ashok et al. find that the amount of information available from the individual disciplines in rotorcraft preliminary design in a traditional design process setup is distinctively diverse. The applied IPPD process aims at improving this imbalance and strives for a more even level of knowledge throughout the disciplines during preliminary design, in order to enable more substantiated decisions, while retaining a larger degree of design freedom at later process stages, as illustrated in figure 2.

Whereas Price et al. agree with the observation of early fixing of the development costs [9], they do not see the SE process as the cause of this issue, but consider it an inherent characteristic of the

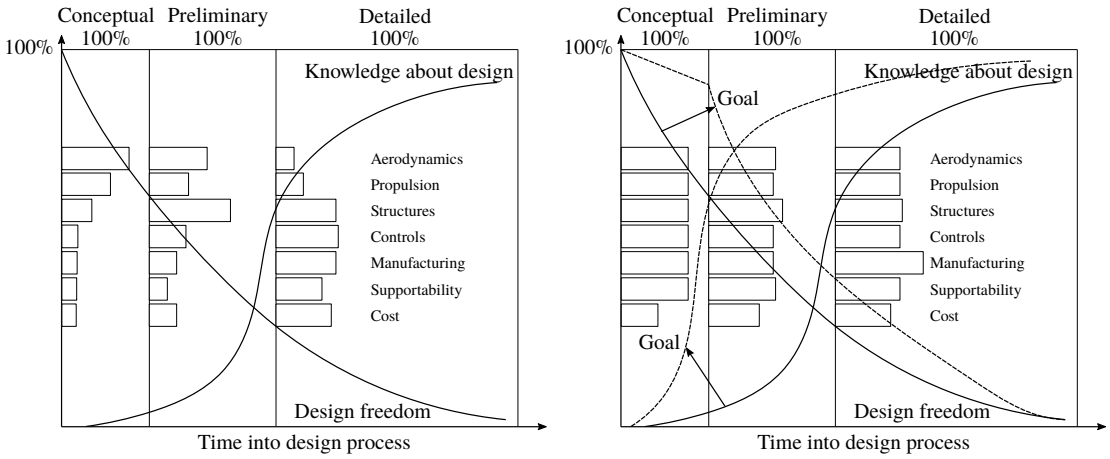

(a) Traditional sequential process

(b) IPPD process

Figure 2 Comparison of Design Knowledge acquisition and Design Freedom per discipline, adopted from [21]

design of complex systems. Therefore, the development of reliable and accurate cost-prediction models is seen as an enabling technology to enable transparent and informed design decisions with respect to their impact on costs.

2.1.2. Key Principles of Systems Engineering

SE is a broadly used framework for integrated product development. Several comprehensive overviews of SE and its applications are available, e.g. [5, 18, 22, 23]. A brief classification of SE in the context of this thesis is provided in this section. The SE principles outlined hereafter represent the state-of-the-art in the aerospace sector, whereas their implementation in the rotary-wing community is generally less wide-spread, as evident from the absence of citable literature in the rotorcraft field.

The ISO/IEC/IEEE standard 15288 describes SE as an interdisciplinary approach to enable the realization of successful systems [23]. SE was developed in response to the unprecedented and ever-growing complexity of man-made systems. As an integrated product development process, SE considers the entire system life-cycle. The aim of SE is to generate systems which satisfy functional, physical and operational needs of the stakeholders. The multitude of stakeholders involved in today's systems typically yields a manifold and frequently conflicting set of interests and constraints. SE seeks a safe and balanced design in the face of these conflicts, while aiming at maximizing the cost-effectiveness of the system. To this end, SE integrates all disciplines into a methodical and holistic approach to generate a coherent system, which satisfies the stakeholder needs.

With the stakeholder needs in the primary focus of the system development, the development objective is not limited to *getting the design right*, i.e. to meet the requirements, but expands to *finding the right design* by optimizing the requirements for overall cost-effectiveness. Therefore, the definition and validation of the requirements becomes a key aspect of the SE development process. Traditionally, requirements have not been treated as an integral part of the design process, but acted as constraints and targets for the design, as Price et al. point out [9]. Mavris and DeLaurentis state

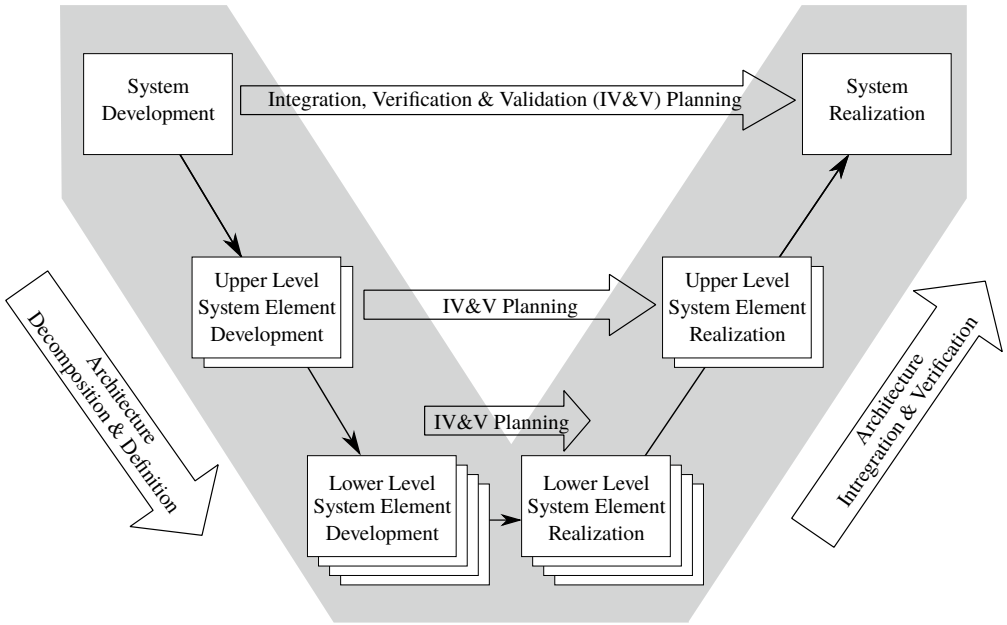

Figure 3 The V-Model - Hierarchical System Development, modified from [5]

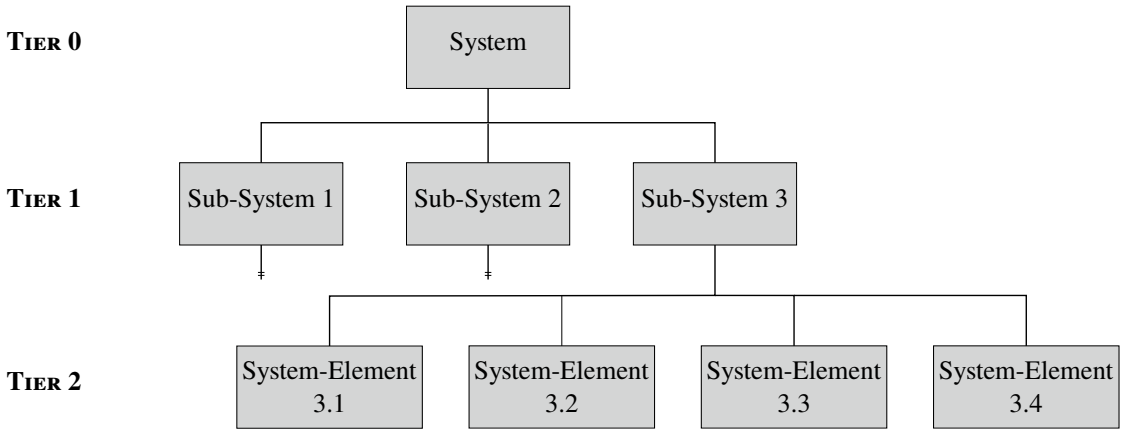

Figure 4 Generic hierarchical system schematic

that end-product user-requirements have historically been treated deterministically and isolated from the actual system development, and consider this to be problematic, as the requirements ultimately define the outcome of the development [20]. This deficiency contributed to the development of non-optimal, i.e. non-cost-effective, systems. The validation of requirements today is an accepted SE principle which aims at ensuring the most cost-effective system to be developed, as opposed to the most-capable one [5, 18, 19].

A frequently deployed representation of a typical SE development logic is the “V-Model”, depicted in figure 3. It illustrates the development principle of following a hierarchical top-down approach. Both the requirements and the design are developed and validated in parallel, whereas the level of system decomposition increases continuously. With the conclusion of the detailed design phase, the system realization commences as a bottom-up activity of integration, validation and verification on the respective levels. Ultimately, a system design emerges, which is validated and verified against the system requirements.

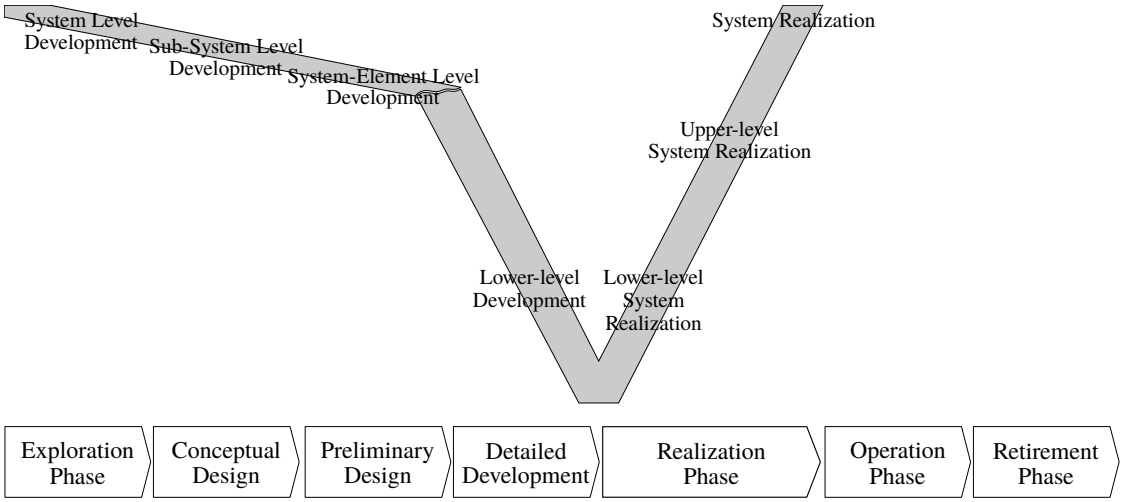

Figure 5 Schematic of a generic Life-Cycle Model

A system in the SE sense is defined as an integrated set of sub-systems and system elements, organized to provide specific functions in fulfillment of one or more stated purposes in a defined environment. Figure 4 shows a generic schematic of a system, composed of an interacting set of system elements and sub-systems. The hierarchy within the system may be described in tiers, whereas "Tier 0" typically denounces the system level, "Tier 1" the first level of decomposition, et cetera. A sub-system poses a system within a system, which itself consists of a number of system elements, or even further sub-systems. A system element is defined in the SE ISO-standard as a discrete part of a system which is implemented to fulfill specified requirements [23]. SE uses such system schematics for the representation of the system hierarchy in a set of architectural views.[2]

Figure 5 shows a simple generic life-cycle model with a focus on the development stages of the system's useful life. The V-model presented in figure 3 is schematically overlaid to indicate the level of decomposition typically achieved in each development phase. After an initial exploration phase, the development is structured into the conceptual, preliminary and detailed design phases. The individual development phases apply the design process iteratively and recursively until the respective objectives are achieved. Subsequently, the system is manufactured in the realization phase. The system is then utilized and supported during its operation phase. The life of the system ends with its withdrawal from service and disposal during the retirement phase.[3]

2.1.2.1 Exploration Phase

The exploration phase serves to develop initial concepts from an explicitly broad spectrum of alternatives. The primary objective of this phase is to develop and validate the top-level end-user needs, whereas the validation follows the SE principle of maximizing the cost-effectiveness of the system. The main outcome of this phase is a set of validated end-user needs, an initial Concept of Operations (ConOps) and a preliminary system-level specification of a feasible system concept.

[2] Chapter 2.1.3 provides a detailed overview of the concept of representing a system in the SE architectural views.
[3] A comparison of popular life-cycle models and a detailed description of the individual phases is given by the International Council on Systems Engineering (INCOSE) [5].

The design activities at this stage are limited to exercises which provide estimates of the expected system behavior in support of the user-needs validation process, which is a distinctively different emphasis than aiming to establish an optimal design solution [18]. This requirement-focused practice is a manifestation of the SE paradigm to adopt a requirement-driven approach, as opposed to a product-driven one.[4] Generally, concepts are developed to the minimum depth needed to assess the initial ConOps, and to establish the principal feasibility of the concept. The relative importance of the individual user needs and their interdependency is assessed to facilitate the validation of conflicting or particularly demanding user needs.

2.1.2.2 Conceptual Design

During the conceptual design phase, the system concept is matured further. In particular, the end-user needs are developed to a state which enables establishing the baseline set of the top-level user-requirements, the ConOps and the system-level requirements. At the end of the conceptual design phase, a down-selected list of candidate system-level architectures is proposed and their feasibility and desirability[5] is evidently substantiated.
Consequently, the representation of competing design candidates is refined until a clear differentiation between the concepts is achieved, to a satisfying degree of uncertainty. In order to generate sufficient insight and maturity to achieve these goals, the design candidates are typically decomposed down to the key sub-systems, i.e. the Tier 1 (T1) level, to provide a substantiated justification for the selection of a system concept for further analysis during the subsequent phase [5]. Some SE handbooks insist on the convergence towards a single baseline architecture in this phase, whereas a less dogmatic approach is arguably favorable when dealing with non-negligible uncertainty or unconventional concepts.

2.1.2.3 Preliminary Design

The preliminary design phase develops the design definition further to a degree of detail and maturity which allows to set it as the baseline for the subsequent detailed design activities. Latest at the end of the preliminary design phase, a singular baseline design is defined.
During this final stage, the emphasis gradually shifts towards optimizing the selected architecture in the course of the preliminary design phase, as the principal feasibility and desirability has been established in the preceding conceptual design phase. The requirements for each element of the evolving system architecture are matured further. A preliminary design for each system element is established, and its feasibility against the established set of requirements is assessed. Trade studies continue where supporting the evolution of the design. At the end of the preliminary design phase,

[4] A product-driven approach is considered one which aims at optimizing the system in terms of maximizing its capabilities, implying an imminent tendency for over-engineering the system and thus driving its life-cycle costs. A requirement-driven approach, in turn, aims at optimizing the cost-effectiveness of a system in its specific mission and application, for example by removing unnecessary capabilities.

[5] The term desirability is used here in the SE sense, implying cost-effectiveness as the primary measure of adequacy. See [5, 18] for further information.

the requirements and design description are typically developed and substantiated down to the Tier 2 (T2) level, and the interfaces between the various system elements are defined.

2.1.3. System Representation via Architectural Views

In terms of design, SE is characterized by its requirement-driven approach and a progressive decomposition of the design problem. As an integrated product development process, SE aims to provide a holistic and coherent view of the system at all times. During development, the design description evolves throughout the process by means of the synchronous hierarchical development and verification of architectural views. These architectural views, in sum, represent a complete view of the system, and of the relationships prevalent between its various elements. Classically, architectural views are established in the requirements, functional and physical domains:

1. The *Requirements Architecture (RA)* holds all needs and constraints to be satisfied by the system and its elements to ensure that the end-user requirements are met. The RA is initially populated by the user requirements. However, it will quickly grow in size during the design process when design decisions are being taken, and corresponding allocated and derived requirements are deduced and validated.

2. The *Functional Architecture (FA)* describes the functions needed to satisfy the requirements. Whereas rather abstract at high levels of the breakdown for a physical system, the functional architecture becomes increasingly concrete along the decomposition path. The FA may be implicitly or explicitly incorporated in the RA. In this case, the RA is created in such a way that it incorporates functional and non-functional requirements.

3. The *Physical Architecture (PA)* describes the system, its elements and its linkages in the physical domain. The PA is developed to yield a system which is capable of fulfilling the required functions in such a way that the requirements are satisfied. Hence, the PA entries can be interpreted as the design space available to the designer. Dimensional and geometrical data such as rotor radius, location, and the selected airfoil are typical examples of the type of information contained in the PA.

Price et al. label this classical practice as the "reductionist" approach [24], as it involves decomposing the system gradually into its sub-systems and system elements in a top-down approach. Whereas Price et al. acknowledge the general viability of this approach, one essential shortcoming is identified in the form of a lack of information on the system's emergent behavior[6], whether designed for or unexpected. Price et al. attribute this deficiency to the strictly hierarchical nature of the reductionist approach. As the system is broken down and more levels are added, the hierarchy becomes increasingly complex. Hence, it becomes more and more challenging to identify and describe interactions between system elements, both physical and functional. These relations may not only arise from inheritance in the hierarchy itself, but also from newly created dependencies when refining the system architecture. This deficiency becomes arguably even more severe in

[6] Emergent behavior describes the characteristic of complex systems to also exhibit behaviors which no subset of their individual elements show. This emergent behavior is generally attributed to interactions between system elements arising when they are integrated into a system.

a model-based design environment. Where empirically based design methodologies rely on implicitly defined interrelations, the behavioral attributes of the individual system elements in a model-based approach are inherently defined by the established system models. In any case, the relations may provoke interactions between system elements with no interface in the physical domain. Thus, for a truly holistic view, a model-based design environment requires to include this information in the architectural views.

In order to achieve a holistic system representation in the face of these challenges, Price et al. propose an extension of the classical hierarchical views:

4. The *Technical Architecture (TA)* is described by Price et al. as a set of rules which govern the interdependence and interconnection between the system elements [24]. The objective of the design task then becomes to establish these linkages in such a way that the emergent behavior of the system is in line with the requirements. The TA thus complements the PA by providing non-physical information. Applied to the context of model-based design, the definition of the TA given by Price et al. can be extended to include information on the chosen modeling and sizing philosophy, since these "links" implicitly yield the system sizing in such an application. Furthermore, the behavioral characteristics of the individual system elements are captured, and the system's emergent behavior is described in the form of system characteristics and performance.

The TA is of particular interest in the context of model-based design, since relationships between dependent system elements arising from the applied modeling in the design and analysis become traceable.[7] The value of this traceability may be illustrated by a simplified view of a system model as derived by Krus [25]: the characteristics of a system (c_{sys}) are generally modeled as a function of a number of system parameters (p_{sys}), such that $F(p_{sys}) \mapsto c_{sys}$, where the set of functional relationships F mimics the behavior and interdependencies present within the design, i.e. within the parameter set p_{sys}. In any design problem, both the system characteristics and the system parameters will be constrained. Constraints imposed on the system characteristics will impact the feasible system parameter domain, and vice versa. Consequently, the design resulting from a model-based design loop built upon the functional relationships F is directly influenced by the system characteristics c_{sys}, but also by F, which encompasses the system model and the sizing algorithms. Therefore, capturing and describing these linkages in the TA is of key importance in a model-based design environment. As for the classical architectural views, the development of the TA follows a hierarchical approach, as Price et al. point out [24].

Figure 6 shows the relationship between the architectural views. In this view, the FA is integrated with the RA, which consequently includes all functional requirements. Interdependencies and interconnections between system elements arising from the applied modeling, the design methodology, or the sizing rules themselves, are now captured in the TA. These relationships enable

[7] The critical importance of this aspect is discussed in detail in chapter 2.4. Only a brief discussion is provided here to ease the introduction of the concept of the Technical Architecture.

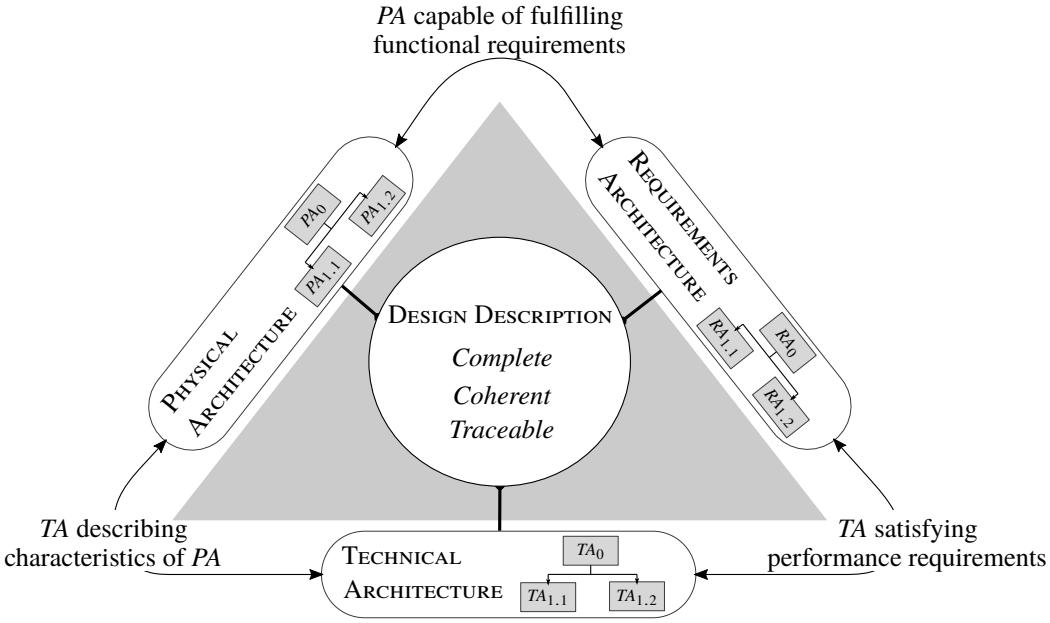

Figure 6 The Systems Engineering architectural views and their interrelation. For simplicity, the Requirements Architecture here integrates the Functional Architecture in the form of functional requirements.

visualizing connections between system elements which are unlinked in the physical domain.

In conclusion, a modern SE process makes use of a series of distinct architectural views for the description of the system architecture of any design candidate. Each architectural view provides a description of the rotorcraft design at hand from a different perspective. However, only the full set of architectural views allows to obtain a coherent and complete description of the design problem, whereas using a model-based design environment advises adding the TA to the classical set of architectural views.

2.1.4. Rotorcraft Preliminary Design Methodologies and Modeling

Chapter 1.1 discusses the reasons for contemporary rotorcraft design methodologies to heavily rely on empirical approaches. The need for a paradigm change towards physics-based modeling for design and analysis is identified. In support of this argument, an overview of the state-of-the-art in methodologies for rotorcraft preliminary design is provided hereafter. Recent research in the field is reviewed and discussed in chapter 2.1.5. The conventional practices depicted hereafter can be classified as the standard approach to preliminary design of rotorcraft, as illustrated by their description in a number of standard textbooks [26–30]. These approaches to the design and analysis of rotorcraft in the preliminary design phase remain predominant today, as their application in more recent publications from several researchers and practitioners show, for example [31–34].

Leishman provides a generic view of this preliminary design process [27], which is depicted in figure 7. The input to the process usually consists of a set of mission requirements. Commonly, these mission requirements are complemented by a series of desired point performances, such as hovering flight in specific conditions with a discrete payload, or a maximum cruise speed threshold value. Furthermore, as depicted previously, key configuration choices, such as the type of rotorcraft

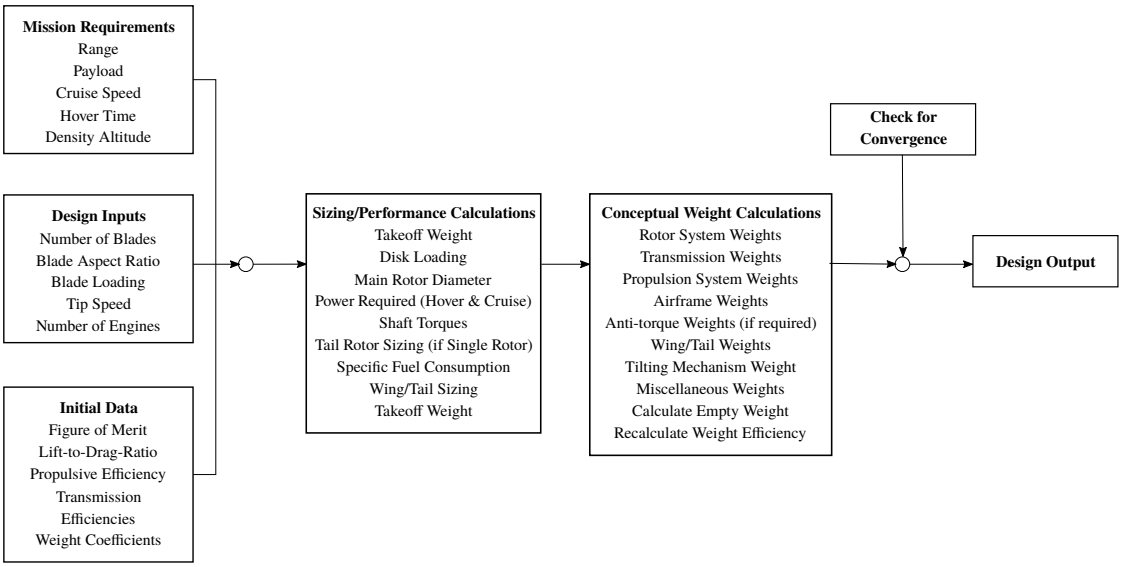

Figure 7 Classical Rotorcraft preliminary design process as described by Leishman [27].

or the number of main rotors, are frequently implicitly defined, reflecting the particular experience and expertise predominant in the respective design organization. Such design choices, and the resulting attributed performance characteristics of the rotorcraft, are categorized as *"Design Inputs"* and *"Initial Data"* in figure 7, and serve as the starting values for the subsequently performed iterative design process. A series of design and analysis tasks are run to determine the needed gross mass, installed power and fuel quantity to satisfy the specified requirements. As for any aerospace-related design problem, the estimation of the empty mass is key. This is primarily the case due to its direct influence on the required design gross mass, and secondarily because of the snowball effects on the required power and the mission fuel associated with a change in the design gross mass of the aircraft. The rotorcraft DGM and its required installed power are typically selected as convergence criteria. The classical design target is to minimize the gross mass required for the specified mission. Other objective functions may be defined, however, depending on the design objectives. Boer et al., for instance, aim to optimize the life-cycle costs [35].[8] Once the design process has converged, the overall development process continues with trade-off studies and comparative analyses of competing concepts, in order to substantiate the selection of a design for the subsequent detailed design phase.

More sophisticated design environments may include an outer loop aiming at the optimization of the design. Crossley and Laananen implement a genetic algorithm to optimize the conceptual design of a helicopter [38, 39]. Celi provides a survey of applications of design optimization to rotorcraft [40]. Celi identifies the limited accuracy of the underlying analyses, as well as the high computational effort associated with the optimization algorithms as issues. Although the continuous development of the performance of computers may help to alleviate this issue, Celi anticipates an increased use of high-fidelity analyses in a strive for a higher degree of accuracy in the future. The correspondingly rising computational effort may then counteract these advances.

[8] Frequently, minimizing DGM is equated with minimizing rotorcraft fly-away costs at the same time, as a first-order correlation between the parameters is drawn. This correlation however is criticized for its inaccuracy by Harris and Scully [36, 37].

Further examples for attempting to enrich contemporary preliminary design tools through the introduction of an outer optimization loop are [41–43].

Typical preliminary design environments use momentum-theory-based modeling for its computational efficiency. When augmented with a number of empirically-calibrated correction factors, momentum theory provides a reasonable accuracy for preliminary design purposes, as for example Leishman emphasizes [27]. Moreover, albeit an increase in model fidelity does improve the resolution of the analysis, it does not necessarily improve its accuracy and reliability.[9]

An important advantage of using empirically-calibrated momentum-theory models consists of the natural built-in robustness, which is obtained from the calibration to measured data from legacy aircraft. The reliability of the models, and of the derived sizing correlations, benefits from the underlying validated database of actual and proven designs. However, once this charted territory is departed from through extrapolation or non-representativeness in terms of architecture and technologies, this advantage quickly reverts into a severe shortcoming. The viability of the empirical models is then compromised depending on the degree of extrapolation, and may even stall the design capacity as a whole. However, as the requirements towards the design capabilities in the rotorcraft domain have remained rather static throughout the past decades, this approach long remained adequate and effective [9].[10]

The preceding paragraphs discuss the classical approach for rotorcraft preliminary design in terms of the design process and methodology, as well as regarding the modeling. Another aspect to consider is the actual sizing of the rotorcraft in the course of the design process. Key configuration choices, such as the type of rotorcraft or the number of main rotors, are frequently implicitly defined in the design organization reflecting its particular experience and expertise. In light of the argument above, this self-imposed restriction of rotorcraft configurations to well-known configurations ensures the validity of the methods and tools of the respective design organization. As Leishman points out, even more detailed design parameters such as the main rotor tip speed or the number of blades per rotor may be fixed and set as input to the design process, rather than remaining a design degree of freedom [27], see figure 7. The remaining design degrees of freedom are then typically sized based on a statistical approach, which derives the sizing of a new rotorcraft by scaling from a database of existing aircraft. Frequently, regression-analysis is used to correlate characteristic rotorcraft parameters to design parameters, yielding fundamental polynomial sizing laws.[11] This simple but effective approach may then be augmented by experience and expertise acquired in past developments, formalized in the form of golden design rules. For instance, these may impose constraints for specific design parameters by restricting the viable design space. As an example, figures 8a and 8b show such golden rules for the main rotor tip speed and the required clearance angle with respect to the tail-boom of a conventional helicopter in order to avoid tail strike.

[9] For a detailed discussion of the question of appropriate model fidelity, see chapter 2.4.1.
[10] Chapter 2.4.2 discusses the suitability of this approach looking forward.
[11] [31], [32] and [33] are good examples for this sizing strategy.

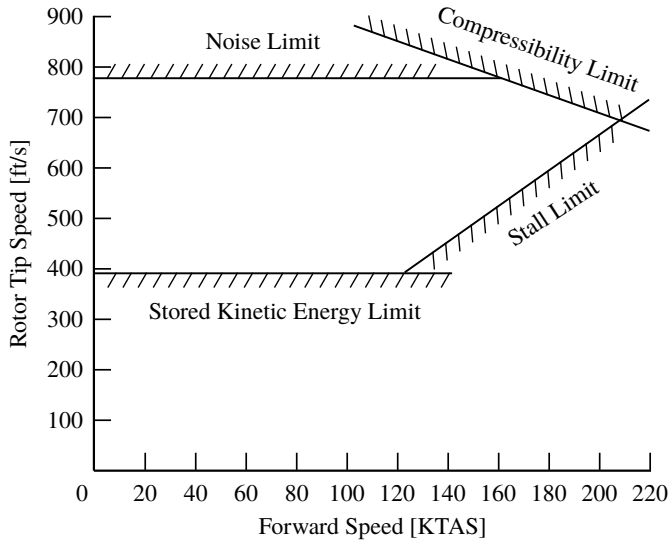

(a) Main rotor tip speed, adopted from [26].

Helicopters	**Clearance angle**
2 blades	16°
3 blades and more	14°
Counter-rotating	10° for both rotors

(b) Main rotor to tail-boom clearance, as proposed by [44].

Figure 8 Examples for "Golden Rules" in helicopter preliminary design in the form of valid design domains.

As argued above, the estimation of the empty mass of a design plays a key role in the design process. Consequently, the accuracy and reliability of the mass estimation is of particular interest. The empty mass of the rotorcraft is typically computed from the sum of the masses of its major components and assemblies. Similar to the common sizing strategies outlined above, popular published mass estimation methodologies employ polynomials which approximate the correlation of selected design parameters and the mass of the respective rotorcraft component. These polynomials stem from statistical analyses of databases of proven and realized rotorcraft designs, from which corresponding mass-estimation-laws are derived.[12] Kalra et al. study the effect of incorporating a series of different mass-estimation-laws from different sources to the same preliminary design scheme [46]. The researchers find the overall characteristics of the resulting designs to be globally comparable, proving the general viability of the approach. However, some deviations are observed in the resulting masses of the individual components, as well as in the characteristics of the identified relationships. These deviations likely result from different perimeters applied in the definition of the respective product breakdowns, and, certainly, of the differing databases feeding the statistical analyses in the course of the generation of the mass-estimation laws.

In review of the discussion above, and as demonstrated by the deviations observed by Kalra et al., it is evident that a profound knowledge of the underlying data is essential when applying empirical design and sizing means. To ensure the validity of the resulting design to a sufficient degree of reliability and accuracy, the inherent limitation of empirical approaches to the confines of the domain of validity of the underlying data must be respected. Significant and uncontrolled uncertainty arises when leaving the valid design space by extrapolation. Nevertheless, the prescribed classical approach to rotorcraft preliminary design proves highly effective and reliable when deployed within viable bounds, and satisfied the needs of the rotorcraft community in the past decades [9, 47].

[12] For examples of the process and concrete mass estimation laws, refer to [26, 31, 45].

2.1.5. Recent Developments in the Field of Rotorcraft Preliminary Design Frameworks

As outlined in chapter 1.1, modern methodologies and tools require the capability to design and evaluate new technologies and rotorcraft concepts. Chapter 2.1.4 presents contemporary design methodologies of rotorcraft, which are built upon models and parametric laws which are calibrated heavily with empirical data. This practice supports the incremental and evolutionary approach to development which has been characteristic of the past decades. However, rising expectations towards rotorcraft call for the infusion of new technologies, and the exploration of unconventional concepts. Roberts et al. agree that legacy comprehensive design and analysis frameworks have proven effective in the past, but are incapable of satisfyingly fulfilling the design tasks of today [2].

Hence, new software environments are required, which are set up to design and analyze generic rotorcraft configurations. Schrage was among the first to recognize the deficiency of legacy codes to meet this need [12]. Schrage concludes that, albeit established codes are sufficient as long as the new design is similar to the rotorcraft reflected in the calibration data, a move to physics-based modeling is required to enable the handling of innovative technologies and rotorcraft concepts, as it allows for incorporating high-fidelity analyses into the design procedure, such as Computational Fluid Dynamics (CFD) and Finite Element Analysis (FEA), as well as experimental results.

To this end, various research organizations actively pursue the development of rotorcraft design and analysis frameworks in this mindset. Arguably, the most renowned among these is NASA Design and Analysis of Rotorcraft (NDARC), a design tool for generic rotorcraft concepts developed by NASA. Johnson outlines the theoretical basis and code architecture in [48], and presents validation and demonstration of NDARC in [49]. A comprehensive documentation is provided in [45]. NDARC has been used in various studies in the recent past, for example [50–52]. NDARC allows for the design and analysis of generic aircraft configurations. The propulsion system architecture supports conventional combustion engines, turbomachines, as well as electric propulsion architectures. NDARC relies on augmented momentum-theory models for performance computations, whereas Blade-Element-Theory (BET) is implemented to enable to fully trim the rotorcraft. An open architecture is provided by the option to use tabulated data as substitute for the incorporated models, allowing to couple higher-fidelity modeling with NDARC in principle.

Similar efforts are reported by the German Aerospace Center (DLR) and The French Aerospace Lab (ONERA). Lier et al. present first results of the DLR project Rotorcraft Integrated Design and Evaluation (RIDE) [53, 54]. The objective of the RIDE project is to develop an automated and integrated toolbox capable of the conceptual and preliminary design of rotorcraft. The design process in RIDE is divided into two stages. In the first conceptual design stage, Lier et al. use statistics and simple models. The second stage is labeled preliminary design stage and relies on higher-fidelity modeling to detail the conceptual design.

CREATION[13] is a research program launched in 2011 at ONERA. Basset et al. define the main goal as the development of a multidisciplinary computational platform for the evaluation of rotorcraft concepts [11]. CREATION is planned to be a modern framework with a hierarchical model structure, i.e. with several levels of modeling fidelity. It is requested to be applicable to various rotorcraft concepts and to problems with very limited input data. The model hierarchy is structured into three levels, whereas the key characteristic of the different levels is the fidelity of the respective flight mechanics model, as described by Basset [55]:

1. *Power Balance and statistics* (PB): The flight performance module here relies on classical momentum theory, while the other modules use simple statistical or analytical modeling, which are either derived from databases or upper-level models. For architecture and geometry, the PB-model relies on statistical trends. The Weight & Balance module is stripped down to characteristic parameters such as the DGM and the Empty Mass (EM).
2. *Analytical Flight Mechanics* (AFM): At this level, the rotor is modeled through an analytical rotor disk model. The resulting forces and moments are calculated from the integration of local blade-force distributions, assuming linear aerodynamic blade characteristics. The Weight & Balance module on the AFM level relies on parametric laws, equivalent to the method outlined in chapter 2.1.4.
3. *Numerical Flight Mechanics* (NFM): The numerical flight mechanics model differentiates from the analytical model by using numerical computation schemes for the calculation of the rotor forces. Other models may use numerical models as well.

In terms of sizing philosophy, Basset et al. present a classical mass-convergence-process based on required power. To date, the publications are limited to the planned tool archicture depicted above, and an example limited to the first level of fidelity [11].

Another example is CONDOR, developed by Roberts et al. at Georgia Tech [2]. CONDOR is a rotorcraft performance analysis and sizing tool focusing on the rapid assessment of the design space across widely differing configurations. In terms of modeling, CONDOR tributes to the main objective of rapid assessment. Rotor modeling can be set by the user to use either momentum theory or blade element theory, the latter being the default setting. CONDOR is structured into five main modules: the Design Space Generator, Sized Vehicle module, Vehicle module, Rotor module and Blade module. The Design Space Generator is the highest-level module. It triggers the generation of aircraft configurations in the design space which are sized and evaluated subsequently. The Sized Vehicle module conducts the actual sizing, which is based on a fuel weight iteration of a specified design mission. The Vehicle module performs the evaluation of the individual Sized Vehicle. For this purpose, the vehicle sizing is completed first, and the characteristic performance attributes are established subsequently. Roberts et al. concludes the presentation of CONDOR with an application example, in which the results of a Monte-Carlo simulation are interpreted in the evaluation of the design space of a conventional helicopter configuration.

[13] The acronym CREATION stands for "Concepts of Rotorcraft Enhanced Assessment Through Integrated Optimization Network".

The activities in rotorcraft design frameworks so far focus primarily on integrating classical engineering aspects like aerodynamics, structural mechanics, et cetera. Comprehensive frameworks from a holistic SE viewpoint however require the integration of further disciplines, such as Production, Support and Maintainability. Their assessment in early design stages is challenging, since more detailed knowledge of the design than typically available at the preliminary design stage is required to calibrate corresponding models. Bhattacharya et al. aim at incorporating Reliability, Availability, and Maintainability (RAM) aspects into the trade-space analysis through integrating respective empirical models into a design framework based on NDARC [56]. Although admitting that several simplifying assumptions are incorporated in this initial work, Bhattacharya et al. conclude that the integration of reliability models into trade-space exploration methods could assist in a significant reduction of life-cycle costs of future designs through the consideration of RAM aspects at early design stages.

The preliminary design frameworks presented above commonly strive to satisfy the need for enabling the design and analysis of generic rotorcraft concepts. In terms of analysis capability, all frameworks appear to be set up to meet this need satisfactorily. In terms of sizing, however, the efforts continue to rely on user-set inputs or parametric scaling-laws, which remain derived from experience and regression-analysis of databases of legacy platforms. The necessary evolution of preliminary design methodologies for model-based design approaches is not addressed by the design frameworks presented above. Chapter 2.4 discusses this aspect further.

2.2. Model-Based Design

2.2.1. Definitions and Terminology

The notion of models in general, and model-based or model-driven design in particular, differs over various fields of science and engineering, depending on the scope, nature and purpose of the modeling. Generally, there is no unambiguous and clear definition of the terminology. Therefore, a classification of the concept of model-based design as used in the context of this work is provided hereafter.

2.2.1.1 Deductive and Inductive Modeling

Raous provides a general definition of the modeling process, describing it as a scientific method which adopts a stepwise approach to explain an observation or an experiment [57]. Another interest may lie in the prediction of behaviors within the bounds of specific assumptions. Raous differentiates between a *deductive* and an *inductive* approach to modeling, whereas this classification is derived from the principles of deductive and inductive reasoning in philosophy.

Deductive reasoning is defined by Woodcock as the form of reasoning in which the premises necessitate the conclusion [58]. Nersessian identifies this soundness as the essential notion of deductive reasoning, since true premises, i.e. assumptions, and sound reasoning inevitably yield

true conclusions [59]. Inductive reasoning, on the other hand, is described as the form of reasoning that is based on inferences, which extrapolate from similarities observed in a set of data to the unobserved [57, 58]. In contrast to deductive reasoning, the soundness in inductive reasoning is not intrinsically embodied, as what has *not* been observed may be in conflict with the data. Therefore, it is logically conceivable that a false conclusion is drawn in spite of true premises. To this end, Woodcock also refers to inductive reasoning as probabilistic reasoning [58]. Nersessian states that a major focus of the work in the field in the 20th century focused on developing a notion of soundness for induction in analogy to the above-mentioned notion related to deduction. The proposed notion for induction assumes that, when starting from maximally probable premises, and when applying scientific, i.e. rational, reasoning, one should obtain maximally probable conclusions [59].

In adoption of the concept of deductive and inductive reasoning, Dresig and Fidlin differentiate between two ways of modeling. *Inductive modeling* starts from a simplified model in order to obtain a better overview of the problems involved, and then gradually increases the size of the model with the benefit of the knowledge obtained form the preceding models. A *deductive modeling* strategy, on the contrary, starts from a large and highly sophisticated model, and breaks it down subsequently into smaller models based on the insight gained from the large model [60]. Pfeiffer sees in the inductive approach the superior methodology for the modeling of complex systems [61]. The inductive approach seems better suited to design applications in particular, as it correlates with the hierarchical top-down approach to design adopted by SE.[14]

Raous sees the primary objective of modeling in providing explanation in the form of *understanding* and *prediction* [57]. Understanding therein prescribes efforts aiming at reconstructing observations noted from experimental or other data. The basis of a model applies the fundamental laws of the respective scientific fields[15] in pursuit of this objective, possibly enriched by additional elements stemming from empirics and experience, in order to facilitate the modeling of complex and interacting systems. However, in the context of design, the primary interest regarding modeling lies in prediction. Raous lists the following main modeling challenges to obtain adequate and reliable predictive capabilities [57]:

1. Validation of the model
2. Determining the reliability of the model
3. Identifying the domains of validity of the model

In review of the above, it is evident that a thorough and substantiated *understanding* in the above-given sense is the basis for the predictive application of a model. Consequently, the higher the complexity of the design problem, the more data is required to develop an adequate modeling, which in turn may not be available or feasible to obtain due to the associated efforts and resources. This issue is prominently known as “postdictive” vs. “predictive” modeling capabilities in the rotorcraft field, and is discussed further in the subsequent chapter 2.2.1.2.

[14] See chapter 2.4 for a discussion of the possible introduction of uncertainty by an unfavorable deductive modeling approach in rotorcraft design.

[15] For instance: mechanics, thermodynamics, aerodynamics, electromagnetism, etc.

	Goal	Engineering Tool	Physics-Based Model
Forward flight performance	1 %	4 %	20 %
Hover performance	0.5 %	2 %	2 % (but flow-field not correct)
Airloads (c_n/c_m), without mean	1 %	10 % / 35 %	6 % / 20 %
Airloads (c_n/c_m), with mean	1 %	10 % / 35 %	15 % / 40 %
Blade loads (flap / chord / torsion)	3 %	20 % / 35 % / 25 %	20 % / 35 % / 25 %
Vibration	10 %	100 %	Not available
Stability (fraction critical damping)	0.002	0.02	Not available
Noise	3 dB	10 dB	15 dB

Table 1 Estimate of predictive capabilities of state-of-the-art rotorcraft tools by Johnson and Datta [63]

2.2.1.2 Modeling of Rotorcraft

Rotary-wing aircraft are characterized by the highly complex aerodynamic flow field induced by the rotors, which gives rise to various highly-interacting aeromechanical phenomena between physical rotorcraft components and also analysis disciplines. The complexity of these phenomena poses an extraordinary challenge to rotorcraft modeling, and even high-fidelity analysis tools today struggle to reliably predict the behavior and performance of a rotorcraft. Typically, rotorcraft models require substantial calibration to relevant data, typically empirical or measured, in order to provide accurate and reliable output. Leishman labels the reliance on such models as *postdictive* methods, whereas the term constitutes the models' substantial need for calibration to become reliable [62]. Achieving true *predictive* capability with rotorcraft models would require significant further progress in the understanding of the above-mentioned phenomena and their modeling. As Sinsay and Nunez point out, no established rotorcraft modeling to date has demonstrated the capability to accurately predict performance in all thinkable modes of operation and application [1]. In support of this argument, table 1 provides the predictive capabilities of current engineering tools and physics-based models as estimated by Johnson and Datta [63]. The physics-based models represent the highest level of fidelity, such as coupled Computational-Fluid-Dynamics and Computational-Structural-Dynamics codes. Johnson and Datta see the need to achieve an increase in predictive capabilities by at least an order of magnitude in each discipline, concluding that new models and analysis tools are required to achieve these improvements, whereby the required development time of these tools is expected to amount to at least two decades. Recently, Sinsay outlined a roadmap for the evolution of rotorcraft design at AMRDEC. A comparison of the current and the desired future capabilities in rotorcraft modeling is given, concluding as well that substantial improvements and development efforts are required to achieve the desired state [47].

Such new tools likely require an immensely increased computational effort compared to contemporary standards. However, preliminary design methodologies demand computationally efficient models in order to support a large number of model executions, which are required to explore the design space effectively. On the other hand, the models need to describe the system behavior in sufficient detail to enable discriminating between competing design solutions. This fundamental dilemma surrounding the definition of optimal-fidelity modeling for preliminary design purposes is discussed further in chapter 2.4.1.

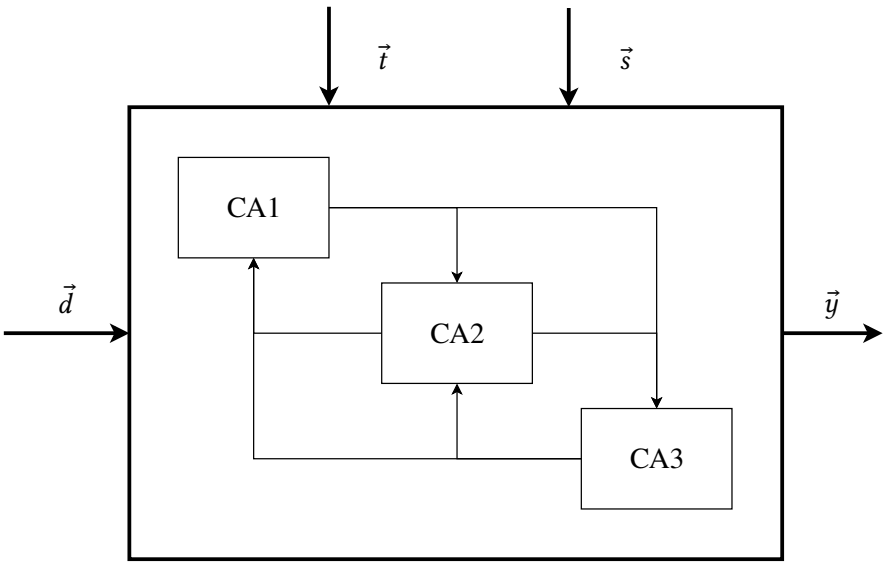

Figure 9 Sketch of general multidisciplinary system analysis modeling augmented with input parameters, modified from [64]

2.2.2. Model-Based Design Logic

2.2.2.1 Model-Based System Analysis Scheme

Batill et al. provide a pragmatic definition of a model as a means to represent a physical artifact and its behavior [64]. This definition adopts Simon's concept of an "artifact", which is defined in terms of its inner and outer environment. According to Simon, an artifact can be understood as an interface between the inner environment, i.e. the substance and organization of the artifact itself, and an outer environment, which describes the surroundings in which it exists and operates [65]. A strong correlation between the definition of a complex system in SE and Simon's definition of an artifact is evident. Simon states that an artifact will only serve its intended purpose when the inner environment is appropriate to the outer environment, or vice versa. This understanding is in line with the holistic approach SE takes to design, in that a successful system requires to consider the needs of all stakeholders in all phases of its development, realization and operation, throughout the entire life-cycle. The terms "system" and "artifact" are hence used interchangeably within this work.

To simplify the following argument, all model parameters are assumed to be real numbers to enable their representation in vectorized form, as for instance proposed by Krosche and Heinze [66]. The entries contained in the architectural views can then be represented by the corresponding vector $\vec{t}$ of TA elements, and the vector $\vec{d}$ of PA elements:

$$\vec{t} := (t_1, t_2, ..., t_n) \subset \mathbb{R} \quad \text{and} \quad \vec{d} := (d_1, d_2, ..., d_n) \subset \mathbb{R} \tag{2.1}$$

This classification of model parameters is developed in adoption of a SE mindset, as it is defined in such a manner that a direct correlation with the SE architectural views is possible. The elements contained in the different architectural views are unambiguously assigned to the corresponding vector of model parameters. A schematic view of a system analysis model of a physical artifact at a given level of abstraction can then be drawn as proposed by Batill et al. [64], see figure 9. In this

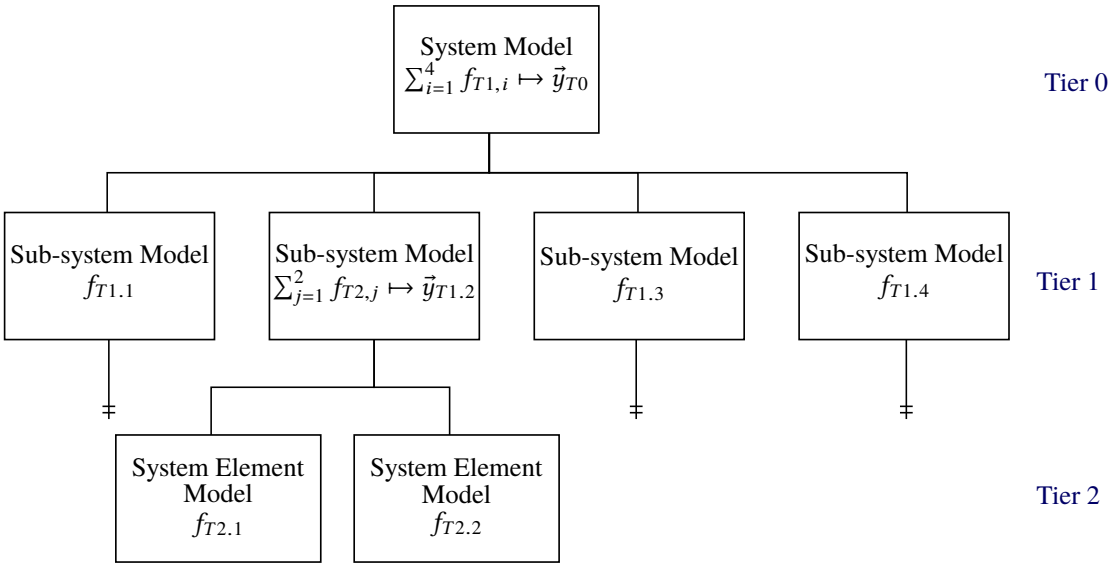

Figure 10 Generic system model topology

example, three individual contributing analysis (CA) elements compose the system analysis. The artifact itself is physically defined by a vector of design variables $\vec{d}$. The artifact's responses, or behavior, is expressed in a vector of system states $\vec{y}$. Batill et al. recognize that there is typically additional information required to perform system analyses – either originating from information related to the outer environment in which the artifact operates, or representing information which is not yet known due to the level of abstraction or model fidelity in the current phase, but is still required to perform the system analyses. Another set of parameters which is required to perform system design and analysis are those which describe the external environment in which the system operates. Batill et al. group these parameters into a single "model parameter" vector. For improved clarity, the convention within this work is to split these fundamentally different elements into two. Consequently, the external environment variables are grouped into a dedicated flight state vector $\vec{s}$. The remaining parameters are allocated to a technical model parameter vector $\vec{t}$.[16]

2.2.2.2 System Model Topology

Figure 10 outlines a generic topology of a system model. The system model is composed of a set of sub-models $f_{Tn,i}$, which predict the behavior of the corresponding modeled system-element in dependency of its respective technical and design parameters, and the flight state vector:

$$f_{Tn,i}(\vec{d}_{Tn,i}, \vec{t}_{Tn,i}, \vec{s}) \mapsto \vec{y}_{Tn,i} \tag{2.2}$$

The system model is organized in a tiered structure, resembling a SE architectural view. The sub-models are identified by the level of decomposition n of the system tree in which the modeled element is located, and an index i to identify the element within the respective tier. The sum of the responses of the set of models of a given tier n then yields the emergent behavior of the system on the upper $(n\text{-}1)^{\text{th}}$ level .

[16] See chapter 2.2.2.4 for a more detailed discussion of the introduced types of model parameters.

It is interesting to recognize the fundamentally different mechanisms in acquiring the behavioral characteristics of an artifact depending on its location in the system model topology. In the example given in figure 10, the behavioral characteristics $\vec{t}_{Tn,i}$ of all artifacts located in T1 and above are obtained from sub-models located in T2, possibly augmented by parameters covering emergent behaviors resulting from the integration of these artifacts into a system. At the lowest level of any branch of the system model, no sub-models are available which may be used to generate computed expectations of system behavior. Instead, each artifact on the T2 level is described by a model, which is restricted to the physical and technical parameters associated with the respective artifact. These parameters are then either known deterministically, or need to be estimated.

2.2.2.3 Model-Driven Rotorcraft Design Logic

A generic system analysis scheme is presented in figure 9 and discussed in chapter 2.2.2.1. Baker et al. describe model-driven design as a process which utilizes models in order to support the system design activities, such as validation, trade-studies and assessments against the functional and non-functional requirements [67]. These models are principally set up as depicted in figure 9. The system model is developed progressively, in order to represent the system in increasing resolution and accuracy.[17] More globally, the usage of Model-Based Systems Engineering (MBSE) over traditional document-centric approaches represents a paradigm shift in system definition, design and qualification, as Estefan points out [68]. MBSE elevates models into a pivotal role, in that they become the governing factor in the specification, design, and integration of a system.[18]

In this newly assigned role, all aspects of modeling demand the utmost degree of attention. The comprehension that the chosen modeling strategy influences the outcome of the design process is agreed among various researchers [24, 64, 70]. The modeling strategy and its possible influence on the outcome of the design loop hence require careful consideration in the paradigm shift towards model-based design methodologies. Chapter 2.4 discusses the associated challenges in detail.

In a pure system analysis environment, system states always represent output. In a design context, however, the system which produces the desired system states is sought to be sized and thus system states in this case are input to the process. This particular set of desired system states are the system requirements represented in $\vec{r}$.

Figure 11 provides a generic rotorcraft design logic. The sizing process takes a set of requirements and constraints as input. Depending on the implemented sizing scheme, some design degrees of freedom may be fixed in the form of design inputs before entering into the actual sizing process. A model-based sizing process requires a system model as an additional input. The iterative sizing loop then commences with the sizing of the design candidate. Contemporary methodologies rely on empirical correlations to define the rotorcraft design parameters. A model-based design environment, in turn, deploys sizing algorithms to size the aircraft. Subsequently, the system

[17] Hence, the inductive modeling approach described in chapter 2.2.1.1 is adopted.
[18] An in-depth discussion of Model-Based Systems Engineering is provided by Wymore [69].

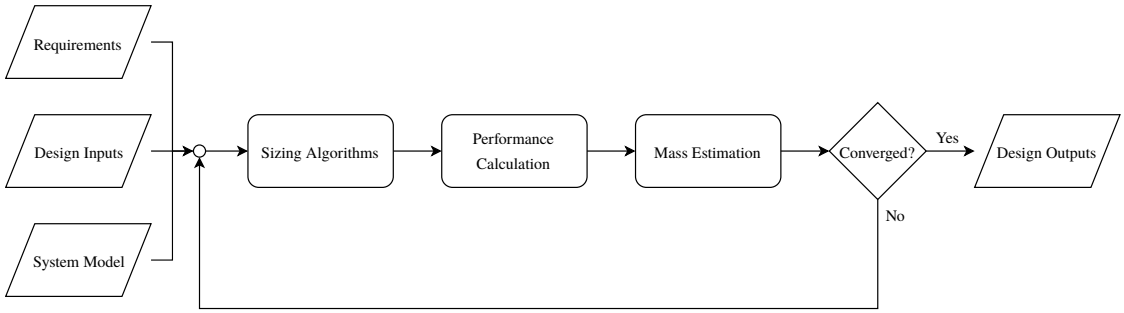

Figure 11 Generic model-driven rotorcraft sizing logic

model is called to execute performance calculations in order to determine the compliance to the performance requirements, and the required fuel or energy to perform the design mission. The mass estimation of the design is then updated. The DGM is commonly selected as the convergence criterion, although other criteria may be defined depending on the global design objectives, as discussed in chapter 2.1.4.

2.2.2.4 Model Parameters

Within this work, the general system analysis terminology presented by Batill et al. is adopted and further refined [64]. The principle elements of system analysis – design parameters, technical parameters and system states – are taken over, see figure 9. Building upon this terminology from Batill et al., these elements are adapted for the field of system design, and, crucially, further refined into sub-vectors. Furthermore, in addition to the parameters described by Batill et al., a requirements vector $\vec{r}$ is defined, holding all requirements established in the course of the system design. Capturing and processing the system requirements is a key element in a system design context. The applied terminology in terms of model parameters is depicted hereafter in detail.

In a systematic design process which is built upon several discrete levels of product decomposition and model fidelity, it is beneficial to further refine the *design parameters*, which describe the design candidate in the physical domain and hence resemble the PA, by adding information on the current state of the respective parameter. The complete design parameter vector $\vec{d}$ is then composed of the following four sub-vectors:[19]

- *Design degrees of freedom* $\vec{d}_{DoF} \subset \vec{d}$
  Elements of this vector represent the design space in the current phase of the design process. The design degrees of freedom reflect the design decisions which are subject of study at the respective level. Typically, these parameters are varied and the resulting system responses are evaluated until design decisions are enabled.
- *Specified design parameters* $\vec{d}_s \subset \vec{d}$
  The vector $\vec{d}_s$ groups all design parameters which are already specified. Specified design

[19] Concrete examples of the contents of the design parameter vector and its evolution over the different tiers are given in the frame of the test cases in chapter 4.

parameters are those which have been fixed in previous loops of the design process. Thus, they are no longer part of the active design space and represent the design decisions already taken.

- *Dependent design parameters* $\vec{d}_{dep} \subset \vec{d}$
  Dependent design parameters are computed from, i.e. modeled in dependency of, other design parameters. These parameters are generally not in the scope of the design space of the current phase in the sense that no design decisions on these parameters are imminent. However, their values depend on design degrees of freedom or specified design parameters. As an example, while the Disk Loading (DL) is a design degree of freedom, the rotor radius R could be an element of $\vec{d}_{dep}$, depending on the DGM and DL.
- *Independent design parameters* $\vec{d}_{indep} \subset \vec{d}$
  These parameters are considered to be not decisive in their impact on the concept assessment at the current tier, but are still required for computations in the design and analysis code. The general practice is to set these parameters to typical values, since they are believed to be independent of the design choices or irrelevant in front of the existing degree of uncertainty at the respective level (to the first order). However, independent design parameters as well as their values may vary between different design candidates, if these differ prominently in their design characteristics. Differing rotorcraft or sub-system architectures, for example, necessitate differentiation between their independent design parameters to achieve an adequate representation of each architecture.
  In the sense of Batill et al. [64], independent design parameters could be attributed to $\vec{t}$ rather than $\vec{d}$, since they represent a lack of information, albeit they are required to run the analyses. However, in the context of system design rather than system analysis, the categorization based on the affiliation to the different SE architectural views is favored for improved clarity and consistency. Therefore, as $\vec{d}$ shall represent the description of the design and $\vec{d}_{indep}$ is set up in such a way that exclusively design parameters are contained, $\vec{d}_{indep}$ is allocated to the design parameter vector, in order to obtain a complete design description through $\vec{d}$.

The *technical parameters* resemble the TA described in chapter 2.1.3. The technical parameter vector consists of the following sub-vectors:[20]

- *Prospect parameters* $\vec{t}_{prosp} \subset \vec{t}$
  In analogy to the TA, the prospect parameters $\vec{t}_{prosp}$ represent the characteristics of the system and its elements rather than its physical parameters. Prospect parameters are meant to mimic the expected physical behavior of the artifact. As outlined in chapter 2.2.2.2, each entry in $\vec{t}_{prosp}$ is generally either computed from a set of sub-models, or estimated. Generally, those entries in $\vec{t}_{prosp}$ at the currently lowest-level of system decomposition are estimated, whereas elements on the upper levels are computed from sub-models.
- *Sizing parameters* $\vec{t}_{size} \subset \vec{t}$
  Sizing parameters are a subset of technical parameters, which are used in the sizing of elements of the dependent design parameters in the physical domain $\left(\vec{d}_{dep}\right)$. These correlations may represent the expertise and experience of the design organization, and may be derived from

[20] As for the design parameter vector, see chapter 4 for concrete examples of the technical parameter vector.

historical data or from data obtained from higher-fidelity analysis. The importance of these additional, i.e. non-functional and non-physical, linkages between system elements progressively increases with the degree of reliance on model-based design. The TA described in chapter 2.1.3 visualizes these interdependencies in a dedicated architectural view. Analogously, the vector t_{size} holds parameters such as sizing constraints and logics, used by the deployed sizing algorithms. As an example, blade stall characteristics may be contained in $\vec{t}_{size}$, in order to govern a valid and effective, but still mass-efficient, rotor blade sizing.

- *Uncertainty parameters* $\vec{t}_{uncert} \subset \vec{t}$
  Uncertainty parameters introduce the probabilistic element to the modeling. These parameters are directly linked to a single corresponding technical parameter of the prospect type. Typically, the uncertainty parameters capture lower and upper bounds as well as the probability distribution of this parameter to comprehensively describe the uncertainty attributes of this design variable. The definition of the uncertainty parameters is most commonly based on the experience and expertise of the designing entity.[21]

The *flight state parameter* vector $\vec{s}$ comprises all variables related to the external environment of the system, such as the state of operation, as well as the operational environment in which the system is operated. For the case of a rotorcraft, these comprise essentially the atmospheric conditions, as well as information on the gross mass, flight velocity vector, et cetera.

The *system states* represent the response of a system to a given set of input parameters and hence describe the behavioral characteristics of a system. Systems discussed in this work are considered deterministic in the sense that one set of input parameters will always yield the same system states in response. All system state or response variables are grouped into the vector $\vec{y}$.

Arguably the most important elements of information which are passed between the different processes during system design consist of the *requirements*. Thus, it is imperative to integrate the requirements into the formal terminology. This is achieved in the form of a requirement vector $\vec{r}$, containing all requirements which the system and its elements are requested to satisfy. For each element of the requirement vector, a dedicated Measure of Performance (MoP) and Measure of Effectiveness (MoE) may be defined to assist in its verification and validation.
As design parameters, requirements may have different states. Requirements may already be specified, i.e. validated and accepted. These requirements are grouped in a dedicated vector $\vec{r}_s \subset \vec{r}$. Requirements may also be in the state of a proposal and as such part of the trade space of the current phase. Such requirements are allocated to the sub-vector $\vec{r}_{prop} \subset \vec{r}$.

[21] See chapter 2.3 for a detailed discussion of uncertainty in the context of this work.

2.3. Uncertainty in the Context of Multi-Fidelity Model-Based Preliminary Design

2.3.1. An Introduction to Uncertainty in System Design

The terminology and classification of uncertainty used throughout this work is introduced in this chapter. Within the engineering sciences, there is neither a commonly shared understanding of the concept of uncertainty, nor an established terminology. Walker et al. provide a conceptual framework for the systematic treatment of uncertainty in a model-based environment, which found wide recognition in various fields [71].

Walker et al. define uncertainty as any deviation from the ideal of total determinism, whereas complete determinism is considered as an unachievable ideal [71]. Funtowicz and Ravetz see in uncertainty a situation of inadequate information, and distinguish between three sorts of uncertainty: inexactness, unreliability, and border with ignorance [72]. However, Asselt and Rotmans point out that uncertainty can prevail in spite of the availability of information [73]. Additional uncertainty may even be unveiled with the introduction of new information. This could be the case, for instance, when unforeseen complexities surface from further research and analysis, or unexpected emergent behavior arises after the integration of system elements into a complex system as a result of unforeseen interactions.

Walker et al. distinguish three *dimensions of uncertainty*, which are the *location*, the *level* and the *nature* of uncertainty [71]. The location of uncertainty describes where the uncertainty resides in the system model and the modeling process. Attributing the location of uncertainty creates transparency with respect to where the uncertainty associated with the model responses is generated and propagated within the system model.

The level of uncertainty places the uncertainty along the spectrum between deterministic knowledge and total ignorance. Therefore, it is a measure of the degree of uncertainty one is faced with. Walker et al. identify four principle states of the level of uncertainty, see figure 12, and recommend to adapt the methodology to handle the uncertainty prevalent in a problem to its level [71]. Statistical uncertainty reflects a level of uncertainty in which the knowledge is sufficiently pronounced for describing it in statistical terms. Statistical uncertainty implies that there is sufficient understanding of the phenomena and their interactions to generate adequate and representative models. Qualitatively and quantitatively appropriate data is available to validate and calibrate the models. This type of uncertainty is the most common in engineering sciences.
Scenario uncertainty is described by Walker et al. as any uncertainty which is related to the external and future environment of a system. Scenarios in this sense represent a plausible forecast of the future. In rotorcraft design, the requirements and the ConOps are examples of items which are subject to scenario uncertainty. This level represents a deeper level of uncertainty for which no data-based probability quantifications are possible. Instead, assumptions are taken and the evaluation of scenario uncertainty is frequently performed by analyzing the effect of different assumptions on the possible outcome. A typical example of this practice in a design context is represented by

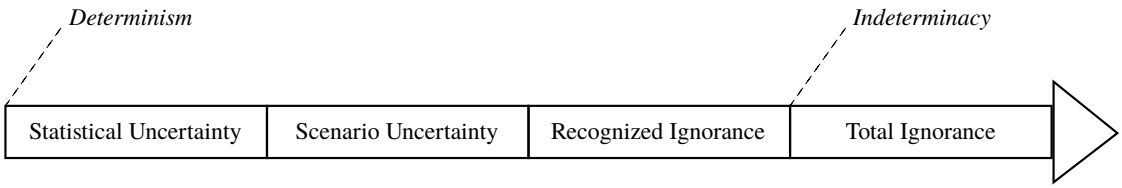

Figure 12 Levels of uncertainty as defined by Walker et al. [71]

trade studies, which are commonly used to simulate the effect of different assumptions or design decisions in front of the set of requirements.
The further levels of uncertainty then represent a pronounced lack of knowledge, in that the actual functional relationships, or indeed the scientific basis, are insufficiently understood even for generating scenarios. Whereas recognized uncertainty prescribes a level in which there is awareness about the extent of the lack of knowledge, total ignorance is the deepest level of uncertainty represented by not even knowing what is unknown. Arguably, the extent of uncertainty in these levels is too pronounced to justify the application of model-based approaches to such design problems.

The third and final dimension of uncertainty is defined by its nature. Several authors generally differentiate between two natures of uncertainty [71, 74–76]. *Epistemic uncertainty* is caused by a lack of knowledge or data. This definition implies that it may be accomplishable to reduce its magnitude, i.e. its level, by gathering additional data or by refining the applied models.
Aleatory uncertainty, in turn, is presumed to represent the intrinsic variability or randomness of a system and its characteristics. Consequently, the modeler has no option to reduce the quantity of this type of uncertainty. Kiureghian and Ditlevsen [74] and Walker et al. [71] agree that the nature of uncertainties should be considered when assessing how to handle the respective uncertainty. Aleatory uncertainty is frequently also referred to as *variability uncertainty*.

The distinction between epistemic and aleatory uncertainty is especially interesting in a model-based design environment, since it allows categorizing uncertainty in terms of its appropriate handling. More interestingly, the categorization enables to effectively identify meaningful and promising starting points for uncertainty reduction activities, if deemed necessary. To this end, epistemic uncertainty is of particular interest in the context of design, as it can be actively acted upon. A SE design process develops a system hierarchically in a top-down approach. Therefore, the knowledge about the system and its behavior is gradually increased. In the introduced terminology, this corresponds to a progressive reduction of the level of uncertainty from Scenario Uncertainty to Statistical Uncertainty. This opens up additional aspects for the modeling of the system under design, since the uncertainty becomes describable, and hence capable of being integrated into the model-based design framework. A model-based design environment accommodating various-fidelity models seems ideally suited to this approach, as the models may correspondingly improve progressively with the evolution of the knowledge about the system under design, and hence enable turning this increasing knowledge into a reduction of epistemic uncertainty, if corresponding elements can be successfully incorporated into the model-based design methodology.

2.3.2. Sources of Uncertainty

Any measured or simulated characteristic of a physical artifact is subject to uncertainty inherent to the measurement or simulation process. Uncertainty arises from variation in the inner and outer environment, as well as from variations between different realizations of the identical system, if tests are conducted on multiple test specimen. In design, additional uncertainty resides in the requirements, and originates from the fact that the system exists only as an abstraction from the designer's point of view. Thus, it is always incompletely described through the established modeling and simulation. Both, the incompleteness and the modeling applied introduce uncertainty to the predicted characteristics of the system, as Batill et al. point out [64].

Kennedy and O'Hagan provide a widely recognized classification of sources of uncertainty in simulation environments which are using complex mathematical models [77]. Kennedy and O'Hagan consider models which are calibrated to fit observed data, and then are applied in a design context to predict future behavior of a system of similar type. The codes themselves thereby are deterministic in the sense that identical inputs always produce the same output. This modeling strategy is representative of model-based design applications in the engineering sciences. The following sources of uncertainty are identified by Kennedy and O'Hagan:

- **Parameter uncertainty:** This type of uncertainty originates from the model calibration parameters, which may be subject to uncertainty or even unknown. Whereas this type of uncertainty typically concerns system characteristics in a particular application context, it may also represent more global system characteristics, which are relevant over a range of contexts. Parameter uncertainty manifests in uncertainty in the model inputs. Kiureghian and Ditlevsen point out that this type of uncertainty concerns so-called *basic variables*, which are defined as variables that are directly observable, and for which empirical data is available [74]. In the case that a probabilistic modeling of these basic variables is established, Kiureghian and Ditlevsen list uncertainty in these probabilistic models and model parameters, which are used to describe the distribution of the basic variables, as an additional source of uncertainty.
  As an example, parameter uncertainty is introduced into rotorcraft modeling when calibrating performance models to sets of observed data. Both the quality and quantity of this data are of finite adequacy, hence introducing variability into the model calibration, and thus the model's predictions.

- **Model inadequacy:** Even in the absence of parameter uncertainty, any model represents a physical artifact only to a limited degree of accuracy. The resulting discrepancy between the model response and the mean value of the true responses of the realized system units is the model inadequacy.
  For instance, trading for code execution runtime frequently causes modelers to opt for lower-order terms to describe an artifact's characteristics to a satisfying degree of accuracy, in spite of higher-order terms potentially providing improved resolution and accuracy of these characteristics.

- **Residual variability** captures variation which results from the repetition of the model-based

prediction process even though the conditions and inputs are identical. The residual variability may be the result of an inherently stochastic process, or a consequence of an inadequate model, which is incapable of discriminating between conditions which affect process-related values. In delineation to model inadequacy, this variability is allocated to the residual variability as these conditions are unrecognized. Unintended emergent behavior of a system due to unknown interactions between system elements may serve as an example for this source of uncertainty.

- **Parametric variability** prescribes variability caused by a deliberate simplification of the model inputs. A simplification of the model inputs may be required or desired, for instance in the case that the model requires more detailed input than is desired or available. As the input parameters are allowed to vary as a result of this simplification, additional uncertainty is introduced into the process. For instance, fuselage aerodynamics modeling in early stages often deliberately neglect the dependency of the aerodynamic properties on the rotorcraft attitude in favor of faster code execution, but also due to the lack of reliable available data on these characteristics at this stage.

- **Observation error:** The calibration of the models is performed based on observed data, which is subject to an observation error, e.g. from limited measurement accuracy. Hence, further uncertainty is introduced. In practice, this type of uncertainty is often not differentiable from the residual variability.

- **Code uncertainty:** Arendt et al. define code uncertainty as the result of a common practice of relying on the availability of only a finite set of simulation results corresponding to a set of discrete model inputs [78]. In case one performs interpolation, or in particular extrapolation, based on these results to alleged outcomes for a specific desired set of inputs, additional uncertainty is introduced.

- In addition to the types of uncertainties outlined above, Kiureghian and Ditlevsen note the possibility of **human errors** occurring during modeling, design, realization or operation of a system, which may be required to be considered depending on the actual engineering problem under question [74].

Evidently, the sources of uncertainty are many and manifold. The distinction between the general categories established by Kennedy and O'Hagan requires an already detailed understanding of the problem and the models. Considering every possible source of uncertainty may quickly lead to unmanageable model and problem complexity, as well as unsurmountable computational effort. Consequently, the prioritization of uncertainty for an actual engineering problem needs to be carefully designed, in order to be efficient and effective at the same time.

2.3.3. Approaches to Handling Uncertainty

Kiureghian and Ditlevsen claim that the nature of uncertainties depends on the context and application in which they are evaluated [74]. Consequently, an appropriate approach to handling uncertainty also depends on the specific context. The following provides an overview of the state-of-the-art of uncertainty handling in rotorcraft preliminary design, before different means of handling uncertainty applied in model-based environments in other fields of engineering are

outlined.

2.3.3.1 Contemporary Practice in Rotorcraft Design

In rotorcraft design, a methodical approach to identifying and quantifying uncertainties is lacking, evident from the absence of respective publications in the literature, and the lack of coverage in relevant textbooks. Instead, the typical approach to managing uncertainty consists of applying system-level design margins, as for instance used by Koch et al. [79]. Frequently, these margins are applied on the estimated empty mass, the computed performance, or both. The quantities of these margins usually vary in the various stages of the development, reflecting the progressively decreasing level of uncertainty present along the progression of the design process. The margin quantities usually stem from the experience and expertise of the designing entity. In the author's personal experience, the empty mass margin may be as high as 10 % in the conceptual design phase, in which the level of uncertainty is highest. In the course of the development, the margin is progressively reduced to an order of magnitude of approximately 3 % before heading into flight-testing. This remaining margin is then intended to cover for future design changes, which frequently become inevitable to solve issues which are only detected during flight. This approach has the advantage of its simplicity. However, there are various shortcomings. With respect to the three dimensions of uncertainty discussed in chapter 2.3.2, the location, the level, and the nature of the uncertainties are undefined.

As a consequence of this historical approach, it is impossible to act on the prevalent uncertainty in a systematic manner. The uncertainty in the present design problem is assessed qualitatively and from experience, which may be an invalid extrapolation for the scenario at hand. As the location and nature of the uncertainty is unknown, the option of deploying particular analyses aiming at reducing uncertainty and thus risk is prohibited. Furthermore, since there is no differentiation of uncertainties into lower levels of product decomposition, the uncertainty resides uncontrolled in the design problem and is allowed to propagate in an uncontrolled manner within the designed system. As a result, the uncertainty resides in the design until testing commences on the system level, i.e. until the final stages of product development. From a designer's point of view, the application of system-level margins on the empty mass of the aircraft effectively results in a systematic over-sizing of the aircraft, which trivially does increase the likelihood of the design meeting the requirements, yet does not represent a cost-effective approach to design.

2.3.3.2 Incorporation of High-Fidelity Analysis in Early Stages

One major challenge in model-based design remains the predictive quality of the models themselves, particularly for unconventional concepts and technologies.[22] The majority of the research in this context strives to integrate high-fidelity models early in the preliminary design process. High-fidelity analyses however are time-consuming and computationally expensive, in particular when

[22] See chapter 2.2.1.2 for a more detailed discussion.

deployed in full scale on the system level. To this end, numerous researchers investigated meta-modeling techniques to alleviate the computational load of incorporating high-fidelity analysis into the design process already at an early stage in various engineering fields. Koch et al. provide a comprehensive overview of this field of activity [80].

Early efforts in this area relied on the Response Surface Methodology (RSM), for instance [81–86]. The RSM aims at generating simple polynomial surrogate models which represent the main trends and behaviors identified in high-fidelity analyses. As Simpson et al. point out, the RSM approaches reach their limits when there are more than 10 factors to be modeled, and when the relationships to be represented are distinctively non-linear [87].

With an increase in computational capabilities, the focus therefore shifted to more sophisticated approximation methods such as Kriging, which are capable of a more complex representation of non-linear responses from high-fidelity analysis. Examples of Kriging application are [70, 79, 88, 89]. Although Kriging is better suited to non-linear problems, the limitation in terms of the maximum number of assessable factors remains an issue.

Consequently, with a further increase in computing power, several recent publications focus on the direct integration of high-fidelity analyses in early design phases. Several researchers aim at selectively and directly implementing high-fidelity models for individual disciplines [90–93]. So far, these efforts are limited to the deeper investigation of particular aspects and disciplines during preliminary design, as full-scale high-fidelity analysis remains too costly in terms of computing power. Besides these technical limitations to the application of high-fidelity analysis at early stages of the design, there are procedural concerns. As discussed in detail in chapter 2.4, prematurely moving to high-fidelity analysis may even introduce more uncertainty into the design problem than is removed.

2.3.3.3 Robust Design

Various authors identify ambiguity and uncertainty as inevitable characteristic of the requirements at the early design stages, and therefore plead for a probabilistic approach to design [12, 20, 94, 95]. Schrage argues that risk and uncertainty are most pronounced at the conceptual design stage, and concludes that a probabilistic approach to design at this stage is thus imperative [12].

Mavris et al. identify three major shortcomings of traditional, non-robust, design methodologies [94]:

1. Traditional design methodologies assume the feasibility of the concept upfront, either through relying on correlated historical data or an incremental-upgrade approach to design. The capability to assess new concepts and technologies is thus impeded.

2. The established deterministic approaches are not set up to account for the variability existing in the economics, the tool fidelity as well as in the requirements and the ConOps. Mavris

et al. see this manifested in the inability of existing design methods to link elementary design variables to system responses, which in turn is considered mandatory to establish feasible design spaces.

3. Mavris et al. see currently used probabilistic modeling approaches as unable to cope with the multi-objective and multi-constraint problems which are characteristic for rotorcraft design.

New methodologies are thus needed, which adopt a probabilistic approach to design, and are set up to efficiently cope with the correspondingly large number of variables and variabilities involved. Such methodologies are commonly labeled *Robust Design*. An overview of the field is given by Park et al. [96]. Chen et al. define the fundamental objective of Robust Design as minimizing the effects of variation, without eliminating the causes [97]. Robust Design problems are classified into two distinct categories by Chen et al., depending on the location of the uncertainty which is evaluated. *Type-I* problems aim to minimize variations caused by uncertainties in the noise factors, i.e. in the technical parameters when considering the terminology adopted in this work. *Type-II* problems, in turn, strive for minimizing the impact caused by variations in the control factors, i.e. in the design variables. The maximum number of parameters to analyze probabilistically may need to be limited for reasons of complexity and computational cost. As pointed out in chapter 2.3.2, the location of uncertainty provides a promising criterion when prioritizing the variations to consider in a particular design problem.[23] In reference to the classification proposed by Chen et al., the evaluation of Type-I variations are of particular interest when evaluating the uncertainty introduced by adopting a model-based design approach.

Analogously to the definition of Robust Design provided by Chen et al., Mavris et al. define Robust Design as the practice of designing for minimizing the sensitivity to the influence of uncontrollable factors [94]. This approach to design is distinctively different to optimizing for maximum capability or cost-effectiveness, as the associated risk and underlying uncertainty is considered prominently. In this sense, Mavris and DeLaurentis develop a design environment which allows the simultaneous investigation of requirements, design variables, and technology infusion [20]. The work is focused on military aircraft systems, but Mavris and DeLaurentis claim that the principles are portable to other complex systems.

Batill et al. qualitatively discuss uncertainty in the context of the design of complex systems [64]. In system analysis, the stochastic behavior of an artifact, but also of the design and environment variables, is usually modeled through stochastic variation of the affected variables. Batill et al. adopt a less differentiated classification of uncertainty than the one presented in chapter 2.3.2. Following Batill et al., the *total uncertainty* is composed of a *bias error* and *stochastic behavior* of the physical artifact. Stochastic behavior is described as the variability in the characteristic states of the realized system. The bias error is defined as the deviation of the mean value of the system states as predicted by the model on the one hand, and as observed from the actualized system in reality on the other hand. The bias error itself corresponds to a combination of uncertainty and an acknowledged error as defined by Chen et al. [97]. Whereby uncertainty in this terminology

[23] To this end, see the discussion on the Problem of Size in chapter 2.4.1.

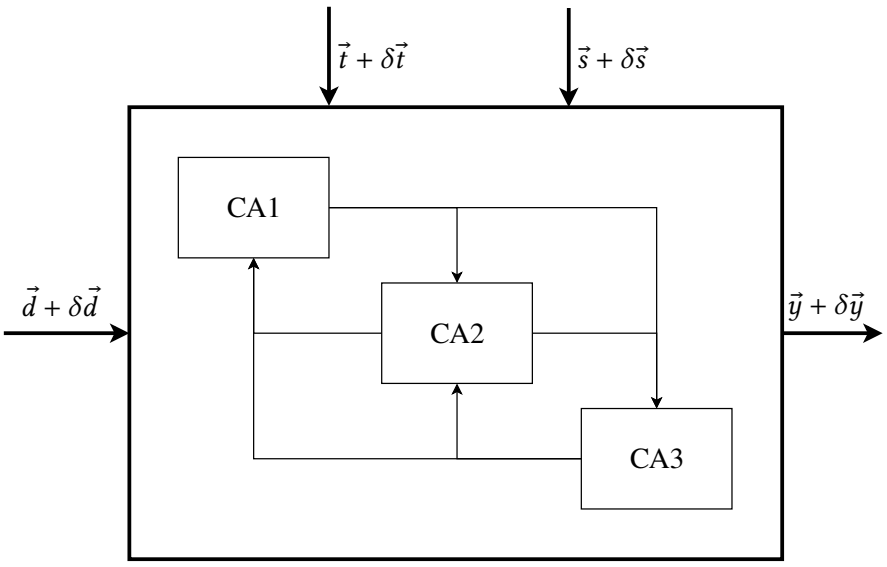

Figure 13 Sketch of a generic multidisciplinary system analysis modeling with input and output variability, modified from [64]

originates from a lack of knowledge or incomplete information, the acknowledged error represents a recognizable deficiency, which is not due to a lack of knowledge and thus usually reproducible and deterministic. Based on this classification of uncertainty, Batill et al. propose the following general four-step process to enable estimating the total uncertainty in a model environment [64]:

1. Select analysis methods and models of appropriate fidelity with respect to the level of abstraction of the artifact at the respective stage of the design process.
2. Define the design variables $\vec{d}$, system (technical) parameters $\vec{t}$, flight state parameters $\vec{s}$, and system states $\vec{y}$, which are required for the system analysis.
3. Estimate the bias errors in the individual contributing analyses. Batill et al. acknowledge that the estimation of the bias error requires information from other sources.
4. Estimate the stochastic properties of the elements in the input vectors $\vec{d}$, $\vec{s}$, and $\vec{t}$.

Once these steps are completed, a modified probabilistic system analysis model is obtained, as depicted schematically in figure 13. The model now considers variability (δ) in the input parameters, which causes variability $\delta\vec{y}$ in the predicted system states $\vec{y}$.

Among the typical stochastic properties which are of interest in a probabilistic design problem are the Cumulative Distribution Function (CDF) and the Probability Density Function (PDF) for each design objective, as Mavris et al. point out [94]. These functions represent the outcome of every permutation of possible designs, i.e. of every combination of design parameters. Thus, the CDF and the PDF can be interpreted as a representation of the feasible design space available to the designer. This output enables trade-off considerations concerning the relaxation of constraints or target values, but also regarding the need for technology infusion. The fundamental concept in CDF and PDF generation lies in the combination of statistical techniques and computer design codes. Fox lists three principle methods [98]:

1. Directly linking a sophisticated design code to a random number generator such as a Monte Carlo Simulation. The PDF and CDF can be obtained from the code responses. A major limitation to this brute force approach is the excessive computational effort required for complex problems such as rotorcraft design.

2. Approximation of a sophisticated analysis code through a meta-model, and subsequently linking the obtained meta-model to a Monte Carlo Simulation. Prominent examples for such approximation methods are Kriging and the RSM. Mavris et al. state that this methodology provides excellent results when the number of design variables is in the range of 12 to 15, whereas it proves unsuitable for more complex design problems [94].

3. Linking a sophisticated design code to an approximation of a Monte Carlo Simulation. This methodology aims at removing the computational expense of method 1 and the design problem complexity limitations of method 2 by reducing the number of high-fidelity design code executions when generating the CDF and the PDF. Mavris et al. names "Fast Probability Integration" (FPI) as a possible technique, which he applies to an example case of a notional Civil Tiltrotor Transport aircraft [94].

More recently, Krosche and Heinze evaluate the robustness of a preliminary design of a STOL-aircraft [66]. The preliminary design is obtained from a deterministic sizing code. This deterministic model is then turned into a probabilistic one through the addition of stochastic properties to selected design characteristics, corresponding to the investigation of a Type-I Robust Design problem in the classification of Chen et al. provided above. The sizing code is then used to determine uncertain samples through stochastically varying these parameters. A Monte-Carlo sampling methodology is deployed. The resulting uncertainty information is ultimately exploited to identify a more robust design solution than the baseline design, which originated from the initial deterministic sizing run. Couturier et al. develop and test a framework for the joint robust design of a fixed-wing aircraft and its engines, when subjected to uncertainty in the model environment, as well as operational and environmental uncertainties [99]. From their test case, Couturier et al. find that neglecting modeling uncertainty may produce designs with an only 30 % chance of meeting all constraints at later design stages, introducing a great risk for costly late design changes.

2.4. Challenges in Hierarchical Model-Based Design

Significant advances have been achieved in both the scientific and practical fields of rotary-wing engineering from the pioneering days. Where early designers had to rely on engineering judgment based on a fragile theoretical foundation,[24] designers today have a more thorough understanding of the underlying physics and, crucially, a vast database of experience, gathered on realized and proven platforms, available to guide the design process.

[24] *"We built the first helicopter by what we hoped was intelligent guess. It was time of crystal ball."* – Igor Alexis Sikorsky (1957), cited from [27].

Nevertheless, rotorcraft design for long remained by no means a straightforward process.[25] Even as recent as in the year 2010, Sinsay and Nunez argue that the incorporation of technology advances into conceptual aircraft designs is "more art than science" [1]. This metaphysical circumscription correlates with the history of the development of comprehensive analysis codes for rotorcraft, collected by Johnson [101]. This chronological overview of the advances in rotorcraft modeling shows that the complex and interacting phenomena characteristic for rotorcraft were for long not captured by the analysis capabilities of the time, and remain tremendously difficult to predict accurately and reliably even today.[26] Leoni illustrates the possible impacts of this shortcoming in a chronology of the development of the UH-60 "Black Hawk" helicopter [100]. As typical for rotary-wing developments, its initial design required a number of major design changes to solve unexpected issues, which were discovered only during flight-testing. These issues, characteristically, originated from complex aeromechanical interaction phenomena, which gave rise to the prescribed unexpected system behavior during flight-testing, and which were not predicted by system analysis before. The development, implementation and verification of these design changes are costly and prolongate the development. Yet, the need for these adaptations after early flight-testing today remains principally accepted as inevitable, and consequently even expected.

In response to the uncertainty in the design process, the rotorcraft industry long adopted a risk-averse incremental development strategy. Empirically-based preliminary design methodologies were developed, relying on observed correlations in databases of already realized artifacts with known characteristics and interdependencies. The availability of this data supported the sizing of many evolutionary designs in the past decades effectively, as discussed in detail in chapter 2.1.4. A major advantage of this conventional approach lies in the intrinsic robustness of such empirical methodologies when used within a validated parameter range, as for instance Price et al. point out [9]. Since the databases and rules are derived from in-service and proven platforms, the level of uncertainty then is comparatively low, and naturally controlled to a large extent.[27] Moving to model-based and hierarchical rotorcraft design methodologies is deemed necessary today, as argued for in chapter 1.1. Yet, little to no publications are concerned with the adaptation of preliminary design methodologies towards model-based design so far. This paradigm change however encompasses new challenges. In particular, the following three major challenges are seen as critical for enabling the transition to model-driven and hierarchical design of rotorcraft:

1. **The Question of Appropriate Model Fidelity**
   In model-driven design, the system model is the primary source of information about the design, feeding design decisions and discriminating competing design candidates. When adopting a hierarchical approach like SE, the level of detail of the information required *from* the model therefore progressively increases, hence calling for higher-fidelity models.

[25] *"During that first up-and-away flight, the YUH-60A gave strong indications that helicopter engineering was still largely an art and not yet a science."* – Ray Leoni, referring to the early flight testing of the Black Hawk in 1974, cited from [100].
[26] See chapter 2.2.1.2 for an overview of the capabilities of contemporary codes.
[27] See chapter 2.3.1 for the classification of uncertainty as aleatory or epistemic.

However, the quality of the model outputs depends on its calibration,[28] and the amount of information required *by* the models generally scales with the models' fidelity. Consequently, the selection of models of appropriate fidelity with respect to the progress of the design process poses a challenge.

2. **Transitioning between model-fidelity levels**
   A hierarchical design environment likely requires models of various fidelity-levels depending on the progress in the design process. In order to ensure the validity of previous design decisions, which are based upon earlier models, the transitioning between model-fidelity levels is of high interest. As switching models, and model-fidelity levels, represents a possible discontinuity in the model-driven design process, transitioning between models needs to be done in such a way that consistency and traceability are maintained.

3. **Quantifying and controlling model-related uncertainty**
   Model-based approaches do not offer the intrinsic robustness of contemporary empirical methodologies. This is particularly true as they will be applied to evaluate new technologies and unconventional concepts. In support of the following discussions, consider the sources of uncertainty in a model-based design environment introduced in chapter 2.3.2. Neglecting *code uncertainty* and *human error*, and attributing any *observation error* to the *residual variability*, the remaining sources of model-related uncertainty to consider are:

   - Model inadequacy
   - Parameter uncertainty
   - Parametric variability
   - Residual variability

   In order to grant model-driven methodologies robustness, a dedicated means to quantify and control this model-related uncertainty is required.

2.4.1. The Question of Appropriate Model Fidelity

In the context of system design, uncertainty is introduced by the modeling and the simulation process as a result of the inherent limitations associated with the used models. Albeit the predictive quality of any model is limited to a certain degree of credibility and accuracy, this is in particular of concern in the rotorcraft field, where the predictive quality of the available models is admittedly limited, particularly for unconventional concepts and technologies.[29] Batill et al. conclude that the epistemic portion of the uncertainty can be influenced by modifying the modeling, or by altering the method of analysis [64]. To this end, various authors advocate for moving to high-fidelity models already early in the design process [64, 79, 90, 92, 93]. This proposal is motivated by the notion of an increased accuracy of the high-fidelity models. Another argument lies in the higher resolution of these models, i.e. in their ability to capture the system behavior to a more refined extent. This approach to minimize uncertainty of the *model-inadequacy* type is intuitive at first view. For postdictive problems, i.e. when striving to understand a phenomenon observed on an already realized rotorcraft, the strategy seems effective. Sufficient reliable data is available in this

[28] Note that calibration here not only refers to technical model parameters, but also to design parameters.
[29] See the discussion of postdictive and predictive methods in chapter 2.2.1.2.

application to calibrate the models to physically and behaviorally represent the system adequately. The *parameter uncertainty* is hence limited and controlled. After successful reproduction of the encountered phenomenon in the model environment, design changes can then be developed with the now validated models, and subsequently implemented to solve the identified issue. However, this strategy is arguably inadequate for design problems of the scale of system design, which are by nature predictive, and therefore inherent a substantial degree of parameter uncertainty.

First, the computational effort associated with high-fidelity analysis is an issue in preliminary design. An inevitable byproduct of an increase in model fidelity is an accompanying step-increase in the number of model parameters, as for instance Price et al. point out [9]. With this increase comes a dilemma Koch et al. label the *Problem of Size* in the model-based design of complex systems [102]. Koch et al. argue that traditional parametric design analysis becomes ineffective when the size of the problem is increased too much due to the computational expense associated with the typically complex and interdependent models. This is problematic for preliminary design, as one of the primary objectives is the exploration of the design space, which requires a large number of model executions. Sinsay and Nunez see the computational effort associated with the model execution as the likely limiting factor in terms of adequate level of model fidelity [1].

Second, the effectiveness of the strategy to deploy high-fidelity analysis early in the design process depends on an alleged dominance of the model-inadequacy uncertainty type over the other uncertainty sources outlined above. This assumption is arguably questionable for rotorcraft modeling, especially when considering the recognized high level of model inadequacy even for the high-fidelity rotorcraft models, see table 1 in chapter 2.2.1.2. Until today, these models do not necessarily show an increased accuracy over lower-fidelity "engineering tools". A gain in accuracy is thus no direct implication. Factoring in the further sources of uncertainty adds to this skepticism. The Problem of Size associated with high-fidelity modeling introduces additional aspects to consider. Increasing the number of model parameters and the model complexity grows the need for model calibration. Parameter uncertainty is a significant aspect in rotorcraft design, as the calibration basis for the models is subject to significant uncertainty. In the absence of data of the realized system, calibration is based on experience, sub-scale testing (e.g. wind-tunnel testing) and analytical understanding of the associated physics. However, in the face of the complex and interacting aeromechanics on a rotary-wing system, uncertainty remains considerably higher for predictive use of the models compared to the above-mentioned postdictive usage. Admittedly, all contemporary rotorcraft codes require significant calibration in order to limit parameter uncertainty to a tolerable degree. In a design application, however, the available information on the design is limited, and therefore the level of parameter uncertainty may rise significantly with an increase in model fidelity. In this regard, Harremoës and Madsen point out that a suitable model requires an appropriate set of data for its calibration [103]. Price et al. share the concern of high-fidelity methods being applied inappropriately prematurely in early design stages [24].

Furthermore, owing to the complexity of rotorcraft aeromechanics, the residual variability may rise by switching to higher-fidelity models, as unrecognized interrelations between sub-models

may yield unexpected emergent behavior. Lastly, the large number of design parameters represents a challenging number of degrees of freedom in the design problem. Koch et al. state that the actual design task becomes extremely difficult in these circumstances, as the sizing task is mathematically under-determined due to the large number of degrees of freedom in the design parameters [102]. To this end, chapter 2.2.2.4 proposes a classification of design parameters, in which the class of independent design parameters are established in order to reduce the complexity of the sizing task. This simplification may however introduce uncertainty of the parametric-variability type. In summary of the above, whereas relying on high-fidelity modeling does potentially decrease uncertainty of the model-inadequacy type, the total uncertainty in the design problem may even increase through the contribution of the other sources of uncertainty.

Evidently, the selection of an appropriate level of model fidelity requires careful consideration and poses a challenging task. Sinsay and Nunez criticize the axiom that the level of fidelity deployed to the analyses poses the primary factor in the perception of the fidelity to which a design problem is understood [1], which they observe in review of previous work in the field. Instead, Sinsay and Nunez propose that fidelity in a design context should be measured by the degree of certainty with which the designs capabilities can be projected. In this sense, the design strategy should put a strong focus on minimizing the total uncertainty in the model-based design problem, considering all contributing sources of uncertainty, as discussed above. To this end, Sinsay and Nunez advocate the concept of "right-fidelity" modeling, in which the right-fidelity model is defined as the lowest-fidelity model capable of discriminating competing design candidates to an acceptable level of uncertainty [1]. The frequent use of empirically defined "technology factors" is used as an example for the introduction of uncertainty through insufficient model fidelity, complicating the ability to identify trade-offs between cost, performance and technology as a result. As an example for the other extreme, Sinsay and Nunez lay out that applying high-fidelity CFD codes on an inaccurate or inappropriate geometry may ultimately not lead to more accurate results than lower-fidelity models, but at the cost of increased computation cost and time. The principles at the heart of right-fidelity modeling are also supported by Harremoës and Madsen [103], Johnson and Sinsay [104] and Juhasz et al. [105].

In conclusion, selecting the appropriate modeling approach should consider two aspects. First, the level of model fidelity needs to be balanced in such a way that answering to the current design questions is achievable with a sufficient level of detail and speed. Second, the selection of the modeling approach needs to carefully consider all possible sources of uncertainty. The interdependence between these aspects is evident when considering any model, and hence any information obtained from model-based analyses, as approximate prior to the realization of the artifact. The design decisions due at the respective phase of the design process reside at increasingly lower levels of the product hierarchy, see chapter 2.1.2. This implies that a suitable model-driven design environment comprises models of varying fidelity in order to provide models of adequate fidelity at each stage of the design process.

2.4.2. Transitioning Between Model-Fidelity Levels

Only little research has been concerned with the adaptation and improvement of design processes and methodologies for model-based design. Price et al. see the need for a paradigm change in which design and analysis methodologies integrate SE principles [9], whereas the model development is identified as an area of particular interest in this regard. To this end, Price et al. present a concept for hierarchical model development named DADI (Dimensional Addition and Detail Insertion). The DADI concept gradually evolves the modeling of a physical artifact based on its geometric dimensions. Starting from 0-D, the representation of the artifact is refined until a detailed three-dimensional model is obtained. The application of DADI depicted by Price et al. is limited to the airframe design of fixed-wing aircraft.

The term "model development" in this thesis describes the refinement of the representation of an artifact in a multi-fidelity model environment. This refinement is achieved by transitioning to a higher-fidelity model. Today, model development is not integrated with the design process. On the contrary, model development is typically conducted in an uncontrolled manner. Models are not designed in such a way that the model parameters are required to correlate with the present progress in the design process, i.e. with the respective states of the PA and TA. This deficiency introduces significant uncertainty, as the models use input parameters which are neither validated and verified, nor under configuration control. As an example, Kalra et al. point out that the parametric mass-estimation-laws by Prouty [26] and from NDARC [45] require input at a level of detail which may not be available at the preliminary design stage. If applied nevertheless, significant uncertainty is introduced into the design process. This uncertainty may either take the form of parametric variability, if the unknown parameters are allowed to change later in the design process, or take the form of model inadequacy, if the model parameters are fixed prematurely to unsuitable values. This uncertainty then remains until the system's realization and testing. At the very least, the design space is artificially restricted. In the terminology introduced in chapter 2.3.3, this uncertainty manifests in uncertainty $\delta\vec{t}$ when predicting the technical characteristics $\vec{t}$ of each modeled system-element. This uncertainty then gives rise to uncertainty $\delta\vec{y}$ in the predicted system states $\vec{y}$. Ultimately, in a design application, these uncertainties propagate into uncertainty $\delta\vec{d}$ in the definition of the values of the design variables $\vec{d}$, i.e. in the sizing of the design candidate. Therefore, if uncontrolled, this uncertainty potentially jeopardizes the validity of the sized aircraft in the face of the requirements.

The previous section indicates the interest in a multi-fidelity design environment in order to tailor the modeling to a level of fidelity which is adequate for each stage of the design process. Furthermore, uncertainty is identified as a key element of the design process. A robust preliminary design methodology built upon a multi-fidelity modeling approach, and adopting SE-principles, then needs a dedicated methodology to handle the transitioning across fidelity levels in such a way that traceability and consistency among the architectural views are ensured. This is required in order to avoid introducing uncontrolled uncertainty, as the complexity of practical modeling approaches, i.e. the number of model parameters used to describe the system and mimic its physical behavior, inevitably evolves in discrete steps. This step-wise evolution of model complexity presents a

significant challenge for the need to sync the model development, contained in the TA, with the development of the RA and PA.

In today's practice, unspecified model parameters are usually set to default values or represent best guesses in the absence of reliable calibration data. Frequently, the link to previous design activities is qualitative at best, since the models use different parameters, and potentially even differ in the underlying basic physical theory, and thus are not directly compatible. As the TA yields the emergent behavior and thus the system characteristics, vast and uncontrolled uncertainty is introduced by the absence of a model development strategy.

In conclusion, a dedicated model development strategy considering uncertainty is seen as a crucial enabler for model-based preliminary design of rotorcraft. In order to integrate a multi-fidelity model-based design environment with a SE process, a strong focus on model development is required in order to ensure the consistency of the architectural views across the transition from one level of model fidelity to another. Furthermore, the transition needs to be conducted in a traceable manner in order to maintain the validity and traceability of design decisions across the different stages of the design process.

2.4.3. Quantifying and Controlling Model-Related Uncertainty

The consideration of uncertainty theory in rotorcraft design research so far is widely neglected, which may be attributed to the long-standing reliance on inherently robust empirical methodologies. Hitherto, the scientific discourse in the field is frequently truncated to a discussion of the ability and reliability of the applied models to represent and predict the behavior of a system in the context of the design problem. Consequently, the strategy to minimize uncertainty has been to maximize the level of model fidelity deployed to the analysis problem already at early stages of the design, whereas the available computational resources posed the limiting factor.[30] In the established uncertainty-sources classification, this strategy aims to minimize the model-inadequacy type of uncertainty. However, this approach may be counterproductive in a design application as it is fragmentary, since the other sources of uncertainty are not factored in. For instance, parameter uncertainty may even dominate the total uncertainty in the design problem, in case high-fidelity models are deployed prematurely without a sound calibration base.[31]

Consequently, a holistic approach to quantifying and controlling uncertainty is required. Besides the need to overcome the limited predicted quality of the available modeling, another challenge lies in the model development itself. The term model development here describes the selection of the modeling strategy in accordance with the needs of each phase of the design process, the generation of the actual system model, as well as its population. Also, the transitioning between the models of varying-fidelity requires consideration, as highlighted in chapter 2.4.2.

Chapter 2.3.3.3 provides the theoretical foundation of a generic methodology to quantify the

[30] See chapter 2.3.3.2 for a discussion of these efforts.
[31] This aspect is discussed in detail in chapter 2.4.1.

impact of uncertainty in system analysis. Arguably, the essential step consists of the attribution, estimation and prioritization of the uncertainty residing in the design problem at hand. In review of the discussion above, the relative contributions of the individual sources of uncertainty are likely to change dramatically in the course of the preliminary design process. Defining a suitable and effective way to identify the propagation of the uncertainty in the process across model-fidelity levels, and across the different phases of the preliminary design process, is challenging, yet necessary to lend viability to model-based design methodologies. Furthermore, the identified uncertainty needs to be controlled at each phase of the process, in order to ensure the robustness of the design.

2.5. Required Characteristics of Modern Preliminary Design Methodologies and Modeling

In this work, it is argued that a paradigm change in rotorcraft preliminary design towards model-based methodologies is required. A multi-fidelity approach to modeling is considered to be well-suited to the hierarchical and progressive approach to design, which is characterizing SE processes. As model-based approaches are naturally subject to model-related uncertainty, and do not benefit from the inherent robustness of contemporary empirical approaches, a dedicated means to cope with this type of uncertainty in the context of design is mandatory, in order to grant validity and robustness to future methodologies.

In conclusion of chapter 2, the identified required characteristics of modern preliminary design methodologies and modeling practices are summarized as follows:

- Capability to design and analyze generic rotorcraft configurations
- Capability to evaluate new technologies
- Adopt and incorporate an integrated and hierarchical top-down approach to design such as SE
- Implement a multi-fidelity modeling strategy, tailoring model fidelity to each individual preliminary design phase
- Maintain traceability and consistency when transitioning across model-fidelity levels
- Ability to prioritize, quantify and control model-related uncertainty

3. Hierarchical, Model-Based and Probabilistic Methodology for Rotorcraft Preliminary Design

3.1. The Overall Preliminary Design Process

A novel methodology for the preliminary design of rotorcraft is developed here. In line with the need identified in chapter 2, this methodology is model-based. A multi-fidelity modeling strategy is developed, in line with the progressive top-down design approach of SE. The methodology is designed to prioritize, quantify and control model-related uncertainty in pursuit of a robust design.

SE provides an overarching theory for the development of complex multidisciplinary systems. SE principles are adopted for the developed methodology. Consequently, the overall preliminary design process shown in figure 14 closely follows SE practices. The process is run iteratively on every level of product decomposition, i.e. on every tier. Within each tier, the process is run recursively until convergence is achieved. The process commences with an initial set of stakeholder needs, which are developed into a set of technical requirements. At the current level of system decomposition n, the RA generally holds the specified requirements from the upper level n-1 and above, and allocated requirements are proposed for the current level n. As outlined in chapter 2.1.3, the convention in this work is that the RA includes functional and non-functional requirements, indicating that the functional analysis is integrated with the Technical Requirements Definition Process. This is considered to be favorable for the ability to validate the proposed requirements, which is an elemental aspect of the process.

With the set of requirements available, the Iterative Design Loop (IDL) is entered. The outcome of the design process is a complete and coherent description of the design candidates. This design description takes the form of the SE architectural views discussed in chapter 2.1.3, developed

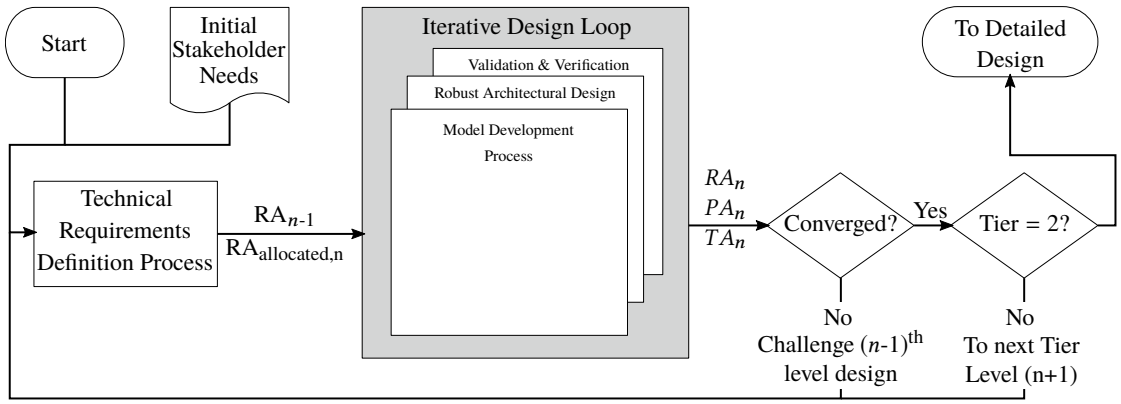

Figure 14 Overview of the overall preliminary design process

down to the current tier of system decomposition. In case the design process does not converge for the current tier, the previous-tier design process is revisited.[1] Successful convergence of the IDL allows the design process to continue to the next tier.

The SE architectural views are naturally characterized by a hierarchical, i.e. tiered, structure. To obtain confirmation of the feasibility of the design to a satisfying degree of certainty, the architectural views need to be developed, validated and verified down to the system-element level, i.e. T2. This level of detail is considered necessary and sufficient in the mathematical sense, as it enables an adequately sophisticated assessment of the characteristics and behavior of the system for preliminary design purposes. In particular, the T2 level of decomposition is required for a sufficiently accurate and reliable estimation of the empty mass of the design, as it allows parametric mass estimation laws to be applied based on input parameters at a level of decomposition which is validated and verified. Consequently, the T2 level concludes the decomposition of the design in the preliminary design process, and the preliminary design phase concludes with the successful validation and verification of the design on the T2 level.

The IDL lies at the center of the preliminary design process. The objective of the IDL is to explore the design space to determine a feasible design, while optimizing its cost-effectiveness against the RA. This is achieved by progressively evolving the design candidate(s) by developing, validating and verifying the architectural views.

3.2. Hierarchical Modeling Strategy of Varying Fidelity

The fundamental law of modeling is defined by Bremer to be "as simple as possible, as complicated as necessary" [106].[2] In a model-based design context, the required complexity is defined by the level of detail in terms of system behavior which is needed to substantiate the pending design decisions. The models are required to be sufficiently accurate and potent to discriminate between competing designs at the level of detail which is requested at the respective stage of the design process. Overly low fidelity models are incapable of predicting the system's behavior in sufficient detail and, consequently, fail to discriminate between candidate designs, effectively stalling the design process as a result. Table 2 shows a generic list of typical design tasks at the different tiers of system decomposition for reference. Evidently, the level of model fidelity which is appropriate may differ for the different stages of preliminary design, as the design decisions which are to be taken reside on an increasingly lower level of system decomposition and require a progressively increasing level of knowledge about the design.

As Johnson and Sinsay recognize, the quantity and quality of the information available in the design description at the current stage of the design may limit the reasonable level of model fidelity [104]. Expressed in the uncertainty terminology introduced in chapter 2.3.2, applying a

[1] See chapter 3.3.1 for a more detailed discussion of this possible outcome.
[2] Chapter 2.4.1 provides a detailed discussion about aspects to consider in this question, and derives a number of guiding criteria for selecting models of adequate fidelity.

Tier 0	Tier 1	Tier 2
• Select rotorcraft configuration	• Select number of rotors and orientation • Define rotor DL • Define number of lifting surfaces • Define lifting surfaces aspect ratio • Select propulsion system technology • Select airframe type • Select landing gear type • . . .	• Size rotor radius and solidity • Size lifting surfaces span and chord • Select propulsion system architecture • Size airframe geometry • . . .

Table 2 Non-exhaustive list of design tasks depending on the progress in system decomposition.

high-fidelity model prematurely may introduce uncontrolled and potentially excessive uncertainty. In explanation of this argument, consider an excessively high-fidelity model as one relying on model parameters at a greater level of product decomposition than has yet been achieved. In this case, unverified and unvalidated design parameters would populate the model, introducing significant uncertainty of the parametric-variability type. Furthermore, technical model parameters then become subject to parameter uncertainty as a result of the impossibility to calibrate the model reliably, as the design parameters may change when actually sized in the future. Even if there is no change in the design parameter values, the design space is artificially restricted by the premature fixing of design parameters, in effect diminishing one of the most-promising benefits of model-driven design. Consequently, the selection of the model fidelity needs to thoroughly consider all possible sources of uncertainty, in order to select the approach with the lowest total uncertainty. In review of these criteria, the level of model fidelity which is appropriate likely varies depending on the respective level of product decomposition typical for the individual preliminary design phases.

Besides the aspect of possible uncertainty introduction, another limiting factor on a sensible degree of model fidelity may be posed by the computational effort associated with the execution of the system model. The model fidelity needs to allow an effective exploration of the design space, i.e. a sufficiently large number of model executions in a suitable time.

In light of the above, the definition of adequate-fidelity modeling is postulated, expanding from the "right-fidelity" modeling definition proposed by Sinsay and Nunez:[3]

> *Adequate-fidelity modeling* in preliminary design applies the lowest-fidelity model capable of discriminating competing design candidates to an acceptable level of uncertainty, implying models to be designed to use parameters which represent elements of the Technical Architecture and Physical Architecture at equal and current levels of decomposition. The design can then be analyzed at the required resolution, while maintaining full design freedom and robustness.

[3] See chapter 2.4.1.

Tier	Modeling Approach	Aeromechanics	Mass & CG	Trim	Propulsion System Model
$T0$	System-level performance metrics	Power Loading, Lift-to-drag ratio	Fraction of gross mass, no CG	no trim	Specific fuel/energy consumption
$T1$	Energy method	Momentum theory	Parametric per sub-system, no CG	4D-trim (forces and yaw-axis)	Parametric model
$T2$	Force-balance method	Blade element theory	Per system element, incl. CG	6D-trim (forces and moments)	Physical model

Table 3 Hierarchical multi-fidelity modeling strategy per preliminary design phase and per discipline.

Contemporary modeling strategies deployed in preliminary design commonly use models of a singular, and often inadequate, fidelity, which is in violation to the proposition of adequate-fidelity modeling given above. In particular in the context of model-based design of complex systems, an inductive modeling strategy appears as the natural choice when considering the top-down and hierarchical approach to the development of a system adopted in SE.[4] Consequently, in order to be well-adapted to the hierarchical nature of SE design processes, a multi-fidelity modeling strategy is applied in the developed methodology. Table 3 shows the proposed modeling strategy for a standard three-tiered preliminary design process. Following the established definition of adequate-fidelity modeling, the models of each phase are selected in such a way that the level of decomposition is consistent across the three architectural views. The model topology is set up to use exclusively model parameters of the current level of the PA and TA. As a result, the models make use of parameters which solely mimic the characteristics of system elements currently under design. In the course of the design, the level of decomposition of the system increases, and the fidelity and resolutive capabilities of the applied models evolve accordingly by transitioning to higher-fidelity models. Subsequently, the modeling principles of each tier are depicted.

3.2.1. Tier-0 Modeling

At the Tier 0 (T0) stage, the system is not decomposed into any sub-systems yet, but only considered as a whole. Consequently, the only design degree of freedom which is available to the designer consists of the definition of the type of rotorcraft, so:

$$\vec{d}_{T0} := (rcType) \tag{3.1}$$

This limited degree of system resolution is insufficient to actually compute the system behavior. Instead, system-level performance metrics are used to attribute the expected behavioral characteristics to the rotorcraft under design. For a conventionally powered rotorcraft:

$$\vec{t}_{T0} := (sfc, PL, L/D, EM/DGM) \tag{3.2}$$

[4] See chapter 2.2.1 for the definition of inductive modeling.

The Specific Fuel Consumption (sfc) allows to describe the energy efficiency of the design in characteristic operating points, such as hover and cruise. Similarly, the aerodynamic benignity of the design is described by its Power Loading (PL) in hovering flight, and by the aircraft Lift-to-Drag ratio (L/D) in cruise flight. Ultimately, the empty-mass fraction of the Design Gross Mass (EM/DGM) allows to rate the mass efficiency of the design. A first estimation of the required DGM of the rotorcraft can then be obtained for the foreseen design mission based upon Breguet's fundamental range equation:

$$Range = \frac{V}{g}\frac{1}{sfc}\frac{L}{D}\ln\left(\frac{W_{initial}}{W_{final}}\right) \tag{3.3}$$

In equation 3.3, W prescribes the aircraft weight before ($W_{initial}$) and after the mission (W_{final}), i.e. the fuel burnt, V is the aircraft speed, and g the gravitational acceleration on earth.

Breguet's equation is not applicable to electrically-powered aircraft. A similar relation however can be derived based on the equations established by Traub [107]. Using the lift-to-drag ratio to prescribe the required power $\left(P_{req} = \frac{WV}{L/D}\right)$, and equating lift to the aircraft's weight in steady-state cruise flight ($W = Mg$), and substituting into Traub's equations yields a relation to compute the range of electric aircraft:

$$Range = (VR_t)^{1-n}\left(\frac{\eta_{tot}}{g}\frac{L}{D}\frac{M_{batt}}{M_{aircraft}}e_{batt}\right)^n \tag{3.4}$$

Analogously to Breguet's range equation, equation 3.4 allows to compute the range of an electric aircraft based upon system-level performance metrics. The discharge time R_t and the discharge parameter n are characteristic parameters of the battery and are correlated to the type of battery being used. The incorporation of these parameters allows for the consideration of the Peukert effect. As described by Sun et al., the Peukert effect can have a significant impact on the batteries' effective capacity C_{batt} [108]. The battery capacity is more commonly used in the form of the specific energy $e_{batt} = {}^{C_{batt}U}/_{M_{batt}}$, given in Wh/kg, where U is the battery voltage. The further parameters in equation 3.4 include the total propulsive efficiency η_{tot} and the total aircraft mass $M_{aircraft}$. The design parameter and technical parameter vectors for an electrically-powered rotorcraft thus comprise:

$$\vec{d}_{T0} := (rcType, battType) \qquad \text{and} \qquad \vec{t}_{T0} := (PL, L/D, EM/DGM, e_{batt}, \eta_{tot}) \tag{3.5}$$

Although the T0 modeling is simplistic and consequently introduces large amounts of parametric-variability-type uncertainty, it allows to mimic the system's behavior at discrete characteristic points of the operating envelope with a reasonable degree of reliability, in case the parameter uncertainty is limited, i.e. in case there is sufficient relevant data of comparable concepts to relate the attributed values in $\vec{t}$ to. For a Vertical Takeoff and Landing (VTOL) system in a design context, the characteristic points typically consist of hovering and cruising flight in design mission conditions. The energy consumption can then be estimated in order to provide a first sizing of the system's DGM, and to provide a first indicative comparison of competing rotorcraft concepts for the design problem at hand. In case the actual design problem is profoundly biased towards

or against a specific concept, the information from this first evaluation may even suffice for a down-selection of suitable concepts.

3.2.2. Tier-1 Modeling

Whereas the T0 models rely on the attributed system characteristics at distinct operating points, the T1 stage introduces a moderately physics-based modeling, which is capable of predicting the system's behavior throughout the flight envelope. The system is now decomposed into its major sub-systems. The major design features and performance characteristics of those are available to serve as model parameters according to the adequate-fidelity modeling paradigm. Taking a rotor as an example, this sub-system is defined by its non-dimensional geometrical properties – Disk Loading (DL) and solidity (σ) – and its blades' tip speed (V_{tip}):

$$\vec{d}_{T1,rotor} = \left(DL, \sigma, V_{tip}\right) \in \vec{d}_{T1} \tag{3.6}$$

The T1 models make use of the Rankine-Froude *momentum theory*[5] to compute the design's behavior off of these sub-system-level parameters, which allows for the prediction of rotor performance using solely characteristic rotor performance parameters such as the mean blade drag coefficient $\bar{c}_d$ and the induced efficiency κ:

$$\vec{t}_{T1,rotor} = (\bar{c}_d, \ldots, \kappa) \in \vec{t}_{T1} \tag{3.7}$$

The higher degree of system decomposition allows for the deployment of parametric mass estimation laws for the prediction of the empty mass of the different sub-systems. As the mass estimation is a critical aspect in any aerospace design problem, the ability to relate design parameters to the mass prediction provides a crucial increase in fidelity to the model-based design process. The rotorcraft is trimmed to obtain a balance of forces in three dimensions, and in terms of momentum with respect to the yaw-axis, in order to enable an appropriate sizing of the anti-torque system, if applicable. The aircraft drag at this stage however is not modeled in depency of the rotorcraft attitude, as the rotorcraft is not trimmed in the pitch and roll axes. The propulsion system is modeled and sized parametrically based on reference characteristics defined per propulsion system technology. An overview of the T1 modeling principles is provided in appendix F.

Im sum, the T1 models represent models of a level of fidelity which is characteristic for contemporary preliminary design environments. These models require extensive calibration in order to be reliable and accurate. Many contemporary empirically-based preliminary design schemes rely on a modeling strategy of the T1 level, as sufficient data is available for calibration in these applications. The difficulty in the assessment of the uncertainty residing in the model lies in the estimation of the involved parametric variability, i.e. in the uncertainty resulting from the simplifications and assumptions. Due to the limited fidelity of the modeling, the emergent behavior resulting from the interrelations and interactions of the various sub-systems are challenging to represent and estimate. Indeed, this holds even more true when investigating novel configurations and technologies. However, capturing these aspects remains challenging also in higher-fidelity models,

[5] Momentum theory is covered extensively in various textbooks, for instance [27, 29, 30, 109].

as outlined in chapter 2.2.1.2. Overall, modeling of the type and fidelity of the T1 category proved effective and efficient in numerous preliminary design investigations.

3.2.3. Tier-2 Modeling

At the T2 stage, the system is decomposed further into the system-element level. Continuing with the example of the rotor, this sub-system is decomposed into the rotor hub and the rotor blade. These system elements are described by their actual dimensional and geometrical properties – Radius (R), number of blades (n_{blades}), chord (c), blade twist (Θ) and taper ratio (tr), and rotational speed (Ω_{rotor}):

$$\vec{d}_{T2,rotor} = (R, n_{blades}, c, \Theta, tr, \ldots, \Omega_{rotor}) \in \vec{d}_{T2} \tag{3.8}$$

With these properties defined, the higher-fidelity Blade Element Theory can be applied to compute the rotorcraft behavior with the Force Balance Method.[6] Generally, the technical parameters, such as the aerodynamic properties of the blades, for instance, are now obtained from a series of sub-models $f_{i,T2}(\vec{p}_{T2})$, which are built upon the T2 model parameters $\vec{p}_{T2}$:

$$\sum_{i}^{N} f_{i,T2}\left(\vec{p}_{T2}\right) \mapsto \vec{t}_{T2,rotor} \in \vec{t}_{T2} \tag{3.9}$$

The formerly attributed sub-system-level performance characteristics are thus now computed as emergent behavior from T2 models. Analogously to the evolution of the rotor modeling, the airframe aerodynamics are now adapted for the airframe attitude in pitch, yaw and roll, allowing for a full six-dimensional trim of the rotorcraft. The propulsion system model is developed synchronously, and now features a full physical model. For example, the turboshaft model considers the Carnot cycle for the sizing and analysis of turbo-machines. The mass prediction models still consider semi-empirical parametric laws. However, these now operate exclusively on fully established design parameters, increasing their accuracy and reliability, and allowing for a reasonably accurate estimation of the location of the Center of Gravity (CG).

Whereas the T0 and T1 models and sizing algorithms are newly developed and implemented in the Python and Matlab computer languages respectively, the T2 modeling uses NASA's NDARC software at its core.[7] Custom software wrappers are coded in Python, which embed NDARC into the design and analysis environment of this work. These wrappers allow to control, parallelize and automate the required NDARC design and analysis tasks as desired.

The T2 modeling is considered fully suitable for the terminal stages of the preliminary design process with regards to the adequate-fidelity modeling paradigm, while still providing the computational efficiency to enable the exploration of the design and probability space in a sensible amount of time. Nevertheless, the open architecture of NDARC and the developed wrappers in principle allow the coupling with higher-fidelity analysis tools. Thus, in case a specific aspect of the design problem calls for an even more refined analysis than provided with the T2 modeling, high-fidelity analysis means such as CFD and FEA may be integrated into the developed design

[6] For a comprehensive description of the Force Balance Method, refer to standard textbooks such as [27, 29, 30, 109].
[7] The underlying theory and modeling of NDARC is described in [45, 48].

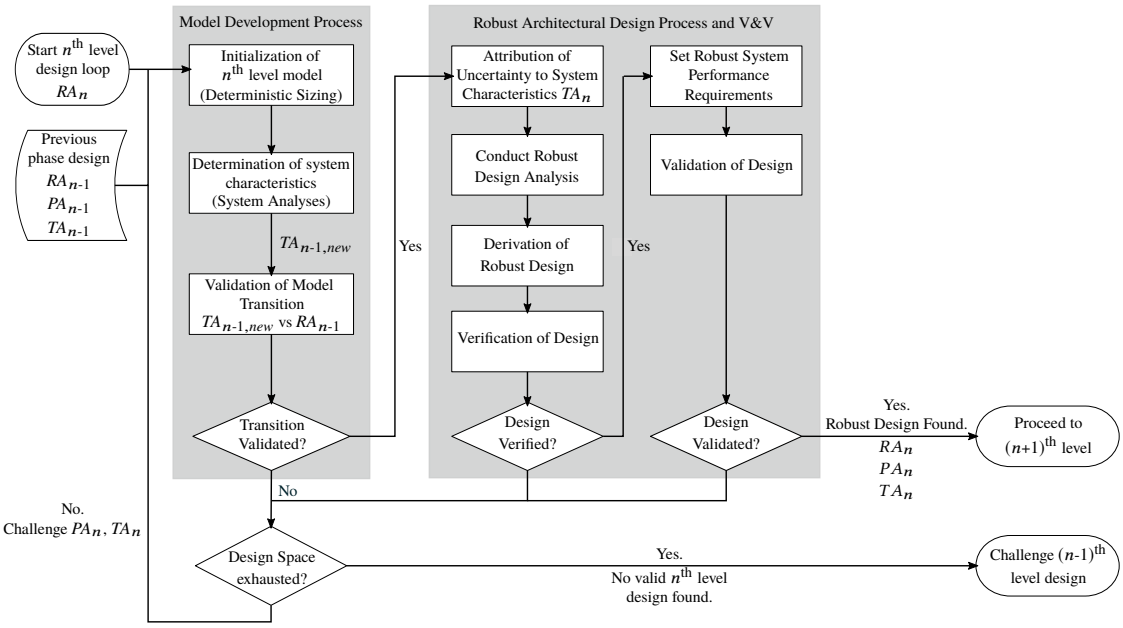

Figure 15 Overview of the revised Iterative Design Loop.

and analysis framework by adding according software wrappers to the T2 framework.

3.3. The Revised Iterative Design Loop

Figure 15 shows an overview of the revised Iterative Design Loop. The IDL is run iteratively and recursively until a converged design at the T2 level is verified and validated. The process is modified over the standard SE design loop to enable quantifying and controlling uncertainty in the context of preliminary design. To this end, two modifications to the otherwise typical SE-type design process are introduced:[8]

1. The Model Development Process (MDP) is introduced. This sub-process incorporates the hierarchical multi-fidelity modeling strategy and provides the procedural framework for transitioning across model-fidelity levels.
2. The Architectural Design Process is modified to yield a design which is robust against uncertainty in the context of preliminary design. In principle, the presented methodology is set up to handle all kinds of uncertainty. The focus of this work, however, is set on uncertainty related to model-based design.

The newly established and modified sub-processes are discussed in detail subsequently.

3.3.1. Infusion of the Model Development Process

The MDP is introduced into the IDL as a prelude to the architectural design process. After the completion of the previous-tier design loop, architectural views at the upper $(n\text{-}1)^{th}$ level

[8] See chapter 2.1.2 for a discussion of SE principles. For detailed information on SE processes, refer to [5, 18, 23].

of decomposition are available. Progressing with the preliminary design process then entails transitioning to the next tier n. Chapter 2.4.2 highlights the challenges which are associated with model development in the context of model-based preliminary design. The use of *adequate-fidelity* models at each tier is identified as a means to avoid the introduction of uncontrolled uncertainty, which is a consequence of using models of inappropriate fidelity. Chapter 3.2 introduces the implemented models of adequate-fidelity of the different tiers, which are set-up to minimize this model-related uncertainty. However, transitioning between these discrete levels of model fidelity represents a major challenge in a hierarchical design environment.

The purpose of the MDP is to validate the transition to the next level of model fidelity. Validation in this sense denotes the confirmation of the *consistency* of the design decisions across the tiers on the one hand, and satisfying the demand for *traceability* in the multi-fidelity SE design environment on the other hand.

For the following argument, consider the direct correlation of the developed model parameters classification with the SE architectural views, presented in chapter 2.2.2.1, and the system model topology discussed in chapter 2.2.2.2. In this mathematical notation, the n^{th}-level models $f_{Tn}(\vec{d}_{Tn}, \vec{t}_{Tn})$ use PA and TA entries of the present level of decomposition n to compute the system states $\vec{y}_{n\text{-}1}$ of the upper $(n\text{-}1)^{\text{th}}$-level:

$$\sum_{i=1}^{N} f_{Tn,i}\left(\vec{d}_{Tn,i}, \vec{t}_{Tn,i}\right) \mapsto \vec{y}_{Tn\text{-}1} \tag{3.10}$$

This logic enables the model development to proceed synchronously with the development of the design, as the model parameters and the design description are logically interrelated, since $\vec{d} \in$ PA and $\vec{t} \in$ TA. Furthermore, in a model-based design environment, this interrelation becomes particularly symbiotic. As the behavioral characteristics attributed to the n^{th}-level artifacts govern the predicted system behavior, the characteristics defined in $\vec{t}$ implicitly yield the design decisions reflected in $\vec{d}_{DoF,Tn} \in \vec{d}_{Tn}$. Acknowledging this dominant significance of the TA, the focus of the model transition aspects consequently is set on the behavioral characteristics, represented in $\vec{t}$ in the model domain.

The aspect of *traceability* is of interest, since the architectural views in SE demand a complete view of all existing hierarchical linkages in all domains. Whereas these linkages are obtainable from functional and logical decomposition in the physical and functional domains, the identification of the linkages in the technical domain is more challenging. This is true in particular for a model-based representation, as the evolution of the representation of the system inevitably needs to respect the available tiered modeling approach. Traceability of the established linkages in the technical domain is obtained by the element-wise allocation of uncertainty to the individual elements of $\vec{t}$. The location of the model-related uncertainty[9] thus becomes transparent at any stage of the design process, since the technical model parameters resemble the TA. Furthermore, since the TA contains information on the sizing practices, the origin of the uncertainty becomes traceable. The

[9] See chapter 2.3.1 for the three dimensions of uncertainty: location, level and nature.

detailed introduction of the individual steps of the MDP later in this chapter presents this concept more illustratively.

The primary argument regarding the criticality of an effective model-transition validation process revolves around the *consistency of the design decisions*. Consider that the design decisions $\vec{d}_{DoF,n\text{-}1}$ taken in the previous tier are linked to the technical characteristics $\vec{t}_{n\text{-}1}$. In SE, these design decisions are taken hierarchically and thus inevitably inherent a degree of sequentiality, which is potentially in conflict with a variable-fidelity modeling strategy, if the variable-fidelity modeling is not synchronized with the needs of the respective design phase. Typically, the values of these technical parameters are set to estimates of expected system behavior under consideration of the values of the corresponding design parameters. As an example, a relatively low disk loading likely increases expectations towards a good hovering efficiency, and vice versa. However, these estimated technical parameters are subject to a certain degree of uncertainty $\delta\vec{t}_{n\text{-}1}$. The Robust Architectural Design Process takes this uncertainty into account in the sizing of the rotorcraft to obtain a robust design.[10] The nature of this uncertainty may be of the epistemic or the aleatory type. In light of the accuracy of rotorcraft modeling and the strong need for calibration of the associated models, a certain portion of the uncertainty remains as aleatory uncertainty until the realization of the system, i.e. until measured data is available. A large share of this uncertainty is arguably of the epistemic type, however. To substantiate this, consider the above-mentioned uncertainty $\delta\vec{t}_{n\text{-}1}$. When moving to the next tier n, and the next level of model fidelity, the previously estimated technical parameters $\vec{t}_{n\text{-}1}$ are now computed from a series of sub-models on the n^{th} level. Consequently, the location of the model-related uncertainty moves from the $(n\text{-}1)^{\text{th}}$ to the n^{th}-level, as the assumptive attribution of artifact behavior is performed on the lowest level of the system model topology.[11] The hypothesis of the hierarchical approach to model-based design founds on the notion that this gradual increase in system decomposition and model fidelity progressively decreases the level of uncertainty in the design problem, as this approach gradually increases and refines the knowledge about the system behavior, and thus serves to decrease epistemic uncertainty. As outlined in chapter 3.2, this hypothesis requires an adequate-fidelity model environment to hold true, as other types of uncertainty than model inadequacy may dominate the total uncertainty in the design problem otherwise.

Figure 15 shows the individual steps of the MDP. The technical requirements of the current tier (RA_n), and the full set of architectural views of the previous $(n\text{-}1)^{\text{th}}$ tier are available as input to the next-level design loop. The focus of the design activities moves to the current level of product hierarchy n, and the system architecture is developed to this n^{th} level accordingly. In line with the adequate-fidelity modeling paradigm, the system model topology evolves to the n^{th} level analogously, enabling the necessary design and analysis activities.

Consequently, the MDP commences with the initialization of the new system model. The new elements of the system model generally take the form $f_{Tn,i}(\vec{d}_{Tn,i}, \vec{t}_{Tn,i}) \mapsto \vec{y}_{Tn,i}$. The initialization

[10] See chapter 3.3.2 for a detailed presentation of the Robust Architectural Design Process (RADP).
[11] This characteristic of hierarchical modeling is outlined in chapter 2.2.2.2.

of the n^{th}-level system model therefore requires the population of the model parameter vectors in the physical ($\vec{d}_{Tn}$) and the technical ($\vec{t}_{Tn}$) domains. The model initialization hence corresponds to a first deterministic sizing. Typically, several system models are generated at this stage, each representing one design candidate.

In a next step, the deterministically sized model is evaluated. The performance characteristics of the $(n\text{-}1)^{\text{th}}$ level are computed. These characteristics represent the emergent behavior of the modeled n^{th}-level system elements. This $(n\text{-}1)^{\text{th}}$-level behavior was hitherto estimated on the previous level, and the design decisions ($\text{PA}_{n\text{-}1}$) taken on this tier consequently base upon these projected characteristics. In order to ensure the consistency of these design decisions across the tiers, the behavioral characteristics in the design points become requirements, as outlined in chapter 3.3.2. The validation of the model transition is then performed by system-element-wise verification of the system characteristics obtained from the newly established model ($\text{TA}_{n\text{-}1,\,new}$) to the behavioral subset of requirements contained in $\text{TA}_{n\text{-}1}$. Using the generic system model topology depicted in figure 10 for illustration, the behavioral characteristics of sub-system 1.2 used during the T1 stage become requirements for the next tier once this stage concludes. When transitioning to the T2 stage, these characteristics are now computed from T2 sub-models, and achieving the previously set behavioral requirements for sub-system 1.2 becomes a criterion for a successful transition to the T2 phase.

The transition is considered validated successfully if all elements of the performance requirements set in the preceding-tier design loop are respected by the next-fidelity-level model. This cross-check of the system behavior across model-fidelity levels ensures that the design decisions taken at the previous $(n\text{-}1)^{\text{th}}$ level are not jeopardized by the switch to the higher-fidelity model. In the case of unsuccessful validation, the deterministic sizing process is revisited to explore whether modifying the assumptions within reasonable bounds can achieve a valid transition. If this iterative process does not converge, the $(n\text{-}1)^{\text{th}}$-level design process is revisited, as unrealistic or unfavorable assumptions during the establishment of the TA may have yielded an infeasible design. Successful validation allows the overall design process to proceed with the full n^{th}-level IDL by triggering the Robust Architectural Design Process.

To illustrate the validation logic more pragmatically, consider the beginning of the preliminary design phase at the T0 level and the three-tiered modeling strategy outlined in chapter 3.2. The sole design degree of freedom available at this initial stage consists of the definition of the type of rotorcraft in the scope, as the architectural views have not yet been developed. The system behavior is not yet known nor computable. However, the system-level performance metrics are capable of mimicking system behavior adequately when applied cunningly and within viable bounds. The T0 models accordingly use these metrics. Before moving to the next tier, the behavioral characteristics used in the T0 sizing loop become requirements for the next tier, in order to ensure the future validity of the taken design decisions. When progressing to the T1 level, the design is developed at the sub-system level, and a corresponding modeling using parameters and characteristics at this level is deployed. Where the low-fidelity T0 models rely on empirically-based values for

parameters such as the Power Loading (PL), the higher-fidelity T1 models substitute these through dedicated Momentum-Theory-based sub-models, which compute actual predicted values for the T0 performance metrics. Applying the higher-fidelity T1 system-model then allows discriminating between various design candidates on the $(n\text{-}1)^{\text{th}}$ level, for instance for the PL:

$$PL = \frac{T}{P_{req}} = f_{T1}\left(\vec{d}_{T1}, \vec{t}_{T1}\right) = \frac{T}{\kappa T v + \frac{\sigma \bar{c}_d}{8} \rho A V_{tip}^3} \tag{3.11}$$

The system behavior is then analyzed with the higher-fidelity T1 models. The transition to the next level of model fidelity is validated in case the behavioral requirements set in the preceding tier, i.e. the performance metrics values set in T0 for the distinct design conditions, are reproduced by the now computed values using the T1 system model. Analogously, the T2 models are validated against behavioral requirements on the T1 level, derived in the course of the T1 design loop.

3.3.2. Adaptation of the Architectural Design Process

As outlined in chapter 2.4.3, model-based design methodologies require a dedicated means for handling uncertainty. The major contributing sources of uncertainty are considered to reside in the definition of the (technical) model parameters, and in the limited accuracy and reliability of the models. The RADP addresses this challenge by adopting a probabilistic approach to the design process.

Chapter 2.3.3.3 introduces a generic four-step process to estimate the total uncertainty in a model environment, proposed by Batill et al. [64]. Furthermore, several methods for computing the stochastic properties of the resulting probabilistic design problem are presented. The first two steps in the process proposed by Batill et al. are performed in the frame of the MDP, in that the selected modeling adheres to the adequate-fidelity modeling paradigm. Even more so, since a multi-fidelity modeling strategy is seen as a necessity for the ability to answer to the increasing needs in the course of the design process, the transition across model-fidelity levels is addressed in the MDP. With the successful completion of the MDP, a validated model of the current tier is available and the RADP commences. In the course of the MDP, the n^{th}-level model is populated in the frame of the deterministic sizing. The design variables $\vec{d}$ are set up to represent the developed architecture of each design candidate. The technical parameters of the current tier are set to baseline values for the expected behavior of the concerned artifact, whereas the degree of certainty about the adequacy of these baseline values correlates with the available knowledge about the design in general, and the experience and expertise of the acting design organization with regards to such design problems in particular. The MDP addresses the procedural aspect of uncertainty in this respect, as it validates the consistency of the design process across the tiers. However, the uncertainty associated with the accuracy of the actual representation of the estimated expected system behavior in the baseline model needs to be addressed. Batill et al. propose to capture this uncertainty by estimating the bias error, and by attributing stochastic properties to the input model parameters, see chapter 2.3.3.3. The bias error is defined as the deviation of the mean values of the predicted system states from the mean values of the actual observed states of the realized system. It thus corresponds to the model-inadequacy type of uncertainty in the terminology introduced in chapter 2.3.2. In

preliminary design, a portion of this uncertainty will remain of the aleatory nature, as the model inadequacy cannot be fully removed. Batill et al. recognize this by admitting that information from other sources is necessary to estimate the quantity of the bias error. However, the developed methodology aims to gradually remove the epistemic portion of this uncertainty by deploying the variable-fidelity modeling strategy in line the the established adequate-fidelity modeling paradigm. As outlined in chapter 2.4.2, this process requires careful balancing in order to minimize the total uncertainty in the design problem, and not the uncertainty of the model-inadequacy type alone. The MDP addresses this challenge, as explained in chapter 3.3.1. The epistemic portion of the total uncertainty present in the design problem is estimated by attributing the expected stochastic quantities to the affected model parameters. It is this epistemic portion of the total uncertainty which is denounced *model-related* uncertainty throughout this work. The RADP aims to quantify and control this uncertainty residing in the design problem, in order to grant the model-based design methodology robustness and validity. The aleatory portion of the uncertainty in the design problem needs to be addressed differently. Whereas out of scope of this work, the contemporary way of handling uncertainty of this nature is outlined in chapter 2.3.3.1, and an outlook of possible future approaches applying the developed methodology is provided in chapter 5.4.

To address model-related uncertainty, the standard SE Architectural Design Process is enhanced by adding probabilistic elements, in order to allow evaluating the robustness of designs against the uncertainty residing in the design problem. In model-based design, the sizing task is performed on the foundation of a series of parameterized surrogate models, with a total number of j parameters. Again, all parameters p_j are assumed to be real numbers to enable representation in vectorized form:

$$\vec{p} := \left(p_1.p_2, ..., p_j\right) \in S \subset \mathbb{R}, \text{where } S \text{ is the parameter space spanned by } \vec{p} \tag{3.12}$$

The deterministic sizing task is performed in the MDP. It is initialized with a set of start values $\vec{p}_0$, and the design loop is run iteratively to find a valid and feasible design, yielding the deterministic reference model with $\vec{p}_{ref} \in S_{feas}$, where $S_{feas} \subset S$ is the feasible design space in the spanned parameter space S. More specifically, with the previously introduced terminology, the design loop varies the design parameters $\vec{d} \in PA \subset \vec{p}$ in search of convergence, whereas the technical parameters $\vec{t} \in TA \subset \vec{p}$ represent the system characteristics, as well as the model topology and the linkage logic. The uncertainty prevalent in the model-based design environment manifests in variations of the expected values of the technical parameters in a probabilistic vector $\delta\vec{t} \in \delta T : \Omega \mapsto \delta T \subset S$, where Ω is the sample space containing the set of all possible outcomes corresponding to the probability space $\mathcal{P} := (\Omega, \mathcal{F}, P)$, where $\mathcal{F}$ is the set of events and P is the function which assigns probabilities to the events. The quantitative definition of the associated probability space $\mathcal{P}$ may originate from experience, expertise or high-fidelity analyses, and represents the model-related uncertainty in the design problem. The RADP then explores the probability space by simulating the probabilistic model defined by $\vec{t}(\omega) := \vec{t}_{ref} + \delta\vec{t}(\omega)$ with $\omega \in \Omega$. The stochastic properties of the spanned probability space, i.e. of the particular design problem at hand, are subsequently computed. These properties can be visualized by means of the CDF and the PDF, which show the impact of the propagated model-based uncertainty on the actual design space. With this data, the uncertainty residing in the models and its impact on the robustness of the design candidate in

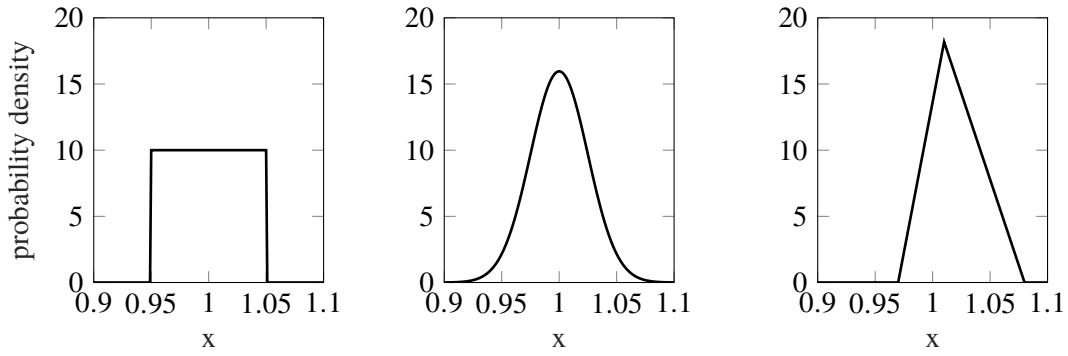

(a) Uniform Distribution (b) Normal Distribution (c) Triangular Distribution

Figure 16 Examples of probabilistic attributes of technical model parameters.

front of the established requirements is quantifiable, and thus becomes controllable. By analyzing the stochastic properties of the characteristic probability space $\mathcal{P}$ of the design problem at hand, a robust design can be derived.

Figure 15 shows the individual steps of the RADP, which adopts the presented principles and adapts the generic methodologies to preliminary design of rotorcraft. The objective of the robust design process is to determine a design $\vec{p}_{rob} \in S_{feas}$ which is robust against the model-related uncertainty. This uncertainty resides in the models' capability to accurately and reliably predict the system's behavior in the design conditions. The deterministic sizing conducted during the MDP sets the baseline values for $\vec{t}_{ref}$ and represents the expected system behavior. This information is now enriched by the definition of $\delta\vec{t}$, which describes the variability associated with the parameters in $\vec{t}_{ref}$ in the form of a probability distribution. Figure 16 shows examples of these probabilistic attributes. Reviewing the discussion in chapter 2.4 around the challenge to populate the system model with reliable and valid baseline values, the introduction of the probabilistic vector $\delta\vec{t}$ resolves this dilemma. On the contrary, any conceivable skepticism in the projected behavioral characteristics of the concerned artifact may be constructively integrated into the system model, since the the degree of certainty of each projection of artifact behavior may be described. Attributing stochastic properties to specific aspects of artifact behavior is a task which is, as the definition of the reference values, fueled by the experience and expertise of the designing entity, and may be substantiated further by relevant data whenever available. Not only are these stochastic properties mirroring the expected accuracy of the model in the design points, but are also defined considering the resolutive capabilities of the model, as the model needs to represent the system's behavior in the entire operating envelope. For instance, whereas the T0 models are capable of mimicking system behavior at characteristic operating points, they certainly fall short of differentiating system behavior in other system operating states due to their very limited resolution. As a result, the uncertainty attributed to the T0 technical parameters likely is significantly higher than for higher-fidelity models.

With the probability space now defined, the identification of its impact on the robustness of the design is of interest. To quantify this impact, the quasi-Monte-Carlo (Method) (qMC) method is widely used to compute the stochastic quantities of the probabilistic model, by approximating

integrals of the form:

$$\int_{\delta T} f\left(\vec{p}\left(\delta\vec{t}\right)\right) dP\left(\delta\vec{t}\right) \approx \sum_{i=1}^{N} \omega_i f\left(\vec{p}\left(\delta\vec{t}_i\right)\right) \tag{3.13}$$

As Siebertz et al. point out, the qMC method offers a superior rate of convergence compared to the regular Monte-Carlo method, yet still requires a comparatively large number of model executions [110]. This is potentially problematic, since the computational effort may pose a primary limiting factor, as discussed in chapter 2.4. To this end, the Latin Hypercube Sampling (LHS) method is deployed to generate the computational grid for the probabilistic analysis, drastically reducing the number of required model executions by up to 50 % compared to the Monte-Carlo method, as Siebertz et al. state.

The LHS-generated computational grid ensures that the entire probabilistic design space S is evaluated. However, it is an evenly-distributed grid, whereas the numeric experiment ought to reflect the probability distributions attributed to the various factors (see figure 16), in order to represent the particular probability space $\mathcal{P}$ adequately. An unevenly-distributed computational grid is hence needed, which resembles the specific probability distributions attributed to the particular elements in $\delta\vec{t}$, which constitute the actual factors of the computational grid. This is achieved by applying the inverse CDF of the attributed probability distributions of these factors to the evenly-generated LHS grid. Figure 17 shows an example of this transformation for one factor x, characterized by a Normal Distribution $f(x)$, which has the CDF $F(x)$. The vertical axis of the PDF exhibits the identical domain of definition as the evenly-distributed and LHS-generated computational grid. Explicitly, $0 \leq F(x) \leq 1$. Since $F(x)$ is a monotonically increasing and continuous function, a unique x-value is obtainable for each function value $F(x)$. Therefore, by utilizing the inverse CDF $F^{-1}(x)$ of each particular factor of the evenly-distributed LHS-grid in this manner, an unevenly-distributed test field is obtained, which accurately resembles the probability distributions characterizing the different factors. As a result, the test field is appropriate to compute the stochastic properties of the spanned probability space $\mathcal{P}$.

In a next step, the probability space $\mathcal{P}$ is evaluated by executing the generated computational grid. For each set of factors, i.e. each set of technical parameters $\vec{t}$ contained in the set of possible outcomes Ω, the sizing routine is executed. The stochastic properties extracted from this analysis include the CDF and the PDF of the response to the design problem. Figure 18 shows illustrative examples of such diagrams. The PDF and the CDF of the DGM required to satisfy the user requirements are shown. In this application context, the CDF may be interpreted as the likelihood with which a design of a specific DGM achieves the design mission in spite of the uncertainty attributed to the underlying system characteristics, described in the form of the probabilistic elements in the technical parameters vector $\vec{t}_{uncert} \subset \vec{t}$.

Since the implemented sizing routine iterates in search of a convergent DGM which enables the rotorcraft to satisfy a set of design missions and conditions, the stochastic properties of the probabilistic analysis can be evaluated to obtain a target value DGM_{rob}, which characterizes a robust design, as opposed to the deterministic DGM_{ref} resulting from $\vec{p}_{ref}$. The desired degree of

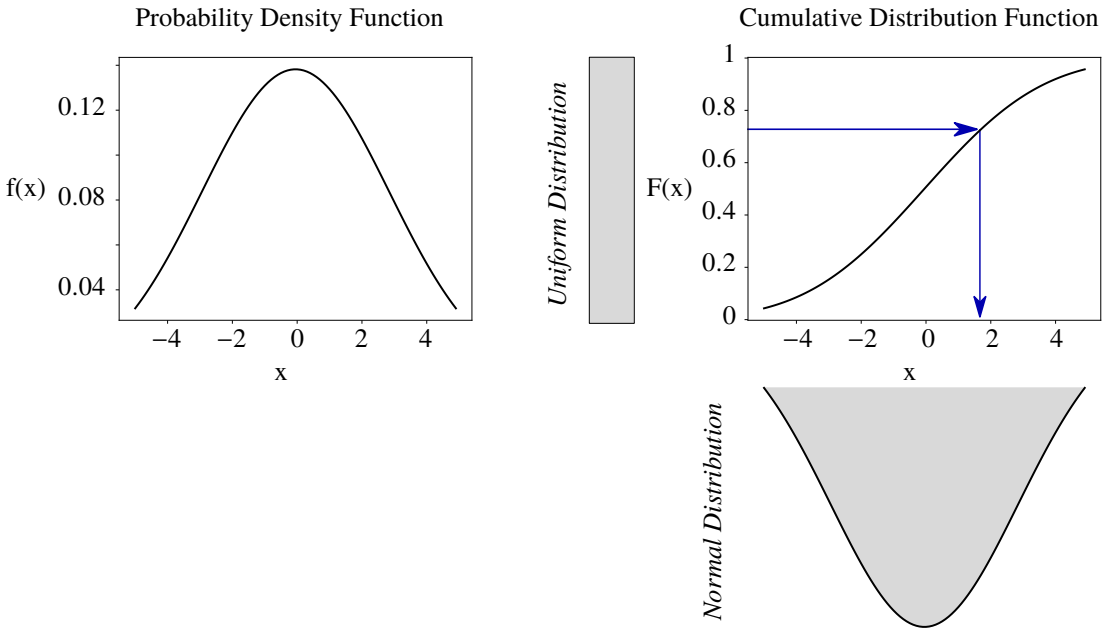

Figure 17 Unevenly-distributed computation grid generation by using the Cumulative Distribution Function, modified from [110].

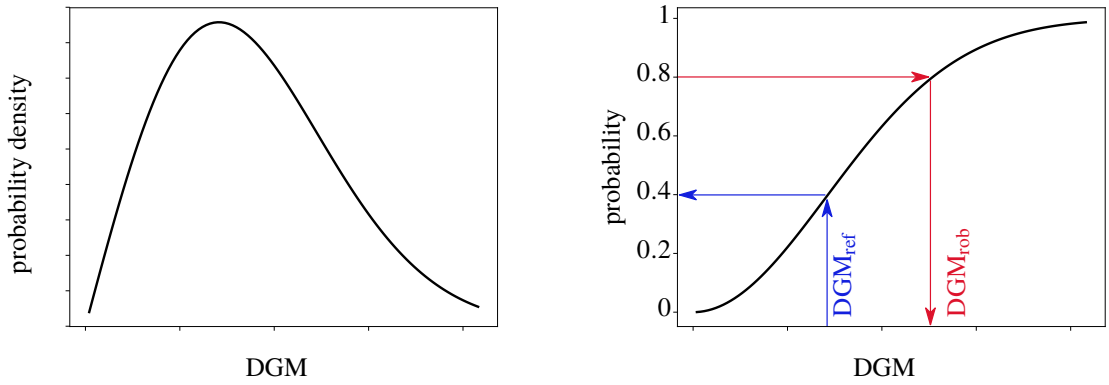

Figure 18 Example of the Probability Density Function and the Cumulative Distribution Function of a Preliminary Design Problem.

robustness of the design can be adjusted by defining the target value of the CDF function of a robust design. For instance, the CDF value of the deterministic reference design results to 0.4 in the example shown in figure 18. This value indicates that the deterministic design ought to be robust against only 40 % of the variability considered present in the model-based design environment. A robust design is typically requested to cover a greater portion of the possible outcomes Ω. For instance, the CDF value of a robust design is set to 0.8 in this illustrative example. The evaluation of the inverse CDF at this target value then yields the target DGM_{rob} of the robust design.

With the target value for the DGM of adequate robustness now known, another iterative run of the model $\vec{p}$ is required to identify the corresponding set of robust model parameters $\vec{p}_{rob}$. This additional model execution is required as the relation between DGM_{rob} and $\vec{p}_{rob}$ is mathematically not an injective mapping. Indeed, this problem is mathematically under-determined. Thus, at least one element of $\vec{p}$ needs to be set as the target parameter. As it is common practice in aircraft design

to control uncertainty by means of a contingency on the empty mass estimation of the design, and due to the dominant influence of the empty mass on the DGM, phrasing this problem as a target search for an empty mass control variable χ_{EM} in the following form proves a pragmatic and effective approach:

$$\text{Find} \quad \chi_{EM} \quad \text{such that} \quad f\left(\vec{p}, \chi_{EM}\right) \stackrel{!}{=} DGM_{rob} \tag{3.14}$$

Once the robust set of design parameters $\vec{d}_{rob}$ and technical parameters $\vec{t}_{rob}$ are determined, and after successful verification of the design against the requirements $\vec{r}$, the robust system characteristics $\vec{t}_{n,rob}$ and the robust design degrees of freedom $\vec{d}_{DoF,n,rob}$ of the current tier then become requirements for the subsequent level n+1. The next-level model is validated against these derived robust system requirements in the MDP as described in chapter 3.3.1. This hierarchical and system-element-wise approach enables the uncertainty to be traced across fidelity levels. Furthermore, the consistency of the taken design decisions is ensured throughout the design process.

The actual robust design margins become visible for each system design parameter by comparing the elements in the set of robust design parameters $\vec{d}_{rob}$ to the ones of the deterministic reference design $\vec{d}_{ref}$. Thus, the design margins become visible per element of the PA. The technical parameters, i.e. system artifact characteristics which make the design robust in the face of the residing uncertainty, are correspondingly identified and quantified per element of the TA. Since contemporary models instead use generic system-level margins, which do not allow any insight into the origin of the uncertainty they aim to cover, this new probabilistic method promises to be an enabler of hierarchical and robust model-based design.

With every step-increase of model fidelity and system decomposition, the allocation of uncertainty in the models becomes increasingly pinpointed, and the designing entity should be able to establish more and more precise descriptions of the uncertainty attributed to the expected reference artifact behavior. Consequently, it is hypothesized that the epistemic model-related uncertainty may be decreased progressively when executing the developed hierarchical model-based design methodology. As knowledge about the design increases with progressing system decomposition and increasing model fidelity, the necessary margins for robustness, i.e. the deviations between $\vec{p}_{ref}$ and $\vec{p}_{rob}$, should gradually decrease accordingly when progressing through the tiered stages of the preliminary design process.

The validation of the design at the current tier includes evaluating whether the granularity of the rotorcraft description is sufficiently decomposed, and whether the level of uncertainty is within acceptable bounds. As argued above, both criteria are interrelated in the established RADP. A measure of "acceptable" bounds is proposed by Sinsay and Nunez, in that the uncertainty associated with the analysis is asked to be less than the projected difference between the competing design candidates [1]. In case of unsuccessful validation, the design space is revisited, since unfavorable design decisions may have yielded an infeasible design. If this search for convergence in the current tier fails, the previous-tier design loop is revisited, as the design decisions taken in this

prior loop may have produced an infeasible design. Successful validation, in turn, allows the product development process to proceed with the next stage of the IDL, or progress to the detailed design phase in case the preliminary design phase is concluded.

4. Example Demonstration of the Proposed Methodology

4.1. Definition of the Example Demonstration Case

A practical test case is performed to demonstrate the proposed design methodology. For this purpose, a generic design problem is defined, and outlined subsequently.

Today, the continued trend towards urbanization is driving the existing infrastructure in many metropolitan areas to and beyond their limits. The integration of air travel into the mobility concept of the affected cities, termed Urban Air Mobility (UAM), promises to provide alleviation to this increasingly severe problem. Holden and Goel provide a comprehensive discussion on the subject [111]. The present issues of urban mobility are outlined, the potential of air travel to solve these are highlighted, and the associated challenges related to realizing UAM are derived.

The UAM scenario seems suitable for the example demonstration case in this work for two reasons. First, it represents a relevant contemporary design question in the field, for which an initial set of user requirements is ascertainable. Second, for reasons of cost [112], as well as operational emissions, noise, speed and safety [111], it is argued that new (electric) rotorcraft concepts are best-suited to the UAM scenario, mandating the usage of model-based methodologies to enable the design and analysis of such configurations.

The emphasis of the test case is set on demonstrating the methodology itself rather than exhaustively investigating this contemporary design question. Therefore, a series of assumptions is taken to simplify the test case in order to maintain a reasonable scope. To this end, the main simplifications and assumptions and their potential impact on the example demonstration are discussed in chapter 5.3.

An initial set of user requirements is needed as input to the design process. The preliminary design phase concludes once the specification, validation and verification is achieved down to the Tier 2 (T2) level. From their analyses, Holden and Goel derive requirements which viable UAM vehicle platforms are asked to achieve [111]. Holden and Goel suggest a minimum range of two trips of

Requirement	**Threshold**
VTOL capability	Yes
Design Mission Range with 2 PAX	2×80.5 km
HOGE Ceiling @DGM, ISA+20 K	2500 m
HOGE Ceiling @DGM, ISA+32 K	1000 m

Table 4 User requirements of the demonstration case.

Parameter	Value
(Flight) Crew	none
PAX	2×90 kg
Cargo	2×6 kg
Fixed Useful Load	250 kg
Ground Level	0 m
Atmospheric Conditions	ISA+20 K
Reserves	10 min @V_{hold}

Table 5 Design Mission parameters.

50 miles (80.5 km) each, while meeting the Instrument Flight Rules (IFR) reserve requirements of the FAA. From the average load factor of 1.6 passengers for commuting trips within the 100 miles range, a passenger capacity of 2 to 4 is considered appropriate, whereat this includes a pilot, if necessary. Duffy et al. found their analysis of cost reduction potential of electric rotorcraft in the UAM mission on comparable mission requirements [112].

From this data, the set of initial user requirements for the example demonstration test-case is derived, and summarized in table 4. A VTOL aircraft is sought which is capable of performing the defined design mission. A number of point performance requirements in the form of Hover out of Ground Effect (HOGE) threshold performances complete the system-level user requirements for this study. The hover requirements are set to cover a warm day in Mexico City (elevation 2250 m), and a hot day in Sao Paolo (elevation 760 m), with some margin.

The design mission is outlined further in table 5 and figure 19. The minimum range suggestion from Holden and Goel is adopted, split into two trips of equal distance. Vertical takeoffs and landings are required. A duration of 2 min per VTOL operation is assumed. The cruise segments are requested to be performed at the maximum cruise speed of the aircraft, as minimizing travel time is a key aspect in the context of UAM. In order to save costs and maximize the mass efficiency of the aircraft, an autonomously piloted vehicle is assumed, which is operated under IFR regulations. The resulting complexity and quantity of the associated avionics and flight control systems is reflected in the rather high value of the required fixed useful load, which represents the needed mission-specific equipment. The existing IFR reserve regulations are based on current aircraft operations, where distances are large and alternate landing fields scarcely available. UAM operations however conceptually rely on a dense grid of potential landing points, and flight times of 30 minutes or less. Both factors significantly decrease the likelihood of a degradation in weather conditions, which is the primary cause for needing to deviate to an alternate destination. In anticipation of a future relaxation of the operational regulations for UAM operations, the reserve requirement for the UAM scenario is therefore reduced to provide for an additional flight time of 10 minutes at holding speed V_{hold} compared to the currently required IFR rules for civil aviation.[1]

[1] IFR reserve regulations for CAT applicable in EASA jurisdiction are depicted in [113, 114]. Usually, no less than final reserve fuel for 30 min and contingency fuel equivalent to 5 % of trip fuel (10 % for helicopters) are demanded.

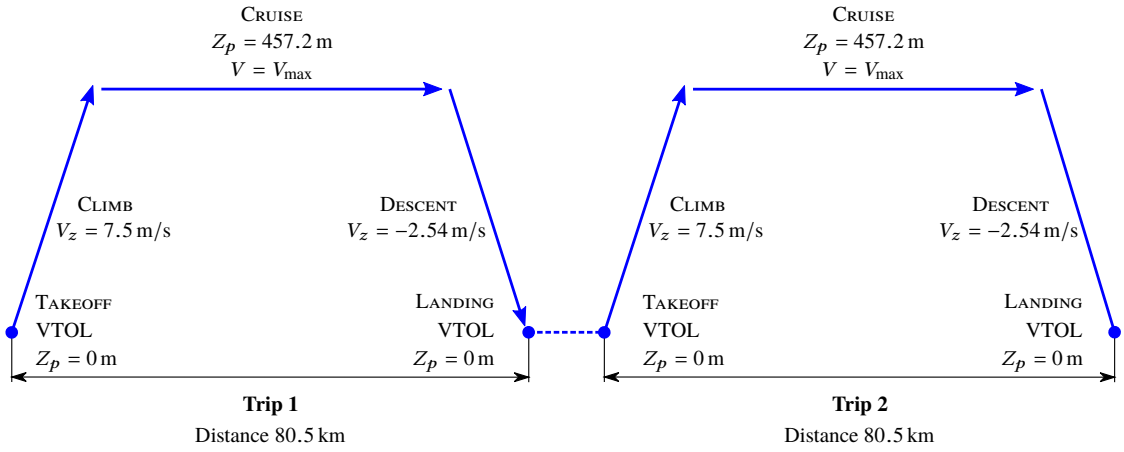

Figure 19 Mission profile for the example demonstration test-case.

4.2. Exploration Phase: Tier-0 Design Loop

With the initial set of stakeholder requirements defined, the hierarchical preliminary design process commences at the system level. The Iterative Design Loop (IDL) begins with the Model Development Process (MDP), see figure 15.

4.2.1. Model Development and Deterministic Reference Design

As the first step of the MDP, the reference T0-level model is initialized. As pointed out in chapter 3.2.1, the sole design parameter at the T0 stage is the type of aircraft to be investigated. The following types of rotorcraft are included in the scope of the example demonstration test-case:

- Helicopter (H/C)
- Tiltrotor (Aircraft) (T/R)
- Electric Vertical Takeoff and Landing (Aircraft) (eVTOL)

The eVTOL concept answers to the depicted UAM scenario, whereas the conventional helicopter and tiltrotor configurations are included to benchmark this novel concept. At the T0 level, the candidate designs are modeled using system-level performance metrics $\vec{t}_{T0} \subset \vec{p}_{T0}$. The T0 model makes use of these parameters to perform a simplified mission computation to obtain a first estimation of the required size of the rotorcraft.

Table 6 provides the reference technical model parameters $\vec{t}_{T0,ref} \subset \vec{p}_{T0,ref}$ for the three candidate concepts, corresponding to the TA entries at the system level. The technical model parameters aim to represent the behavior of each system element and hence are determined with respect to the corresponding design parameters $\vec{d}_n \subset \vec{p}_n$. For the T0 design loop, the expected system behavior is typically defined based on a representative database of existing rotorcraft, enriched by the available experience and expertise. For the conventional configurations (helicopter and tiltrotor), a large amount of empirical data is available to guide the definition of reference baseline values.[2] The

[2]For example, data is published in [34, 115–120].

	Parameter	Baseline Value	Confidence Interval
H/C	*PL* in hover	46.5 N/kW	41.7 to 51.3 N/kW
	L/D in cruise	3.1	2.9 to 3.5
	EM fraction of DGM	0.735	0.71 to 0.78
	sfc in cruise	0.365 kg/kWh	0.34 to 0.39 kg/kWh
T/R	PL in hover	37.5 N/kW	35.3 to 41.6 N/kW
	L/D in cruise	5.3	4.5 to 6.8
	EM fraction of DGM	0.809	0.79 to 0.86
	sfc in cruise	0.415 kg/kWh	0.39 to 0.44 kg/kWh
eVTOL	PL in hover	40.5 N/kW	37.3 to 45.7 N/kW
	L/D in cruise	11.0	8.5 to 13.5
	EM fraction of DGM (excl. Battery)	0.47	0.45 to 0.52
	Battery cell specific energy	250 Wh/kg	232 Wh/kg to 272 Wh/kg
	Total Propulsive Efficiency	0.68	0.65 to 0.77

Table 6 Tier-0 reference technical model parameters. Values for design mission conditions.

baseline specific fuel consumption (*sfc*) value represents the performance of a modern turboshaft engine, assuming identical engine technology levels for both configurations. The tiltrotor engine is assumed to perform at worse efficiency, since the power demand discrepancy between hovering and cruising flight is typically larger for this configuration, leading to operation further off the design point in cruising flight.
The Lift-to-Drag ratios (L/D) correspond to typical aerodynamic cruise efficiencies of the respective rotorcraft configurations, see [29, 34, 49]. The power loading (*PL*) prescribes the aircraft efficiency in hovering flight. In this field, the helicopter configuration is superior to the other configurations due to its lower disk loading. Finally, the empty mass (*EM*) fraction gives the mass efficiency of the rotorcraft in relating the empty mass to its design gross mass (DGM). The *EM*-fraction values attributed in table 6 are approximately 10 % to 20 % greater than typical helicopter and tiltrotor values, see [34]. Typically, rotorcraft are multi-role aircraft which represent a best-compromise design to satisfy a manifold set of mission requirements, containing both long-range and high-payload missions. The selected UAM scenario of the test case however contains only a comparatively low required Useful Load (UL) scenario, i.e. a short-range and low-payload design mission. The sizing algorithm optimizes the design for this discrete mission in determining the lowest required DGM. In the absence of other high-payload missions, a comparatively high *EM*-fraction value is expected due to the low required UL.

Whereas a broad database is available to take reasonable experience-based assumptions for the conventional rotorcraft in the scope, an empirical approach is not possible for the eVTOL concept in the absence of previously realized designs. Furthermore, the energy efficiency parameter *sfc* needs to be substituted for a corresponding electrical efficiency metric.[3] The reference assumptions for the eVTOL are discussed subsequently in the order of their listing in table 6.

As pointed out above, conventional rotorcraft achieve rather moderate L/D ratios of about 3 to 6, depending on the configuration and the priorities set during its design. The UAM scenario

[3] See equation 3.4 for the parameters of emphasis for electric aircraft in the T0 design loop.

however requires electric aircraft to achieve greater L/D ratios in order to become viable solutions for this application, as Fredericks et al. point out [121]. Hepperle also stresses the sensitivity of electric aircraft to the L/D ratio [122]. As the power-to-weight ratio of the battery as primary energy source is comparatively low, the overall vehicle mass correlates strongly with its cruising efficiency. Consequently, an electric VTOL design should focus on aerodynamics and strive for high L/D ratios. Fredericks et al. study a distributed propulsion concept with a L/D ratio of 20. Hepperle suggests a design with a L/D ratio of 16.35. Moore et al. consider L/D ratios of 9 to 15 [123], whereas the rather extreme designs described by Pornet et al. achieve values of up to 28 [124]. These high-advance-ratio designs rely on a low wing-loading, and thus large wing spans, to boost the aerodynamic efficiency in cruise flight. Rotorcraft operating in an urban environment however need to maintain a reasonable exterior footprint in order to allow operation, takeoff and landing in these confined spaces. Therefore, a L/D ratio of 11.0 is assumed for an eVTOL aircraft designed with these dimensional constraints of the UAM scenario in mind in the T0 loop.

Hepperle suggests typical aircraft empty mass fractions (EM/DGM) to be in the range of 0.4 to 0.7. Electric aircraft typically reside at the lower end of this spectrum, benefiting from the relatively low level of complexity. This is supported by Hepperle and Fredericks et al., who use empty mass fractions of 0.53 [122] and 0.4 to 0.498 [121] for their design studies, respectively. Obviously, the battery mass is not included in these values. As a rule of thumb, and depending on the range requirements, approximately one third of the total aircraft mass is made up of the batteries for fully electric aircraft.[4] Considering the autonomous flight capability and anticipating usage of speed-controlled thrust units, the reference EM/DGM fraction for the T0 eVTOL design example is set to 0.47.

The battery energy density e, given in Wh/kg, is a primary parameter of interest for electric aircraft. The inferior energy density of contemporary batteries when compared to fossil fuels represents a major disadvantage for an airborne application, in which weight is of utmost importance. A brief review of recent progress in the field is given hereafter.
Moore and Fredericks see an energy density of 400 Wh/kg as a critical threshold value enabling electric propulsion aircraft, and forecast a time-line of 7 years to achieve this level, assuming that battery technology continues to evolve at the same rate as exhibited currently [125]. Among the established battery technologies, lithium-ion batteries surpass other electrochemical compositions like lead-acid or nickel-type batteries in terms of energy density, and are expected to achieve up to 250 Wh/kg near-term on the cell level [122, 126–128]. However, further improvements are required in order make electric vehicles competitive in terms of range and endurance, as Choi and Aurbach point out [129].[5] Choi and Aurbach argue that existing battery technologies achieve a volumetric energy density of 491 Wh/l, and that the application of new technologies such as lithium-air batteries may lead to an increase in battery energy density by a factor of three in a time-frame of only a decade. Rahman et al. even anticipate an increase in energy density by a

[4] The rule of thumb for kerosene-fueled rotorcraft attributes approx. 25 % of the aircraft mass to the carried fuel. A direct comparison however is flawed as these aircraft will exhibit much larger range potential due to the higher energy density of kerosene compared to batteries.
[5] Petrol achieves an effective energy density of approximately 1750 Wh/kg [127].

factor of 5 to 10 compared to lithium-ion technology, yet point out that numerous technological challenges remain to be overcome [128]. Hepperle expects lithium-air batteries to achieve 800 to 1750 Wh/kg by 2025, and up to 500 Wh/kg more short-term [122]. Pornet et al. assume future energy densities of up to 2000 Wh/kg, applying a value of 1400 Wh/kg at pack level for the studied design. After reviewing the state-of-the-art research activities in lithium-air battery technology, Grande et al. come to a more conservative conclusion, forecasting the possibility of future batteries to achieve practical energy densities of 500 Wh/kg on the pack level, considering all identified constraints.
In view of the above, the battery for the example test-case is assumed of the lithium-ion type. The potential of this technology is exploited to the maximum, yielding a specific energy density at the cell level of $e_{cell} = 250\,\text{Wh/kg}$. An integration factor of 1.2 is applied to obtain the actual battery energy density at pack level, yielding an effective battery specific energy of $e_{batt} = e_{cell}/1.2 = 208.3\,\text{Wh/kg}$. Based on the battery technology selection and the data published by Omar et al., the battery Peukert factor is set to 1.03 [130].

The total efficiency η_{tot} of the propulsive chain is another decisive factor for eVTOL viability, as evident from the T0 modeling description in chapter 3.2. The contributing factors are the efficiencies of the power electronics η_{pe}, the electric motor η_{mot} and the propeller η_{prop}. Fredericks et al. give a range of 81 % to 90 % for the total propulsive efficiency of electric aircraft [121]. Moore et al. suggest efficiencies for the electric chain (motor and power electronics) of up to 95 % [123], and Hepperle suggests similar values of up to 94 % [122]. Compared to contemporary technology, these values appear optimistic. Exploiting modern silicon-carbide technology to its full potential allows power electronics to reach efficiencies of up to 98 % according to Zhang and Tolbert [131]. Electric motors would then need to reach efficiencies of 96 % to 97 % to achieve the total electric efficiencies stated by Moore et al. and Hepperle. Whereas carefully designed electric motors may reach such efficiencies in peak, the motor efficiency is a function of its rotational speed, which will likely be sub-optimal in cruise flight. Consequently, the efficiency of the electric motor is assumed at 95 %. According to Raymer, well-designed turboprop propellers may reach efficiencies above 80 % [132]. However, propellers sized for both hovering and cruising flight are a compromise design, in which the hovering thrust requirements will significantly influence the propeller sizing. The propeller is hence expected to not achieve these peak levels of efficiency in cruise flight, as the thrust level and rotational speed will likely be sub-optimal in this flight state.[6] This holds particularly true in case fixed-pitch and rpm-controlled propellers are used. The propulsive efficiency of the propeller is thus set to 73 %, derived from typical propeller operating maps as published by Raymer [132]. Overall, this yields a total propulsive chain efficiency of 68 %:

$$\eta_{tot} = \eta_{pe}\eta_{mot}\eta_{prop} = 0.98 \times 0.95 \times 0.73 = 0.68 \tag{4.1}$$

With the projected performance characteristics at the current level of decomposition established,

[6] Balancing conflicting objectives for cruising and hovering flight is a well-known dilemma in rotorcraft design, strikingly illustrated by Prouty's postulation of the "helicopter designer's dilemma": *Whatever helps forward flight hurts hover, and whatever helps hover hurts forward flight* [133].

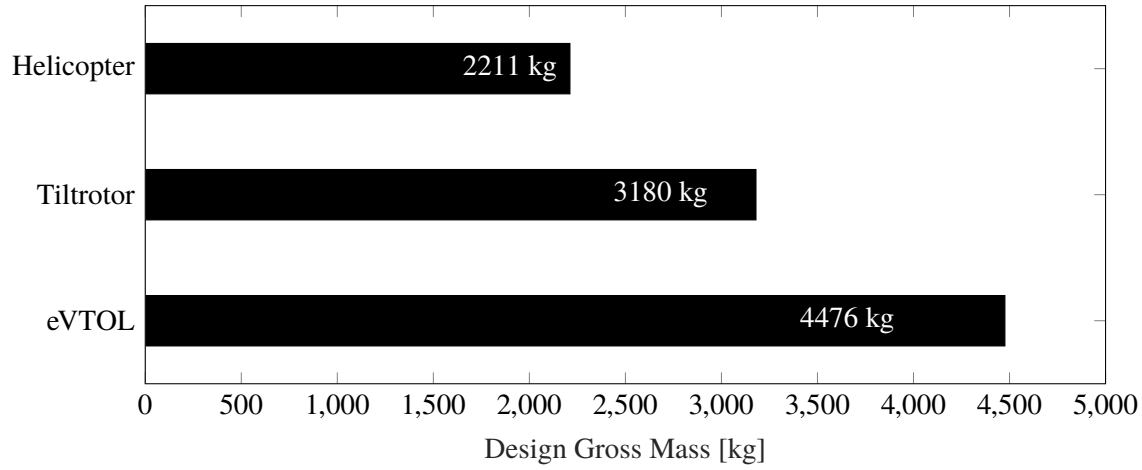

Figure 20 Tier-0 deterministic reference DGM per rotorcraft type for the UAM mission.

the actual design loop is performed. As the initial sizing applies the reference baseline values for the technical model parameters, i.e. the expected behavior, the deterministic reference design is obtained from the automated T0 sizing framework, built upon the T0 models:

$$\sum_{i=1}^{k} f_{i,T0}\left(\vec{p}_{T0,ref}\right) \mapsto \mathrm{DGM}_{T0,ref} \tag{4.2}$$

With the reference assumptions taken in table 6, and the requirements outlined in chapter 4.1, the resulting deterministic reference DGM required to satisfy the specified UAM mission is obtained. Figure 20 shows the results for all rotorcraft types in the scope. As expected, the helicopter configuration proves the most mass-efficient and exhibits the lowest DGM. The tiltrotor requires a 969 kg or 44 % higher DGM to achieve the mission. The required mission trip distance is apparently too short to allow the superior cruise efficiency of the tiltrotor to compensate for its inferior mass efficiency. The discrepancy in DGM is even more significant for the eVTOL aircraft, which requires a 2265 kg or 102 % larger mission takeoff mass for the same set of requirements. The inferior energy density of the battery compared to kerosene apparently dominates over the significantly improved cruise efficiency.

As there is no previous-level model yet against which to validate a model-fidelity transition, this concludes the MDP for the T0 phase.

4.2.2. Attribution of Uncertainty and Generation of the Computation Grid

The IDL progresses with the Robust Architectural Design Process (RADP), and the attribution of uncertainty to the previously determined system characteristics as the first step. Naturally, the level of uncertainty present at the T0 stage is vast. The simplistic modeling introduces significant model-inadequacy-type uncertainty. Furthermore, uncertainty of the parametric-variability kind is severe, since no specificities of the design candidates are yet established. Hence, the correlation between the PA and the assumptions taken in the TA inevitably is generalizing the system behavior significantly at this point. More concretely, the expected performance characteristics of the investigated rotorcraft types, see table 6, are set to typical values for the particular type

	H/C	T/R	eVTOL
PL	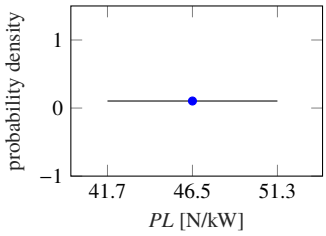	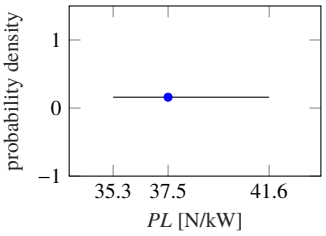	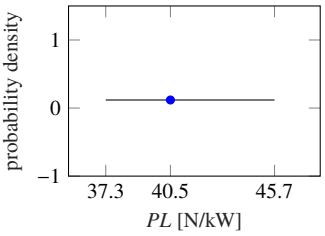
L/*D*	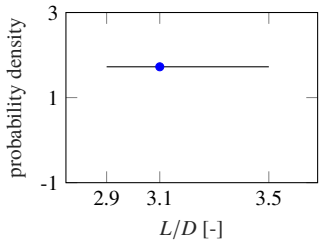	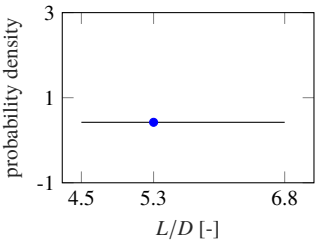	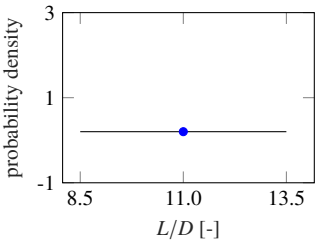
EM	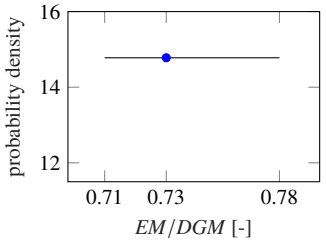	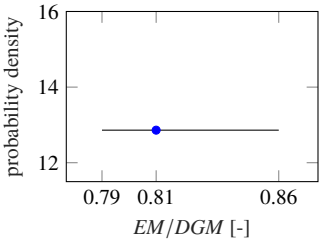	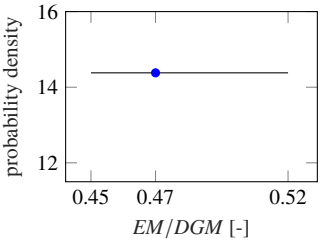
sfc	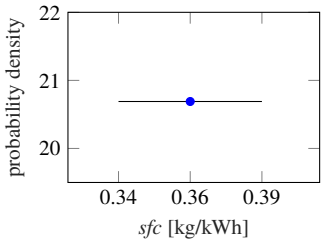	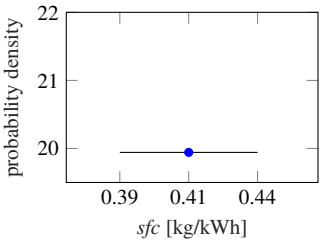	Not applicable
e_{cell}	Not applicable	Not applicable	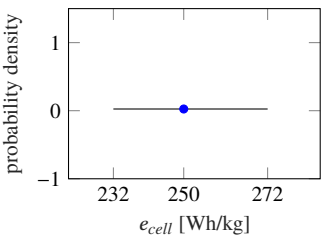
η_{tot}	Not applicable	Not applicable	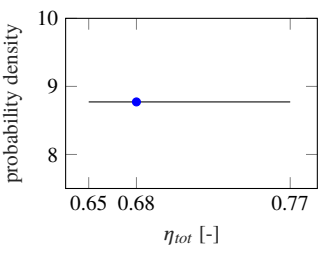

Table 7 Tier-0 uncertainty allocation to technical model parameters. The reference value is indicated as a blue marker.

of rotorcraft. Whereas this empirical data may be refined by adjusting the projected values for anticipated specificities of the future design resulting from the mission scenario,[7] the level of parametric-variability uncertainty inevitably remains vast at the T0 stage due to the simplistic modeling.

Therefore, as a first step of the probabilistic analysis of the design problem, the prevailing uncertainty in the system characteristics $\vec{t}_{T0}$ is estimated in order to define the probability space $\mathcal{P}_{T0}$ of the specific design problem at hand, as foreseen in the RADP. The confidence interval attributed to each parameter of system behavior is shown in table 6 alongside the predicted system performance, i.e. the baseline values of the reference design.
Overall, a consistent strategy is applied in the definition of the confidence intervals and the probability distributions per technical model parameter for all configurations. Arguably, the confidence intervals for the eVTOL architecture, and to a lesser degree for the tiltrotor configuration, could be enlarged compared to the conventional helicopter as a concession to the notionally deeper level of uncertainty inherent to these configurations. This notion is based on the low number of realized designs of these types, and hence the small or non-existent sample size present in the database, reducing the certainty of the projected reference values $\vec{t}_{T0,ref}$ for the system behavior. Furthermore, the development and manufacturing experience for these configurations is certainly lower than for the more common helicopter, indicating that uncertainty of the residual-variability type in the form of "unknown-unknowns" may be increased. However, the example demonstration executed here aims at demonstrating the developed methodology rather than at exploring the defined generic UAM scenario as a real design problem. Therefore, in order to enhance the direct comparability of the competing designs with the user requirements, and to provide more clarity about the methodologies' characteristics and virtues, the confidence intervals in this test case are globally defined in a comparable manner for all configurations in the scope.

In reference to the vast uncertainty at this stage, the confidence intervals are defined correspondingly broad. The most-influential parameter is the *EM*/*DGM* ratio. Due to the high level of uncertainty at the T0 stage, the confidence intervals are generally defined asymmetrically towards the higher end of the spectrum, which is defined comparably for all configurations. As an exception, a symmetrical *PL* interval is selected for the helicopter with respect to the reference value, whereas a bias towards the lower end of the spectrum is chosen for the other configurations. The L/D ratios for the helicopter and the tiltrotor are asymmetrical, since improvement potential is seen compared to previous designs in case a strong focus is laid on aerodynamics. A more broad but symmetrical distribution for this parameter is adopted for the eVTOL, in line with the discussion in chapter 4.2.1. Finally, the *sfc* for the conventional configurations, and e_{cell} and η_{tot} for the eVTOL design, are considered analogously as energy efficiency parameters. Whereas identical intervals are applied to the helicopter and tiltrotor, the interval for η_{tot} is extended towards higher efficiencies in light of the discussion in the previous chapter.

With the confidence intervals defined, the definition of the probability space $\mathcal{P}_{T0}$ is completed by

[7] For example, hover-centered missions likely yield designs of low disk load and hence high power loading.

attributing a probability distribution for the expected values in these intervals. As discussed above, it is not possible to justify an informed assumption about how the realized designs will compare to those available in the database at this stage, as the design is described only on the system level yet. In the terminology introduced in chapter 2.3.1, the level of uncertainty in the T0 stage is of the "recognized ignorance" degree, cf. figure 12. Consequently, a uniform Probability Distribution Type (PDT) is selected for all parameters, as depicted in table 7, in order to reflect this pronounced ignorance concerning the system characteristics. The reference assumptions are shown in table 7 in the form of blue markers.

With the probability space defined, the computational grid for the subsequent probabilistic analysis is generated with the LHS method. The factors listed in table 6 are stochastically varied. Up to 30 individual instances per factor populate the computational grid, which in total contains 6 420 000 design candidates. The applied method ensures that the defined design space is fully covered, and that the probability distributions per uncertainty variable are correctly represented.[8] With the probability space defined and the computational grid set up accordingly, the probabilistic properties of the design problem are now determined in the next step.

4.2.3. Probabilistic Analysis and Robust Design

The generated computational grid maps the probabilistic design space S_{T0}. Every entry m in this grid corresponds to a design candidate with a specific set of technical model parameters $\vec{t}_{T0,m} \in \vec{t}_{T0} + \delta\vec{t}_{T0}$ out of the defined probability space. In order to compute the stochastic properties of S_{T0}, each of these design candidates is sized to achieve the requirements. The simulation requires a runtime of only several minutes despite the large number of necessary sizing routine executions on a standard desktop PC with 8 CPU cores, as the computational effort associated with the T0 model is low.

Figures 21 and 22 show the outcome of the T0 probabilistic analysis. The PDF of the DGM required to satisfy the user requirements are shown for the three studied configurations in figure 21. A series of configuration-related characteristics can be observed. The difference in overall rotorcraft size for the different configurations observed in the deterministic sizing, cf. figure 20, shows again in terms of DGM. More notably, however, is the severe difference in the obtained probability distributions for the different rotorcraft types. The helicopter shows the densest DGM probability distribution, indicating that this configuration is the most robust against the uncertainty in its design space. Compared to the helicopter, the tiltrotor proves more affected by the uncertainty. However, a viable solution is found for all entries in the tiltrotor computational grid. This is not the case for the eVTOL configuration, for which 9.5 % of the design candidates do not converge successfully. The respective system performance characteristics $\vec{t}_{T0,m}$ of this subset of eVTOL design candidates are insufficient to allow performing the design mission. A further 10.9 % of the eVTOL designs converge to DGM above 12 000 kg and hence can be considered non-viable solutions as well. Consequently, as also evident from its widely-scattered probability distribution, the robustness of the eVTOL configuration is significantly lower compared to the conventional

[8] See chapter 3.3.2 for the description of this method.

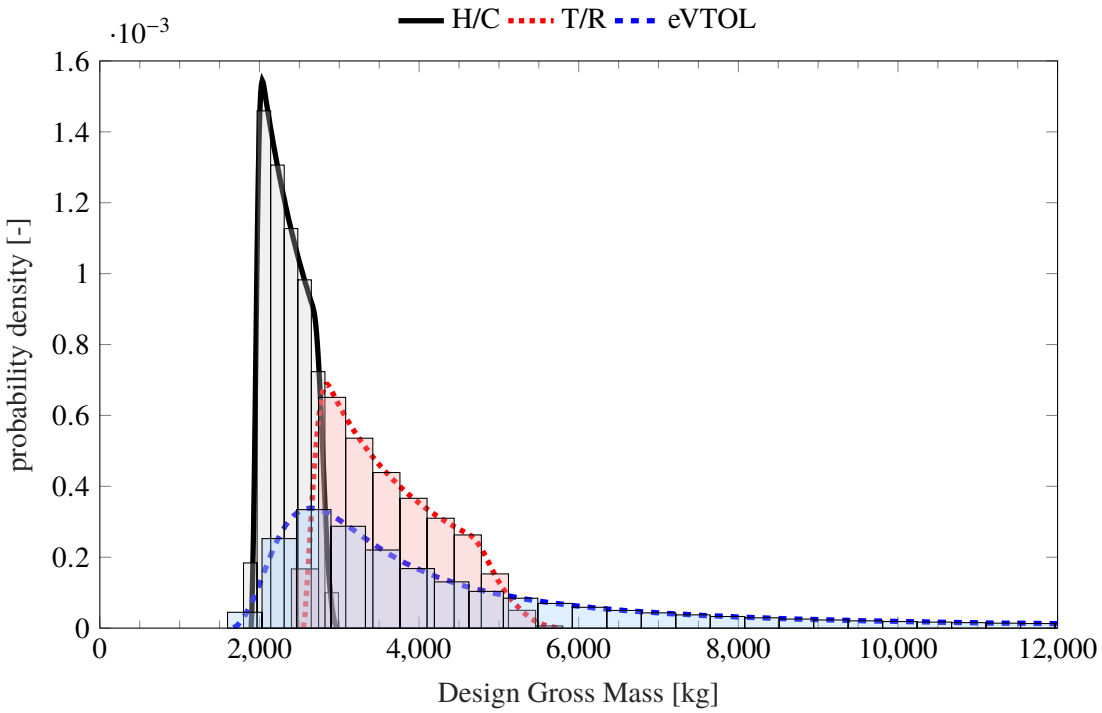

Figure 21 Tier-0 Robust Design results: Probability Density Function for the required DGM.

designs for the design mission of two successive 80.5 km trips. Different than for the conventional configurations, the eVTOL configuration is not robust against the uncertainty in the probability space $\mathcal{P}_{T0}$. However, a significant viable design space is evidently existing nonetheless. The experience-based T0 model, in lieu with the established confidence intervals, therefore proves insufficient to evaluate the robustness of the eVTOL concept. Due to the lack of available data, the confidence intervals need to be set too broadly to obtain a conclusive analysis.

In interpretation of the T0 results, the mass efficiency of a rotorcraft configuration seems a primary impact factor in terms of its influence on the robustness in the defined design problem. Those rotorcraft configurations with relatively large *EM* fractions (tiltrotor and eVTOL) show an increased sensitivity to the model-related uncertainty. Apparently, the impact of requiring additional mission energy capacity by increasing the fuel tank or battery capacity in order to compensate for lower than expected performance characteristics is more severe for these aircraft, as the associated snowball effect on the overall gross mass increase exceeds that of the more mass-efficient helicopter configuration, detrimentally affecting the configuration's robustness for a fixed-distance design mission. If confirmed in the subsequent tiers, this represents a first interesting configuration-related finding of the example test-case.

With the probability density functions of the design problem available, the analysis progresses with the evaluation of the CDF, depicted in figure 22. As introduced in chapter 3.3.2, the CDF corresponds to the likelihood with which a design of a specific DGM achieves the design mission in spite of the prevalent uncertainty. The helicopter configuration achieves a greater robustness in its reference design than the tiltrotor, with a robustness against 38 % and 34 % of the failure cases,

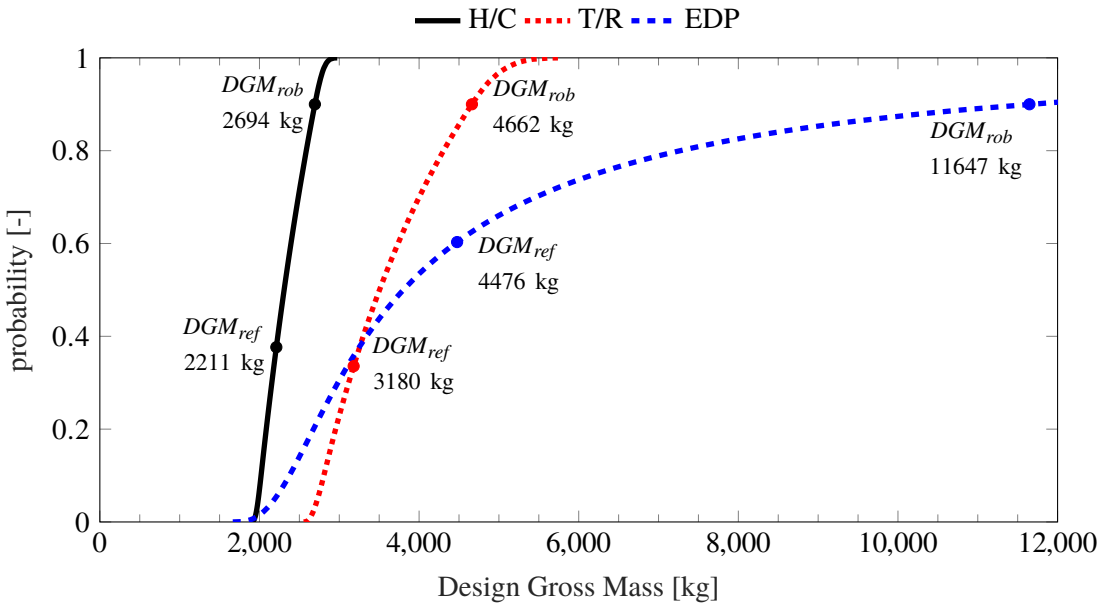

Figure 22 Tier-0 Robust Design results: Cumulative Distribution Function for the required DGM.

respectively. For the eVTOL configuration, however, the deterministic reference design achieves a significantly higher value of 60 %, which to a large degree may be attributed to the fact that the significant subset of eVTOL design candidates which fail to converge is not included in the genesis of the CDF. Further analysis in the subsequent design loops based on model-based design will provide a more meaningful analysis of this concept.

The probabilistic properties of the T0 design problem are now known. To exploit this data, a robust DGM for each rotorcraft type is derived in a next step. The robustness sought is customizable, as the definition for the CDF value constituting a robust design is an user input. This choice should be defined in harmony with the global risk strategy for the design task at hand. For example, in case the confidence intervals and probability distributions are set conservatively, a more aggressive strategy for defining a robust design may be suitable, and vice versa. Within the framework of this study, a design is considered robust when it copes with 90 % of the uncertainty range, i.e. at a CDF value of 0.9.

The varying sensitivity against the underlying uncertainty manifests in the respective required increase of the robust DGM compared to the reference ones, shown in figure 22 and summarized in figure 23. The T0 design loop positively verifies that all studied rotorcraft configurations are capable of complying with the specified user requirements. However, whereas an increase of DGM of 22 % suffices to cover the proclaimed uncertainty at the T0 level for the helicopter configuration, the gross mass margin required to reliably satisfy the design mission increases to 47 % for the tiltrotor, and even 160 % for the eVTOL. The helicopter configuration hence proves the most robust candidate for the present design problem at this initial stage. The eVTOL configuration in turn shows the lowest level of robustness, and even exhibits convergence issues, which indicate insufficient overall robustness in the T0 probability space.

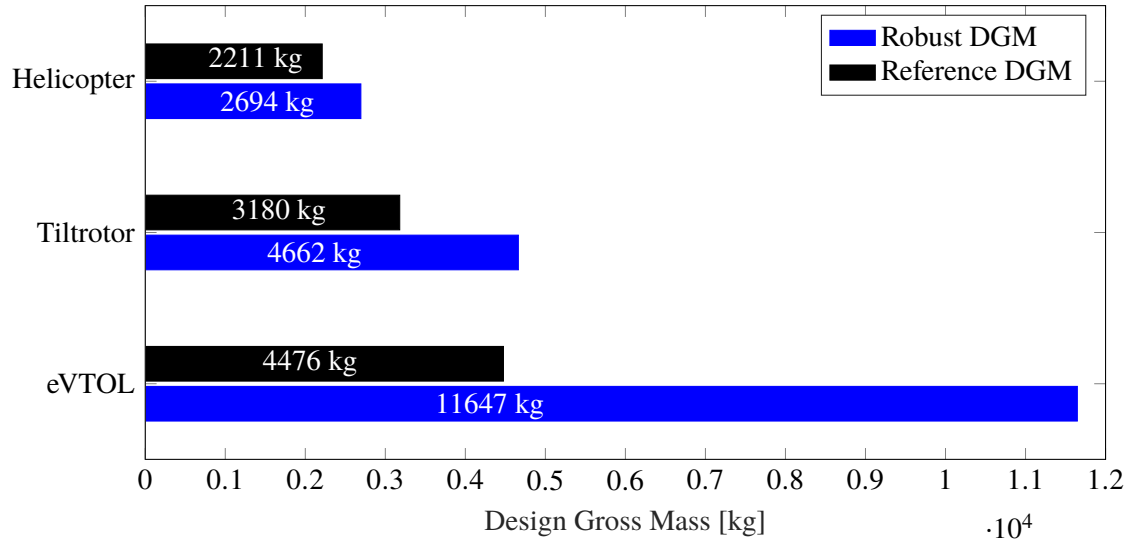

Figure 23 Tier-0 robust DGM per rotorcraft type for the UAM mission.

	$(EM/DGM)_{ref}$	χ_{EM}	$(EM/DGM)_{rob}$	Δ_{EM}
H/C	0.735	4.99 %	0.772	0.037
T/R	0.809	5.61 %	0.854	0.045
eVTOL	0.470	12.94 %	0.531	0.061

Table 8 Tier-0 resulting empty mass control variable χ_{EM} and robust EM/DGM fractions to obtain a robust design.

To conclude the T0 phase, and in order to prepare the subsequent design phase, robust system performance requirements are derived from the obtained data. Using the determined robust DGM as the target values, iterative model executions of the T0 sizing framework are performed. A target-search algorithm is deployed in the quest for the corresponding control variable on the EM χ_{EM}, which yields the respective target robust DGM of each configuration. For the T0 model, the EM of any design is directly derived from the EM/DGM fraction contained in $\vec{t}_{T0}$ during the sizing. The EM of the robust design is then obtained by applying χ_{EM} on the reference design EM as follows:

$$EM_{rob} = (1 + \chi_{EM})\, EM_{ref} \tag{4.3}$$

The outlined target search approach ensures that χ_{EM} results to exactly the value needed for controlling the determined uncertainty magnitude. The T0 EM control variables are shown in table 8 alongside the resulting robust EM fractions. Note that the stated design margin exclusively covers the specified model-related uncertainty, whereas a real design problem should take further epistemic and aleatory uncertainties into consideration in a more holistic approach.[9] As expected from the results presented above, the helicopter configuration requires the lowest Δ_{EM} to obtain a robust design, followed by the tiltrotor and the eVTOL designs.

In conclusion of the T0 design loop, the baseline values for the remaining T0 system characteristics, and the design decisions taken on the T0 level, are set as requirements for the subsequent phase in

[9] See chapter 5.4 for a detailed discussion of aspects to consider when applying the developed methodology to practical design problems.

the RA:

$$\vec{d}_{T0,DoF,rob} = (rcType)_{T0,rob} \subset RA_{T0} \quad \text{and} \tag{4.4}$$

$$\vec{t}_{T0,rob} = (sfc, PL, L/D)_{T0,ref} \subset RA_{T0} \quad \text{for H/C and T/R and} \tag{4.5}$$

$$\vec{t}_{T0,rob} = (\eta_{tot}, e_{cell}, PL, L/D)_{T0,ref} \subset RA_{T0} \quad \text{for eVTOL.} \tag{4.6}$$

4.3. Conceptual Design: Tier-1 Design Loop

The design space now opens up significantly as the system's architecture is being developed into the major sub-systems at the T1 level of decomposition, while developing the functional and technical requirements in parallel. In a real design problem, numerous trade studies and optimization routines would be performed to determine ideal values for sub-system design parameters such as disk load, wing loading or tail rotor type. However, as the aim of this test case is to demonstrate the developed methodology and a full design study is out of scope, the design degrees of freedom in $\vec{d}_{T1}$ are instead set to reasonable values, and this single design of each rotorcraft type is developed further. Table 9 provides an overview of selected primary T1 design parameters ($\vec{d}_{T1,sel} \in \vec{d}_{T1} \subset \vec{p}_{T1}$) and their chosen values.

	Parameter	Baseline Value
H/C	Main Rotor Number	1
	Anti-Torque Type	Shrouded tail rotor
	Disk Load	365 N/m^2
	Rotor Tip Speed	210 m/s
	Landing Gear Type	Retractable wheels
	Engine Type	Turboshaft
	Engine Number	2
	Fuselage Type	Fishtail
T/R	Rotor Number	2
	Disk Load	634 N/m^2
	Rotor Tip Speed	225 m/s
	Landing Gear Type	Retractable wheels
	Engine Type	Turboshaft
	Engine Number	2
	Fuselage Type	Fishtail
	Wing Loading	3686 N/m^2
eVTOL	Thrust Unit Number	6
	Disk Load	634 N/m^2
	Rotor Tip Speed	225 m/s
	Landing Gear Type	Retractable wheels
	Engine Type	Electric motor, direct drive
	Engine Number	6
	Fuselage Type	Fishtail
	Wing Loading	3541 N/m^2
	Battery Cell Energy Density	250 Wh/kg

Table 9 Selected Tier-1 Design Degrees of Freedom ($\vec{d}_{T1,DoF,sel} \in \vec{d}_{T1}$).

	Parameter	Baseline Value	Confidence Interval
H/C	κ in hover	1.12	1.08 to 1.16
	f_{RC} in cruise	Computed	$\pm$ 0.2 m^2
	k_{DL} fraction of DGM	0.03	−0.01, +0.03
	$\bar{c}_d$ in cruise	0.0112	0.008 to 0.013
	EM/DGM	Computed	−0.015, +0.03
	k_{FF}	0.03	$\pm$ 0.02
	f_{Int}	*Not applicable*	
T/R	κ in hover	1.05	1.03 to 1.10
	f_{RC} in cruise	Computed	$\pm$ 0.1 m^2
	k_{DL} fraction of DGM	0.108	−0.03, +0.05
	$\bar{c}_d$ in cruise	0.0103	0.008 to 0.013
	EM/DGM	Computed	−0.02, +0.04
	k_{FF}	0.03	$\pm$ 0.02
	f_{Int}	*Not applicable*	
eVTOL	κ in hover	1.05	1.03 to 1.10
	f_{RC} in cruise	Computed	$\pm$ 0.1 m^2
	k_{DL} fraction of DGM	0.01	−0.005, +0.005
	$\bar{c}_d$ in cruise	0.0109	0.008 to 0.013
	EM/DGM	Computed	−0.02, +0.04
	k_{FF}	*Not applicable*	
	f_{Int}	1.2	$\pm$ 0.05

Table 10 Subset of Tier-1 reference technical model parameters subjected to uncertainty.

4.3.1. Model Development and Deterministic Reference Design

The T1 design loop commences with the generation and validation of the T1 model. To this end, the model is first populated with the baseline design parameters ($\vec{d}_{T1,sel}$) presented above. Second, baseline assumptions are taken for the parameters in the further developed TA, which now resides on the major sub-system level as the design resolution progresses one level. With this increase in fidelity, the model is now capable of computing the performance characteristics contained in $\vec{t}_{T0}$ from a set of sub-models $f_{i,T1}(\vec{p}_{T1})$. These sub-models take inputs from the T1 level and operate on basic momentum theory with classical empirical correction factors.[10] Table 10 provides an indicative subset of selected high-impact T1 model parameters $\vec{t}_{T1,sel} \in \vec{t}_{T1} \subset \vec{p}_{T1}$. The generation of the T1 deterministic reference model follows the established logic, in that the sub-system characteristics $\vec{t}_{T1} \subset \vec{p}_{T1}$ are set under consideration of the design decisions taken, listed in $\vec{d}_{T1}$.

With the reference model parameters set, the MDP progresses. A regular deterministic sizing is conducted. Subsequently, the resulting reference design is analyzed in off-design conditions. The data generated then allows to evaluate the system's behavior and characteristics against the technical requirements, which were set on the preceding level of decomposition. The resulting reference DGM for the T1 model are shown in figure 24. Comparing the T1 reference DGM to the ones from the previous T0 loop, cf. figure 20, the consistency between the tiers is favorable. For all configurations, a minor but recognizable decrease in reference DGM is obtained, indicating

[10] See chapter 3.2.1 for a detailed description of the T1 model.

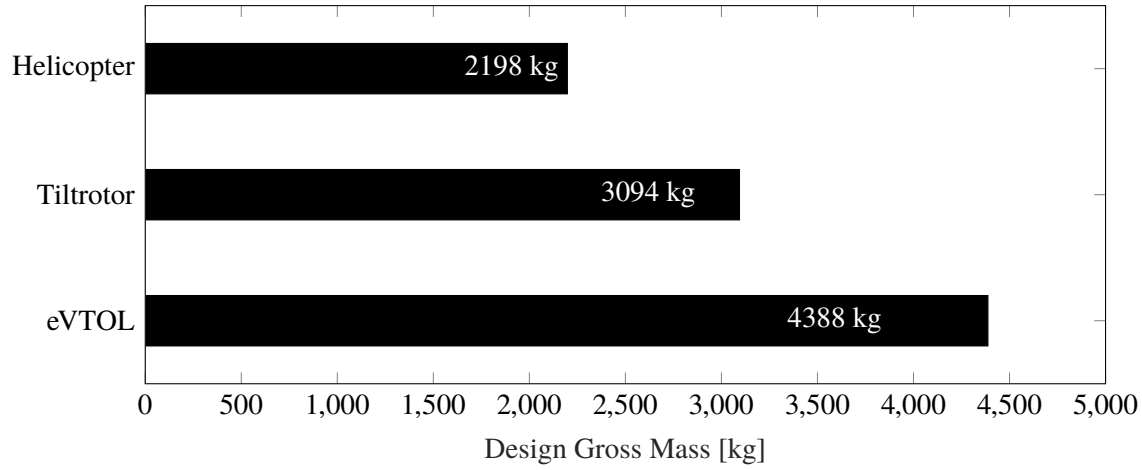

Figure 24 Tier-1 deterministic reference DGM per rotorcraft type for the UAM mission.

that the T0 performance metrics $\vec{t}_{T0}$ were estimated reasonably. The subsequent model transition validation provides substantiation of this hypothesis.

The objective of the model transition validation is to confirm the consistency across the model fidelity levels. As an integral element of the proposed design methodology, consistency is ensured by requesting the design of any subsequent phase to satisfy the threshold system performance specified in the preceding phase. To this end, the previously estimated (T0 design loop), and now computed (T1), performance characteristics of the $(n\text{-}1)^{\text{th}}$ level are compared in the relevant design mission conditions.[11] At the T1 stage, the upper-level performance characteristics consequently correspond to the system-level (T0) performance parameters.

The validation plots for the T0-to-T1 model transition for the three rotorcraft configurations are shown in figures 25, 26 and 27. The system's emergent behavior as computed by the T1 model is compared to the performance requirements set at the T0 level, whereas these requirements correspond to the baseline values listed in table 6. The increased fidelity of the T1 model is immediately evident from the more pronounced resolution of system behavior compared to the metric-based T0 model, which is limited to distinct characteristic operating points. Alongside the performance of the T1 initial deterministic design, the robust design of the T0 stage is indicated on the graphs for reference. Due to the excessive robust DGM of the eVTOL configuration in the T0 loop, the T0 robust design does not appear in the power loading chart in figure 27. However, as the valid system behavior range extends well above the reference eVTOL $DGM_{T0,ref}$, this is considered unproblematic for model validation purposes. The model transition is deemed validated successfully if the T1 model does not violate the robust technical parameter requirements ($\vec{t}_{T0,req} \in RA_{T0}$), set at the end of the T0 loop. Projected system behavior within these bounds corresponds to achieving the requested performance in the relevant conditions of the underlying design mission, and hence serves to ensure the consistency of the T0 design decisions henceforth across the tiers. As evident from figures 25, 26 and 27, all threshold values are achieved by the three configurations. The model transition is therefore considered validated, and the T1 robust

[11] The developed model transition logic and methodology is outlined in detail in chapter 3.3.1.

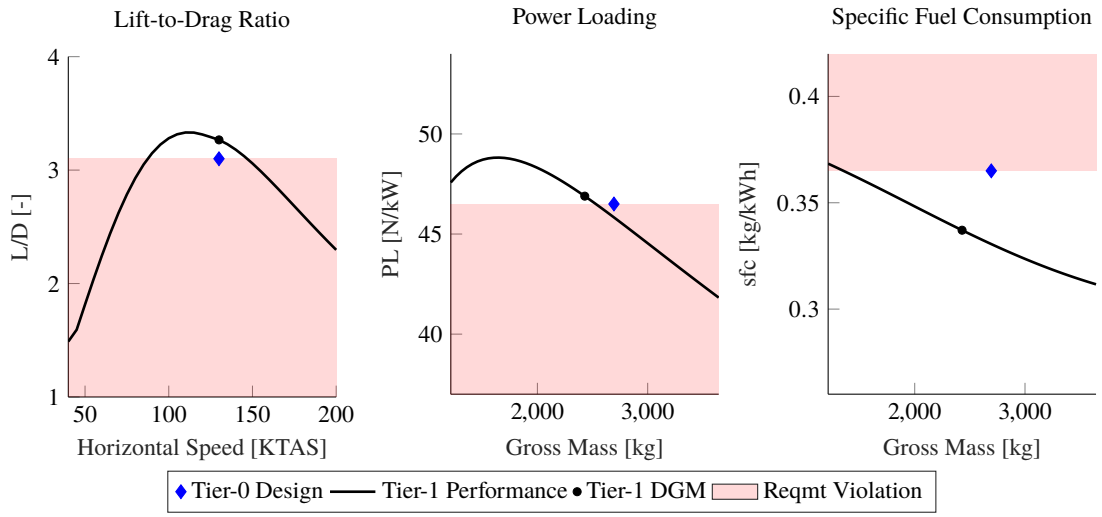

Figure 25 Tier-0 to Tier-1 model transition validation plots for the H/C configuration.

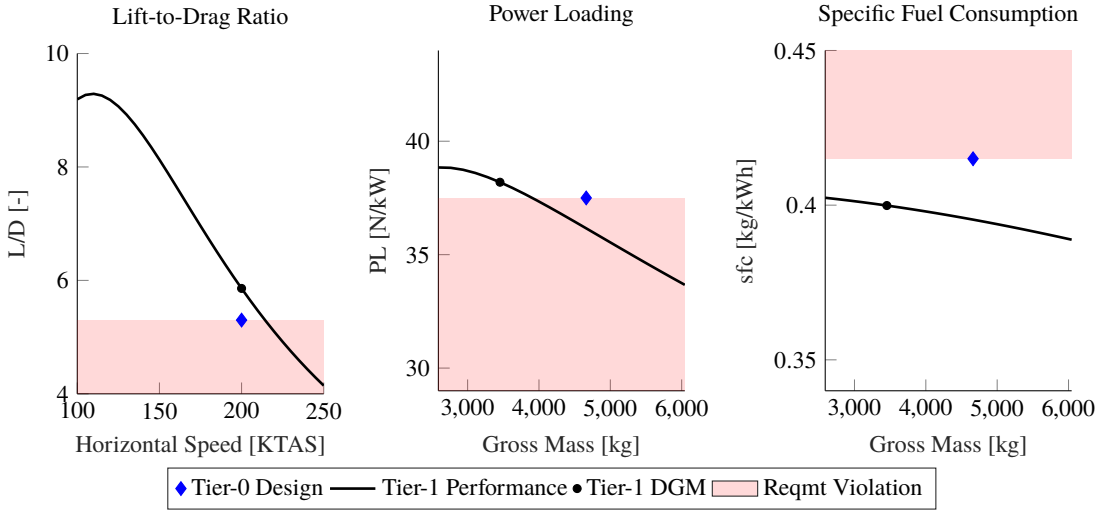

Figure 26 Tier-0 to Tier-1 model transition validation plots for the T/R configuration.

design loop is continued. Also indicative from the model transition plots is that the T1 designs outperform the T0 designs in the operating conditions relevant for the design mission, which explains the decreasing trend in reference DGM observed above.

4.3.2. Attribution of Uncertainty and Generation of the Computation Grid

With the consistency and adequacy of the established models confirmed, and the reference designs sized, the focus turns to investigating the model-related uncertainty prevalent in the T1 environment. Different to the metric-based T0 model, the system performance is now determined in the form of emergent behavior, resulting from estimates generated from sub-models of the performance characteristics at the sub-system level. The increase in model fidelity, however, is inevitably accompanied by a step-increase in the number of model parameters, i.e. $\dim(\vec{p}_{T1}) \gg \dim(\vec{p}_{T0})$. This increase is causing a dilemma which Koch et al. refer to as the *Problem of Size* in the model-based design of complex systems [102], already highlighted as a challenge in robust model-based

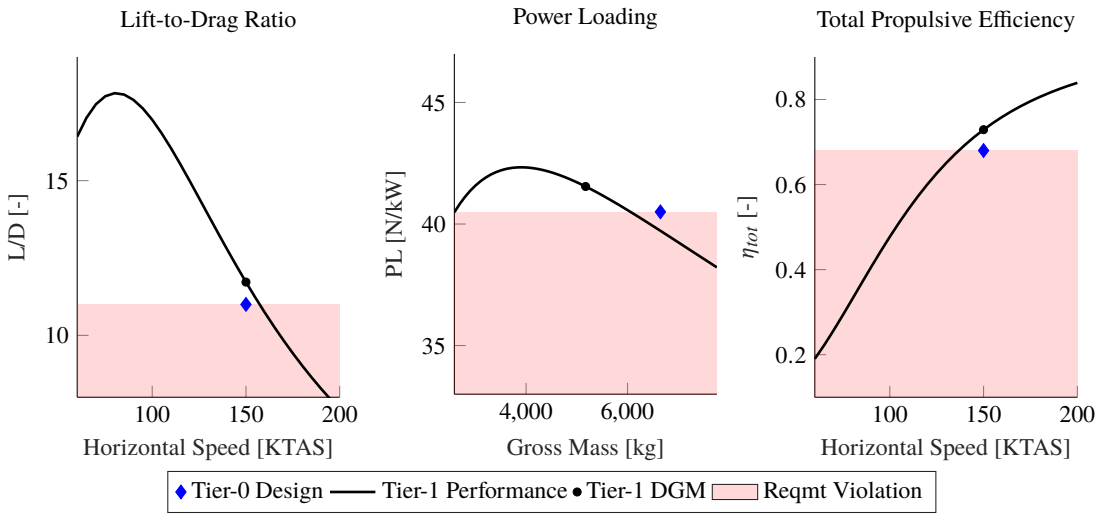

Figure 27 Tier-0 to Tier-1 model transition validation plots for the eVTOL configuration.

design in chapter 2.4.1. Koch et al. argue that traditional parametric design and analysis becomes ineffective once the size of the problem exceeds a certain threshold, whereby the number of model parameters is directly related to the problem size, as the increasingly complex and interdependent modeling causes excessive computational efforts. As the correlation between the number of model parameters and increasing model fidelity is usually exponential, and as probabilistic analysis requires numerous model executions to generate sufficiently reliable data, the problem of size poses a significant challenge to probabilistic model-based design. This dilemma is certainly relevant in the set-up of the probabilistic numerical experiments in this work, as the number of execution points Ω_n in the probability space $\mathcal{P}$ increases exponentially with the number of factors exposed to uncertainty $n_f = \dim(\Delta\vec{t})$, and the number of cases evaluated per factor n_c:

$$\Omega_n = n_c^{n_f} \tag{4.7}$$

Thus, Ω_n corresponds directly to the number of design candidates to be sized and evaluated in the frame of the probabilistic analysis. Considering that numerous model executions are required to perform the sizing and probabilistic analysis of each design candidate, the total number of model executions is further orders of magnitude above Ω_n.

At the T0 stage, both the dimension of the model and the computational effort for the model execution are low. Therefore, the problem of size is not yet relevant and does not mandate any limitation of the numerical experiment. All technical model parameters $\vec{t}_{T0}$ can be subjected to uncertainty. However, this is no longer the case for the T1 stage, in which the model complexity reaches significantly higher levels, as demonstrated by the dimension of the model parameter vector:

$$\dim\left(\vec{t}_{T1}\right) = 53 \qquad \text{whereas} \qquad \dim\left(\vec{t}_{T0}\right) = 5 \tag{4.8}$$

As evident from equations 4.7 and 4.8, the number of factors $n_{f,T1}$ subjected to uncertainty in

the T1 probabilistic analysis thus requires restriction, in order to maintain surmountable levels of computational expense. The inclusion of model parameters into $n_{f,TI}$ should be driven by their respective influence on the design in the specific design problem at hand. In case the most-influential parameters can not be selected conclusively, a complementary series of sensitivity studies on the baseline model may be conducted. The most-influential T1 technical model parameters to be subjected to uncertainty during the probabilistic analysis of the test case are selected from previous studies and experience. Table 10 lists these parameters for each investigated rotorcraft configuration. Although $\dim(n_{f,TI}) = 6 < \dim(\vec{t}_{TI})$, a comprehensive coverage of the main impact parameters for cruising, hovering and mass efficiency is achieved.

The probability distribution for each uncertainty parameter is shown in table 11. By increasing the degree of system decomposition and model resolution to the sub-system level, significant epistemic uncertainty is removed from the design environment compared to the simplistic T0 stage. One major contributing factor in this context is related to removing configuration-related uncertainty. As the system is now defined in more detail, i.e. first design parameters are set on the sub-system level, the projection of the system characteristics $\vec{t}_{TI}$ for the model generation can now be performed on a sounder basis. As the technical model parameters on the T1 level are more physical and less abstract than for the T0 metric-based model, a more precise and more refined prediction of their expected value in correlation to the relevant design parameters is possible. In probabilistic terms, model-inadequacy uncertainty is significantly reduced by moving to the next-level design stage. Moreover, as the model fidelity is developed in parallel, the increased resolution of system behavior in the T1 model mimics system behavior more accurately, and therefore reduces the level of parametric variability.

In view of the above, it is deemed appropriate to move to triangular probability distributions, as depicted in table 11. This is a significant improvement, as the description of the probability space no longer only entails solely its span, but its topology as well. Furthermore, the confidence intervals are considerably reduced compared to the T0 stage. The probability data presented is generated from an evaluation of the scenario prescribed in chapter 4.1 in a holistic approach, which includes aspects of requirements, design, as well as as the established ConOps. Naturally, this assessment is subject to a certain degree of subjectivity. Chapter 5.3 discusses the possible impact of this subjectivity on the analysis, and recommendations for future activities in this field are discussed in chapter 6.2.

	H/C	**T/R**	**eVTOL**
κ_{hover}	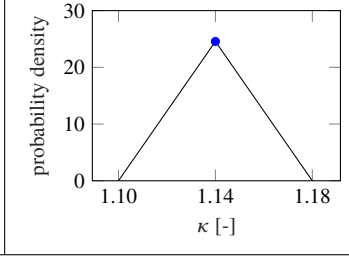	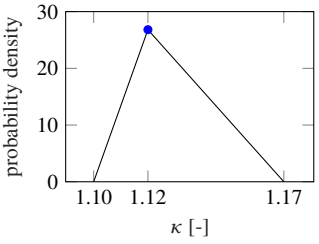	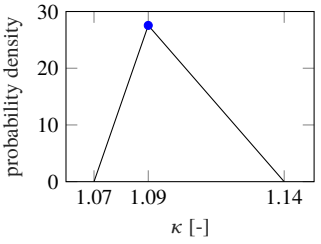

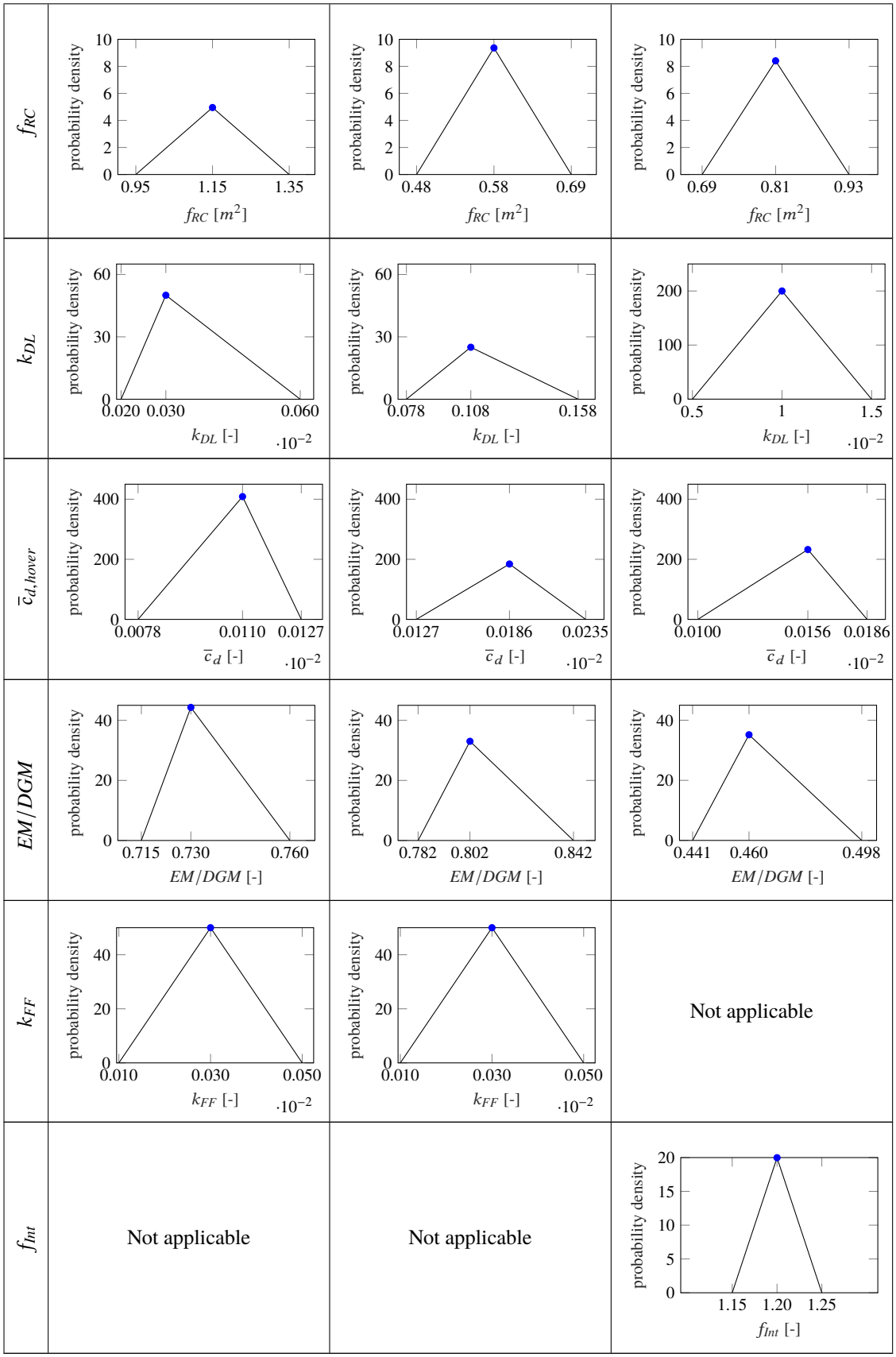

Table 11 Tier-1 uncertainty allocation to technical model parameters. The reference value is indicated as a blue marker.

The following particularities in the definition of the probability space are highlighted, cf. table 11. As pointed out by Harris, the complex aerodynamics of helicopters make predicting their flat plate drag area f_{RC} a particularly challenging task [34]. Consequently, the confidence interval is increased compared to the other configurations. On the contrary, the uncertainty in the EM fraction is slightly increased for the tiltrotor and the eVTOL configuration, reflecting the less profound database underlying the parametric mass estimation. Globally, however, the probability distributions and confidence intervals are deliberately defined on a comparable level for the sake of methodology demonstration. Hence, configuration-related probabilistic properties of the designs are obtained, in contrast to uncertainty-attribution-biased results which may complicate the assessment of the developed methodology in an example-demonstration context.

The probability space $\mathcal{P}_{T1}$ is defined by the probability distributions shown in table 11. The LHS method is deployed once more in the genesis of the computational grid to ensure probabilistically representative coverage of the entire probability space $\mathcal{P}_{T1}$, while minimizing computational effort. Owing to the known disproportionately high significance of the empty mass in the design of airborne vehicles, the number of instances in the computation grid for this factor is increased compared to the other technical parameters in the probability space. More specifically, $n_{c,EM/DGM} = 10$, whereas $n_{c,others} = 6$. The total size of the computational grid results to 233 280. The runtime of the outlined T1 experiment is approximately 22 h per investigated rotorcraft type on a standard desktop PC with 8 CPU cores.

4.3.3. Probabilistic Analysis and Robust Design

The stochastic quantities of the T1 design loop are shown in the form of histrogram plots of the probability distributions of the resulting DGM, and the corresponding PDF, for each rotorcraft concept in figure 28. The CDF is presented in figure 29. Comparing the T0 and T1 probability density functions qualitatively, three distinct differences are apparent. First, the width of the probability distributions is significantly reduced, reflecting the reduced model-related uncertainty in the design space. The increase in model fidelity allows a more precise evaluation of system behavior, manifesting in reduced confidence intervals for the uncertain parameters, and ultimately in reduced scatter of the DGM responses corresponding to discrete sets of $\vec{t}_{T1}$. Second, the shape of all probability distributions is now more centered. This is primarily attributed to the change in the probability distribution type from uniform to triangular distributions, again enabled by the more refined representation of system behavior in the T1 model. Third, whereas the design domains of the three rotorcraft types show significant overlap in the T0 loop, see figure 21, distinctively separated design domains in terms of DGM are obtained in the T1 loop. Consequently, the staggering of the expected gross masses of the different configurations turns from a likely outcome observed in the T0 analysis into a certainty. Therefore, the conclusion that the helicopter configuration promises to turn out the lightest aircraft for the design problem at hand, followed by the tiltrotor and the eVTOL, can now be drawn confidently.

Analyzing figure 28 further, the sensitivity to the underlying uncertainty leads to a significantly reduced interval of possible resulting DGM values compared to the T0 results. This dramatic

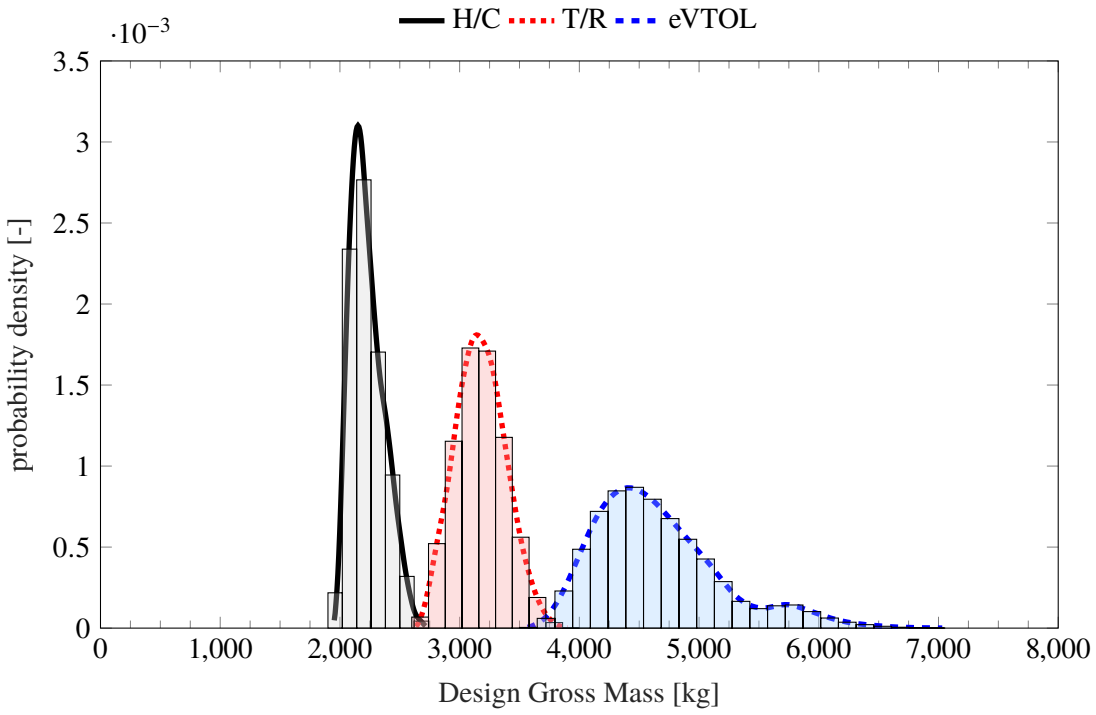

Figure 28 Tier-1 Robust Design results: Probability Density Function

reduction is expected, as the move from the simplistic metrics-based T0 model to the model-based T1 modeling significantly increases the accuracy and reliability of the model. The improvement is relatively the least significant for the helicopter configuration. This is attributed to the fact that the transforming tiltrotor and eVTOL configurations benefit to a larger degree from the improved model resolution, as their system behavior differs to a larger extent depending on the flight state and vehicle flight mode. Interestingly, the eVTOL experiences the largest benefit: a viable design is now obtained for all eVTOL entries in the probability space, as all design candidates converge. However, the fundamental characteristic observed already in the T0 loop remains valid. The helicopter configuration proves the most robust against the uncertainties in the design problem, evident from its probability distribution being the most dense. The tiltrotor configuration is more sensitive, but closes the gap substantially. The eVTOL configuration remains the most volatile, although its feasibility throughout the entire probability space is now confirmed.

Turning to figure 29, this general trend is also observable in the CDF. The benefit from removing epistemic uncertainty by switching to the higher-fidelity model shows in decreased model-inherent uncertainty in the design loop. This is evident from the dramatic decrease in the gap between the deterministic reference and the obtained robust DGM for all configurations, see figure 30. After the T1 design loop, a design margin of 231 kg or 10.5 % in terms of DGM is needed for the helicopter, decreasing the magnitude compared to the previous design loop by a factor of 2. For the tiltrotor, the necessary DGM margin reduces to 360 kg or 11.6 %, representing a reduction by a factor of 4. Again, the most significant gain is generated for the eVTOL configuration. The more-refined T1 model removes the parametric-variability-type uncertainty to a degree that all convergence issues experienced in the T0 design are resolved. A robust design margin of 1005 kg or 22.9 % is

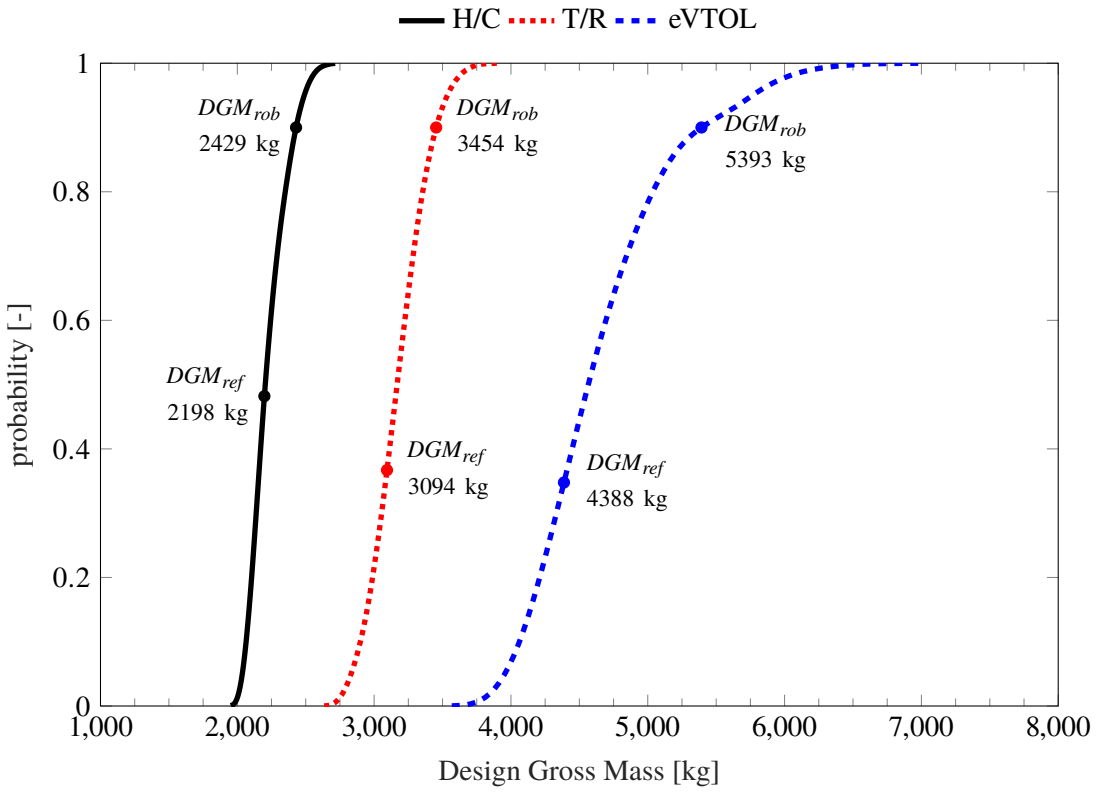

Figure 29 Tier-1 Robust Design results: Cumulative Distribution Function

determined, which is seven times less than the T0 value. As a result, the eVTOL configuration becomes a viable design candidate since the impact of the model-related uncertainty now becomes controllable by a still large but no longer excessive margin on DGM.

Table 12 shows the empty mass control variable values required to achieve robust designs of the determined target design gross masses DGM_{rob}. Interestingly, the control variables do not decline to the same extent as the DGM margins themselves. For the helicopter, $\chi_{EM,T1}$ actually increases compared to $\chi_{EM,T0}$, cf. table 8. The reason for this counterintuitive phenomenon is related to a difference in the way χ_{EM} is applied in the T0 and the T1 models. In the absence of any mass estimation methodology, the T0 model directly applies $\chi_{EM,T0}$ on the reference design EM to obtain $EM_{T0,rob}$, see equation 4.3. The T1 model, in turn, is capable of computing the empty mass of the design depending on sub-system-level parameters, mandating a modification to the way χ_{EM} is used to obtain the robust design. The actual empty mass of the robust design is no longer directly derived from the control variable value, but results from the sub-model in the sizing loop. The EM of the robust design is computed during the sizing loop by applying χ_{EM} on the estimated EM of the design as follows:

$$EM_{rob} = (1 + \chi_{EM})\, EM_{computed} \tag{4.9}$$

As a result, the robust design control variable χ_{EM} from the T0 and the T1 design loops are not directly comparable. To this end, the actual EM difference $\Delta_{EM} = (EM/DGM)_{rob} - (EM/DGM)_{ref}$ is provided in table 12 to provide a directly comparable measure. As expected, the required empty

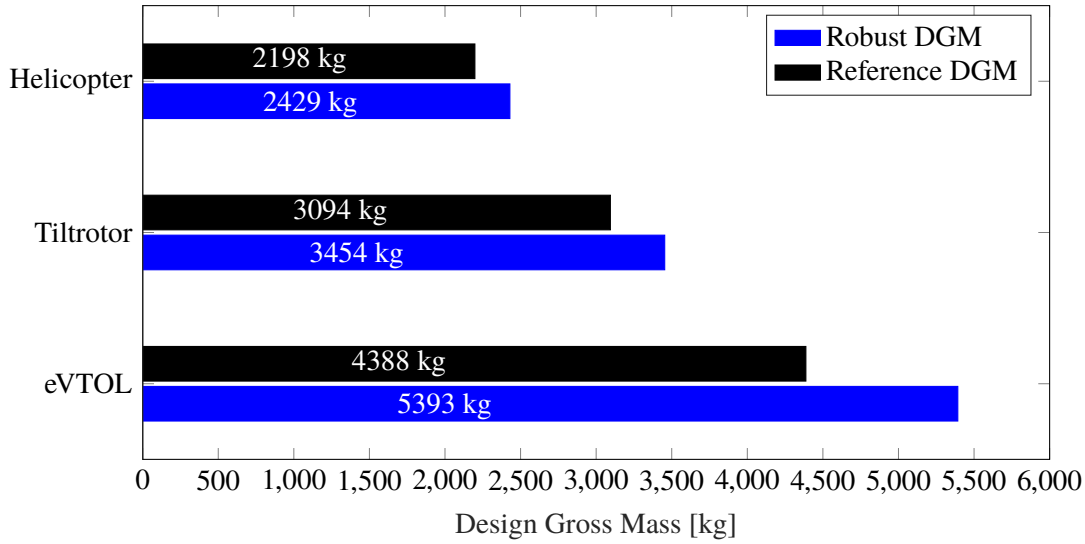

Figure 30 Tier-1 robust DGM per rotorcraft type for the UAM mission.

	$(EM/DGM)_{ref}$	χ_{EM}	$(EM/DGM)_{rob}$	Δ_{EM}
H/C	0.730	6.45 %	0.750	0.020
T/R	0.802	4.59 %	0.818	0.016
eVTOL (excl. Battery)	0.460	6.51 %	0.468	0.008
eVTOL (incl. Battery)	0.899	6.51 %	0.918	0.019

Table 12 Tier-1 resulting empty mass control variables χ_{EM} and robust EM/DGM fractions to obtain a robust design.

mass margins Δ_{EM} decrease considerably compared to the T0 design loop. Reviewing the data in table 12, and the necessary design margins in terms of DGM discussed in the previous paragraph, it becomes evident that the EM control variable is an effective means to control the uncertainty in the model-based design process, however itself is not a suitable measure of the actual robust design margins incorporated into the design across the different rotorcraft types. The tiltrotor configurations requires a lower relative and absolute EM control variable value to control a larger required margin in terms of DGM. For the eVTOL, $\chi_{EM,T1}$ results to comparable levels as for the helicopter when including battery mass, in spite of an even larger discrepancy in required DGM margins. Apparently, due to the more pronounced sensitivity to the EM,[12] a smaller EM control variable value has a larger impact on the high-mass configurations tiltrotor and eVTOL.

In conclusion, all rotorcraft configurations are now viable configuration choices in terms of the ability to control the inherent model-related uncertainty via the developed probabilistic design methodology, although significant differences in overall rotorcraft mass remain. Moreover, the relative staggering of the DGM of the rotorcraft configurations manifests as distinct characteristic property of the investigated design problem in the T1 loop.

In the final step of the T1 design loop, the RA is updated with the determined robust design parameters, as well as its technical model parameters. Using the Main Rotor (MR) as an example,

[12] This larger sensitivity for the tiltrotor and eVTOL configurations on EM is already observed in the T0 loop, see chapter 4.2.3.

the RA now includes:

$$\vec{d}_{T1,DoF,rob,rotor} = \left(DL, \sigma, V_{tip}\right)_{T1,rob} \in \vec{d}_{T1,rob} \quad \text{and} \tag{4.10}$$

$$\vec{t}_{T1,rob,rotor} = \left(f\left(\vec{p}_{T1}\right) \mapsto \kappa, \ldots, f\left(\vec{p}_{T1}\right) \mapsto \overline{c}_d\right)_{T1,rob} \in \vec{t}_{T1,rob} \tag{4.11}$$

Evidently, the complexity of the RA rises analogously with the increasing model fidelity and the inherently soaring resolution of system behavior. The elements contained in $\vec{t}_{T1}$ are no longer restricted to discrete entries at specific operating points. Instead, the actual system behavior[13] is recorded in the updated RA_{T1}, now incorporating $\vec{t}_{T1,rob} \subset RA_{T1}$. Likewise, the design decisions taken on the T1 level are assigned to the RA: $\vec{d}_{T1,DoF,rob} \subset RA_{T1}$.

4.4. Preliminary Design: Tier-2 Design Loop

The final stage of the preliminary design phase is marked by the T2 design loop. The system under design is decomposed down to the system-element level. The fidelity of the applied models increases synchronously, as requested by the adequate-fidelity modeling paradigm. The T2 models mimic the characteristics of the system elements on the T2 level, and the sub-system (T1) and system (T0) behavior is computed:

$$f_{i,T2}\left(\vec{p}_{T2}\right) \mapsto \left(\vec{t}_{T1,computed}, \vec{t}_{T0,computed}\right) \tag{4.12}$$

As for the T1 design, the T2 design degrees of freedom $\vec{d}_{T2,DoF}$ are set to reasonable values for the three competing design concepts instead of comprehensively optimizing the designs via trade-studies, sensitivity studies and optimization routines, in order to limit the scope of the example test-case, focusing on methodology demonstration. Table 13 gives an indicative overview of selected T2 design parameters ($\vec{d}_{T2,DoF,sel} \in \vec{d}_{T2}$).

4.4.1. Model Development and Deterministic Reference Design

Routinely, the T2 loop begins with the generation of the T2 reference model, which is subsequently validated by confirming its conformity with the previously established performance requirements. The first step of the model population attributes the selected design degrees of freedom. Using the MR as the example once again, the design degrees of freedom established at the T2 level include the geometric properties of the rotor blades, such as the number of blades, twist and taper. The projected performance characteristics of the blades are then estimated on the T2 level of fidelity, which relates blade performance to the blade angle of attack and advance ratio. Table 13 shows an indicative overview of baseline values for further selected T2 design degrees of freedom. The model population is then completed by executing the deterministic reference design, in which the dependent design parameters are computed in the frame of the rotorcraft sizing. Subsequently, the generated deterministic reference design is analyzed in off-design conditions, and the model transition validation plots are generated in order to evaluate the consistency of the model transition to the requirements which entered the RA in the previous design phase, since $\vec{t}_{T1} \subset RA_{T1}$.

[13] As presented in figures 25, 26 and 27.

	Parameter	Baseline Value
H/C	Rotor control	Cyclic and collective
	(Main) Rotor solidity	0.0994
	(Main) Rotor blade number	5
	(Main) Rotor twist	linear, $-10°$
	(Main) Rotor taper ratio	1.0
	Empennage configuration	Horizontal and Vertical Stabilizers
T/R	Rotor control	Cyclic and collective
	Rotor solidity	0.12
	Rotor blade number	3
	Rotor twist	non-linear
	Rotor taper ratio	0.8
	Tilting mechanism	Rotor and nacelle fold
	Empennage configuration	H-Tail
eVTOL	Propeller control	rpm control
	Propeller solidity	0.13
	Propeller blade number	5
	Propeller twist	non-linear
	Propeller taper ratio	0.8
	Tilting mechanism	Wing fold
	Empennage configuration	V-Tail
	Battery Cooling	Yes

Table 13 Selected Tier-2 Design Degrees of Freedom ($\vec{d}_{T2,DoF,sel} \in \vec{d}_{T2}$).

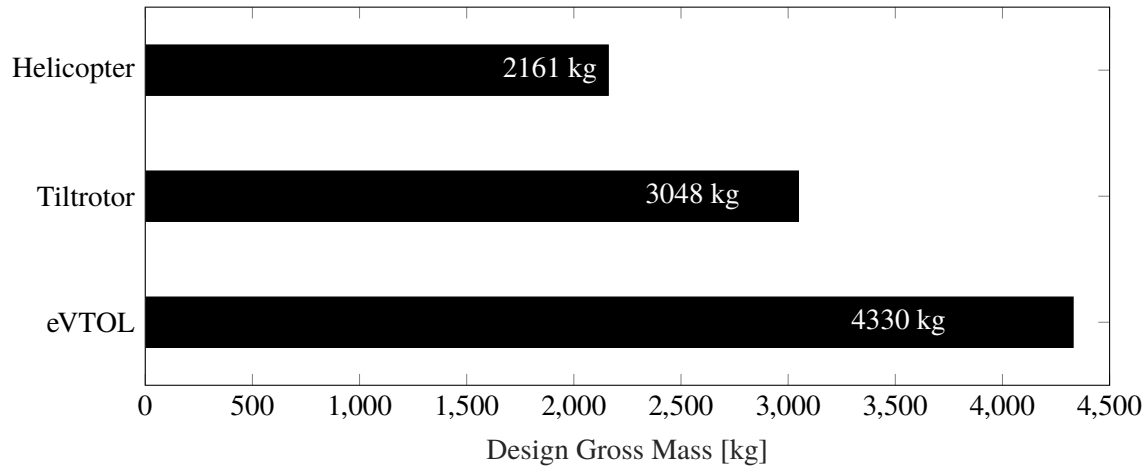

Figure 31 Tier-2 deterministic reference DGM per rotorcraft type for the UAM mission.

Figure 31 shows the resulting reference DGM for the three rotorcraft types in the scope of the example case. The system behavior is now computed from the sub-models deployed on system-element level (T2). The T2 stage marks the highest-fidelity modeling deployed in the methodology. Whereas the T1 model uses constant empirically-defined technical model parameters for model calibration, the T2 model computes these parameters from semi-physical sub-models $f_{T2}(\vec{p}_{T2})$. These sub-models are either calibrated based on the expertise and experience of the designing entity, or alternatively may be calibrated by correlation to high-fidelity analysis, if available. As the T2 model resolution is of sufficient fidelity to effectively implement data from such analysis, deploying selective high-fidelity analyses at this stage may improve the overall quality of the design. Chapter 4.5 discusses the potential of this strategy, and executes a simulated example in this sense. As already observed after the transition from the T0 to the T1 level, the DGM of the T2 sizing routines turn out below the ones sized during the T1 loop, whereas the differences are less pronounced for the step from the T1 to the T2 stage. Overall, the DGM development of each rotorcraft design shows great consistency across the tiers, demonstrating the adequacy of all performed design loops. The evolutionary characteristic in terms of progressively decreasing DGM is desired, as it indicates that the generalizing system performance estimations of the previous tiers globally captured the system behavior well, whereas the refinement of the TA in subsequent tiers enabled a more precise and optimized sizing of the rotorcraft.

The T1 to T2 model transition plots are shown in figures 32, 33 and 34. The relevant design conditions are indicated on each plot, in order to highlight the domains of interest. The design conditions correspond to the mission and point performance requirements described in chapter 4.1. In forward flight, two vertical lines indicate the maximum cruise speed point performance requirements, and the design mission cruise speed. For the eVTOL configuration, these requirements correspond to the same advance ratio μ, see figure 34. In hovering flight, the blade loading for the point performance requirements and for the design mission takeoff is indicated.

The further increase in model fidelity is evident from the improved resolution of sub-system behavior compared to the T1 model. Whereas the T1 model uses almost exclusively constant assumptions for the sub-system level performance characteristics, the T2 model computes actual sub-system behavior based on the design parameters and technical model parameters on the system-element level. In line with the model transition regulation established in the methodology, the transition is considered successful and valid in case the T2 reference design satisfies the performance requirements set in the T1 loop in the relevant design conditions. The T2 design is analyzed at various gross masses, in order to ensure adequate performance in the entire mass envelope. The mass envelope for the model transition is defined broadly and spans well-above the T2 deterministic reference DGM, cf. figure 31. This practice increases the robustness of the model transition as it adds a degree of conservatism.

Overall, the transition-validation plots show good consistency of the T2 model off-design analyses with the assumptions taken in the course of the T1 design loop. The interest in deploying a full trim computation is illustrated particularly clearly in the plots of the equivalent flat plate drag area

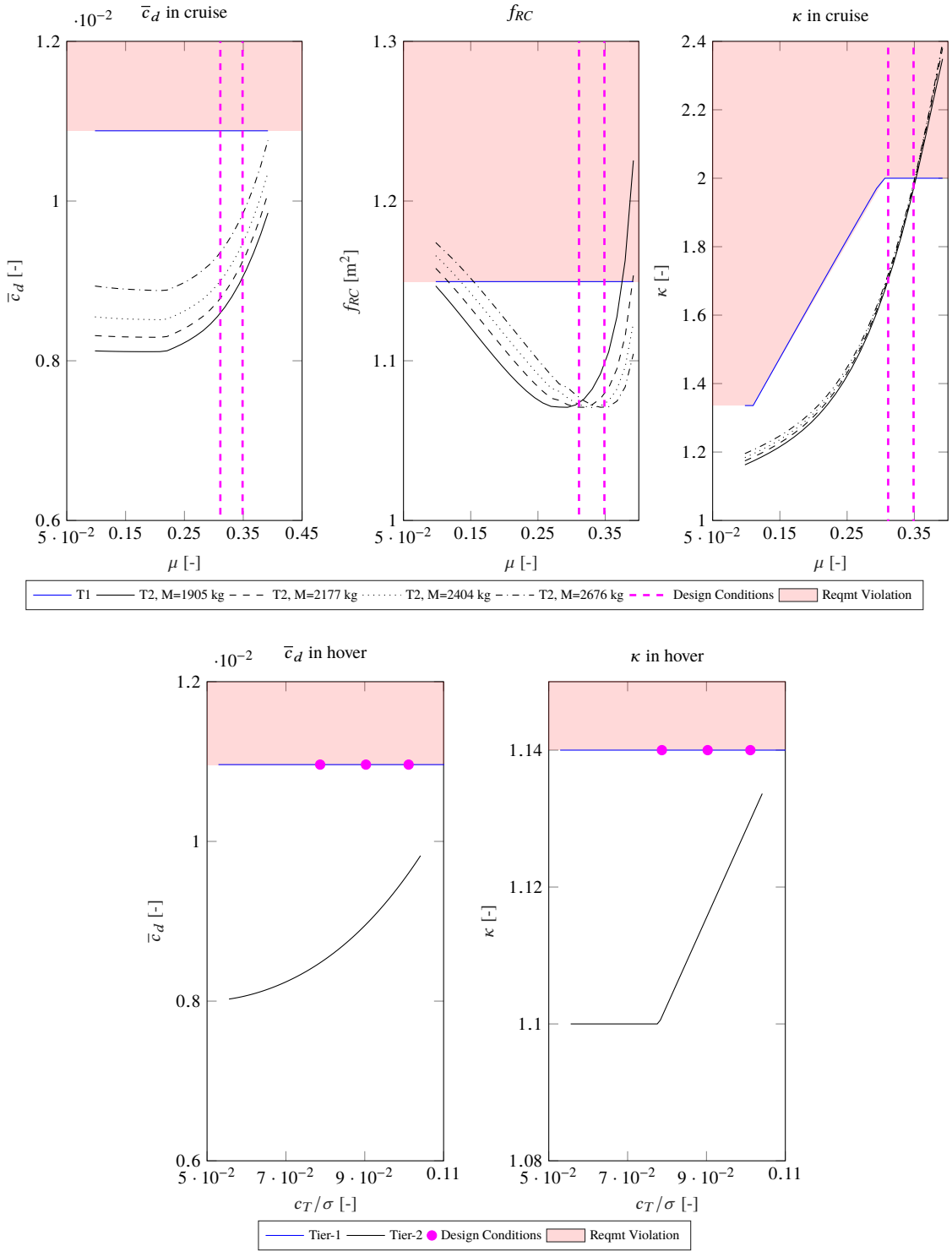

Figure 32 Tier-1 to Tier-2 model transition validation plots for the helicopter configuration.

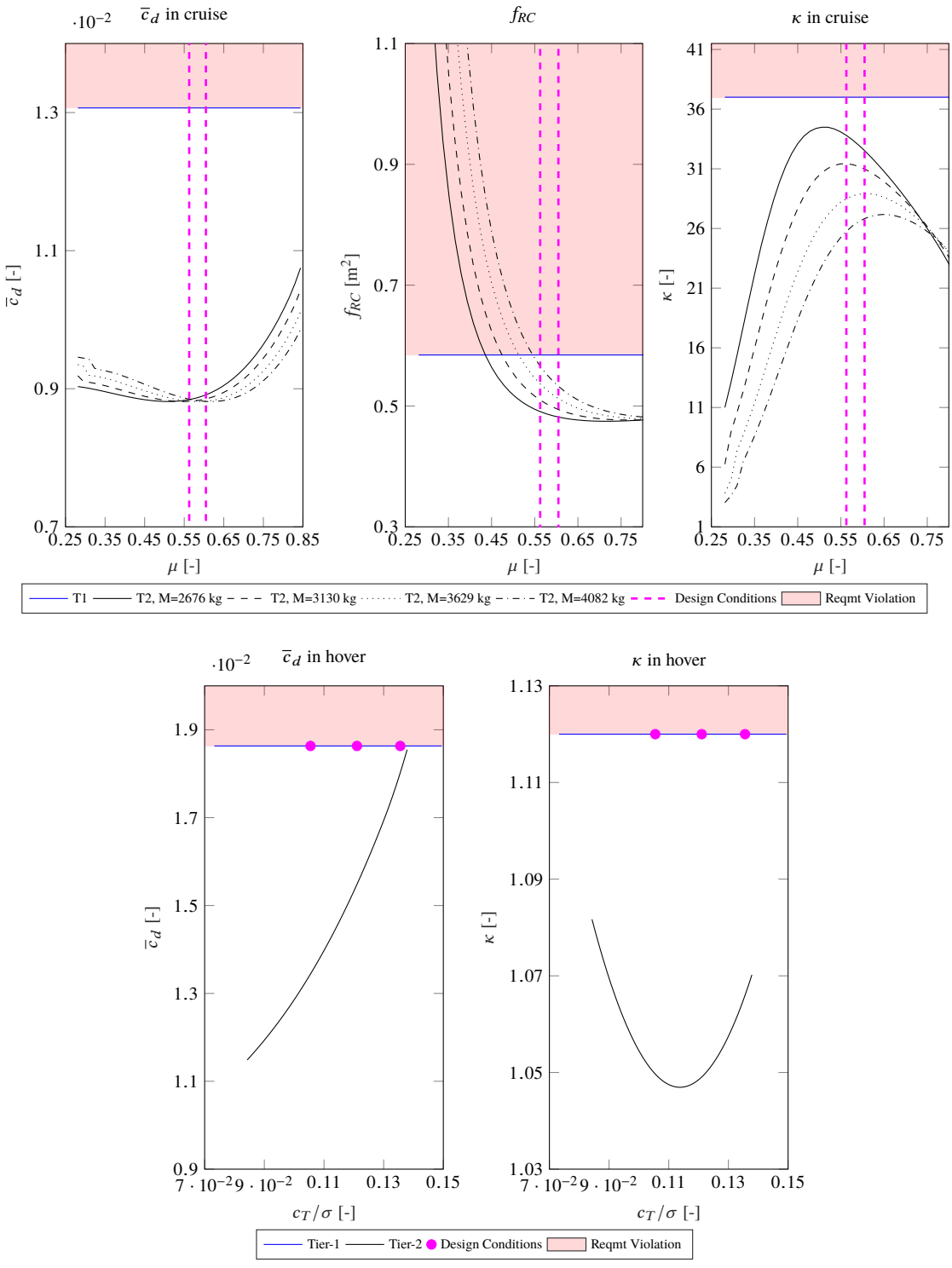

Figure 33 Tier-1 to Tier-2 model transition validation plots for the T/R configuration.

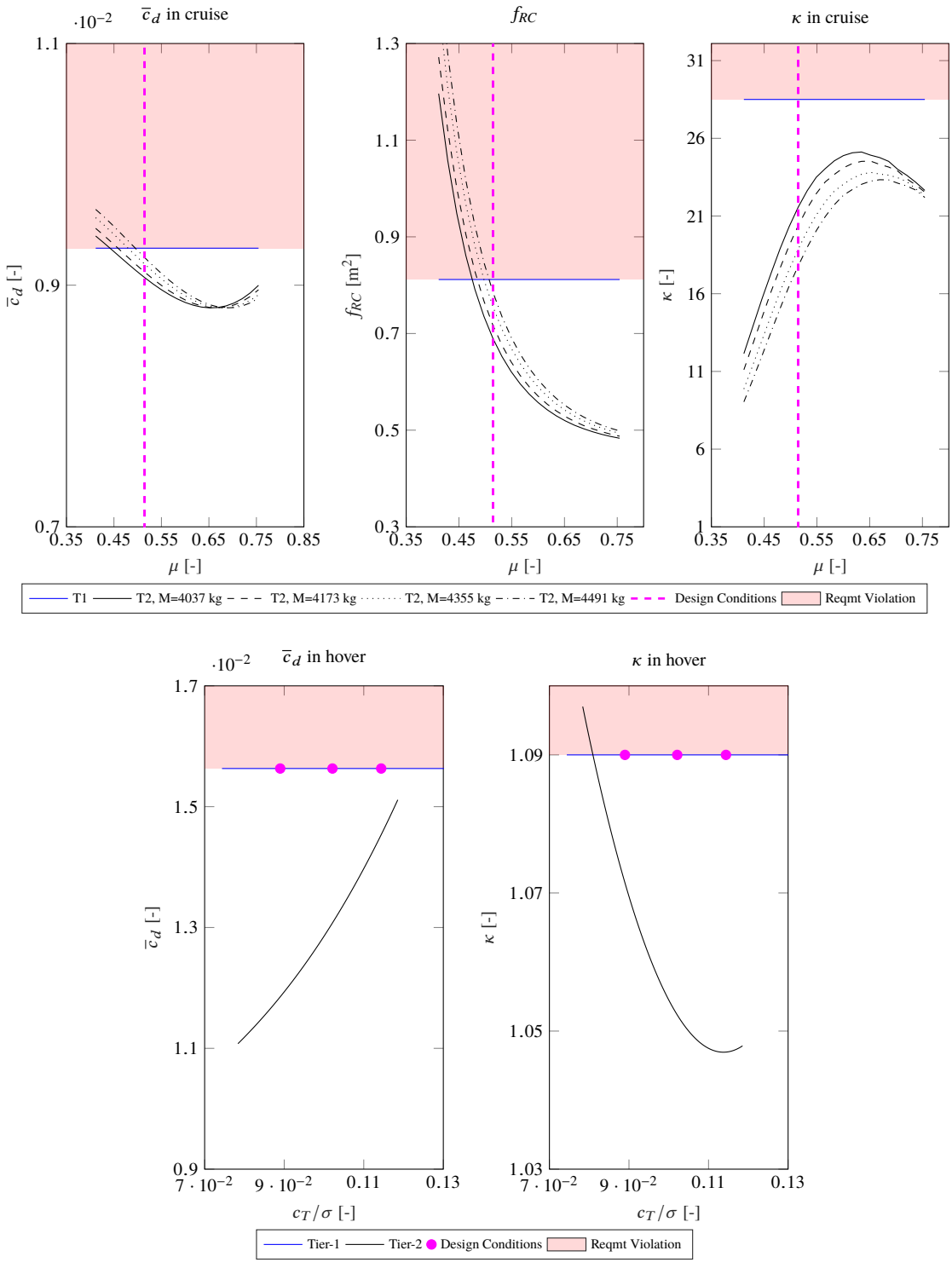

Figure 34 Tier-1 to Tier-2 model transition validation plots for the eVTOL configuration.

	Parameter	Baseline Value	Confidence Interval
H/C	κ in hover	Computed, $f(\vec{p}_{T2})$	± 0.04
	f_{RC} in cruise	Computed, $f(\vec{p}_{T2})$	± 0.2 m^2
	k_{DL} fraction of DGM	Computed, $f(\vec{p}_{T2})$	−0.01, +0.03
	$\bar{c}_d$ in cruise	Computed, $f(\vec{p}_{T2})$	−0.0032 to +0.0018
	EM/DGM	Computed, $f(\vec{p}_{T2})$	−0.015, +0.03
	k_{FF}	Computed, $f(\vec{p}_{T2})$	± 0.02
	f_{Int}	*Not applicable*	
T/R	κ in hover	Computed, $f(\vec{p}_{T2})$	−0.02, +0.05
	f_{RC} in cruise	Computed, $f(\vec{p}_{T2})$	± 0.1 m^2
	k_{DL} fraction of DGM	Computed, $f(\vec{p}_{T2})$	−0.03, +0.05
	$\bar{c}_d$ in cruise	Computed, $f(\vec{p}_{T2})$	−0.0023, +0.0027
	EM/DGM	Computed, $f(\vec{p}_{T2})$	−0.02, +0.04
	k_{FF}	Computed, $f(\vec{p}_{T2})$	± 0.02
	f_{Int}	*Not applicable*	
eVTOL	κ in hover	Computed, $f(\vec{p}_{T2})$	−0.02, +0.05
	f_{RC} in cruise	Computed, $f(\vec{p}_{T2})$	± 0.1 m^2
	k_{DL} fraction of DGM	Computed, $f(\vec{p}_{T2})$	−0.005, +0.005
	$\bar{c}_d$ in cruise	Computed, $f(\vec{p}_{T2})$	−0.0029, +0.0021
	EM/DGM	Computed, $f(\vec{p}_{T2})$	−0.02, +0.04
	k_{FF}	*Not applicable*	
	f_{Int}	1.2	± 0.05

Table 14 Subset of Tier-2 reference technical model parameters subjected to uncertainty.

f_{RC} of the different designs. All designs satisfy the technical requirements $\vec{t}_{T1,req} \subset RA_{T1}$ in the relevant operating conditions, even for the high gross masses. Therefore, the T2 model transition is considered successful and validated, and the T2 RADP commences.

4.4.2. Attribution of Uncertainty and Generation of the Computation Grid

As mentioned afore, the T2 model incorporates the highest-fidelity modeling deployed in the presented methodology. The complexity of the model is consequently the highest as well, as illustrated by the dimension of the technical model parameter vector. Whereas the dimension of $\vec{t}_{T1}$ is 53, $\vec{t}_{T2}$ already contains several hundred entries for each rotorcraft. Evidently, the problem-of-size dilemma discussed during the T1 loop, see chapter 4.3.2, poses a challenge for the T2 design loop as well. The number of technical model parameters included in the probabilistic analysis hence needs to be limited again. Generally, the selection of those parameters to be subjected to uncertainty requires the more careful consideration, the larger the dimension of $\vec{t}$. Table 14 lists the model parameters which are selected for the T2 stage. In order to cover the performance characteristics comprehensively with the limited number of factors available for probabilistic analysis, the same sub-system-level performance factors selected for the T1 loop are subjected to uncertainty in the T2 loop as well. However, different to the constants used in the T1 loop, all sub-system-level performance characteristics are now computed from T2 sub-models. The battery integration factor f_{Int} poses the sole exception to this rule, as no sub-model is available relating the battery pack integration penalty to specific design parameters. For the sake of consistency, its reference value and confidence interval remain at the T1 prospects. In conclusion, the increasing

model fidelity is reflected in the following probabilistic analysis, while maintaining a manageable number of factors for the probabilistic analysis.

	H/C	T/R	eVTOL
κ_{hover}	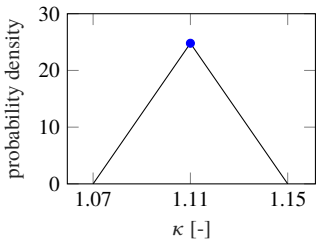	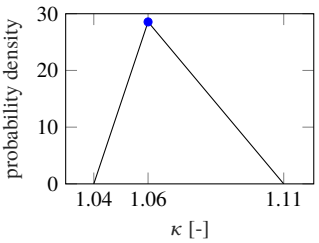	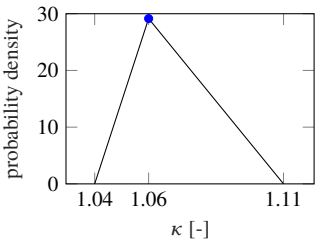
f_{RC}	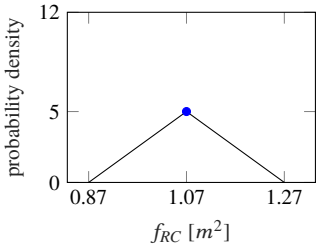	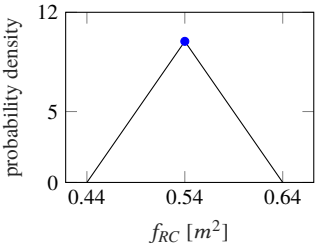	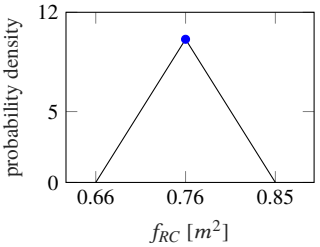
k_{DL}	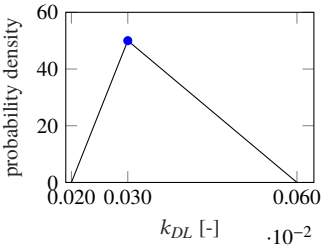	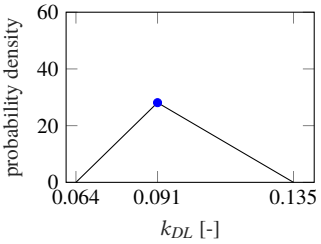	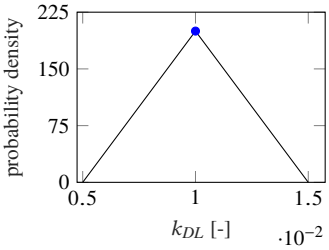
$\bar{c}_{d,hover}$	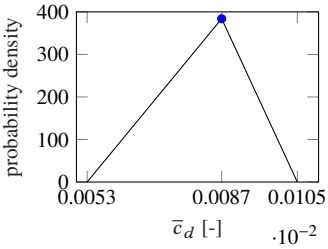	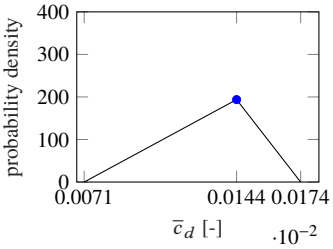	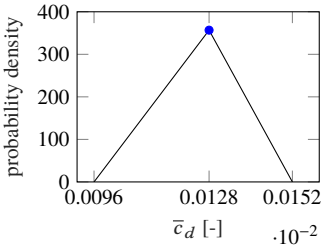
EM/DGM	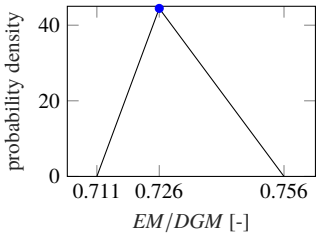	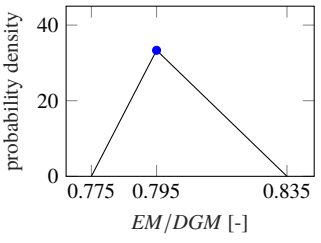	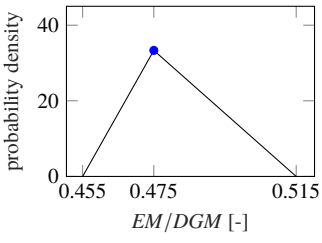

k_{FF}	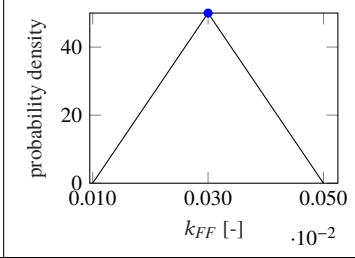	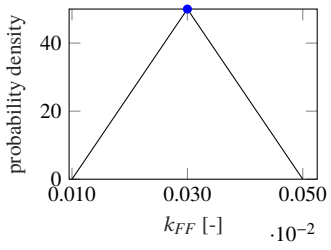	Not applicable
f_{Int}	Not applicable	Not applicable	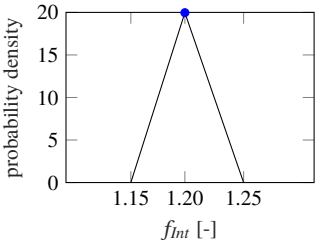

Table 15 Tier-2 uncertainty allocation to technical model parameters. The reference value is indicated as a blue marker.

With the uncertainty factors identified, the attribution of the uncertainty characteristics associated to these factors is due. As the T2 stage marks the final phase of preliminary design, complementary activities in the spirit of Concurrent Engineering (CE) are usually performed in practical preliminary design projects. Typically, several further analyses are performed in parallel at this concluding design stage. Examples of typical analyses include computational high-fidelity analysis such as CFD and FEA, but also experimental activities such as wind-tunnel-testing. The objective of these activities generally lies in determining the behavioral characteristics of the specific design to a larger degree of precision and maturity. This information may then be fed into the probabilistic analysis by decreasing the levels of uncertainty associated to the particular technical model parameters.

In spite of the potential outlined in the preceding paragraph, the initially performed T2 probabilistic analysis assumes identical confidence intervals as for the T1 model, as evident when comparing the data in the tables 9 and 13. This approach is chosen in order to explore the benefits stemming solely from the increase in model fidelity first. Consistent with the T1 design loop, triangular probability distributions are deployed for the T2 probabilistic analysis as well. Overall, uncertainty characteristics of comparable level for the T1 and T2 analyses result, cf. tables 11 and 15. As the T2 model deploys sub-models in the computation of the sub-system performance characteristics, the data in table 15 generally presents the uncertainty intervals for the values corresponding to the design mission conditions, and are generated with the deterministic reference design of each configuration. For the off-design domain of the envelope, the algorithm is set up in such a way that the confidence intervals are identical in relative terms, i.e. identical percentage deviation from the baseline value.

The T2 computational grid spans the probability space $\mathcal{P}_{T2}$ and is generated using the developed customized LHS method. The total size of the computational grid is 77 760 per rotorcraft type, yielding a total size of 233 280 design candidates to be evaluated. The T2 computer experiment is

executed on a high-performance computation cluster with 28 CPU cores, and requires a runtime of approximately 26 h.

4.4.3. Probabilistic Analysis and Robust Design

Figures 35 and 36 show the stochastic properties of the T2 design space in the form of the PDF and CDF functions, respectively. Comparing the evolution of the PDF from the previous stage, it is notable that a further removal of epistemic uncertainty is achieved for all configurations, as the width of the probability distributions decreases further, cf. figures 28 and 35. Although the improvement is not as dramatic as for the T0-to-T1 transition, the benefit is still significant. This is particularly noteworthy since similar levels of uncertainty are applied in both the T1 and the T2 simulations, whereas the T0 design loop considers significantly greater uncertainty levels than the T1 analysis. Hence, the further improvement is directly attributable to the improved capabilities of the applied T2 modeling, proving the added value of the increased model fidelity. In consideration of the comparable uncertainty levels attributed, the further reduction in the density of the probability distributions of the DGM is impressive. The size of the domain of the possible DGM decreases by approximately 50 % for each rotorcraft configuration.

Unlike the results of the previous tier, the tiltrotor PDF shows two distinct probability peaks around the center of its probability distribution. As all designs converged successfully, this phenomenon cannot be attributed to convergence issues in the design space. Such behavior may either indicate a characteristic of the tiltrotor configuration, or result from a non-ideal set-up of the computational grid. As for the T1 design loop, the number of instances per factor in the T2 computational grid is set to $n_{c,EM/DGM} = 10$ for the empty mass, and to $n_{c,others} = 6$ for the other factors, in order to save computational effort. In order to further explore this phenomenon, two additional tiltrotor design loops are performed, modifying the settings for n_c. In one run, the number of EM instances is increased to $n_{c,EM/DGM} = 30$, whereas a second test of this possible cause is investigated by setting the number of instances for all factors to $n_c = 8$. The resulting PDF are displayed in appendix D in comparison to the nominal T2 case presented here. Evidently, the same behavior is observed also with the modified settings for the probabilistic analysis. It is therefore concluded that the behavior observed is indeed a characteristic of the tiltrotor configuration, which is only unveiled by the highest-fidelity preliminary design model. As outlined in chapter 6.2, it is recommended to further investigate the robustness properties of the different rotorcraft configurations depending on the nature of the design problem in further executions of the methodology. However, the two-peak characteristic observed in the tiltrotor PDF in figure 35 is considered non-problematic for the evaluation of the results from the probabilistic analysis.

As illustrated in figure 37, the DGM margin to control the prevalent uncertainty remaining at the end of the T2 phase is 114 kg, or 5.3 % of the reference DGM for the helicopter. For the tiltrotor, the remaining margin is 195 kg (6.4 %), and for the eVTOL configuration 378 kg (8.7 %). For all rotorcraft types, the required margins decrease relative to the T1 stage. Whereas the gain is comparable for the helicopter and tiltrotor configurations, i.e. a decrease by approximately a factor of 2, it is even more pronounced for the eVTOL configuration. The same trends are already

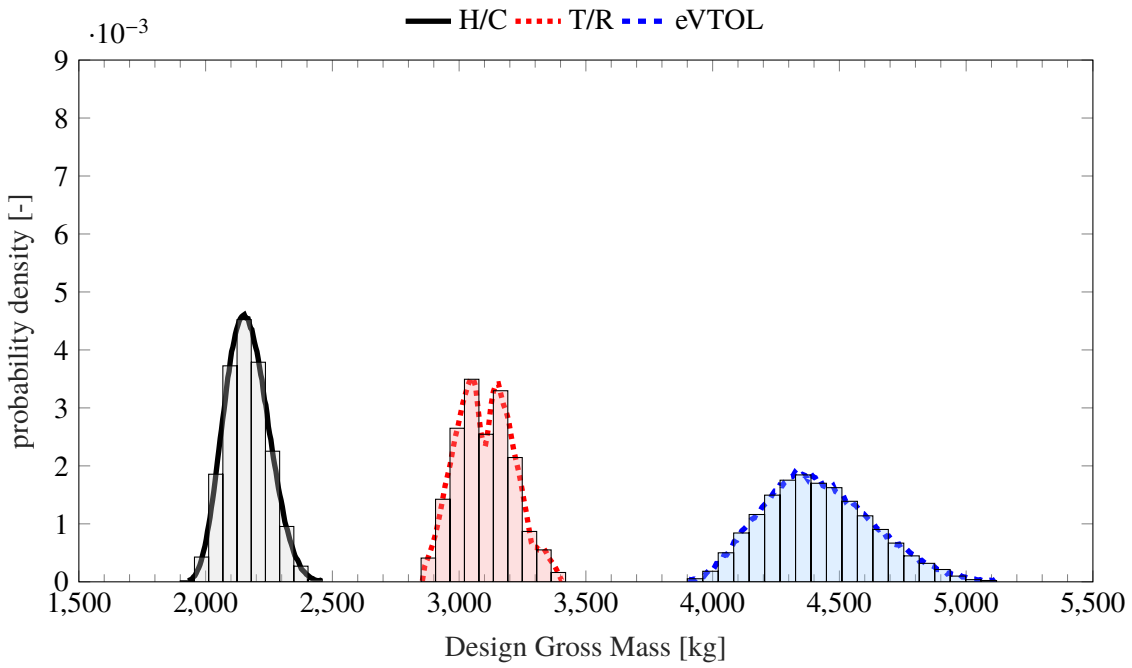

Figure 35 Tier-2 Robust Design results: Probability Density Function

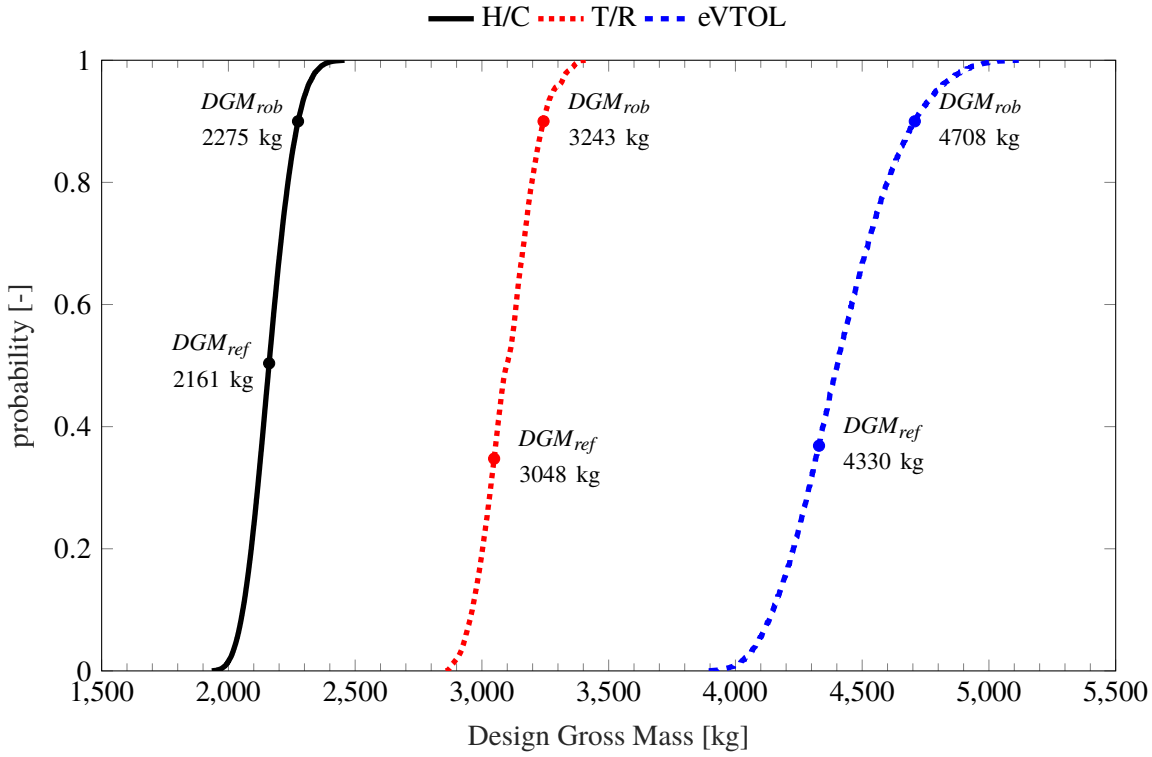

Figure 36 Tier-2 Robust Design results: Cumulative Distribution Function

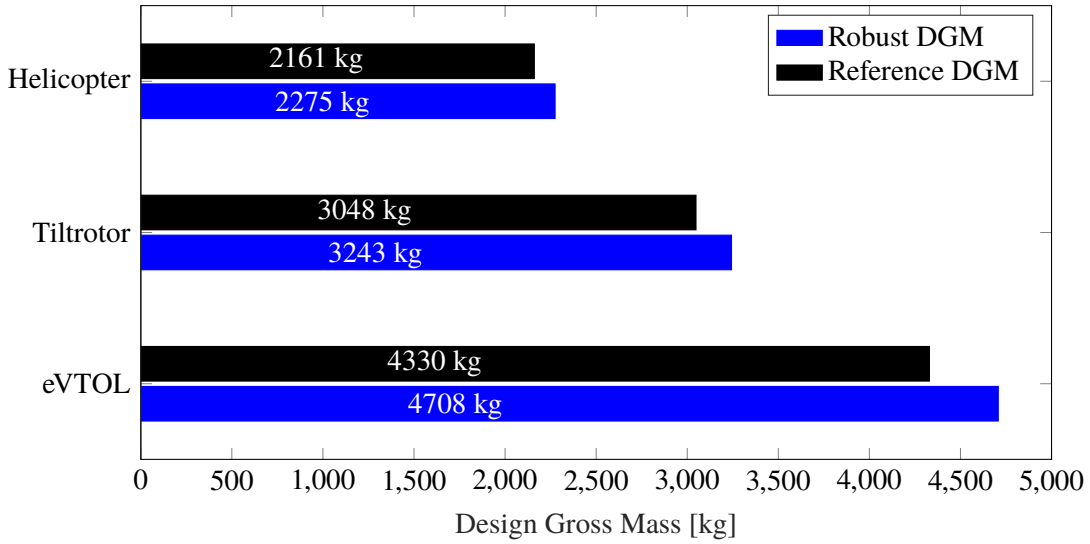

Figure 37 Tier-2 robust DGM per rotorcraft type for the UAM mission.

	$(EM/DGM)_{ref}$	χ_{EM}	$(EM/DGM)_{rob}$	Δ_{EM}
H/C	0.726	4.37 %	0.737	0.011
T/R	0.795	3.87 %	0.806	0.011
eVTOL (excl. Battery)	0.475	5.72 %	0.487	0.012
eVTOL (incl. Battery)	0.895	5.72 %	0.904	0.009

Table 16 Tier-2 resulting empty mass control variables χ_{EM} and robust EM/DGM fractions to obtain a robust design.

observed in the transition from the T0 to the T1 level.[14]

To complete the probabilistic analysis, the EM control variable values yielding the determined robust DGM are determined, and are shown in table 16. As the T2 stage concludes the preliminary design phase, these values correspond to the empty mass margins which are required to control the model-related uncertainty which remains before entering into the detailed design. The required EM control variable value χ_{EM} for the helicopter and the tiltrotor result to 4.37 % and 3.87 %, respectively. For the eVTOL, a larger value of 5.72 % is needed. As outlined in chapter 4.3.3, the actual DGM margin is a more suitable parameter than the control variable value to indicate the degree of investment needed to turn the deterministic into the robust design. To this end, as evident from figures 36 and 37, the helicopter continues to prove the most robust rotorcraft in the face of the model-related uncertainty, whereas the increasing model fidelity serves to decrease this advantage in terms of required DGM margin for the trailing tiltrotor and eVTOL configurations compared to the previous-tier design loops.

In closure of the preliminary design IDL, the T2 designs are verified and validated against the established RA. In order to prepare the detailed design phase, the RA is updated to include the determined T2 design degrees of freedom, $\vec{d}_{T2,DoF,rob} \subset RA_{T2}$. Essentially, the derived robust technical model parameter values are added to the RA, $\vec{t}_{T2,rob} \subset RA_{T2}$, in order to allow validating the transition into the detailed design phase in the same manner as performed in-between the

[14] A more detailed discussion of this behavior is provided in chapter 5.1.

different preliminary design stages of this example test-case.

4.5. Further Tier-2 Design Loop Boosted by Concurrent Engineering

As briefly pointed out in chapter 4.4.2, CE techniques are typically deployed in the late stages of the preliminary design phase. These additional activities generally serve the purpose of increasing the available information about the design candidate, and may be used in multiple ways. Selective high-fidelity analysis may further substantiate or even enable design decisions in active trade-studies, for which even the highest preliminary design model may not be sufficiently refined. The more interesting motivation with respect to the example demonstration lies in increasing the certainty about the assumptions on the behavior and performance of the system under design. For example, detailed bottom-up mass predictions would be desirable. Stress computations based on FEA may be performed to substantiate the mass estimation of key structural parts in addition. Numerical CFD computations as well as wind-tunnel-testing may be used to increase the knowledge and maturity about the aerodynamic properties of the airframe and the rotor blades. A model of the resolutive capabilities of the T2-fidelity model is a pre-requisite to enable incorporating the information obtained from such high-fidelity analyses into the preliminary design procedure, as only a model operating on the system-element level of decomposition is capable of mimicking system behavior in a sufficient level of detail.[15] Hence, the T2 model can be considered as the basis for implementing any additional information in the form of a reduced probability space, and correspondingly calibrated sub-models. Consequently, the T2 phase is considered to be the earliest stage in the overall development process to initiate CE activities appropriately.

In the probabilistic terminology adopted in this work, outlined in chapter 2.3.2, such complementary activities may in many cases remove further epistemic uncertainty of the parameter-uncertainty type. Arguably, this type represents the dominant share of uncertainty at the end of the preliminary design phase, as the model-inadequacy and parametric-variability types are significantly diminished by the accomplished progressive transition to higher-fidelity modeling in the course of the design process. To investigate the potential of deploying such CE analyses, another execution of the T2 design loop is conducted. In delineation from the previous T2 loop, all data from the Tier-2 scenario boosted by Concurrent Engineering ($T2_+$) is marked with the subscript "+". In the absence of actual high-fidelity analysis data for the fictive example demonstration test-case, the removal of epistemic uncertainty is simulated by reducing the confidence intervals for this CE-boosted scenario compared to the regular T2 loop, which is described in chapter 4.4. In order to obtain the isolated impact of the uncertainty reduction, all other parameters in the simulation are kept identical to the previous T2 run.

The confidence intervals of the T2 stage, presented in table 14, are reduced by 50 % for all factors in the experiment. The reference baseline values for the technical model parameters $\vec{t}_{T2+}$

[15] In illustration of this claim, compare the model transition plots in chapters 4.3.1 and 4.4.1.

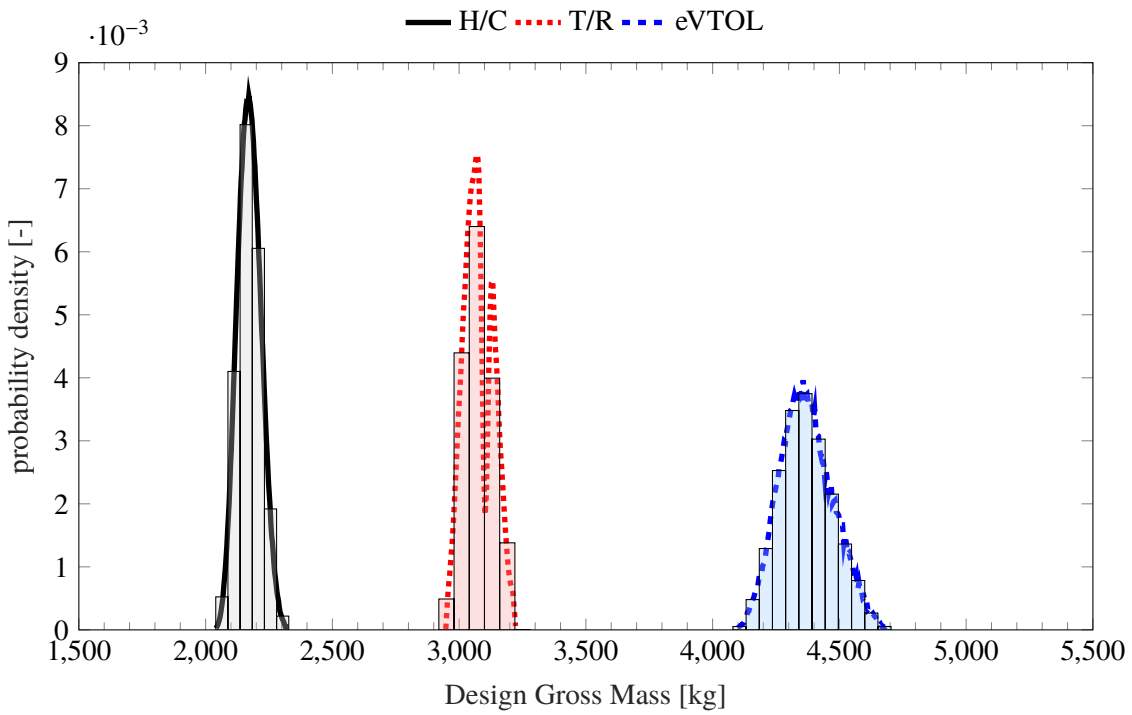

Figure 38 $T2_+$ CE-boosted scenario Robust Design results: Probability Density Function

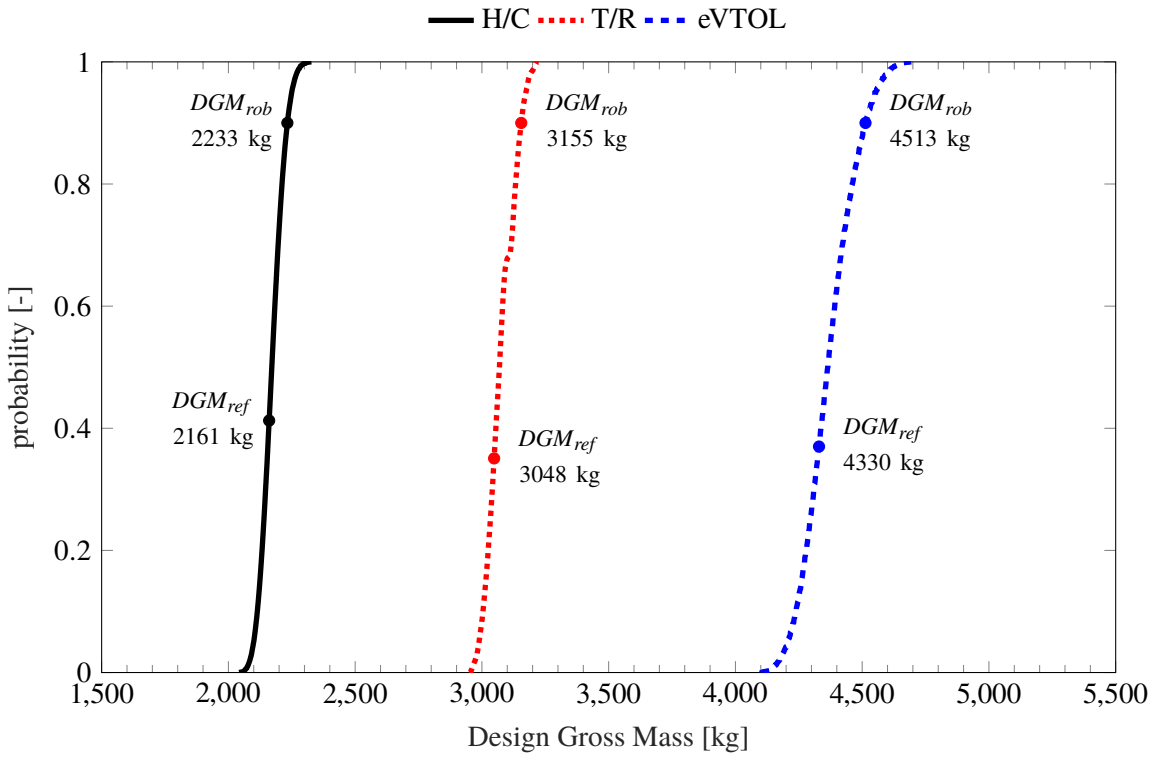

Figure 39 $T2_+$ CE-boosted scenario Robust Design results: Cumulative Distribution Function

	T2 DGM margin	$T2_+$ DGM margin	Reduction
H/C	114 kg	72 kg	42 kg (36.8 %)
T/R	195 kg	107 kg	88 kg (45.1 %)
eVTOL	378 kg	183 kg	183 kg (51.6 %)

Table 17 Reduction of required DGM margin for a robust design for the $T2_+$ scenario compared to the initial T2 loop.

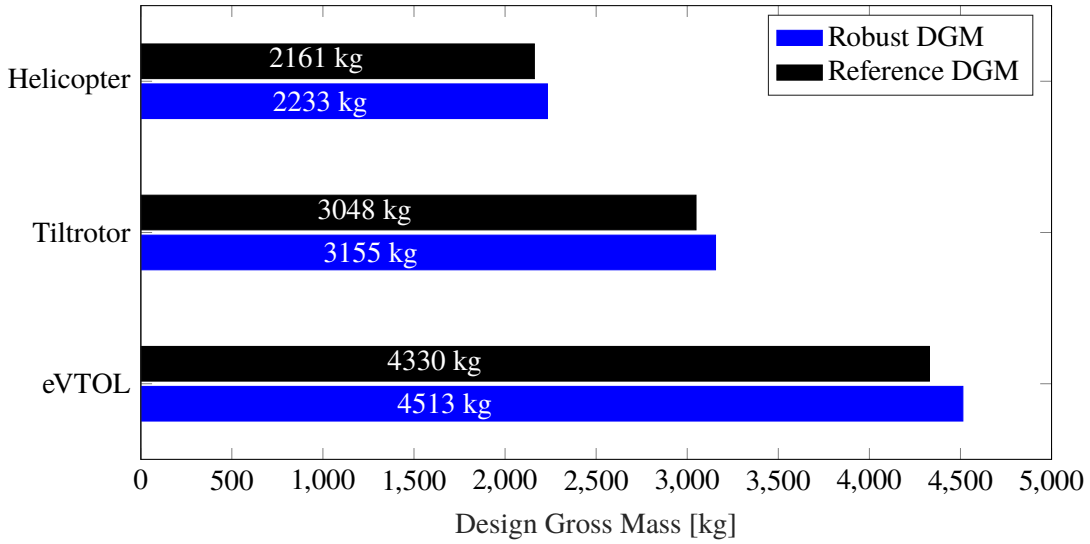

Figure 40 $T2_+$ CE-boosted scenario robust DGM per rotorcraft type for the UAM mission.

remain at the original T2 values. Unaltered to the T2 stage, triangular PDT are applied to all factors. Consequently, the probability space $\mathcal{P}_{T2+}$ is effectively halved in each particular dimension compared to $\mathcal{P}_{T2}$. The concrete confidence intervals and probability distributions are outlined in appendix E.

Figure 38 shows the PDF of the resulting DGM in the $T2_+$ scenario. Comparing the data to the identically formatted figure 38 from the initial T2 loop, the effect of the reduced epistemic uncertainty shows in significantly denser probability distributions for all investigated rotorcraft types. The same trend is evident in the CDF, shown in figure 39. As a result from the more-constricted probability space $\mathcal{P}_{T2+}$, the required design margins in terms of DGM decrease considerably, see table 17. Interestingly, however, the effectiveness of the uncertainty removal differs for the different configurations, despite the fact that each probability space is truncated to the same extent. The eVTOL configuration again benefits the most from the uncertainty reduction, decreasing the required robust DGM margin by 183 kg and thus 52 %. The tiltrotor experiences a reduction by 88 kg (45 %), whereas the helicopter experiences the smallest benefit with 42 kg (37 %). This indicates that the benefit from removing epistemic uncertainty seems to be non-linear, and the more effective the larger the difference between the deterministic and robust designs. Additional analyses should be conducted to test this hypothesis further. Recommendations for future work on this aspect are provided in chapter 6.2.

The empty mass control variable values $\chi_{EM,T2+}$ to control the reduced uncertainty in this boosted scenario decrease further compared to the initial T2 loop, and exhibit the same trend as observed for the actual DGM margin. Table 29 in appendix E contains the detailed data on the $T2_+$ control variables. The control variable value decreases by 1.56 percentage points to a value of $\chi_{EM,T2+} = 2.81\,\%$ for the helicopter configuration. The tiltrotor experiences a more significant decrease, concretely a reduction by 1.93 down to a value of $\chi_{EM,T2+} = 1.94\,\%$. The effect is largest for the eVTOL, for which a value of $\chi_{EM,T2+} = 2.85\,\%$ remains after a decrease by 2.87 percentage

points.

In summary of the $T2_+$ scenario, a great interest in accompanying high-fidelity analyses during the final stage of the preliminary design phase is identified. Complementary and parallel activities show the potential to significantly reduce the robust design margin remaining at the end of the preliminary design stage. These high-effort analyses promise to exploit their maximum potential in the probabilistic design context when aimed directly at reducing the epistemic uncertainty in the technical model parameters $\vec{t}_{T2}$, since this information can then be fed into the probabilistic analysis in the form of a reduced probability space.

5. Discussion of the Proposed Methodology

A novel probabilistic methodology for preliminary design is developed in line with the required characteristics identified in chapter 2, and is described in detail in chapter 3. An example execution of this methodology for a fictive design problem is performed and presented in chapter 4. The model-related uncertainty residing in this design problem is quantified by attributing probabilistic elements to the applied models, spanning the specific probability space of the analyzed design problem. The probabilistic elements comprise user-defined attributions of uncertainty characteristics to the estimated model behavior at the lowest level of decomposition in each design phase. The probability space is subsequently analyzed numerically, and its probabilistic characteristics are derived. From this data, the required empty-mass control-variable magnitude needed to control the model-related uncertainty is determined, enabling turning the deterministic reference design into a design which is inherently robust against the uncertainty in the probability space. The main observations drawn from the test case are summarized hereafter, and conclusions on the effectiveness and virtues of the developed methodology are derived.

5.1. Evolution of the Designs over the Preliminary Design Phases

The design of each investigated candidate configuration is established hierarchically and chronologically in accordance with the developed probabilistic methodology for the preliminary design of rotorcraft. The evolution of the deterministic reference design as well as of the robust design throughout the three-tiered process is presented in figures 41, 42 and 43. The numerical values are presented alongside in tables 18, 19 and 20.

Reviewing the evolution of the reference design gross mass DGM_{ref} first, a general trend for all configurations is evident. DGM_{ref} decreases continuously across the design phases, whereas the general consistency between all tiers and for all rotorcraft configurations is adequate. Even the simplistic metric-based T0 framework already achieves a reasonable accuracy compared to the higher-fidelity models. A cause for the decreasing trend for DGM_{ref} with increasing model fidelity may be identified in the model-transition-validation plots presented in chapters 4.3.1 and 4.4.1. As the assumptions of artifact performance taken on the $(n\text{-}1)^{\text{th}}$ level are of lower resolutive capability compared to the next-level models of the n^{th} level, the calibration of the $(n\text{-}1)^{\text{th}}$ level focuses on the domains which are of special interest in the set of requirements, see for example figure 33. As a result, the resulting artifact performance on the $(n\text{-}1)^{\text{th}}$ level is conservative for a significant portion of the flight envelope, ultimately providing a likely root cause for an over-prediction of the reference DGM on the $(n\text{-}1)^{\text{th}}$ level compared to the n^{th} tier. Whereas the exhibited evolutionary behavior is considered desirable in both trend and relative quantities, this phenomenon could be reduced or even reversed by opting for a more aggressive strategy in the definition of the technical model parameters $\vec{t}$ in the early phases of the design process. However, the probability space for

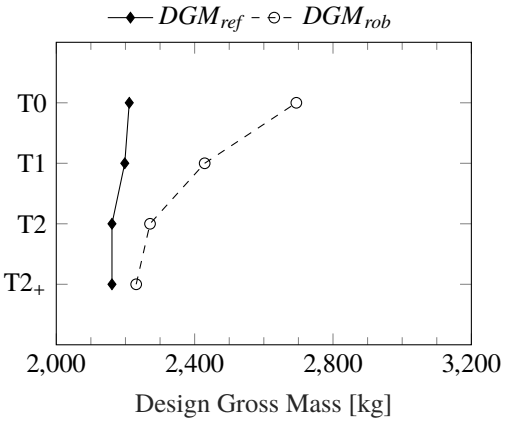

Figure 41 Evolution of the DGM throughout the preliminary design phases for the H/C.

	DGM_{ref}	DGM_{rob}	Δ_{DGM}
Tier-0	2211 kg	2694 kg	483 kg
Tier-1	2198 kg	2429 kg	231 kg
Tier-2	2161 kg	2275 kg	114 kg
Tier-2_+	2161 kg	2233 kg	72 kg

Table 18 Resulting reference and robust DGM for the H/C.

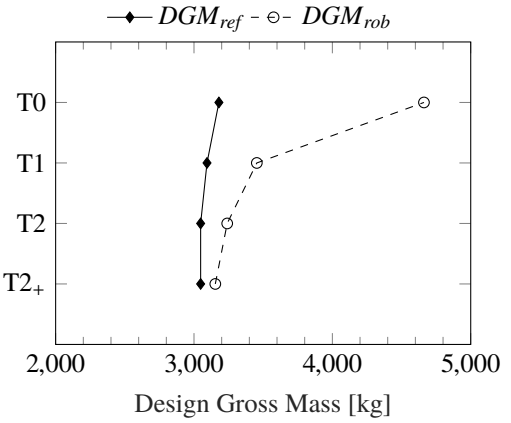

Figure 42 Evolution of the DGM throughout the preliminary design phases for the T/R.

	DGM_{ref}	DGM_{rob}	Δ_{DGM}
Tier-0	3180 kg	4662 kg	1482 kg
Tier-1	3094 kg	3454 kg	360 kg
Tier-2	3048 kg	3243 kg	195 kg
Tier-2_+	3048 kg	3155 kg	107 kg

Table 19 Resulting reference and robust DGM for the T/R.

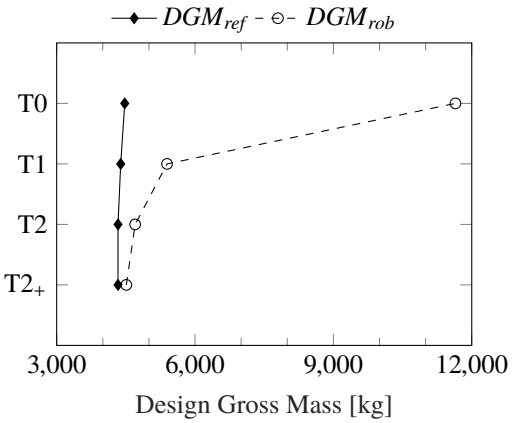

Figure 43 Evolution of the DGM throughout the preliminary design phases for the eVTOL.

	DGM_{ref}	DGM_{rob}	Δ_{DGM}
Tier-0	4476 kg	11 647 kg[a]	7171 kg
Tier-1	4388 kg	5393 kg	1005 kg
Tier-2	4330 kg	4708 kg	378 kg
Tier-2_+	4330 kg	4513 kg	183 kg

Table 20 Resulting reference and robust DGM for the eVTOL.

[a] See chapter 4.2.3 for the discussion on the excessive eVTOL T0 robust DGM value.

the subsequent probabilistic analysis would then need to be set accordingly, i.e. asymmetrically towards deteriorated performance, yielding a larger gap to the robust DGM as a result.

Turning to the evolution of the robust design gross mass DGM_{rob} and the actual design margin Δ_{DGM} to obtain this robust design, a series of interesting observations can be drawn. Firstly, the vast reduction in the required Δ_{DGM} in the course of the preliminary design phase is apparent. As expected, the design margins are initially high at the end of the T0 stage due to the simplistic modeling and, even more so, resulting from the vast uncertainty level present at this early stage. However, the transition to the model-driven T1 design, deploying models on the sub-system level, already decreases the robust DGM of the helicopter and the Tiltrotor (Aircraft) to reasonable levels when compared to the deterministic reference DGM. For the eVTOL however, the gap remains inappropriately large also at the T1 level. This is attributed to the detrimental effect of a low mass efficiency on the overall robustness of a rotorcraft concept, identified and outlined in chapters 4.2.3, 4.3.3 and 4.4.3. The low power-to-weight ratio of the energy storage technology compared to conventional kerosene-powered aircraft adds to the dilemma for the eVTOL configuration when compared to the tiltrotor, which also does not achieve helicopter-level mass efficiencies as an inherent characteristic of this type of rotorcraft. Inaccuracies in the performance characteristics of system elements trivially influence the amount of energy required to perform the design mission. The eVTOL concept however is more sensitive to such variations, as its means of energy storage, i.e. the battery, represents a significantly larger fraction of the overall aircraft mass than for conventional designs. Consequently, the additional mass to provide a certain excess energy is larger for the electric rotorcraft. Whereas this first-order influence already yields a disadvantage compared to the kerosene-powered aircraft, the indirect snowball effect on the overall aircraft size from the additional energy demand is also augmented, increasing the gap in the respectively needed design gross mass increments even further.

At the end of the T2 phase, the required design margins decrease further for all configurations. The different configurations continue to converge in terms of required Δ_{DGM} towards comparable values, although the differences remain significant. With the move to the T2 level, the eVTOL finally achieves a robust design margin satisfyingly moderate to be considered a viable design alternative in the face of the associated uncertainty. The CE-boosted scenario investigated in the $T2_+$ design loop further continues this trend. As outlined in chapter 4.4.3, the tiltrotor and in particular the eVTOL configurations take stronger benefit from the reduced uncertainty, although the probability spaces are truncated to the same extent for all configurations. This non-linearity in the benefit from the uncertainty-removal from parallel CE activities is already highlighted in chapter 4.5. This observation is consistent with the hypothesis deduced above, in that the configurations which are more susceptible to model-related uncertainty exhibit more significant gains from the removal of epistemic uncertainty of similar levels than less susceptible ones. This implies that the interest in performing concurrent high-fidelity analysis is especially high in case a strong sensitivity of the investigated concept against the prevalent uncertainty is identified. However, a model of the fidelity of the T2 level is a prerequisite to incorporate the additional data effectively into the probabilistic analysis, restricting the earliest point of embodiment of such analyses to the

T2 phase. This observation constitutes a significant finding with potentially high relevance for practical preliminary design investigations. Consequently, recommendations to further investigate and analyze this phenomenon are given in chapter 6.2.

In differentiation of the individual investigated rotorcraft concepts, the helicopter configuration consistently proves the most robust against the uncertainty in its probability space throughout all tiers. In the initial T0 phase, this may have been attributable to the slightly more confined confidence intervals for the uncertainty factors for the helicopter compared to the tiltrotor and eVTOL configurations. However, as the confidence intervals for the T1 and the T2 phases are defined comparably for all rotorcraft concepts, this observation reveals a general configuration-related characteristic, at least for the investigated UAM scenario.[1] Indeed, a similar behavior is already observed in previous work of the author, in which identical relative confidence intervals are applied, published by Wirth and Hajek in [134]. The tiltrotor configuration in this study exhibits a required DGM margin that is larger by a factor of two than for the helicopter at the T0 stage, although a direct comparison to the test case presented in this work is flawed, as a different design problem is investigated in [134].[2]

It is hence hypothesized that the probability space certainly is an influencing factor, however another primary cause for the configuration-related differences in robustness is suspected, as the test case is deliberately set up to minimize this influence. Notably, the robustness of a configuration against the model-related uncertainty, i.e. the magnitude of the required Δ_{DGM}, seems to correlate with its mass efficiency, as highlighted above. The high EM/DGM-ratio configurations, i.e. the tiltrotor and in particular the eVTOL, appear more susceptible to variability in their performance characteristics. In line with this hypothesis, these more versatile configurations benefit to a larger extent from the increasing model fidelity than the helicopter, resulting in larger reductions in Δ_{DGM} across the tiers, when epistemic model-related uncertainty is removed. Since the uncertainty intervals develop analogously in-between all configurations throughout the tiers, this behavior is attributed directly to the improvements in model fidelity.

5.2. Comparison of the Deterministic and Robust Designs

The sizing algorithm for the test case is set up to search for the minimum Design Gross Mass which allows to satisfy the mission and point performance requirements. As outlined in chapter 2.2.2.3, this approach represents the most-commonly adopted strategy for aircraft design. Consequently, the resulting deterministic reference DGM and the obtained target DGM of a robust design are chosen in chapter 4 and chapter 5.1 as the primary parameters in the analysis of the results. However, one of the virtues of the developed methodology lies in the unveiling of the actual robust design margins not only on this system-level parameter, but throughout the entire design space, i.e. throughout the PA and the TA. The propagation of the uncertainty to the actual design parameters is thus revealed. To highlight the significance of this aspect of the developed methodology, a

[1] Compare the data in tables 6, 10, 14 and 27 for the uncertainty intervals applied in the different tiers.
[2] Wirth and Hajek explore a significantly longer-range design mission, which should benefit the tiltrotor.

Parameter	H/C Tier-1 Deterministic	H/C Tier-1 Robust	Δ_{T1}	H/C Tier-2_+ Deterministic	H/C Tier-2_+ Robust	Δ_{T2+}
Design Gross Mass	2198 kg	2429 kg	10.5 %	2161 kg	2231 kg	3.2 %
Empty Mass	1605 kg	1823 kg	13.6 %	1568 kg	1635 kg	4.3 %
Fuselage Length	n/a	n/a	n/a	8.02 m	8.09 m	0.9 %
Overall Wetted Surface	n/a	n/a	n/a	38.9 m^2	39.3 m^2	1.0 %
Design Mission Fuel	151 kg	164 kg	8.6 %	136.2 kg	139.5 kg	2.4 %
MR Disk Load†	365 N/m^2	365 N/m^2	n/a	365 N/m^2	365 N/m^2	n/a
MR Solidity†	0.0994	0.0994	n/a	0.0994	0.0994	n/a
MR Tip Speed†	210 m/s	210 m/s	n/a	210 m/s	210 m/s	n/a
MR Rotational Speed	47.74 rad/s	45.40 rad/s	−4.9 %	48.85 rad/s	48.08 rad/s	−1.0 %
MR Radius	4.40 m	4.63 m	5.2 %	4.30 m	4.37 m	1.6 %
MR Chord	n/a	n/a	n/a	277 mm	283 mm	2.2 %
MR Blade Number	n/a	n/a	n/a	5	5	n/a
TR Radius	0.504 m	0.512 m	1.6 %	0.851 m	0.864 m	1.5 %
TR Solidity	0.2925	0.3029	3.6 %	0.160	0.160	n/a
TR Blade Number	n/a	n/a	n/a	10	10	n/a
Horizontal Stabilizer Area	n/a	n/a	n/a	0.773 m^2	0.773 m^2	0.0 %
Vertical Stabilizer Area	n/a	n/a	n/a	1.121 m^2	1.121 m^2	0.0 %
Installed Power (MCP SLS)	2×312 kW	2×327 kW	4.8 %	2×402 kW	2×412 kW	2.5 %
Fuel Flow (MCP SLS)	62.3 kg/h	67.7 kg/h	8.7 %	57.3 kg/h	58.7 kg/h	2.4 %
Drive System Limit	619 kW	673 kW	8.7 %	591 kW	603 kW	2.0 %
Normalized Fly-away Price	n/a	n/a	n/a	100 %	102.1 %	2.1 %

Table 21 Comparison of selected characteristic design parameters of the T1 and T2_+ Deterministic and Robust Helicopter Designs. Parameters marked with † indicate system-level design parameters fixed during the T1 design phase.

Parameter	T/R Tier-1 Deterministic	T/R Tier-1 Robust	Δ_{T1}	T/R Tier-2_+ Deterministic	T/R Tier-2_+ Robust	Δ_{T2+}
Design Gross Mass	3094 kg	3454 kg	11.6 %	3048 kg	3154 kg	3.5 %
Empty Mass	2482 kg	2823 kg	13.7 %	2423 kg	2522 kg	4.1 %
Fuselage Length	n/a	n/a	n/a	10.36 m	10.45 m	0.9 %
Overall Wetted Surface	n/a	n/a	n/a	90.2 m^2	91.8 m^2	1.8 %
Design Mission Fuel	170 kg	188 kg	10.6 %	133.4 kg	136.3 kg	2.2 %
Disk Load†	634 N/m^2	634 N/m^2	n/a	634 N/m^2	634 N/m^2	n/a
Rotor Solidity†	0.120	0.120	n/a	0.120	0.120	n/a
Rotor Tip Speed†	225 m/s	225 m/s	n/a	225 m/s	225 m/s	n/a
Rotor Rotational Speed	77.65 rad/s	73.49 rad/s	−5.4 %	82.33 rad/s	80.95 rad/s	−1.7 %
Rotor Radius	2.90 m	3.07 m	5.9 %	2.74 m	2.79 m	1.8 %
Rotor Chord	n/a	n/a	n/a	366 mm	372 mm	1.6 %
Rotor Blade Number	n/a	n/a	n/a	3	3	n/a
Wing Loading†	3686 N/m^2	3686 N/m^2	n/a	3686 N/m^2	3686 N/m^2	n/a
Wing Aspect Ratio	8.51	8.23	−3.3 %	7.73	7.65	−1.0 %
Wing Span	8.37 m	8.70 m	−3.9 %	7.92 m	8.01 m	1.1 %
Horizontal Stabilizer Area	n/a	n/a	n/a	2.141 m^2	2.228 m^2	4.1 %
Vertical Stabilizer Area	n/a	n/a	n/a	2.507 m^2	2.581 m^2	3.0 %
Installed Power (MCP SLS)	2×516 kW	2×577 kW	11.8 %	2×439 kW	2×443 kW	0.9 %
Fuel Flow (MCP SLS)	106.6 kg/h	119.2 kg/h	11.8 %	124.9 kg/h	126.0 kg/h	0.9 %
Drive System Limit	1033 kW	1153 kW	11.6 %	864 kW	897 kW	3.8 %
Normalized Fly-away Price	n/a	n/a	n/a	100 %	101.6 %	1.6 %

Table 22 Comparison of selected characteristic design parameters of the T1 and T2_+ Deterministic and Robust T/R Designs. Parameters marked with † indicate system-level design parameters fixed during the T1 design phase.

Parameter	eVTOL Tier-1 Deterministic	eVTOL Tier-1 Robust	Δ_{T1}	eVTOL Tier-2$_+$ Deterministic	eVTOL Tier-2$_+$ Robust	Δ_{T2+}
Design Gross Mass	4388 kg	5393 kg	22.9 %	4330 kg	4510 kg	4.2 %
Empty Mass	3946 kg	4951 kg	25.5 %	3877 kg	4056 kg	4.6 %
Battery Cell Spec. Energy†	250 Wh/kg	250 Wh/kg	n/a	250 Wh/kg	250 Wh/kg	n/a
Battery Mass	1927 kg	2426 kg	25.9 %	1818 kg	1886 kg	3.7 %
Fuselage Length	n/a	n/a	n/a	7.35 m	7.50 m	2.0 %
Overall Wetted Surface	n/a	n/a	n/a	71.5 m^2	73.2 m^2	2.4 %
Design Mission Energy	401.5 kWh	474.5 kWh	18.2 %	378.9 kWh	391.9 kWh	3.4 %
Disk Load†	634 N/m^2	634 N/m^2	n/a	634 N/m^2	634 N/m^2	n/a
Propeller Solidity†	0.130	0.130	n/a	0.130	0.130	n/a
Propeller Tip Speed†	225 m/s	225 m/s	n/a	225 m/s	225 m/s	n/a
Propeller Rotational Speed	118.26 rad/s	106.68 rad/s	−9.8 %	119.66 rad/s	117.24 rad/s	−2.1 %
Propeller Radius	1.91 m	2.11 m	10.5 %	1.88 m	1.92 m	2.1 %
Propeller Chord	n/a	n/a	n/a	204 mm	207 mm	1.5 %
Propeller Blade Number	n/a	n/a	n/a	4	4	n/a
Wing Loading†	3541 N/m^2	3541 N/m^2	n/a	3541 N/m^2	3541 N/m^2	n/a
Wing Aspect Ratio	8.20	7.82	−4.6 %	7.89	7.89	0.0 %
Wing Span	9.98 m	14.94 m	49.7 %	9.73 m	9.93 m	2.1 %
V-Tail Stabilizer Area	n/a	n/a	n/a	5.164 m^2	5.164 m^2	0.0 %
V-Tail Dihedral Angle	n/a	n/a	n/a	45°	45°	n/a
Installed Power (Cont.)	6×192 kW	6×236 kW	22.9 %	6×168 kW	6×175 kW	4.2 %
Normalized Fly-away Price	n/a	n/a	n/a	100 %	103.1 %	3.1 %

Table 23 Comparison of selected characteristic design parameters of the T1 and T2$_+$ Deterministic and Robust eVTOL Designs. Parameters marked with † indicate system-level design parameters fixed during the T1 design phase.

comparison of the obtained deterministic and robust designs is conducted hereafter.

A number of selected characteristic design parameters of the deterministic and robust designs from the T1 and the T2$_+$ design loops are listed in tables 21, 22 and 23 for the three investigated rotorcraft configurations.[3] Those parameters representing system-level design degrees of freedom, which are fixed in the course of the T1 design loop, are marked with the symbol † for improved clarity. Whereas the T1 framework is built on newly developed sizing code, the T2 stage uses NDARC's built-in sizing functionality. Therefore, the T1 and T2$_+$ designs are both presented, in order to explore the consistency between the different sizing codes. Overall, the presented data illustrates that the margins to obtain the robust rather than the deterministic design are transparently captured for every element of the design space, comprised of the physical and technical model parameters $\vec{d}$ and $\vec{t}$.

Comparing the deterministic helicopter designs in table 21, two parameters show noteworthy differences between the tiers. First, a notable disparity is visible in the sizing strategy of the ducted tail rotor, for which the T1 sizing code yields a design of higher disk load and hence greater solidity compared to NDARC. As the tail rotor parameters are part of the dependent design parameters $\vec{d}_{T1,dep}$ and hence are not fixed in the T1 design loop, this is considered non-problematic.[4] The suspected origin of this difference lies in a presumably different set of data, from which the respective ducted-tail-rotor sizing-algorithms were derived for the T1 sizing code and NDARC. Second, a relevant difference is observed in the installed power levels of the T1 and T2 designs.

[3] The T2 data is provided in addition in appendix A.2 for the helicopter, B.2 for the tiltrotor and C.2 for the eVTOL for completeness.

[4] The model parameter terminology is defined in chapter 2.2.2.4.

Whereas the T1 turboshaft model uses a parametric modeling, NDARC uses a physics-based thermodynamical model.[5] In the requirements of the test case, depicted in chapter 4.1, the decisive sizing points for the required installed power are the hovering flight point performance requirements at high density altitudes, at least for the conventionally-propelled configurations, as turboshaft engines deteriorate considerably in terms of the power capacity available with increasing density altitude. The higher-fidelity T2 model apparently obtains a different engine characteristic with respect to its available power depending on the density altitude than the T1 model, which applies a generalized characteristic of a generic turboshaft engine. However, the fuel flow data between the tiers shows excellent consistency, which is considered to be the more relevant parameter with respect to the overall rotorcraft sizing. However, the observed deviation demonstrates the relevance of deploying a physics-based model before the end of the preliminary design phase, at the end of which the engine characteristics are ultimately specified. In view of the above, the overall consistency of the T1 and T2 sizing algorithms is considered as acutely satisfactory for the helicopter configuration.

Turning to the analysis of the remaining differences Δ_{T2+} between the deterministic and the robust design at the end of the preliminary design phase, the design margins required for a robust design become visible for every design parameter. Generally, the required margins are rather minor for the helicopter, as evident from table 21. Interestingly, an increase of 70 mm (1.6 %) in main rotor radius, and 10 kW (2.5 %) for installed engine power, is sufficient to control the remaining uncertainty in the probability space to the requested degree, ensuring a robust design. In the face of relatively challenging user requirements for hovering flight at high density altitudes, these margins represent a modest investment for achieving robustness. The most significant deviation is observed in the EM. Since the uncertainty is being controlled by a single control variable acting on the EM of the design, this behavior is expected. As NDARC includes a parametric cost-estimation module, the estimated fly-away price is given in table 21. This parameter is normalized with the deterministic reference value, since the validity of the cost module is not considered to be on the same level as the actual sizing code, and thus should be interpreted cautiously. Nevertheless, the obtained projected price difference of 2.1 % indicates that investing into the robustness of the design may be an interesting economic risk-mitigation strategy, as dramatic cost and schedule overruns may be encountered for a non-robust design, if design changes become necessary at a later stage of the development due to insufficient robustness of the design.

For the tiltrotor, the data is listed in table 22. The consistency of the T1 and T2 sizing codes yield equally good consistency as for the helicopter, whereas the observation and remarks on the installed engine power are valid for this configuration as well. Different than for the helicopter, however, the fuel flow at Maximum Continuous Power (MCP) in Sea Level Standard Conditions (SLS) deviates to a noteworthy extent for the tiltrotor. However, as the projected design mission fuel results are consistent between the tiers, this difference is also attributed to a difference in the engine characteristics with respect to the sensitivity to density altitude resulting from the different fidelity of the sub-models of each tier. Also for the tiltrotor, remarkably moderate design margins

[5] See chapter 3.2 for the description of the modeling of the different tiers.

are necessary to turn the reference design into a robust design. An increase of the rotor radius of only 50 mm (1.8 %), mandating a corresponding elongation of the wing span of 90 mm (1.1 %), suffices to achieve robust characteristics for these sub-systems.

Lastly, the consistency of the T1 and T2 sizing algorithms is equally satisfactory for the unconventional eVTOL configuration, see table 23. In particular, the battery mass, the design mission energy and the electric motor power match well between the tiers, when taking the larger gross mass and the moderate conservatism in the technical model parameters of the T1 design into consideration.[6] Although larger margins are required to ensure a robust design for the eVTOL concept compared to the more conventional architectures, the obtained design margins at the end of the preliminary design phase appear reasonably moderate also for this novel configuration. Accounting for a margin of 13 kWh (3.4 %) in battery energy capacity, resulting in an increase of 68 kg (3.7 %) in battery mass, suffices to obtain a robust battery system. This excess energy serves to compensate for the additional power required due to the larger gross mass of the robust design, and for the accordingly increased electric motor power, which rises by 7 kW (4.2 %) per motor. However, comparing the design evolution presented in chapter 4, and comparing the $T2_+$ design margins Δ_{T2+} to the ones at the end of the T1 phase, it is evident that the eVTOL only achieves manageable robust design margins in the T2 phase.

The established hierarchical design paradigm to exclusively specify design variables at the current level of system decomposition is a significant contributing factor to minimizing the magnitude of the required design margins on the design parameters. As only design parameters on the sub-system level are baselined in the T1 design loop, other dependent design parameters remain free to be adapted by the sizing algorithm during the T2 phase. As a result, the impact of modifying the reference model for robustness on these rotorcraft design parameters is alleviated. Using the (main) rotor as an example, the parameters fixed in the T1 design loop include the rotor DL and solidity. Consequently, the geometrical dimensions of the system-element rotor blade remain adaptable in the T2 sizing loop. The rotor radius is hence automatically adjusted during the sizing loop, contributing to minimizing the ramifications on the required increase in engine power and design gross mass. As evident from the data in tables 21, 22 and 23, this characteristic of the developed methodology effectively benefits all rotorcraft configurations. Besides the increased transparency from the unveiling of the propagation of the uncertainty into the design space, which is a significant improvement over contemporary approaches in itself, this alleviation of the impact of the identified uncertainty on the robust design represents another important advantage of the developed methodology.

[6] See the model validation plots in figure 34 for the comparison of the technical model parameters.

5.3. Synthesis of the Simplifications and Assumptions and their Potential Impact on the Results

In the course of the example demonstration test-case execution, described in chapter 4, a series of simplifications and assumptions were taken. The necessity for some of these assumptions originates from the desire to limit the test case to a practical scope, thus ensuring that the focus is set on the methodology demonstration itself, rather than on the exploration of the fictive design scenario. Other simplifications and assumptions are needed to enable the methodology itself. Subsequently, the main simplifications and assumptions are outlined, and their potential impact on the obtained results of the test case, and the possible implications on the validity of the developed methodology, are discussed. The order of presentation does not constitute any relation to the relative significance of the individual items.

- **Simulation of Concurrent Engineering Activities**
  Typically, CE techniques are applied during late stages of the preliminary design phase in order to generate additional information about the design candidates, as outlined in chapter 4.5. These analyses may be performed to substantiate due design decisions between competing design options, or to increase the certainty about the assumed performance characteristics of a system element. For example, the expected aerodynamic properties of the fuselage and rotor blades may be validated by wind-tunnel-testing and CFD analysis. The increased confidence in the associated model parameter values may then be implemented into the model-based design logic, as performed in the example in chapter 4.5. This example shows that considerable benefit may arise from effective use of CE activities during preliminary design. However, as no resources have been available in the frame of this work to perform CE activities, the restriction of the confidence intervals simulated in chapter 4.5 is based on an assumed confidence improvement, rather than stemming from the analysis of actual data from corresponding CE activities. The confidence intervals for the CE-boosted $T2_+$ scenario are reduced by 50 % for all uncertainty factors compared to the initial T2 run. Whereas the general conclusions drawn are considered valid regardless of this assumption, the quantitative potential outlined in the example in chapter 4.5 may differ from an application in a practical use case, depending on the magnitude of the confidence interval reductions which can be justified by actual high-fidelity CE analyses.

- **Mass estimation**
  The mass-estimation method selected for each tier of model fidelity is depicted in table 2 in chapter 3.2. The fraction-based method in the T0 model, as well as the parametric mass estimation laws implemented in the T1 framework are considered consistent with the relative fidelity of the other sub-models of the respective model tier. In these cases, the design candidates make use of system parameters at the lowest current level of decomposition. For the T2 model, however, the system is decomposed further, whereas the fidelity of the mass estimation method does not develop to the same degree. The T2 mass estimation remains based on parametric laws, albeit these are now fed exclusively by already validated and verified model parameters. The decrease of the necessary robust DGM for all concepts from the T1 to the T2 stage demonstrates

the benefits from this improvement, which is considered to be a contributing factor. However, owing to the relative importance of the mass estimation in preliminary design, it is always desirable to deploy the highest-fidelity mass-estimation method which can be realized. For the T2 stage, a move from a top-down approach to a bottom-up methodology may hence be advisable. In this bottom-up approach, the masses of individual elements of the product breakdown may be derived based on high-fidelity stress calculations. Even actual mass data may be available for individual items of the avionics, for example. However, the generation of a bottom-up mass estimation is both complex and laborious, and therefore out of scope for this work.

In terms of the potential impact on the presented results of the example case, a more sophisticated mass estimation methodology would allow to further restrict the uncertainty attribution to the EM estimate. As a result, the required robust design margins required to control the model-related uncertainty would decrease, as indicated by the CE-boosted scenario explored in chapter 4.5

- **Hierarchical Design Approach**

  The developed methodology is based on a hierarchical approach to design. Generally, design decisions are taken on the currently active level of decomposition, and become requirements for the subsequent phases of the design process. This approach is considered to represent an enabler for an equally hierarchical approach to modeling, which in turn is a prerequisite for satisfying the established adequate-fidelity modeling paradigm. Other researchers, however, criticize hierarchical design approaches for their early fixing of design parameters, and advocate for a different approach, aiming at preserving the design freedom to as late a stage in the design process as possible. Examples for this argument are [20, 21]. The criticism circles around the hypothesis that hierarchical approaches are prone to premature fixing of design parameters, driven by the motivation to progress in spite of potentially insufficient available data at the respective point in time. As a result, sub-optimal designs may be obtained with respect to their cost-effectiveness.[7] This risk is certainly present when applying conventional empirically-based design methodologies, since design entities in this case inevitably are biased towards previously realized design, if only for risk-minimization reasons. Model-based design methodologies however allow to investigate competing design candidates in parallel until sufficient information is available to take an informed decision, thus avoiding this conflict of objectives. The limit to this parallel investigation is posed only by the available computing resources. The example case in chapter 4 demonstrates the principle by investigating three competing rotorcraft concepts throughout all phases.

- **Waiver of Trade Studies**

  Arguably, the most effective technique to generate data which enables informed decisions about competing design options is constituted in performing trade studies. The rivaling design options are evolved into design candidates, the subsequent analysis of which then provides the data to take a well-founded decision for the superior alternative. As the purpose of the example test-case lies in methodology demonstration, no such trade studies are performed in

[7] See chapter 2.1.1 for more information.

the scope of the example execution. Instead, design parameters are set to reasonable values and a sole baseline design for each rotorcraft concept in the scope is explored further. As a result, the obtained rotorcraft designs at the end of the preliminary design phase likely do not represent optimal designs for the particular design problem depicted in chapter 4.1. Depending on the optimization strategy, either design could likely be optimized for example for reduced DGM, or potentially even for decreased susceptibility to uncertainty. The aspects to consider when applying the developed methodology to a practical design problem are discussed more comprehensibly in chapter 5.4. However, as each baseline design is considered to be defined reasonably, the results derived from the test-case execution provide a meaningful and representative basis for the purpose of methodology demonstration.

- **Uncertainty attribution**

  The probability space of each design phase is a result of the attribution of uncertainty to those technical parameters which are subjected to uncertainty. This attribution is performed by the designer during the set-up of the probabilistic analysis. A number of potential sources of information is available in the definition of the confidence intervals and the respective probability distributions. First, empirical data of previously realized designs may be available. As argued for the conventional design methodologies, this data is particularly relevant when strong correlations can be obtained between distinct design features and resulting characteristics of the respective artifact. Second, additional analyses may be launched, either computational or experimental, to obtain complementary information about specific characteristics of the particular system-element of interest. The availability of such information may assist in objectifying the attribution of uncertainty to a certain extent.

  Finally, however, the spanned probability space always entails the subjectivity of the designing entity, yet significantly influences the resulting design margins required to control the prevalent uncertainty, as evident when comparing the results from chapters 4.4 and 4.5. Consequently, it is advisable to base the attribution of the uncertainty characteristics on objective data to the largest degree possible. In particular when competing concepts are evaluated, the consistency between the uncertainty allocations for these design candidates needs to be carefully established in order to avoid a potential bias. For the example test-case in this work, this bias is deliberately minimized as the confidence intervals are set comparably between the competing rotorcraft configurations, although a differentiation may be justified considering the larger level of residual-variability-type uncertainty stemming from the lack of experience with the novel eVTOL configuration. In any case, further research on this aspect is considered to be promising, as depicted further in chapter 6.2.

- **Problem of Size**

  The problem of size is introduced in chapter 4.3.2, limiting the dimension of the probability space in the T1 and, more so, in the T2 design loop. Ideally, all technical model parameters would be subjected to uncertainty. The computational expense however increases exponentially with the number of factors in the experiment. To limit the impact of the problem of size, a dedicated method for the generation of the computational grid was developed in order to

minimize the number of instances required to adequately represent the probability space.[8] However, the number of instances per factor, as well as the number of uncertainty factors in the probabilistic design space itself, requires limitation for the T1 and T2 analyses. This highlights the relevance of the problem of size already for design tasks of the size of the test case. Whereas this challenge is overcome to a reasonable degree by using modern high-performance computing clusters for the T2 level of model fidelity already today, the problem of size may limit the transferability of the developed methodology to high-fidelity analysis until sufficient progress in computing power is achieved, so that adequate computing resources for such applications become available.

- **Down-selection of Concepts**
  The test case developed in chapter 4 compares three competing concepts along all stages of the preliminary design phase for demonstration purposes. A practical design case would aim to select a superior concept earlier in the design process, typically during the T0 or T1 phases, in order to concentrate the available resources on the development of the most-promising design candidate. Classical SE theory proposes the cost-effectiveness of a design as a primary decision criterion. Whereas this is widely agreed in terms of principle, it is challenging to establish cost-estimation models of satisfying accuracy and reliability for rotorcraft. Existing models operate similar to parametric mass-estimation-laws, sharing their deficiencies. Normalized cost-estimations from NDARC, based upon such a methodology, are presented in chapter 5.2, but are considered to be of insufficient reliability, in particular for the cross-evaluation of different concepts. The most critical shortcoming in the context of this work is the inability to predict new concepts and technologies due to the lack of empirical data. Reliable cost estimation methods including eVTOL rotorcraft are not yet available, although this field is actively researched, e.g. by Duffy et al. [112]. In order to allow for the evaluation of competing concepts in terms of cost-effectiveness rather than pure capability, a practical design problem should include a cost estimation methodology in the assessment of the concepts. Once such models are available, it will be interesting to include cost parameters into the probabilistic analysis in a similar fashion as performed for the DGM for the example test-case.

- **Battery Technology**
  The fundamental assumption regarding the battery technology underlying the design of the eVTOL configuration concerns the specific energy of the battery cells. For the test case, it is assumed that the lithium-ion battery technology is exploited to its limits, yielding a battery specific energy of 250 Wh/kg on the cell level. As discussed in chapter 4.2.1, higher levels of specific energy require the adoption of new battery technologies such as lithium-air, although both the potential of new technologies as well as their readiness is assessed quite differently by various researchers. In any case, as the battery mass constitutes approximately 42 % of the total eVTOL design gross mass, a substantial improvement in battery cell energy density would significantly improve the competitiveness and viability of the eVTOL configuration compared to the design outlined in the example test-case.
  In a first-order evaluation of the impact of this assumption on the test-case eVTOL design,

[8] This methodology is outlined in detail in chapter 3.3.2.

consider the sketch of the configuration provided in figure in appendix C.1. The low energy density of the battery drives the DGM to a two-times higher value than for the helicopter. As a result, lifting this mass with reasonable levels of power yields rotor radii which necessitate to position two thrust-units at the trailing edge of the eVTOL wing. This however is an unfavorable design, for example as rotor-to-rotor interactions are stronger. Also, these rotors will be positioned in close proximity of the ground in hover mode. An increase in the battery specific energy would reduce the overall eVTOL mass, and hence enable a more-favorable architecture for the selected eVTOL configuration.

5.4. On the Applicability of the Proposed Methodology to Practical Preliminary Design Problems

Chapter 2.3.1 introduces the three dimensions of uncertainty: level, location, and nature. The presented methodology focuses on model-related uncertainty, as the design methodology is set up to systematically reduce epistemic uncertainty residing in the model environment. Hence, in terms of its location, this uncertainty resides in the representation of the design by the applied modeling. The hierarchical approach to design, and the associated adequate-fidelity modeling paradigm ensure a level of uncertainty of the statistical-uncertainty degree, which is thus quantitatively describable and hence controllable. By gradually but continuously progressing to the T2 level, the epistemic portion of the model-related uncertainty is progressively removed, and the remaining aleatory share is controlled via a dedicated control variable at all times. The effectiveness of the methodology to deal with model-related uncertainty is successfully demonstrated, enabling the adoption of model-based design in future preliminary design methodologies. However, further sources of uncertainty exist in practical preliminary design problems, which are not covered by the test case. From the perspective of the model-based design methodology, these uncertainties can be categorized into the residual-variability type, and are classified as aleatory. A practical preliminary design study however needs to include these uncertainties in a holistic approach. To this end, a brief discussion of further non-model-related uncertainties is provided below.

Variability in the system requirements is among the most relevant further sources of uncertainty. These changes may have a particularly severe impact if detrimental developments in the requirements occur at late stages of the development phase, at which point re-designs are excessively costly and time-consuming, see [5]. The uncertainty in the requirements may be of the epistemic or the aleatory nature. Extensive market research, for example, may pose a means to further substantiate system-level requirements. On the other hand, the market environment may evolve during the system's development, commanding requirement changes which are not avoidable by early research.

Further aleatory uncertainty resides in the design itself at any given stage of the design process, which may only be treated at later stages when additional information, for example from testing activities, becomes available. At any stage of the preliminary design process, the total uncertainty may be categorized according to its level, see figure 12. It is argued in chapter 2.3.1 that the lack of

knowledge for the deep levels of uncertainty, i.e. recognized ignorance and total ignorance, is too pronounced to be suitable to be treated by model-based approaches. According to Walker et al., this level of uncertainty is uncommon in engineering sciences [71], and arguably even more so in actual product development, in which the anticipated market and the needed system characteristics are usually known at least on the theoretical level. Nonetheless, as discussed in chapter 2.4, detecting unexpected emergent behavior in the developed rotorcraft only after its realization is by no means unprecedented in rotorcraft design, but more the norm in rotorcraft development to date, due to the high degree of complexity of the underlying aeromechanical phenomena. Evidently, a significant portion of uncertainty may reside in the design on the level of recognized-ignorance, trivially of the aleatory nature. Most commonly, this kind of uncertainty is attempted to be controlled by preserving contingencies on the empty mass as well as on the performance characteristics of the rotorcraft, which are then consumed by necessary re-designs or accepted deviations in rotorcraft performance. An adequate dimensioning of these margins is a delicate task. Preserving insufficient margins may endanger the compliance of the design to the user requirements, whereas overly conservative margins represent a self-fulfilling prophecy, since a non-ideal design in terms of cost-effectiveness then becomes a certainty. The developed methodology may assist in reducing the total uncertainty in a rotorcraft design problem by controlling the model-related portion of the total uncertainty, and by attributing these to the actual design parameters and hence increasing the design's robustness. As a result, the magnitude of the contingencies covering the aleatory recognized-ignorance portion of uncertainty may possibly be reduced.

For the epistemic portion of the non-model-related uncertainty, one can distinguish between statistical and scenario uncertainty in practical rotorcraft preliminary design problems. In the proposed hierarchical design approach, the statistical uncertainty at any stage of the design may be described and treated with the developed methodology. The probabilistic design space is analyzed, the impact of the uncertainty quantified, and a control variable is defined in order to control the technical uncertainty of this level. The scenario uncertainty however resides at a deeper level which eludes its description by probabilistic means. To this end, it is best practice to define, and subsequently explore, distinctive design problem scenarios which represent the different possible assumptions for a given factor in the design problem. These scenarios may be built around a differing set of anticipated requirements, or may be focused on varying technical assumptions, or a combination of both. Although the developed methodology does not treat scenario uncertainty itself, it arguably provides a significant boost in the ability to discriminate between different scenarios. As the statistical uncertainty potentially varies itself among the scenarios, but most certainly at least in terms of its influence, the developed methodology should allow for a more substantiated judgment of the competing scenarios by including aspects of design robustness.

Chapter 5.3 discusses the attribution of uncertainty among the main assumptions in the developed methodology, and its relevance to the value of the obtained results. The quantification of the residing model-related uncertainty becomes most valuable when it is integrated into a coherent and consistent risk management strategy for the system development at hand. For example, the definition of the desired target value for the robustness of the design should resemble the

stance taken in the definition of the confidence intervals and probability distributions. If the probability distributions are established in a conservative way, i.e. biased towards detrimental developments of system characteristics compared to the actually anticipated domain, a lower target robustness against the defined uncertainty may be tolerated for the robust design than in the case of an optimistically defined probability space. Equally, the baseline reference values may be defined rather conservatively or aggressively, with the corresponding implication on the degree of robustness requested from the robust design.

6. Conclusion and Recommendations for Future Work

6.1. Conclusion

A novel methodology for the preliminary design of rotorcraft was developed. The methodology is model-based, enabling the design and analysis of generic rotorcraft concepts, new technologies and novel configurations. A hierarchical approach to both design and model development was adopted, in order to facilitate the development of the Systems Engineering (SE) architectural views synchronously with the development of the system model. The deployed modeling strategy implements newly developed models of varying fidelity, whereby the respective model fidelity is tailored to the needs of the three design stages. To support the developed methodology, a standard SE-type design process was altered twofold. First, a dedicated Model Development Process (MDP) was introduced, which integrates model development into the hierarchical design approach. Second, the SE Architectural Design Process was enhanced by incorporating probabilistic elements into its core, allowing to prioritize and quantify model-related uncertainty, enabling controlling this uncertainty in a robust design.

The following main conclusions regarding the characteristics of the developed methodology are drawn:

- **Effectiveness and validity of the deployed models**
  As outlined in chapter 5.1, the deterministically sized reference designs show consistent and meaningful results in terms of the respective Design Gross Mass (DGM) required to satisfy the example case requirements. This consistency is observed in all of the three design tiers, and for all investigated rotorcraft concepts alike. More notably, this observation is not limited to the sizing-algorithm's target-parameter DGM, but is also evident throughout the entire spectrum of design parameters, as highlighted in chapter 5.2. Since the final tier of the design and analysis framework incorporates a validated design tool with NDARC, the validity of the newly developed code for the other tiers is considered to be confirmed by yielding consistent results for all rotorcraft types. Therefore, the established models of all three tiers are considered adequate for effectively designing and analyzing the broad range of rotorcraft concepts included in the scope of the model.
- **Integration of model development into a hierarchical design scheme**
  Moving to model-based preliminary design attributes a critical role to the modeling itself. The developed methodology thus integrates the model development into the hierarchical SE design process. In line with the established adequate-fidelity-modeling paradigm, the model development is performed equally hierarchically, and, crucially, synchronously with the concurrent development of the system representation in the SE architectural views. By

progressing the model and system development in parallel, the introduction of uncontrolled uncertainty is avoided, as outlined in chapter 3.3.1.

- **Consistent transitioning across model-fidelity levels**
  The MDP includes a dedicated model transitioning logic, avoiding any discontinuity when transitioning across the discrete levels of model fidelity. By incorporating the behavioral characteristics of the system under development into the Requirements Architecture, and subsequently verifying the model behavior in the next tier, a consistent and traceable model transition between the tiered preliminary design stages is ensured. The example demonstration case successfully establishes the effectiveness of the developed logic, indicated by the observed consistency in the model-transition plots depicted in chapters 4.3.1 and 4.4.1, as well as in the consistent DGM for all tiers after passing validation in the preceding MDP. These results highlight the ability to ensure the consistency of design decisions taken at the various levels of the system architecture, representing an important contribution to the hierarchical modeling strategy, and thus to the overall methodology.

- **Ability to quantify and control model-related uncertainty**
  The model-related uncertainty is successfully quantified in the analysis of the probabilistic design space, and subsequently controlled by means of a dedicated control variable on the EM. The resulting robust design margins are unveiled for each design parameter, which represents a major improvement over contemporary methodologies. The uncertainty is thus controlled in a traceable manner throughout the entire design, tracking the propagation of the identified uncertainty into the individual elements of the design. The ability to prioritize and quantify uncertainty of the model-related kind is a key element for the robustness and overall viability of model-based design methodologies.

- **Removal of epistemic uncertainty by increasing model fidelity**
  As hypothesized during the development of the methodology, model-related uncertainty of the epistemic nature is progressively removed with increasing model fidelity, as demonstrated in the example test-case. The results are particularly noteworthy for the transition from the Tier 1 (T1) phase to the initial Tier 2 (T2) scenario, in which comparable levels of uncertainty are maintained across the tiers in the set-up of the probability spaces, in order to determine the isolated impact of the further increase in model fidelity. While this mechanism was expected, the magnitude of the epistemic uncertainty reduction induced by moving to the higher-fidelity models is impressive.

- **Visibility of uncertainty propagation into the design space**
  The prevalent model-related uncertainty is transparently captured at all stages of the development, and its location is attributed to specific elements of the Technical Architecture of the system under design. As evident from the comparison of the deterministic and robust designs in chapter 5.2, the propagation of this uncertainty in the design space is visible for each design parameter, vastly improving this important aspect of preliminary design compared to historical approaches.

- **Adaptation of the required design margins to the design problem**

The capability of the methodology to determine the magnitude of the specific design margins for robustness for the particular design problem at hand represents a major improvement over contemporary approaches, which typically apply a pre-defined design margin on the system level. In these historical approaches, the magnitude of this margin is derived from experience, frequently leading to over- or under-sizing of the rotorcraft, depending on the adequacy of the initial design margins. Consequently, the developed methodology is expected to produce designs which are either more optimized for the particular application or more robust. At the same time, the confidence in the design is increased, as the robust design margins may now be tailored to the specific design problem.

To demonstrate its effectiveness and validity, the developed methodology was tested in a fictive Urban Air Mobility (UAM) scenario, presented in chapter 4. Conventional helicopter and tiltrotor configurations were explored, alongside a novel Electric Vertical Takeoff and Landing (Aircraft) (eVTOL) concept. These design candidates were developed from the initial exploration stage down to the system-element level of decomposition, demonstrating the sizing capabilities of the developed software. The most relevant findings from the example test-case execution are as follows:

- **Comparison of the obtained designs**
  Reviewing the reference designs of the investigated rotorcraft concepts, the helicopter configuration requires the lowest DGM to satisfy the design scenario (2161 kg), followed by the tiltrotor (3048 kg), and then the eVTOL (4330 kg).

- **Moderate design margins achieve robustness**
  Among the most interesting findings of the test case is the moderate level of the design margins in terms of needed DGM increase which are required to modify the reference designs for robustness against the model-related uncertainty remaining at the end of the preliminary design phase. Chapter 5.2 compares the differences in the obtained designs in detail. The helicopter configuration requires the smallest absolute robust design margin (72 kg), followed by the tiltrotor (107 kg). Even for the most-sensitive eVTOL configuration, a reasonably modest required design margin is ultimately achieved (183 kg), despite the robustness issues experienced for this configuration in the initial Tier 0 (T0) stage. Therefore, the robustness of the methodology itself is assessed favorably.

- **Configuration-specific sensitivity to uncertainty**
  Interestingly, the investigated rotorcraft configurations exhibit distinctly different degrees of sensitivity to model-related uncertainty, in spite of comparable levels of uncertainty applied in the definition of the respective probability spaces. The difference in robustness is particularly pronounced in the early tiers of the development process, whereas the gap is largely diminished at the final stage. Apparently, specific characteristics of the configurations impact their robustness characteristics. It is hypothesized that the mass efficiency plays a dominant role in this behavior, as the relative sensitivity of the investigated rotorcraft configurations against the model-related uncertainty appears to correlate with their relative Empty-Mass (EM) ratios EM/DGM.

- **Non-linear effectiveness of uncertainty-reducing activities**
  In the Tier-2 scenario boosted by Concurrent Engineering ($T2_+$), the more sensitive tiltrotor and eVTOL configurations benefit disproportionately from the assumed reduction in uncertainty levels compared to the already more robust helicopter, see chapter 4.5. This finding promises to inspire strategies for exploring competing design candidates or technologies more efficiently in the future.

- **Assessment of the eVTOL concept for the UAM scenario**
  The eVTOL concept is generally considered to be well-suited for the investigated UAM scenario, due to an alleged reduction in complexity, and hence purchase price and maintenance costs. Other anticipated advantages of the concept are reduced noise and improved safety, as detailed in chapter 4.1. The example test-case focuses on methodology demonstration rather than the comprehensive investigation of the UAM design problem, resulting in a series of simplifications and assumptions, summarized in chapter 5.3, which may limit the validity of any conclusions drawn from the test case in terms of the general suitability of the competing concepts for the investigated scenario. However, since the differences in overall rotorcraft size are substantial, an evaluation is offered. Since a reliable means of cost estimation eludes current capabilities in rotorcraft modeling,[1] no conclusion in terms of relative price and maintenance costs between the competing concepts is possible. However, considering the vast difference in DGM between the helicopter and the eVTOL configurations, it is considered unlikely that this penalty can be recovered by the eVTOL economic properties or noise emissions, at least with the assumption of state-of-the-art technology level regarding the battery cell energy density taken for the example demonstration. Therefore, the test case results indicate that a breakthrough in battery technology is indeed needed for fully-electric propulsion vehicles to satisfactorily comply with an UAM design scenario as outlined in chapter 4.1.

Overall, the example case presented in chapter 4, as well as the discussion in chapter 5, demonstrate that the developed probabilistic and hierarchical methodology provides an effective and valid framework for the model-based preliminary design of rotorcraft. The required properties of modern preliminary design methodologies established in chapter 2.5 are achieved. Thus, it is concluded that this methodology provides an effective framework for the broad adoption of model-based methodologies in the field of rotorcraft preliminary design.

6.2. Recommendations for Future Work

The following recommendations are made for future investigations and improvements to the methodology developed in this work:

- The example case successfully demonstrates the capability of the developed methodology to quantify model-related uncertainty in a preliminary design problem. Hence, it may be of interest to explore sizing strategies which directly target maximized design robustness, instead

[1] Schwabe et al. provide a comprehensive review of the state-of-the-art in aerospace cost estimation methods [135].

of optimizing for maximum capabilities. The comparison of the designs obtained from these fundamentally different objectives may allow the relevance of such a strategy to be assessed.

- As discussed in chapter 6.1, a configuration-specific sensitivity to uncertainty is observed, and an interrelation of this phenomenon with the model fidelity is also identified. Apparently, specific features of the design, and potentially of the probability space, cause this characteristic behavior. The mass efficiency of a rotorcraft configuration is suspected as a primary influencing parameter in this respect. It would be of great interest to further test this hypothesis, and to seek further insights into the nature of uncertainty in preliminary design. If distinct correlations can be identified, these could assist in improving preliminary designs for robustness in the future.

- As discussed in chapter 5.3, the developed methodology currently entails subjectivity as it allows for the incorporation of engineering judgment in the set up of the probabilistic design space. This choice is mainly driven by the absence of capable objective methods for the generation of uncertainty attributes. Expert engineering judgment supported by relevant data is considered the most capable substitute for such a method for the time being. However, increasing the degree of objectivity by adding equally-capable objective methods remains desirable for improving the developed Robust Architectural Design Process (RADP) further.

- It may be advisable to perform a sensitivity study before the definition of the probabilistic design space, in order to ensure that the most-influential model parameters are included in the probabilistic analysis. For the example case performed in this work, this selection was based upon previous experience with the methodology, which is considered sufficiently reliable for most preliminary design problems. However, sensitivity studies could further substantiate this selection, in particular for unusual design problems. For instance, a possible implementation could build upon a series of full-factorial numerical experiments. Interaction plots could then be derived from the generated data, in order to analyze the combined influence of particular sets of model parameters on the resulting DGM.

- In chapter 4.5, the potential of concurrently performed high-fidelity activities to augment the preliminary design process is highlighted. In order to maximize the effectiveness of this design technique, a methodical investigation is recommended. These studies should explore at which phase of the preliminary design process higher-fidelity analyses may provide the greatest benefit.

- The presented methodology focuses on model-related uncertainty, whereas practical design problems require a holistic approach to risk management in order to ensure a viable design with a high probability of success. The incorporation of the developed methodology into an overall product development process may therefore be of interest, especially for application in industry. An initial discussion of this aspect is provided in chapter 5.4.

- A limitation in the methodology encountered in the exploration of the example case is posed by the “Problem of Size”. This issue was addressed by optimizing the computational grid for efficiency, and by restricting the number of factors in the probabilistic analysis to the most-influential. Continuously growing availability of computing power is likely to alleviate this issue. However, as the model complexity and hence associated computational effort

increases in parallel, the incorporation of methodologies which reduce the burden of the probabilistic analysis without sacrificing its effectiveness remain worthy of exploration. The comprehensive review of research in the related field of Uncertainty-Based Multidisciplinary Design Optimization (UMDO) by Yao et al. may assist in identifying starting points [136].

A. Helicopter Data

A.1. Sketch of the Helicopter Design

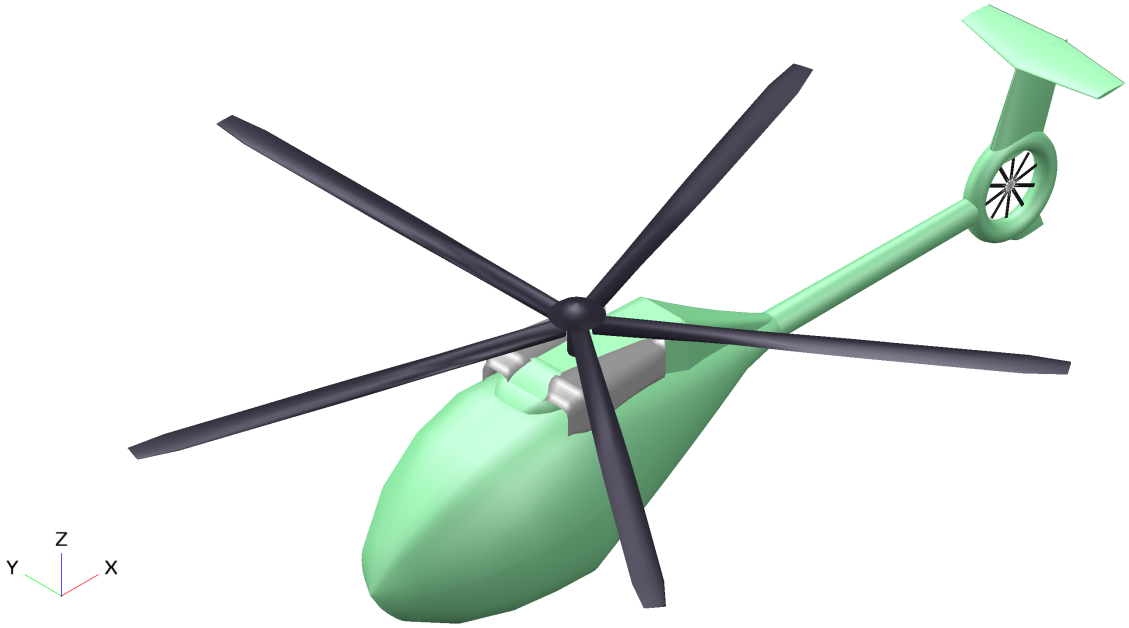

Figure 44 Sketch of the Helicopter Design.

A.2. Comparison of the T2 and T2$_+$ Deterministic and Robust Helicopter Designs

Parameter	Tier-2 Deterministic	Tier-2 Robust	Δ_{T2}	Tier-2$_+$ Robust	Δ_{T2+}
Design Gross Mass	2161 kg	2271 kg	5.1 %	2231 kg	3.2 %
Empty Mass	1568 kg	1673 kg	6.7 %	1635 kg	4.3 %
Fuselage Length	8.02 m	8.13 m	1.4 %	8.09 m	0.9 %
Overall Wetted Surface	38.9 m^2	39.6 m^2	1.8 %	39.3 m^2	1.0 %
Design Mission Fuel	136.2 kg	141.5 kg	3.9 %	139.5 kg	2.4 %
MR Disk Load	365 N/m^2	365 N/m^2	n/a	365 N/m^2	n/a
MR Solidity	0.0994	0.0994	n/a	0.0994	n/a
MR Tip Speed	210 m/s	210 m/s	n/a	210 m/s	n/a
MR Rotational Speed	48.85 rad/s	47.65 rad/s	−2.5 %	48.08 rad/s	−1.0 %
MR Radius	4.30 m	4.41 m	2.6 %	4.37 m	1.6 %
MR Chord	277 mm	284 mm	2.5 %	283 mm	2.2 %
MR Blade Number	5	5	n/a	5	n/a
TR Radius	0.851 m	0.871 m	2.4 %	0.864 m	1.5 %
TR Solidity	0.160	0.160	n/a	0.160	n/a
TR Blade Number	10	10	n/a	10	n/a
Horizontal Stabilizer Area	0.773 m^2	0.773 m^2	0.0 %	0.773 m^2	0.0 %
Vertical Stabilizer Area	1.121 m^2	1.121 m^2	0.0 %	1.121 m^2	0.0 %
Installed Power (MCP SLS)	2×402 kW	2×417 kW	3.7 %	2×412 kW	2.5 %
Fuel Flow (MCP SLS)	57.3 kg/h	59.4 kg/h	3.7 %	58.7 kg/h	2.4 %
Drive System Limit	591 kW	610 kW	3.2 %	603 kW	2.0 %
Normalized Fly-away Price	100 %	103.4 %	3.4 %	102.1 %	2.1 %

Table 24 Comparison of selected characteristic design parameters of the T2 and T2$_+$ Deterministic and Robust Helicopter Designs.

B. Tiltrotor Data

B.1. Sketch of the Tiltrotor Design

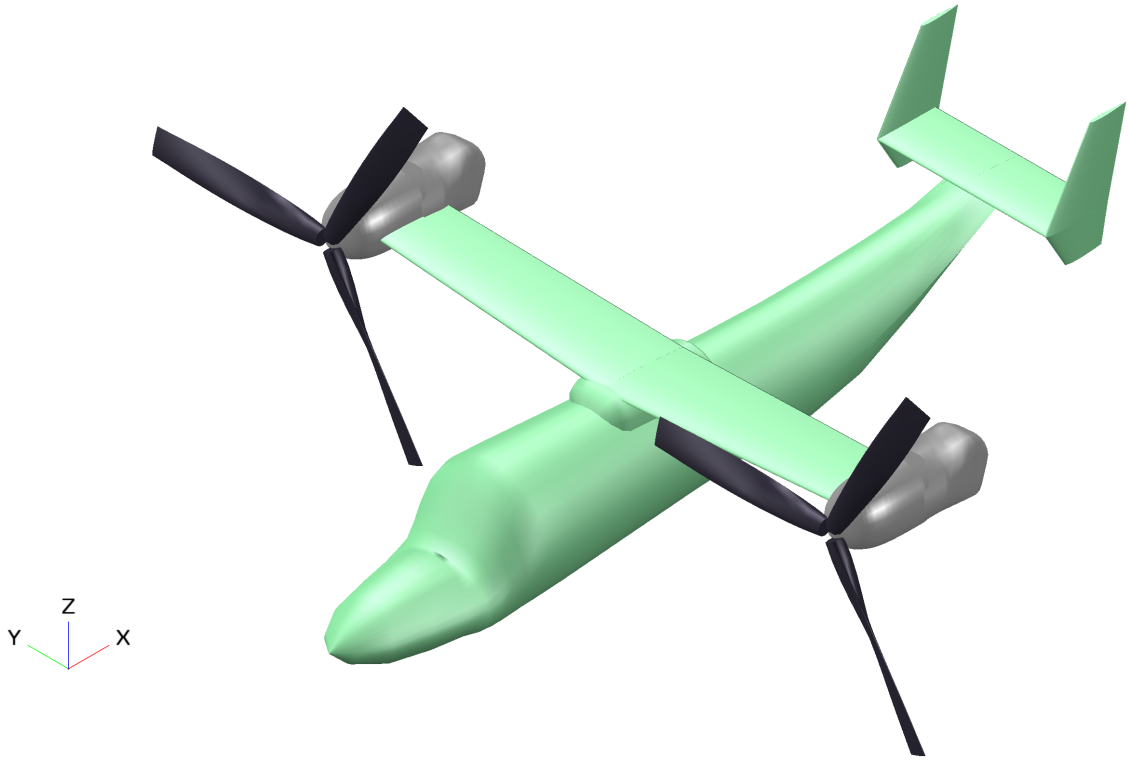

Figure 45 Sketch of the Tiltrotor Design.

B.2. Comparison of the T2 and T2$_+$ Deterministic and Robust Tiltrotor Designs

Parameter	Tier-2 Deterministic	Tier-2 Robust	Δ_{T2}	Tier-2$_+$ Robust	Δ_{T2+}
Design Gross Mass	3048 kg	3240 kg	6.3 %	3154 kg	3.5 %
Empty Mass	2423 kg	2611 kg	7.8 %	2522 kg	4.1 %
Fuselage Length	10.36 m	10.52 m	1.5 %	10.45 m	0.9 %
Overall Wetted Surface	90.2 m^2	93.1 m^2	3.2 %	91.8 m^2	1.8 %
Design Mission Fuel	133.4 kg	138.7 kg	4.0 %	136.3 kg	2.2 %
Disk Load	634 N/m^2	634 N/m^2	n/a	634 N/m^2	n/a
Rotor Solidity	0.120	0.120	n/a	0.120	n/a
Rotor Tip Speed	225 m/s	225 m/s	n/a	225 m/s	n/a
Rotor Rotational Speed	82.33 rad/s	79.86 rad/s	−3.0 %	80.95 rad/s	−1.7 %
Rotor Radius	2.74 m	2.82 m	2.9 %	2.79 m	1.8 %
Rotor Chord	366 mm	375 mm	2.5 %	372 mm	1.6 %
Rotor Blade Number	3	3	n/a	3	n/a
Wing Loading	3686 N/m^2	3686 N/m^2	n/a	3686 N/m^2	n/a
Wing Aspect Ratio	7.73	7.59	−1.8 %	7.65	−1.0 %
Wing Span	7.92 m	8.09 m	2.1 %	8.01 m	1.1 %
Horizontal Stabilizer Area	2.141 m^2	2.297 m^2	7.3 %	2.228 m^2	4.1 %
Vertical Stabilizer Area	2.507 m^2	2.640 m^2	5.3 %	2.581 m^2	3.0 %
Installed Power (MCP SLS)	2×439 kW	2×446 kW	1.6 %	2×443 kW	0.9 %
Fuel Flow (MCP SLS)	124.9 kg/h	126.8 kg/h	1.5 %	126.0 kg/h	0.9 %
Drive System Limit	864 kW	920 kW	6.5 %	897 kW	3.8 %
Normalized Fly-away Price	100 %	103.0 %	3.0 %	101.6 %	1.6 %

Table 25 Comparison of selected characteristic design parameters of the T2 and T2$_+$ Deterministic and Robust Tiltrotor Designs.

C. Electric VTOL Data

C.1. Sketch of the eVTOL Design

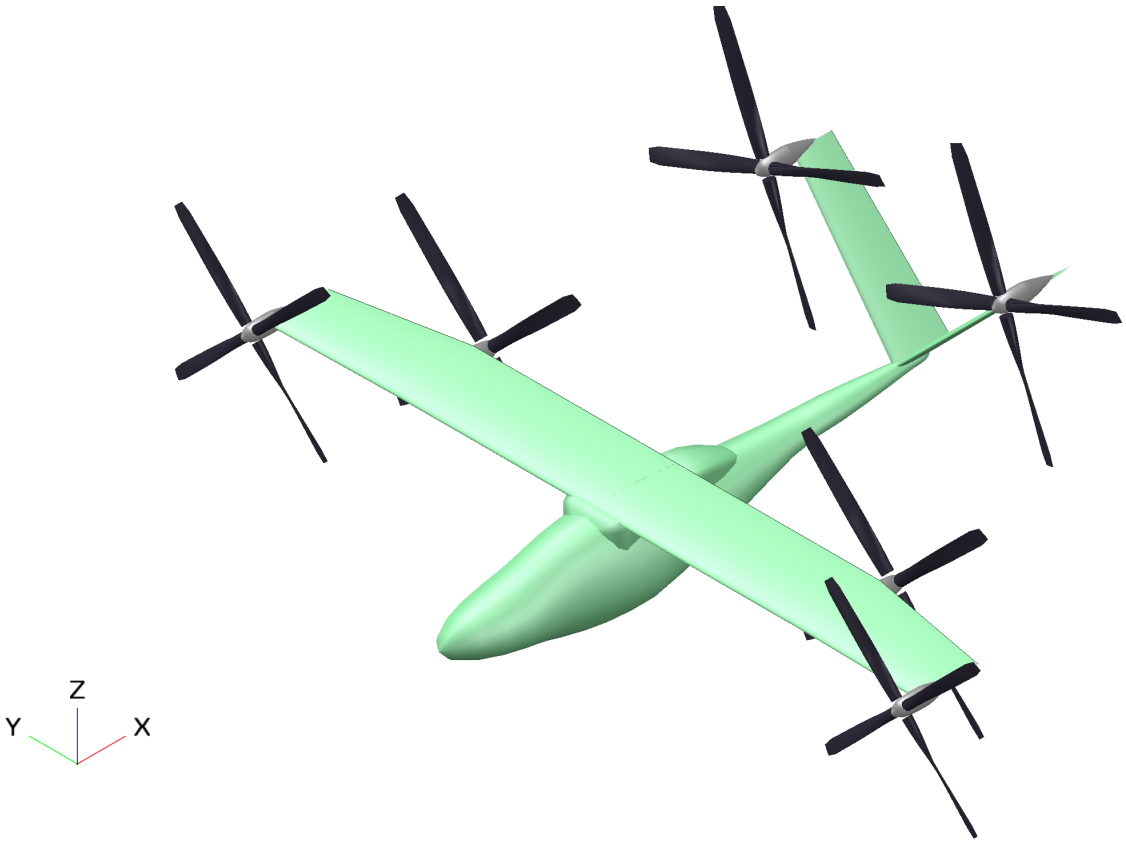

Figure 46 Sketch of the Electric VTOL Design.

C.2. Comparison of the T2 and T2$_+$ Deterministic and Robust eVTOL Designs

Parameter	Tier-2 Deterministic	Tier-2 Robust	Δ_{T2}	Tier-2$_+$ Robust	Δ_{T2+}
Design Gross Mass	4330 kg	4701 kg	8.6 %	4510 kg	4.2 %
Empty Mass	3877 kg	4248 kg	9.6 %	4056 kg	4.6 %
Battery Cell Specific Energy	250 Wh/kg	250 Wh/kg	n/a	250 Wh/kg	n/a
Battery Mass	1818 kg	1957 kg	7.6 %	1886 kg	3.7 %
Fuselage Length	7.35 m	7.66 m	4.2 %	7.50 m	2.0 %
Overall Wetted Surface	71.5 m^2	75.0 m^2	4.9 %	73.2 m^2	2.4 %
Design Mission Energy	378.9 kWh	405.8 kWh	7.1 %	391.9 kWh	3.4 %
Disk Load	634 N/m^2	634 N/m^2	n/a	634 N/m^2	n/a
Propeller Solidity	0.130	0.130	n/a	0.130	n/a
Propeller Tip Speed	225 m/s	225 m/s	n/a	225 m/s	n/a
Propeller Rotational Speed	119.66 rad/s	114.84 rad/s	−4.0 %	117.24 rad/s	−2.1 %
Propeller Radius	1.88 m	1.96 m	4.3 %	1.92 m	2.1 %
Propeller Chord	204 mm	213 mm	4.4 %	207 mm	1.5 %
Propeller Blade Number	4	4	n/a	4	n/a
Wing Loading	3541 N/m^2	3541 N/m^2	n/a	3541 N/m^2	n/a
Wing Aspect Ratio	7.89	7.89	0.0 %	7.89	0.0 %
Wing Span	9.73 m	10.14 m	4.2 %	9.93 m	2.1 %
V-Tail Stabilizer Area	5.164 m^2	5.164 m^2	0.0 %	5.164 m^2	0.0 %
V-Tail Dihedral Angle	45°	45°	n/a	45°	n/a
Installed Power (Continuous)	6×168 kW	6×182 kW	8.3 %	6×175 kW	4.2 %
Normalized Fly-away Price	100 %	106.5 %	6.5 %	103.1 %	3.1 %

Table 26 Comparison of selected characteristic design parameters of the T2 and T2$_+$ Deterministic and Robust eVTOL Designs.

D. Probability Density Functions of Further Tier-2 Tiltrotor Runs

D.1. Larger Number of Instances per Uncertainty Factor

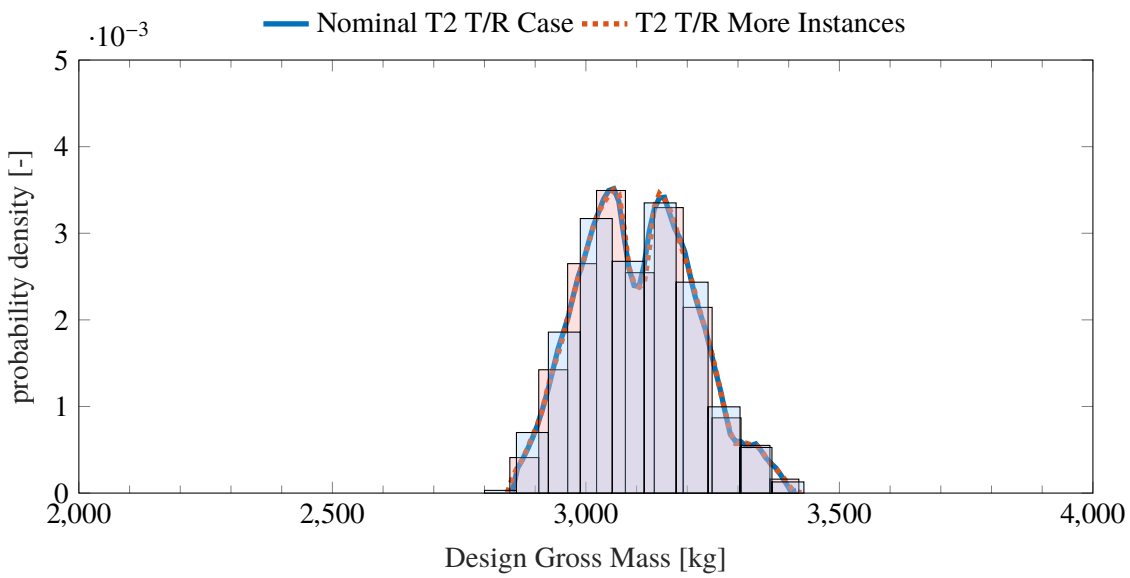

Figure 47 Tiltrotor Tier-2 Probability Density Function for an increased number of instances per uncertainty factor compared to the regular Tier-2 scenario.

D.2. Larger Number of Instances for the Empty-Mass-Related Uncertainty Factor

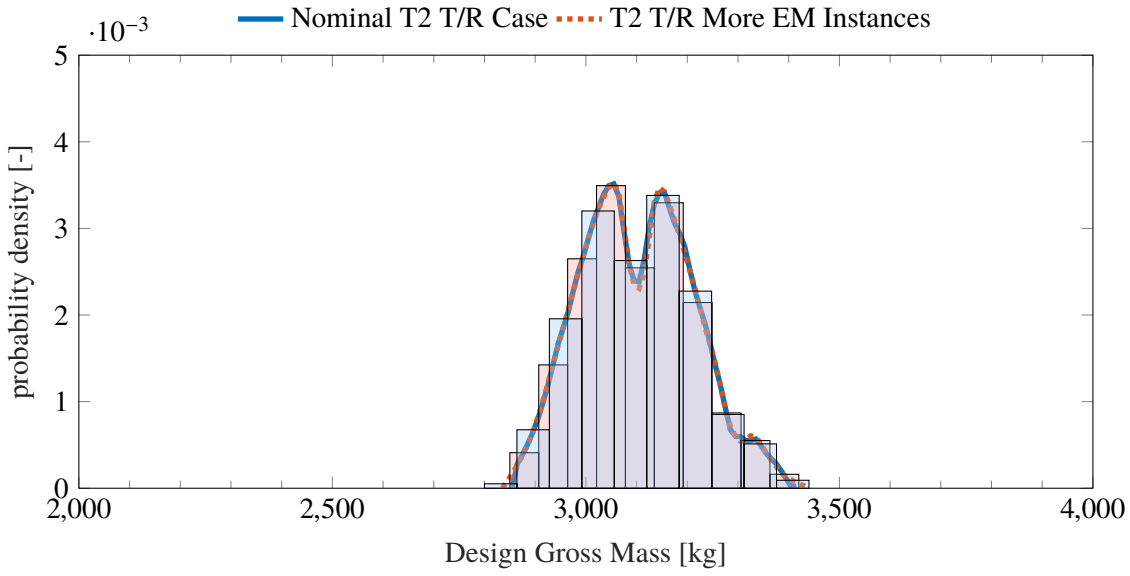

Figure 48 Tiltrotor Tier-2 Probability Density Function for an increased number of instances for the empty-mass uncertainty factor compared to the regular Tier-2 scenario.

E. Uncertainty Allocation for the CE-boosted $T2_+$ Scenario

	Parameter	Baseline Value	Confidence Interval
H/C	κ in hover	Computed, $f(\vec{p}_{T2})$	$\pm$ 0.02
	f_{RC} in cruise	Computed, $f(\vec{p}_{T2})$	$\pm$ 0.1 m^2
	k_{DL} fraction of DGM	Computed, $f(\vec{p}_{T2})$	-0.002, $+0.015$
	$\bar{c}_d$ in cruise	Computed, $f(\vec{p}_{T2})$	-0.0016 to $+0.0009$
	EM/DGM	Computed, $f(\vec{p}_{T2})$	-0.0075, $+0.015$
	k_{FF}	Computed, $f(\vec{p}_{T2})$	$\pm$ 0.01
	f_{Int}	*Not applicable*	
T/R	κ in hover	Computed, $f(\vec{p}_{T2})$	-0.01, $+0.025$
	f_{RC} in cruise	Computed, $f(\vec{p}_{T2})$	$\pm$ 0.05 m^2
	k_{DL} fraction of DGM	Computed, $f(\vec{p}_{T2})$	-0.015, $+0.025$
	$\bar{c}_d$ in cruise	Computed, $f(\vec{p}_{T2})$	-0.00115, $+0.00135$
	EM/DGM	Computed, $f(\vec{p}_{T2})$	-0.01, $+0.02$
	k_{FF}	Computed, $f(\vec{p}_{T2})$	$\pm$ 0.01
	f_{Int}	*Not applicable*	
eVTOL	κ in hover	Computed, $f(\vec{p}_{T2})$	-0.01, $+0.025$
	f_{RC} in cruise	Computed, $f(\vec{p}_{T2})$	$\pm$ 0.05 m^2
	k_{DL} fraction of DGM	Computed, $f(\vec{p}_{T2})$	-0.0025, $+0.0025$
	$\bar{c}_d$ in cruise	Computed, $f(\vec{p}_{T2})$	-0.00145, $+0.00105$
	EM/DGM	Computed, $f(\vec{p}_{T2})$	-0.01, $+0.02$
	k_{FF}	*Not applicable*	
	f_{Int}	1.2	$\pm$ 0.025

Table 27 Subset of $T2_+$ CE-boosted scenario reference technical model parameters subjected to uncertainty.

	H/C	T/R	eVTOL
κ_{hover}	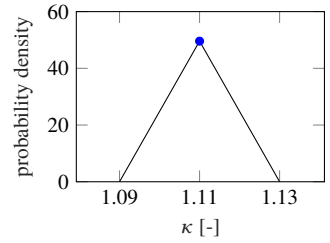	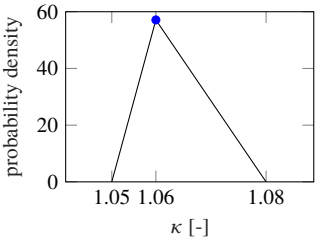	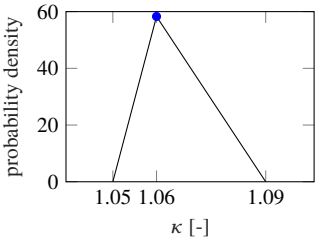
f_{RC}	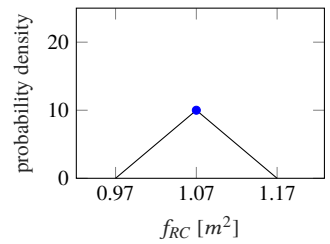	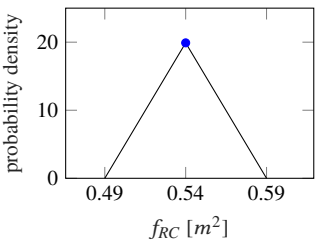	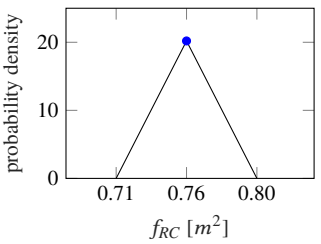
k_{DL}	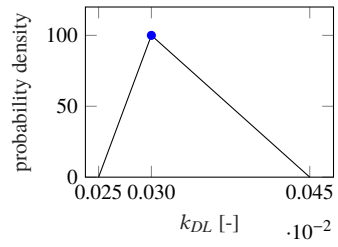	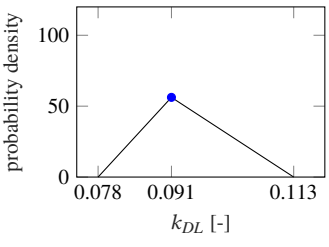	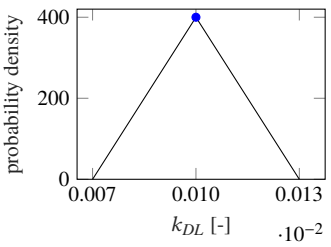
$\bar{c}_{d,hover}$	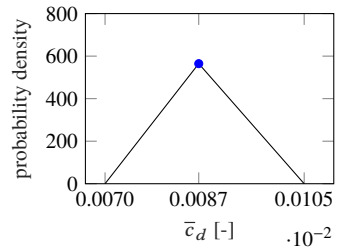	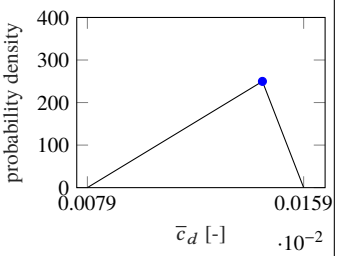	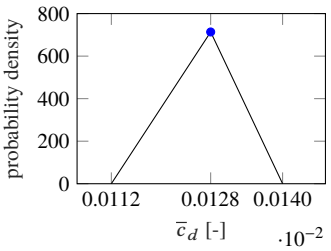
EM/DGM	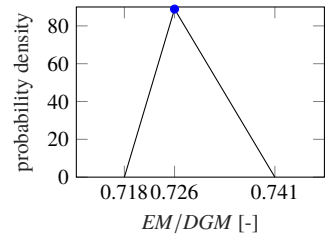	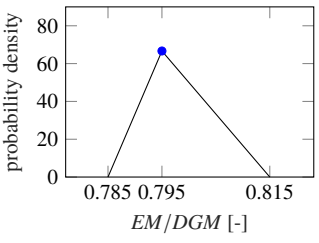	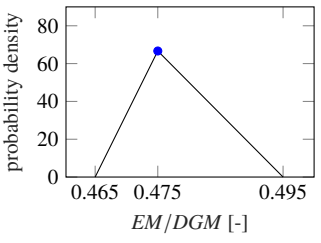
k_{FF}	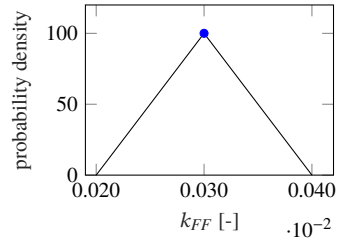	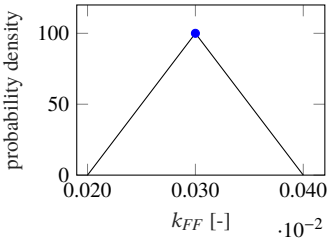	Not applicable

f_{Int}	Not applicable	Not applicable	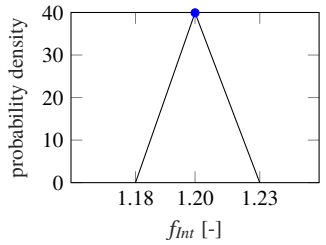

Table 28 Tier-2 CE-boosted scenario uncertainty allocation to technical model parameters. The reference value is indicated as a blue marker.

	$(EM/DGM)_{ref}$	χ_{EM}	$(EM/DGM)_{rob}$	Δ_{EM}
H/C	0.726	2.81 %	0.733	0.007
T/R	0.795	1.94 %	0.800	0.005
eVTOL (excl. Battery)	0.475	2.85 %	0.481	0.006
eVTOL (incl. Battery)	0.895	2.85 %	0.899	0.004

Table 29 $T2_+$ CE-boosted scenario resulting empty mass control variable values χ_{EM} and robust EM/DGM fractions to obtain a robust design.

F. Overview of the Tier-1 Modeling

The hierarchical modeling strategy adopted in this work is presented in chapter 3.2. As the Tier 1 (T1) modeling consists of newly developed code, a summary of the main aspects of its modeling is presented hereafter to provide an overview of the T1 modeling principles.

F.1. Symbols

Symbol	Unit	Description
A	m^2	Rotor disk area, $A = \pi R^2$
a_w	–	Tail rotor wake contraction rate
AR	–	Wing aspect ratio
$\bar{c}_d$	–	Rotor blade mean drag coefficient
C_D	–	Wing drag coefficient
C_{D0}	–	Wing zero lift drag coefficient
C_L	–	Wing lift coefficient, $C_L = \frac{L}{qS}$
C_T	–	Rotor thrust coefficient, $C_T = \frac{T}{\rho A V_{tip}^2}$
c_T/σ	–	Rotor blade loading
D_{RC}	N	Rotorcraft drag force
D_{Wing}	N	Drag force due to wing lift
D_{Total}	N	Total drag force
e	–	Oswald efficiency factor
f_{RC}	m^2	Rotorcraft equivalent flat plate drag area
FM_{tr}	–	Tail rotor figure of merit
g	m/s^2	Gravitational acceleration constant
i_{disk}	rad	Rotor disk angle of attack
K	–	"Drag-due-to-lift factor", $K = \frac{1}{\pi ARe}$
k_{DL}	–	Download factor, where $k_{DL} = f(V_x)$
$k_{mrDrive}$	–	Main rotor drive system losses, fraction of main rotor power
$k_{trDrive}$	–	Tail rotor drive system losses, fraction of tail rotor power
k_{ts}	–	Thrust share coefficient per rotor. Either equally distributed among all rotors (default), or user-specified
l_{antiQ}	m	Anti-torque system lever arm. Corresponds to the distance of main and tail rotor shaft axes for conventional helicopters.
L_{Wing}	N	Wing lift force
M	kg	(Rotorcraft) mass
P_0	W	Profile power
$P_{accessories}$	W	Power off-take for accessories
P_c	W	Climb (or descent) power
P_h	W	Ideal rotor power
P_i	W	Induced rotor power

P_{losses}	W	Sum of power losses, $P_{losses} = P_{accessories} + P_{loss,mr} + P_{loss,tr}$
$P_{loss,mr}$	W	Main rotor drive mechanical losses
$P_{loss,tr}$	W	Tail rotor drive mechanical losses
P_{mr}	W	Main rotor power, $P_{mr} = P_i + P_0 + P_p + P_c$
P_p	W	Parasite power
P_{req}	W	(Total) power required
P_{tr}	W	Tail rotor power
q	kg/ms^2	Dynamic pressure, $q = \frac{1}{2}\rho V^2$
Q_{mr}	Nm	Main rotor torque
R	m	Rotor radius
R_{tr}	m	Tail rotor radius
S	m^2	Wing area
T	N	Rotor thrust force
T_{antiQ}	N	Anti-torque system thrust force
v	m/s	Induced velocity
v_h	m/s	Ideal induced velocity in hovering flight
V	m/s	Rotorcraft speed
V_{tip}	m/s	Rotor tip speed, $V_{tip} = \Omega R$
V_x	m/s	Horizontal speed
V_y	m/s	Lateral speed
V_z	m/s	Vertical speed
W	N	Weight force, $W = Mg$
κ	–	Induced power factor, indicating the ratio between real induced power to ideal power
λ	–	Rotor inflow ratio $\lambda = \frac{V \sin i_{disk} + v}{\Omega R} = \mu \tan i_{disk} + \lambda_i$
λ_i	–	Rotor induced inflow ratio $\lambda_i = \frac{v}{\Omega R}$
μ	–	Rotor advance ratio $\mu = \frac{V}{\Omega R}$
Ω	rad/s	Rotor rotational speed
ρ	kg/m^3	Air density
σ_r	–	Rotor solidity
Θ_{FP}	rad	Flight path angle

Table 30 List of Symbols for the Tier-1 modeling overview.

F.2. Performance

F.2.1. Forces

The flight path angle is determined applying the small angles approximation, i.e. assuming $T \approx W$. The rotor disk angle of attack then follows from:

$$\Theta_{FP} = 0, \text{ in vertical flight.}$$

$$\Theta_{FP} = \arcsin\left(\frac{V_z}{\sqrt{V_x^2 + V_y^2 + V_z^2}}\right), \text{ in cruise mode.}$$

$$i_{disk} = \Theta_{FP} + \arctan\left(\frac{D_{Total}}{W}\right)$$

$$i_{disk} = \frac{\pi}{2}, \text{ in cruise mode with tilted rotors.}$$

The T1 drag forces are computed for the global rotorcraft and the lifting surfaces, if present, as follows:

$$D_{RC} = \frac{1}{2}\rho f_{RC}\left(V_x^2 + V_y^2\right), \text{ where } f_{RC} = \text{const. in T1.}$$

$$C_D = C_{D0} + KC_L^2$$

$$D_{Wing} = qSC_D$$

$$D_{Total} = D_{RC} + D_{Wing}$$

The rotor thrust is determined in accordance with the number of rotors and the lifting share convention established. The default logic assumes an equally distributed lifting share between all lifting rotors.

$$T = \frac{k_{ts}W(1 + k_{DL})}{\cos(i_{disk})}, \text{ in hovering mode.}$$

$$T = D_{Total}, \text{ in cruise mode.}$$

For the single-main-single-tail-rotor helicopter configuration, the rotorcraft is trimmed in the yaw-axis to ensure an appropriate anti-torque system sizing:

$$T_{antiQ} = Q_{mr}/l_{antiQ}$$

F.2.2. Power

F.2.2.1 Induced Power

The induced velocity is computed from basic momentum theory. For vertical flight:

$$v_h = \sqrt{\frac{C_T}{2}}\Omega R$$

$$v = -\frac{V_z}{2} + \left(\left(\frac{V_z}{2}\right)^2 + v_h^2\right)^{1/2}, \text{ where } V_z \geq -v_h.$$

$$v = -\frac{V_z}{2} - \left(\left(\frac{V_z}{2}\right)^2 + v_h^2\right)^{1/2}, \text{ where } V_z < -2v_h.$$

$$v \approx V_z\left(0.373\left(\frac{V_z}{v_h}\right)^2 - 1.991\right), \text{ for flight in Vortex Ring State or Turbulent Wake State.}$$

In forward flight, the default model uses a Newton-Raphson algorithm to solve Glauert's inflow formula iteratively to obtain the induced velocity:

$$\lambda_i = \frac{C_T}{2\sqrt{\mu^2 + \lambda^2}}$$

$$v = \lambda_i \Omega R$$

The default model for the induced power correction factor κ sets constant correction factors depending on the rotorcraft flight state and type. The model values are recommended to be set by the user in accordance with the anticipated characteristics of the rotorcraft. The following default values are applied in case no user input is provided:

For the helicopter:	$\kappa = 1.14$	in hover.
	$\kappa = 1.30$	in low-speed forward flight.
	$\kappa = 2.00$	in cruise flight.
For the tiltrotor:	$\kappa = 1.13$	in hover.
	$\kappa = 37.0$	in low-speed forward flight.
	$\kappa = 37.0$	in cruise flight.
For the eVTOL:	$\kappa = 1.09$	in hover.
	$\kappa = 28.5$	in low-speed forward flight.
	$\kappa = 28.5$	in cruise flight.

Alternatively, a polynomial-based model is implemented, which computes κ from a base value. The variable x is a function of the blade loading c_T/σ and the advance ratio μ. The coefficients k_i of the polynomial are scaled to match literature data in their default state, and may be user-specified

if desired.

$$\kappa = \kappa_{base} + k_1 x + k_2 x^2$$

The induced power per rotor is then computed from:

$$P_i = \kappa T v$$

F.2.2.2 Profile Power

The default profile power model is built around the rotor blade mean drag coefficient $\overline{c}_d$ to compute the profile power. For the helicopter configuration, a polynomial correction is included to account for the detrimental aerodynamic effects on the rotor in edgewise forward flight:

$$P_0 = \frac{\sigma_r \overline{c}_d}{8} \rho A (\Omega R)^3 \left(1 + 4.5\mu^2 + 1.61\mu^{3.7}\right)$$

For a rotor tilting for forward flight, this simplifies to:

$$P_0 = \frac{\sigma_r \overline{c}_d}{8} \rho A (\Omega R)^3$$

As for the induced power correction factor, the mean drag coefficient $\overline{c}_d$ is set in dependency of the rotorcraft flight state and type. A linear interpolation scheme is implemented to smoothen the transition between the distinct flight state regimes. The $\overline{c}_d$ values are recommended to be set by the user in accordance with the anticipated characteristics of the rotorcraft. The following default values are used in case no user input is provided:

For the helicopter:	$\overline{c}_d = 0.0120$	in hover.
	$\overline{c}_d = 0.0120$	in low-speed forward flight.
	$\overline{c}_d = 0.0120$	in cruise flight.
For the tiltrotor:	$\overline{c}_d = 0.0190$	in hover.
	$\overline{c}_d = 0.0140$	in low-speed forward flight.
	$\overline{c}_d = 0.0140$	in cruise flight.
For the eVTOL:	$\overline{c}_d = 0.0190$	in hover.
	$\overline{c}_d = 0.0125$	in low-speed forward flight.
	$\overline{c}_d = 0.0125$	in cruise flight.

As an alternative to this default model, a polynomial based model is implemented which computes

$\overline{c}_d$ as the sum of a series of contributing terms:

$$\overline{c}_d = \overline{c}_{d,basic} + \overline{c}_{d,sep} + \overline{c}_{d,stall} + \overline{c}_{d,comp}$$

The basic term $\overline{c}_{d,basic}$ assumes a quadratic relation of $\overline{c}_d$ with the blade loading c_T/σ.

$$\overline{c}_{d,basic} = b_0 + b_1 \frac{c_T}{\sigma} + b_2 \left(\frac{c_T}{\sigma}\right)^2$$

The coefficients b_i are set to default values, but may be set by the user as desired. The same input options are implemented for the coefficients s_i, t_i and c_i of the further contributing terms outlined below. The separation term $\overline{c}_{d,sep}$ increases $\overline{c}_d$ once the blade loading exceeds a threshold value $(c_T/\sigma)_{sep,crit}$, i.e. once $\Delta_{sep} = c_T/\sigma - (c_T/\sigma)_{sep,crit} > 0$. The term covers aerodynamic losses due to separation effects at sub-stall flow states. Δ_{sep} is set to zero at blade loadings below $(c_T/\sigma)_{sep,crit}$:

$$\overline{c}_{d,sep} = s_0 \Delta_{sep} + s_1 \Delta_{sep}^2$$

The stall term $\overline{c}_{d,stall}$ follows the same logic, and hence becomes effective once $\Delta_{stall} = c_T/\sigma - (c_T/\sigma)_{stall,crit} > 0$:

$$\overline{c}_{d,stall} = t_0 \Delta_{stall} + t_1 \Delta_{stall}^2 + t_2 \Delta_{stall}^3$$

Finally, the compressibility term $\overline{c}_{d,comp}$ increases the mean rotor blade drag coefficient as a function of the advance ratio μ to model compressibility effects. The model incorporates the rotor blade thickness ratio τ_{tip} at the blade tip, and the local Mach-number at the advancing blade tip Ma_{at}:

$$\overline{c}_{d,comp} = c_0 (K_1 + 1)^2 \left((1+\mu)\,\tau_{tip}\right)^{c_1} (1+\gamma)^{c_2}, \text{ where } K_1 = \frac{Ma_{at}^2 - 1}{\left(\tau_{tip} Ma_{at}^2 (1+\gamma)\right)^{2/3}}$$

F.2.2.3 Other Power Fractions

The parasite power is computed from the rotorcraft total drag:

$$P_p = D_{Total} V$$

The climb and descent power is computed as follows. The vertical flight efficiency factor η_{vf} accounts for the variation in fuselage download and trim drag in vertical flight, among other influencing phenomena, and varies between climbing and descending flight. The climb speed V_c corresponds to $V_c = V_z$ when $V_x = 0$, and is computed from $V_c = V \sin(\Theta_{FP})$ otherwise.

$$P_c = \eta_{vf} W V_c$$

For a conventional single-main-single-tail-rotor helicopter, a dedicated tail rotor power model is

implemented. It is differentiated between shrouded fan-in-fin-type tail rotors and conventional tail rotors. In hovering flight, the tail rotor thrust for a given flight state is derived from the rotorcraft trim in the yaw-axis. The tail rotor power for a shrouded fan-in-fin-type tail rotor is then computed from:

$$P_{tr} = \frac{1}{FM_{tr}} \frac{T_{antiQ}^{3/2}}{\sqrt{4a_w \rho \pi R_{tr}^2}}$$

For a conventional tail rotor, the required power for hovering flight results from:

$$P_{tr} = \frac{1}{FM_{tr}} \frac{T_{antiQ}^{3/2}}{\sqrt{2\rho \pi R_{tr}^2}}$$

In forward flight, the tail rotor power is computed as a fraction of the main rotor power:

$$P_{tr} = k_{tr} P_{mr}$$

The tail rotor power fraction in cruising flight may be defined by the user, whereas the following default values are defined. A polynomial of the second order is implemented as an interpolation scheme in the transitioning region between hovering and cruising flight.

$k_{tr} = 0.040$ for a conventional tail rotor

$k_{tr} = 0.015$ for a shrouded fan-in-fin-type tail rotor

The power off-take $P_{accessories}$ to supply accessories is user input. Mechanical losses are computed separately for the main rotor and tail rotor drive system:

$$P_{loss,mr} = P_{mr} \left(\left(\frac{1}{1 - k_{mrDrive}} \right) - 1 \right)$$

$$P_{loss,tr} = P_{tr} \left(\left(\frac{1}{1 - k_{trDrive}} \right) - 1 \right)$$

$$P_{losses} = P_{accessories} + P_{loss,mr} + P_{loss,tr}$$

F.2.2.4 Total Power Required

The total power required for a given flight state results from the sum of the contributing power fractions:

$$P_{mr} = P_i + P_0 + P_p + P_c$$

$$P_{req} = P_{mr} + P_{tr} + P_{losses}$$

Bibliography

[1] Jeffrey D. Sinsay and Gerardo Nunez. "Toward Right-Fidelity Rotorcraft Conceptual Design". In: *51st AIAA/ASME/ASCE/AHS/ASC Structures, Structural Dynamics, and Materials Conference*. AIAA-2010-2756. American Institute of Aeronautics and Astronautics (AIAA), Apr. 2010, p. 2756. DOI: 10.2514/6.2010-2756.

[2] Michael D P Roberts, Sylvester V Ashok, and Daniel P Schrage. "Design Space Exploration Tool for Future Rotorcraft Applications". In: *AHS 69th Annual Forum*. 2013.

[3] C. Linares, C. P. Lawson, and H. Smith. "Multidisciplinary optimisation framework for minimum rotorcraft fuel and air pollutants at mission level". In: *Aeronautical Journal* 117.1193 (2013), pp. 749–767.

[4] Carl Russell and P.-M. Basset. "Conceptual Design of Environmentally Friendly Rotorcraft – A Comparison of NASA and ONERA Approaches". In: *Annual Forum Proceedings-AHS International*. 2015.

[5] International Council on Systems Engineering. *Systems Engineering Handbook v3.2.2*. 2011.

[6] Clément Pornet et al. "Methodology for Sizing and Performance Assessment of Hybrid Energy Aircraft". In: *Journal of Aircraft* 52.1 (2015), pp. 341–352.

[7] Aerospace Industries Association. *The Unseen Cost: Industrial Base Consequences of Defense Strategy Choices*. Special Report. July 2009.

[8] Glen R. Whitehouse, Todd R. Quackenbush, and Alexander H. Boschitsch. "Variable Fidelity Preliminary Design Tools for Advanced Vertical Flight Vehicles". In: *Presented at the American Helicopter Society 66th Annual Forum*. 2010.

[9] M. Price, S. Raghunathan, and R. Curran. "An integrated systems engineering approach to aircraft design". In: *Progress in Aerospace Sciences* 42 (2006), pp. 331–376. DOI: 10.1016/j.paerosci.2006.11.002.

[10] Frank Patterson and Daniel P Schrage. "Comparison of Probabilistic and Fuzzy Multi-Attribute Decision Making Methods for Capturing Uncertainty in Concept Selection". In: *Annual Forum Proceedings-AHS International*. 2015.

[11] P Basset et al. "The C.R.E.A.T.I.O.N. project for rotorcraft concepts evaluation: The first steps". In: *37th European Rotorcraft Forum*. Italy, Sept. 2011, pp. 1–13.

[12] Daniel P. Schrage. "Technology for Rotorcraft Affordability Through Integrated Product/Process Development (IPPD)". In: *Annual Forum Proceedings-AHS International*. 1999.

[13] Klaus Ehrlenspiel and Harald Meerkamm. *Integrierte Produktentwicklung*. 5. Auflage. Carl Hanser Verlag München Wien, 2013.

[14] Sándor Vajna. *Integrated Design Engineering*. Springer-Verlag Berlin Heidelberg, 2014.

[15] Martin Eigner, Daniil Roubanov, and Radoslav Zafirov. *Modellbasierte Virtuelle Produktentwicklung*. Springer-Verlag Berlin Heidelberg, 2014.

[16] Josef Ponn and Udo Lindemann. *Konzeptentwicklung und Gestaltung technischer Produkte*. Springer-Verlag Berlin Heidelberg, 2011.

[17] SAE Aerospace. *ARP4754A: Guidelines for Development of Civil Aircraft and Systems*. Dec. 2010.

[18] National Aeronautics and Space Administration. *NASA Systems Engineering Handbook*. Tech. rep. NASA/SP-2007-6105. NASA, 2007.

[19] Federal Aviation Administration. *FAA Systems Engineering Manual*. Manual. June 2014.

[20] Dimitri N. Mavris and Daniel A. DeLaurentis. "Methodology for Examining the Simultaneous Impact of Requirements, Vehicle Characteristics, and Technologies on Military Aircraft Design". In: *ICAS 2000 Congress*. 2000, pp. 1–12. DOI: 10.1016/j.phrs.2010.10.003.

[21] Sylvester V Ashok, Daniel P Schrage, and Alexander Robledo. "A Systems Engineering Modeling and Simulation Approach for Rotorcraft Drive System Optimization". In: *Annual Forum Proceedings-AHS International*. 2011.

[22] Andrew P. Sage and William B. Rouse. *Handbook of Systems Engineering and Management*. 2nd. Hoboken, New Jersey: John Wiley & Sons Inc., 2009.

[23] *ISO/IEC/IEEE International Standard 15288 - Systems and software engineering – System life cycle processes*. 1st ed. ISO/IEC/IEE 15288:2015. ISO/IEC/IEE, May 2015.

[24] Mark Price et al. "Identifying Interfaces in Engineering Systems". In: *AIAA Journal* 44.3 (Mar. 2006), pp. 529–540.

[25] Petter Krus. "Systems Engineering in Aircraft System Design". In: *INCOSE International Symposium*. Vol. 11. 1. July 2001, pp. 723–728.

[26] Raymond W. Prouty. *Helicopter Performance, Stability and Control*. Krieger Publishing Company, 2002.

[27] J. Gordon Leishman. *Principles of Helicopter Aerodynamics*. Cambridge University Press, 2006.

[28] Wayne Johnson. *Helicopter Theory*. Dover Publications, Inc., 1994.

[29] Wayne Johnson. *Rotorcraft Aeromechanics*. Cambridge University Press, 2013.

[30] Berend Gerdes van der Wall. *Grundlagen der Hubschrauber-Aerodynamik*. Springer-Verlag Berlin Heidelberg, 2015.

[31] Marat N. Tishchenko, Vengalattore T. Nagaraj, and Inderjit Chopra. "Preliminary Design of Transport Helicopters". In: *Journal of the American Helicopter Society* 48 (2003), pp. 71–79. DOI: 10.4050/JAHS.48.71.

[32] Omri Rand and Vladimir Khromov. "Helicopter Sizing by Statistics". In: *Journal of the American Helicopter Society* 49 (2004). DOI: 10.4050/JAHS.49.300.

[33] Max Lier. "Statistical Methods for Helicopter Preliminary Design and Sizing". In: *37th European Rotorcraft Forum*. Gallarate, Italy, 2011.

[34] Franklin D Harris. *Introduction to Autogyros, Helicopters, and Other V/STOL Aircraft Volume II: Helicopters*. Tech. rep. NASA/SP-2012-215959 Vol II. NASA, 2012.

[35] J F Boer et al. *Multi-role Helicopter Life Cycle Cost (LCC) Optimisation: The Pre-Design Strategy*. Tech. rep. NLR-TP-2007-857. National Aerospace Laboratory NLR, 2007, pp. 11–13.

[36] Franklin D. Harris and Michael P. Scully. "Rotorcraft Cost Too Much". In: *Journal of the American Helicopter Society* (1997).

[37] Franklin D Harris and Michael P. Scully. "Supplemental Appendix Helicopters Cost Too Much". In: *Annual Forum Proceedings - American Helicopter Society* 53 (1997), pp. 121–132.

[38] William A. Crossley and David H. Laananen. "Conceptual design of helicopters via genetic algorithm". In: *Journal of Aircraft* 33.6 (1996), pp. 1062–1070. DOI: 10.2514/3.47058.

[39] Wlliam A. Crossley and David H. Laananen. "The Genetic Algorithm as an Automated Methodology for Helicopter Conceptual Design". In: *Journal of Engineering Design* 8.March (1997), pp. 231–250. DOI: 10.1080/09544829708907963.

[40] Roberto Celi. "Recent applications of design optimization to rotorcraft-a survey". In: *American Helicopter Society 55th Annual Forum*. Montréal, Canada, May 1999. DOI: 10.2514/2.2424.

[41] Joel E Hirsh et al. "An Integrated Approach to Rotorcraft Conceptual Design". In: *Aiaa* 1252 (2007), pp. 1–18.

[42] JaeHoon Lim and SangJoon Shin. "Modularization and Formula Upgrade for a Rotorcraft Preliminary Design Framework". In: *50th AIAA/ASME/ASCE/AHS/ASC Structures, Structural Dynamics, and Materials Conference*. AIAA-2009-2207. Palm Springs, CA, USA, May 2009, pp. 1–7.

[43] Jaehoon Lim, Sangjoon Shin, and Junemo Kim. "Development of an Advanced Rotorcraft Preliminary Design Framework". In: *International Journal Aeronautical and Space Sciences* 10.2 (2009), pp. 134–139. DOI: 10.5139/IJASS.2009.10.2.134.

[44] P.-M. Basset et al. "C.R.E.A.T.I.O.N. the Onera multi-level rotorcraft concepts evaluation tool: the foundations". In: *Presented at the Future Vertical Lift Aircraft Design Conference*. ONERA. San Francisco, CA, USA, Jan. 2012, pp. 1–14.

[45] Wayne Johnson. *NDARC - NASA Design and Analysis of Rotorcraft*. Tech. rep. NASA/TP-2009-215402. Moffett Field, CA, USA: NASA, 2009.

[46] Tarandeep S Kalra, James D Baeder, and College Park. "A Comparative Study of Different Weight Formulations Affecting Preliminary Sizing of Rotorcraft". In: *Annual Forum Proceedings-AHS International*. 2012.

[47] Jeffrey D. Sinsay. "Re-imagining Rotorcraft Advanced Design". In: *Presented at the Rotorcraft Virtual Engineering Conference*. Liverpool, U.K., Nov. 2016.

[48] Wayne Johnson. “NDARC - NASA Design and Analysis of Rotorcraft Theoretical Basis and Architecture”. In: *Presented at the American Helicopter Society Aeromechanics Specialists Conference 2010*. 2010.

[49] Wayne Johnson. “NDARC - NASA Design and Analysis of Rotorcraft Validation and Demonstration”. In: *Presented at the American Helicopter Society Aeromechanics Specialists Conference 2010*. San Francisco, CA, USA, 2010.

[50] C. W. Acree. “Integration of Rotor Aerodynamic Optimization with the Conceptual Design of a Large Civil Tiltrotor”. In: *Presented at the AHS Aeromechanics Conference*. San Francisco, CA, USA, Jan. 2010.

[51] Christopher Silva, Hyeonsoo Yeo, and Wayne Johnson. “Design of a Slowed-Rotor Compound Helicopter for Future Joint Service Missions”. In: *American Helicopter Society* (2010).

[52] Carl Russell and Wayne Johnson. “Conceptual Design and Performance Analysis for a Large Civil Compound Helicopter”. In: *Presented at the AHS Future Vertical Lift Aircraft Design Conference*. Vol. AHS Future Vertical Lift Design Conference. San Francisco, CA, USA, Jan. 2012.

[53] Max Lier et al. “Studies on Rotorcraft Integrated Design and Evaluation At DLR - First Results -”. In: *38th European Rotorcraft Forum*. 2012, pp. 568–580.

[54] Max Lier et al. “A Toolbox for Rotorcraft Preliminary Design”. In: *Annual Forum Proceedings-AHS International*. 2015.

[55] P.-M. Basset. “Some meta-modeling and optimization techniques for helicopter pre-sizing”. In: *38th European Rotorcraft Forum*. Jan. 2012.

[56] Saikath Bhattacharya et al. “Rotorcraft Tradespace Exploration incorporating Reliability Engineering”. In: *Annual Forum Proceedings-AHS International*. Virginia Beach, VA, USA, May 2015.

[57] Michel Raous. “Art of Modeling in Contact Mechanics”. In: *The Art of Modeling Mechanical Systems*. Springer, 2017, pp. 203–276.

[58] Brian A. Woodcock. “The Scientific Method as Myth and Ideal”. In: *Science & Education* 23.10 (2014), pp. 2069–2093. DOI: 10.1007/s11191-014-9704-z.

[59] Nancy J. Nersessian. “Model-Based Reasoning in Conceptual Change”. In: *Model-Based Reasoning in Scientific Discovery*. Ed. by Lorenzo Magnani, Nancy J. Nersessian, and Paul Thagard. Boston, MA: Springer US, 1999, pp. 5–22. DOI: 10.1007/978-1-4615-4813-3_1.

[60] Hans Dresig and Alexander Fidlin. *Schwingungen mechanischer Antriebssysteme*. Springer Berlin Heidelberg, 2014.

[61] Friedrich Pfeiffer. “Modeling Objectives and Realization”. In: *The Art of Modeling Mechanical Systems*. Vol. 570. Springer, 2017, pp. 1–82.

[62] J. Gordon Leishman. *The Helicopter – Thinking Forward, Looking Back*. The College Park Press, 2007.

[63] Wayne Johnson and Anubhav Datta. “Requirements for Next Generation Comprehensive Analysis of Rotorcraft”. In: *AHS Specialist’s Conference on Aeromechanics*. San Francisco, CA, USA, 2008, pp. 1–8.

[64] Stephen M Batill, John E Renaud, and Xiaoyu Gu. “Modeling and Simulation Uncertainty in Multidisciplinary Design Optimization”. In: *8th AIAA/USAF/NASA/ISSMO Symposium on Multidisciplinary Analysis & Optimization* AIAA-2000-4803 (2000), pp. 1–11. DOI: 10.2514/6.2000-4803.

[65] Herbert Alexander Simon. *The Sciences of the Artificial*. 3rd ed. The MIT Press, 1996.

[66] Martin Krosche and Wolfgang Heinze. “Robustness Analysis of an Aircraft Design for Short Takeoff and Landing”. In: *Journal of Aircraft* 52.4 (July 2015).

[67] Loyd Baker et al. “Foundational concepts for model driven system design”. In: *INCOSE Model Driven System Design Interest Group* 16 (2000).

[68] Jeffrey A. Estefan. “Survey of model-based systems engineering (MBSE) methodologies, Rev. B”. In: *Incose MBSE Focus Group* 25.8 (2008).

[69] A Wayne Wymore. *Model-based systems engineering*. Vol. 3. CRC press, 1993.

[70] Natalia M. Alexandrov et al. “Approximation and Model Management in Aerodynamic Optimization with Variable-Fidelity Models”. In: *Journal of Aircraft* 38.6 (2001), pp. 1093–1101. DOI: 10.2514/2.2877.

[71] Warren E Walker et al. “Defining Uncertainty: A Conceptual Basis for Uncertainty Management in Model-Based Decision Support”. In: *Integrated assessment* 4.1 (2003), pp. 5–17.

[72] Silvio O Funtowicz and Jerome R Ravetz. *Uncertainty and quality in science for policy*. Vol. 15. Springer Science & Business Media, 1990.

[73] Marjolein B. A. van Asselt and Jan Rotmans. “Uncertainty in Integrated Assessment Modelling”. In: *Climatic Change* 54.1 (2002), pp. 75–105. DOI: 10.1023/A:1015783803445.

[74] Armen Der Kiureghian and Ove Ditlevsen. “Aleatory or epistemic? Does it matter?” In: *Structural Safety* 31 (2009), pp. 105–112. DOI: 10.1016/j.strusafe.2008.06.020.

[75] L. Jaeger et al. “Aircraft Multidisciplinary Design Optimization Under Both Model and Design Variables Uncertainty”. In: *Journal of Aircraft* 50.2 (Mar. 2013), pp. 528–538.

[76] C. Siva, M. S. Murugan, and Ranjan Ganguli. “Uncertainty Quantification in Helicopter Performance Using Monte Carlo Simulations”. In: *Journal of Aircraft* 48.5 (2011), pp. 1503–1511.

[77] Marc C Kennedy and Anthony O’Hagan. “Bayesian calibration of computer models”. In: *Journal of the Royal Statistical Society: Series B (Statistical Methodology)* 63.3 (2001), pp. 425–464.

[78] Paul D Arendt, Daniel W Apley, and Wei Chen. “Quantification of model uncertainty: Calibration, model discrepancy, and identifiability”. In: *Journal of Mechanical Design* 134.10 (2012).

[79] Patrick N. Koch et al. “Facilitating probabilistic multidisciplinary design optimization using kriging approximation models”. In: *9th AIAA/ISSMO Symposium on Multidisciplinary Analysis and Optimization*. AIAA 2002-5415. 2002, pp. 1–11.

[80] G. Gary Wang and S. Shan. “Review of Metamodeling Techniques in Support of Engineering Design Optimization”. In: *Journal of Mechanical Design* 129.April 2007 (2007), p. 370. DOI: 10.1115/1.2429697.

[81] Wei Chen et al. “A Concept Exploration Method for Determining Robust Top-Level Specifications”. In: *Engineering Optimization* 26 (1996), pp. 137–158. DOI: 10.1080/03052159608941114.

[82] Debora D. Daberkow and Dimitri N. Mavris. “New Approaches to Conceptual and Preliminary Aircraft Design: A Comparative Assessment of a Neural Network Formulation and a Response Surface Methodology”. In: *SAE Technical Paper*. SAE International, Sept. 1998. DOI: 10.4271/985509.

[83] Dimitri N. Mavris and Daniel A. DeLaurentis. “A Stochastic Design Approach for Aircraft Affordability”. In: *Proceedings of the 21st Congress of the International Council on the Aeronautical Sciences* (1998).

[84] Patrick N Koch, Dimitri Mavris, and Farrokh Mistree. “Partitioned, multilevel response surfaces for modeling complex systems”. In: *AIAA journal* 38.5 (2000), pp. 875–881.

[85] D. A. DeLaurentis and D. N. Mavris. “Uncertainty Modeling and Management in Multidisciplinary Analysis and Synthesis”. In: 38th Aerospace Sciences Meeting and Exhibit. American Institute of Aeronautics and Astronautics, 2015/08/19 2000, pp. 2–12. DOI: 10.2514/6.2000-422.

[86] Timothy W Simpson et al. “Metamodels for computer-based engineering design: survey and recommendations”. In: *Engineering with computers* 17.2 (2001), pp. 129–150.

[87] Timothy W. Simpson et al. “On the Use of Statistics in Design and the Implications for Deterministic Computer Experiments”. In: *Proceedings of DETC’97*. DETC97DTM3881. 1997, pp. 1–14.

[88] Timothy Simpson et al. “Comparison of response surface and kriging models for multidisciplinary design optimization”. In: *7th AIAA/USAF/NASA/ISSMO Symposium on Multidisciplinary Analysis and Optimization*. AIAA-98-4755. 1998, pp. 1–11. DOI: 10.2514/6.1998-4755.

[89] Jose Valenzuela del Rio and Dimitri Mavris. “Stochastic Process Model for the Optimization of a Rotorcraft with Categorical Variables”. In: *Journal of the American Helicopter Society* 59 (2014), pp. 1–14. DOI: 10.4050/JAHS.59.042007.

[90] J Beedy et al. “Using CFD to Improve Simple Aerodynamic Models for Rotor Codes”. In: *Presented at the AHS 4th Decennial Specialist’s Conference on Aeromechanics*. San Francisco, CA, USA, Jan. 2004, pp. 1–26.

[91] Michael Avera and Rajneesh Singh. “OpenMDAO/NDARC Framework for Assessing Performance Impact of Rotor Technology Integration”. In: *Annual Forum Proceedings-AHS International*. Québec, Canada, May 2014.

[92] Michael Avera, Hao Kang, and Rajneesh Singh. “Comprehensive Rotorcraft Analysis for Preliminary Design and Optimization”. In: *Annual Forum Proceedings-AHS International*. Virginia Beach, VA, USA, May 2015.

[93] Francesca Fusi et al. “Multifidelity Physics-Based Method for Robust Optimization Applied to a Hovering Rotor Airfoil”. In: *AIAA Journal* 53.11 (Nov. 2015), pp. 3448–3465.

[94] Dimitri N Mavris, Andrew P Baker, and Daniel P Schrage. “Development of a methodology for the determination of technical feasibility and viability of affordable rotorcraft systems”. In: *Annual Forum Proceedings - American Helicopter Society* 2 (1998), pp. 1070–1081.

[95] Bryce Alexander Roth, Dimitri N Mavris, and Don Elliott. “A Probabilistic Approach to UCAV Engine Sizing”. In: *Presented at 1998 Joint Propulsion Conference*. AIAA98-3264. Georgia Institute of Technology, 1998.

[96] Gyung-Jin Park et al. “Robust Design: An Overview”. In: *AIAA Journal* 44.1 (Jan. 2006).

[97] Wei Chen et al. “A Procedure For Robust Design: Minimizing Variations Caused By Noise Factors And Control Factors”. In: *Journal of Mechanical Design* 118.4 (1996), pp. 478–485.

[98] Eric Fox. “The Pratt & Whitney Probabilistic Design System”. In: *35th Structures, Structural Dynamics, and Materials Conference*. AIAA-94-1442-CP. Hilton Head, SC, USA: American Institute of Aeronautics and Astronautics, Apr. 1994. DOI: 10.2514/6.1994-1442.

[99] Philippe J Couturier, Christophe Tribes, and Jean-Yves Trépanier. “Framework for the Robust Design Optimization of an Airframe and its Engines”. In: *Journal of Aerospace Engineering* (2013).

[100] Ray D Leoni. *Black Hawk: The Story of a World Class Helicopter*. American Institute of Aeronautics & Astronautics, Aug. 2007.

[101] Wayne Johnson. *A History of Rotorcraft Comprehensive Analyses*. Tech. rep. NASA/TP-2012-216012. Moffett Field, CA, USA: NASA, 2012.

[102] Patrick N. Koch et al. “Statistical Approximations for Multidisciplinary Design Optimization: The Problem of Size”. In: *Journal of Aircraft* 36.1 (1999).

[103] Poul Harremoës and H. Madsen. “Fiction and Reality in the Modelling World – Balance Between Simplicity and Complexity, Calibration and Identifiability, Verification and Falsification”. In: *Water Science and Technology* 39.9 (1999), pp. 1–8.

[104] Wayne Johnson and Jeffrey D Sinsay. “Rotorcraft Conceptual Design Environment”. In: *Presented at the 2nd International Forum on Rotorcraft Multidisciplinary Technology*. Seoul, Korea, 2009.

[105] O. Juhasz et al. “Comparison of Three Coaxial Aerodynamic Prediction Methods Including Validation with Model Test Data”. In: *Journal of the American Helicopter Society* 59.January 2011 (2014), pp. 1–14. DOI: 10.4050/JAHS.59.032006.

[106] Hartmut Bremer. “Fascination of Making Models - Truth-Reality-Illusion?” In: *The Art of Modeling Mechanical Systems*. Vol. 570. Springer, 2017, pp. 83–172.

[107] Lance W Traub. “Range and endurance estimates for battery-powered aircraft”. In: *Journal of Aircraft* 48.2 (Mar. 2011), pp. 703–707.

[108] Y. H. Sun, H. L. Jou, and J. C. Wu. “Multilevel Peukert Equations Based Residual Capacity Estimation Method for Lead-Acid Battery”. In: *2008 IEEE International Conference on Sustainable Energy Technologies*. Nov. 2008, pp. 101–105. DOI: 10.1109/ICSET.2008.4746980.

[109] W. Z. Stepniewski and C. N. Keys. *Rotary-Wing Aerodynamics*. Dover Publications, 1984.

[110] Karl Siebertz, David van Bebber, and Thomas Hochkirchen. *Statistische Versuchsplanung - Design of Experiments (DoE)*. Springer-Verlag Berlin Heidelberg, 2010.

[111] Jeff Holden and Nikhil Goel. *Fast-Forwarding to a Future of On-Demand Urban Air Transportation*. Tech. rep. UBER Technologies, Oct. 2016.

[112] Michael J. Duffy et al. “A Study in Reducing the Cost of Vertical Flight with Electric Propulsion”. In: *AHS International’s 73rd Annual Forum*. 2017.

[113] The European Commission. *Commission Regulation (EU) No 965/2012*. Tech. rep. Official Journal of the European Union, 2012.

[114] European Aviation Safety Agency. *Acceptable Means of Compliance (AMC) and Guidance Material (GM) to Part-CAT*. Tech. rep. 2. European Aviation Safety Agency, Apr. 2014.

[115] Franklin D Harris. *Introduction to Autogyros, Helicopters, and Other V/STOL Aircraft Volume I: Overview and Autogyros*. Tech. rep. NASA/SP-2011-215959 Vol I. NASA, May 2011.

[116] Franklin D Harris. *Introduction to Autogyros, Helicopters, and Other V/STOL Aircraft Volume III: Other V/STOL Aircraft*. Tech. rep. NASA/SP-2015-215959 Vol III. NASA, Nov. 2015.

[117] Antonio Filippone. “Data and performances of selected aircraft and rotorcraft”. In: *Progress in Aerospace Sciences* 36 (2000), pp. 629–654. DOI: 10.1016/S0376-0421(00)00011-7.

[118] Edwin D. McConkey et al. *Helicopter Physical and Performance Data*. Tech. rep. DOT/FAA/RD-90/3. Springfield, VA, USA: U.S. Department of Transportation, 1991.

[119] W. Z. Stepniewski. *A Comparative Study of Soviet vs. Western Helicopters Part 1 - General Comparison of Designs*. Tech. rep. NASA-CR3579. NASA, 1983.

[120] W. Z. Stepniewski. *A Comparative Study of Soviet vs. Western Helicopters Part 2 - Evaluation of Weight, Maintainability and Design Aspects of Major Components*. Tech. rep. NASA-CR3580. NASA, 1983.

[121] William J Fredericks, Mark D Moore, and Ronald C Busan. “Benefits of hybrid-electric propulsion to achieve 4x increase in cruise efficiency for a VTOL aircraft”. In: *AIAA Aviation Technology, Integration, and Operations (ATIO) Conference*. Vol. 12. 14. 2013.

[122] Martin Hepperle. *Electric Flight - Potential and Limitations*. Tech. rep. STO-MP-AVT-209. DLR - German Aerospace Center, Oct. 2012.

[123] Mark D Moore et al. “High Speed Mobility through On-Demand Aviation”. In: *Aviation Technology, Integration, and Operations Conference, AIAA AVIATION Forum*. AIAA 2013-4373. 2013. DOI: 10.2514/6.2013-4373.

[124] C. Pornet et al. “Methodology for Sizing and Performance Assessment of Hybrid Energy Aircraft”. In: *Aviation Technology, Integration, and Operations Conference*. AIAA 2013-4415. 2013.

[125] M.D. Moore and B Fredericks. “Misconceptions of electric propulsion aircraft and their emergent aviation markets”. In: *52nd AIAA Aerospace Sciences Meeting - AIAA Science and Technology Forum and Exposition, SciTech 2014*. Jan. 2014.

[126] Geoffrey Hammond and Tom Hazeldine. “Indicative Energy Technology Assessment of Advanced Rechargeable Batteries”. In: *Applied Energy* 138 (Nov. 2014).

[127] Lorenzo Grande et al. “The Lithium/Air battery: Still an Emerging System or a Practical Reality?” In: *Advanced materials* 27.5 (2015), pp. 784–800.

[128] Arafat Md Rahman, Xiaojian Wang, and Cuie Wen. “A review of high energy density lithium–air battery technology”. In: *Journal of Applied Electrochemistry* 44 (Jan. 2014).

[129] Jang Choi and Doron Aurbach. “Promise and Reality of Post-Lithium-Ion Batteries with High Energy Densities”. In: *Nature Reviews Materials* 1 (Mar. 2016), p. 16013. DOI: 10.1038/natrevmats.2016.13.

[130] Noshin Omar et al. “Rechargeable Energy Storage Systems for Plug-In Hybrid Electric Vehicles – Assessment of Electrical Characteristics”. In: *Energies* 5.8 (2012), pp. 2952–2988.

[131] Hui Zhang and Leon M Tolbert. “Efficiency Impact of Silicon Carbide Power Electronics for Modern Wind Turbine Full Scale Frequency Converter”. In: *IEEE Transactions on Industrial Electronics* 58.1 (2011), pp. 21–28.

[132] Daniel P. Raymer. *Aircraft Design: A Conceptual Approach*. Ed. by Joseph A. Schetz. 5th ed. American Institute of Aeronautics and Astronautics, Inc., 2012.

[133] Raymond W. Prouty. *Helicopter Aerodynamics, Volume II*. Eagle Eye Solutions, LLC, 2009.

[134] Dominik Wirth and Manfred Hajek. “Probabilistic Methodology for Multi-Fidelity Model-Based Robust Preliminary Design of Rotorcraft”. In: *AHS International’s 73rd Annual Forum*. Fort Worth, Texas, USA, May 2017.

[135] O. Schwabe, E. Shehab, and J. Erkoyuncu. “Uncertainty quantification metrics for whole product life cycle cost estimates in aerospace innovation”. In: *Progress in Aerospace Sciences* (2015).

[136] Wen Yao et al. “Review of uncertainty-based multidisciplinary design optimization methods for aerospace vehicles”. In: *Progress in Aerospace Sciences* 47 (2011), pp. 450–479.